Universidade Federal Fluminense
Instituto de Física

Quantum Spacetimes and Physics Beyond the Standard Model

Arthur Ferreira Vieira

Niterói, 2024

ARTHUR FERREIRA VIEIRA

QUANTUM SPACETIMES AND PHYSICS BEYOND THE STANDARD MODEL

A thesis submitted to the Departamento de Física - UFF in partial fulfillment of the requirements for the degree of Doctor in Sciences (Physics).

Advisor: Prof. Dr. Antônio Duarte Pereira Junior
Co-advisor: Dr. Gustavo Pazzini de Brito

Niterói-RJ
2024

Ficha catalográfica automática - SDC/BIF
Gerada com informações fornecidas pelo autor

V657q Vieira, Arthur Ferreira
Quantum Spacetimes and Physics Beyond the Standard Model / Arthur Ferreira Vieira. - 2024.
164 p.: il.

Orientador: Antônio Duarte Pereira Junior.
Coorientador: Gustavo Pazzini De Brito.
Tese (doutorado)-Universidade Federal Fluminense, Instituto de Física, Niterói, 2024.

1. Gravitação quântica. 2. Grupo de renormalização. 3. Teorias alternativas de gravitação. 4. Física além do modelo padrão. 5. Produção intelectual. I. Pereira Junior, Antônio Duarte, orientador. II. De Brito, Gustavo Pazzini, coorientador. III. Universidade Federal Fluminense. Instituto de Física. IV. Título.

CDD - XXX

Bibliotecário responsável: Debora do Nascimento - CRB7/6368

BANCA EXAMINADORA

MEMBROS TITULARES:

Prof. Dr. Antônio Duarte Pereira Junior - (IF-UFF)

Profa. Dra. Leila Lobato Graef - (IF-UFF)

Prof. Dr. Gabriel Santos Menezes - (UFRRJ)

Prof. Dr. Marcelo Guimarães - (UERJ)

Prof. Dr. Rodrigo Ferreira Sobreiro - (IF-UFF)

MEMBROS SUPLENTES:

Prof. Dr. Rudnei de Oliveira Ramos - (UERJ)

Profa. Dra. Raissa Fernandes Pessoa Mendes - (IF-UFF)

Prof. Dr. Luis Oxman - (IF-UFF)

Para o homem que moldou o homem que sou hoje,
para o meu herói, para o meu amado pai,
Luiz Henrique Ferreira Vieira, dedico esta tese.
Te amo para sempre!

Acknowledgments

Throughout my PhD, I truly understood that science is a truly collaborative activity. I say this in every sense of the word. In this way, I would like to first of all thank my parents for the support and love throughout my whole life. I cannot find the right words to express what you both meant and mean to me. I love you, my dear mom and my forever beloved father (*in memoriam*)!

I had the amazing opportunity to learn how to do better scientific research with many people. So, I will move on to thanking each one that contributed to this. Starting with my supervisor Antônio Duarte, I would like to thank him for accepting me as his first student on the field of asymptotically safe quantum gravity at the Fluminense Federal University. I appreciate all the moments we had discussing physics in your office and coffee breaks. No doubt, he had a major positive impact on my scientific formation. I also thank my co-supervisor Gustavo de Brito, whom I am deeply grateful for the patience and scientific support at every stage of my PhD.

In the final year of the PhD, I had the incredible opportunity to work in the group of Astrid Eichhorn at the CP^3-Origins - University of Southern Denmark at the city of Odense, as a visiting PhD student for a one-year period. I would like to thank Astrid for the fruitful collaboration and for the kind hospitality and support I had during that time. I am grateful for sharing with me her knowledge about different approaches to quantum gravity and about team-work in scientific research. I extend my gratitude once again to Gustavo for helping me settling in in Odense and to Rafael Lino dos Santos for the enjoyable and fruitful friendship we developed. My time in Odense certainly was a lot better with the company of amazing people: Mattias Thing, Hélöise Delaporte, Pedro Fernandes, Juan Cruz, Gustavo de Brito, Rafael dos Santos and Shouryya Ray. Thank you all!

I also had the amazing opportunity to spend one month at the Institute of Physics of the University of Graz in Austria. I was invited by prof. Reinhard Alkofer to collaborate on a project and give a seminar for the graduate students. I am grateful to Reinhard for the hospitality and for all the fruitful discussions on non-perturbative Yang-Mills theories and various aspects of classical formulations of gravity.

During my time in Odense, I could attend many conferences where I met many people with whom I had enlightening discussions that somehow contributed to my understanding on non-perturbative quantum field theories: Holger Gies, Markus Fröb, Manuel Reichert, Christof Wetterich, Benjamin Knorr, Roberto Percacci, Aaron Held and Daniel Litim.

I also extend my gratitude to the people at the Fluminense Federal University. Those who had a

positive impact in my scientific formation: professors Jorge Sá Martins, Antonio Zelaquette, Rodrigo Sobreiro, Nivaldo Lemos, Kaled Dechoum, Andrea Latgé, Marco Moriconi, Raissa Fernandes and Luis Oxman, and those dear colleagues that turned this journey a lot easier and funnier: Bernardo França, Maron Anka, Anderson Tomaz and Samuel Motta. Thank you all!

I would like to thank the one that is a blue sky on my cloudy days, the love of my life: Bruna Oliveira. Thank you for giving me the love I never knew I needed and for the support and encouragement to pursue all my plans, my desires and dreams. Thank you for making my life happy again and for being my best friend. Te amo, minha princesa!

Finally, I am grateful to CNPq for financial support along the last years.

Abstract

In this thesis, we investigate the interplay of quantum fluctuations of matter with different incarnations of gravity. In particular, both quantum properties of the background spacetime and its fluctuations are put to the test in order to provide constraints on dark matter models, on the fate of chiral symmetry for fermions and on kinematically classical siblings of gravity itself. Non-perturbative renormalization techniques in the context of the functional Renormalization Group will be the main tools for the three investigations, and, in particular, to probe the existence of a suitable UV fixed point for quantum gravity-matter systems within the asymptotic safety perspective. Our first investigation regards dark matter. The nature of dark matter is a problem with too many potential solutions. We investigate whether a consistent embedding into quantum gravity can reduce the number of solutions to the dark-matter problem. Concretely, we focus on a hidden sector composed of a gauge field and a charged scalar, with gauge group $\mathrm{U}(1)_\mathrm{D}$ or $\mathrm{SU}(2)_\mathrm{D}$. The gauge field is the dark-matter candidate, if the gauge symmetry is broken spontaneously. Phenomenological constraints on the couplings in this model arise from requiring that the correct dark matter relic density is produced via thermal freeze-out and that recent bounds from direct-detection experiments are respected. We find that the consistent embedding into asymptotically safe quantum gravity gives rise to additional constraints on the couplings at the Planck scale, from which we calculate corresponding constraints at low energy scales. We discover that phenomenological constraints cannot be satisfied simultaneously with theoretical constraints from asymptotically safe quantum gravity, ruling out these dark-matter models. Our second study will probe the mechanism of chiral symmetry breaking for fermionic systems in a gravitational background with curvature and torsion. The analysis is based on a scale-dependent effective potential derived from a bosonized version of the Nambu-Jona-Lasino model in a Riemann-Cartan background. We have investigated the fate of chiral symmetry in two different regimes of curvature and torsion. Our main finding is that, in the scenario where only torsion is present, there is no indication of a mechanism of gravitational catalysis. Our third and final endeavor is the study of Renormalization Group flows of unimodular quantum gravity. In particular, we search for non-trivial fixed-point solutions for polynomial expansions of the $f(R)$-type as well as of the $F(R_{\mu\nu}R^{\mu\nu}) + RZ(R_{\mu\nu}R^{\mu\nu})$ family. Furthermore, we consider the inclusion of matter fields without self-interactions minimally coupled to the unimodular gravitational action and we find evidence for compatibility of asymptotically safe unimodular quantum gravity with the field content of the Standard Model and some of its common extensions.

Resumo

Nesta tese, investigamos a interação das flutuações quânticas da matéria com diferentes formulações da gravidade. Em particular, tanto as propriedades quânticas do espaço-tempo de fundo como as suas flutuações são postas à prova, a fim de fornecer restrições aos modelos de matéria escura, ao destino da simetria quiral dos férmions e aos irmãos cinematicamente clássicos da própria gravidade. Técnicas de renormalização não-perturbativas no contexto do Grupo de Renormalização funcional serão as principais ferramentas para as três investigações e, em particular, para sondar a existência de um ponto fixo UV adequado para sistemas quânticos de gravidade-matéria na perspectiva da segurança assintótica. Nossa primeira investigação diz respeito à matéria escura. A natureza da matéria escura é um problema com muitas soluções em potencial. Investigamos se uma incorporação consistente na gravidade quântica pode reduzir o número de soluções para o problema da matéria escura. Concretamente, concentramo-nos em um setor oculto composto por um campo de calibre e um escalar carregado, com grupo de calibre $\mathrm{U}(1)_\mathrm{D}$ ou $\mathrm{SU}(2)_\mathrm{D}$. O campo de calibre é o candidato à matéria escura, se o a simetria de calibre é quebrada espontaneamente. Restrições fenomenológicas nos acoplamentos neste modelo surgem da exigência de que a correta densidade de relíquia de matéria escura seja produzida por meio de congelamento térmico e que os limites recentes dos experimentos de detecção direta sejam respeitados. Descobrimos que a incorporação consistente na gravidade quântica assintoticamente segura dá origem a restrições adicionais nos acoplamentos na escala de Planck, a partir dos quais calculamos as restrições correspondentes em baixa escalas de energia. Descobrimos que as restrições fenomenológicas não podem ser satisfeitas simultaneamente com restrições teóricas da gravidade quântica assintoticamente segura, descartando estes modelos de matéria escura. Nosso segundo estudo irá investigar o mecanismo de quebra de simetria quiral para sistemas fermiônicos em um fundo gravitacional com curvatura e torção. A análise baseia-se em um potencial efectivo dependente de escala derivado de uma versão bosonizada do modelo de Nambu-Jona-Lasino em uma geometria de Riemann-Cartan. Investigamos o destino da simetria quiral em dois regimes diferentes de curvatura e torção. Nossa principal conclusão é que, no cenário onde apenas a torção está presente, não há indicação de um mecanismo de catálise gravitacional. Nosso terceiro e último empreendimento é o estudo dos fluxos do Grupo de Renormalização de gravidade quântica unimodular. Em particular, procuramos soluções de ponto fixo não-triviais para expansões polinomiais do tipo $f(R)$, bem como do tipo $F(R_{\mu\nu}R^{\mu\nu}) + RZ(R_{\mu\nu}R^{\mu\nu})$. Além disso, consideramos a inclusão de campos de matéria sem autointerações minimamente acopladas à ação gravitacional unimodular e encontramos evidências de compatibilidade da gravidade quântica unimodular assintoticamente segura com o conteúdo de matéria (além) do Modelo Padrão.

List of Publications

Here I present my complete list of publications and on-going projects that are associated to the content of this thesis:

- *"Exploring new corners of asymptotically safe unimodular quantum gravity,"*
  Gustavo P. de Brito, Antônio D. Pereira and Arthur F. Vieira,
  Phys. Rev. D **103**, no. 10, 104023 (2021)

- *"Fate of chiral symmetry in Riemann-Cartan geometry,"*
  Gustavo P. de Brito, Antônio D. Pereira and Arthur F. Vieira,
  Phys. Rev. D **108**, no. 4, 045012 (2023)

- *"Ruling out models of vector dark matter in asymptotically safe quantum gravity,"*
  Gustavo P. de Brito, Astrid Eichhorn, Mads T. Frandsen, Martin Rosenlyst, Mattias E. Thing and Arthur F. Vieira,
  arXiv:2312.02086 [hep-ph] (accepted in Physical Review D after the submission of the thesis.)

- *"Four-fermions in quantum Poincaré gauge gravity,"*
  Gustavo P. de Brito and Arthur F. Vieira,
  (In preparation)

- *"Cosmological constant from low-energy QCD in Riemann-Cartan gravity theories,"*
  Arthur F. Vieira, Antônio D. Pereira, Niko Heinemann and Reinhard Alkofer,
  (In preparation)

This thesis intends to cover in detail the first three projects. The last two projects will appear soon.

Content

Chapter 1

Introduction

1.1 Setting the stage: What do we know about the fundamental building blocks of Nature?

Our current knowledge of the fundamental building blocks of Nature is encoded in two formidable theories: in the Standard Model (SM) of particle physics on the one side and in General Relativity (GR) on the other side. Nevertheless, both theories are actually incomplete in the sense that they have regimes of validity and break down at certain circumstances. This breakdown calls us to go beyond in order to fully understand the fundamental microscopic building blocks of Nature. In the next section, we will briefly review how and where these two theories break down, so that we can get an indication of what is the type of theory or formalism that is needed to be developed to go beyond our current status of understanding.

1.1.1 The Standard Model and the scale of new physics

The status of the SM pre-LHC (some 12 years ago) was that it worked quite well at energy scales of around 100 GeV or so, but the particle physics community had a very clear indication where the next scale of new physics had to be, because, from measuring the masses of the weak gauge bosons, it is actually possible to infer that, if there is a Higgs particle, then its vacuum expectation value (VEV) has to be $v_{\text{Higgs}} = 246$ GeV (see, *e.g.*, [1]). If there is not a Higgs particle, then the electroweak sector runs into a problem below the TeV scale. Therefore, before the LHC was switched on, there was a very good and robust theoretical understanding of the scale of new physics. Indeed, this new physics turned out to be the simplest possibility of them all, namely just a Higgs particle that has to be added or that was already part of the SM. In Fig. 1.1, we can see the Renormalization Group (RG) running of the bottom- and tau-quark Yukawa couplings $y_{b,\tau}$ at 2-loops, and $\mathrm{U}(1)_{\mathrm{Y}}$ hypercharge gauge coupling $g_1 = \sqrt{\frac{5}{3}} g_{\mathrm{Y}}$, $\mathrm{SU}(2)_{\mathrm{L}}$ gauge coupling g_2, $\mathrm{SU}(3)_{\mathrm{C}}$ gauge coupling g_3, quartic self-coupling λ and top-quark Yukawa y_t at 3-loops, which are all measured in the infrared, and their RG-evolution up to the Planck scale ($M_{\text{Planck}} = 1.221 \times 10^{19}$ GeV) and even beyond [2].

Interestingly, the exciting discovery of the Higgs [3, 4] at ATLAS and CMS detectors is telling us

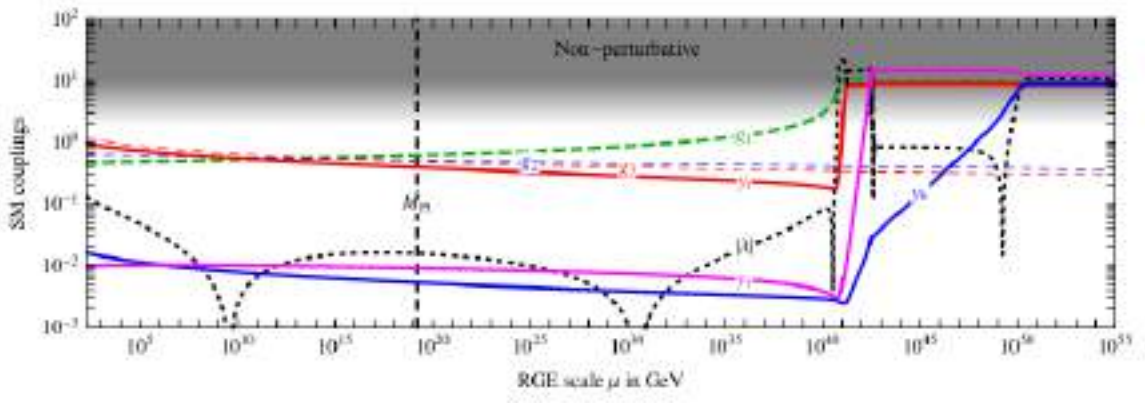

Figure 1.1: Renormalization Group flow of all couplings in the SM at 3 loops in the $\mathrm{U}(1)_\mathrm{Y}$ hypercharge gauge coupling $g_1 = \sqrt{\frac{5}{3}} g_\mathrm{Y}$, $\mathrm{SU}(2)_\mathrm{L}$ gauge coupling g_2, $\mathrm{SU}(3)_\mathrm{C}$ gauge coupling g_3, quartic self-coupling λ and top-quark Yukawa y_t and at 2 loops in the bottom- and tau-quark Yukawa couplings $y_{b,\tau}$. Figure extracted from [2].

where the understanding that we have of the building blocks of matter breaks down. For that, we have to take a look at the mass of the Higgs, which is related to its VEV and the coupling λ that parameterizes the quartic Higgs self-interaction. This relation is given by $M_\mathrm{H} = \sqrt{2\lambda} v_\mathrm{Higgs} \approx 125$ GeV and we see that the Higgs mass depends on the quartic coupling only very weakly (cf. Fig. 1.1) up to very large trans-Planckian energies (or very small distance scales), where it actually starts to diverge. This divergence is the so-called *Landau pole* and signals that this is a scale where new physics has to exist.

Furthermore, there is only a very narrow range of Higgs masses where we can extend our understanding of the degrees of freedom of the fundamental building blocks of matter until very high scales. This is due to the fact that, if the quartic coupling is tuned to a larger value at low energies, then the Higgs mass is somewhat higher and, consequently, the Landau pole sets in much earlier and we run into the so-called *triviality problem* (see, *e.g.*, [5, 6]). Therefore, if we demand that the SM to be consistent for a very large range of scales, then this bounds the range of allowed masses from above. Moreover, there is also a bound from below. This is because the quartic coupling dips into a negative, almost flat, regime (cf. Fig. 1.1) and, if it becomes truly negative and does not become positive again, then that would represent an instability of the vacuum, which would be a significant theoretical problem. In this sense, a small change in the mass of the Higgs by changing the quartic coupling would lead to a prediction that the scale of new physics has to exist around 10^6 to 10^7 GeV.

However, what the measurement of the Higgs mass at low energies is actually telling us is that we could be facing what has been conjectured as the *desert scenario*, where the SM is really basically everything there is for a very long range of scales and then new physics that significantly interacts with the SM only comes in beyond the Planck scale. Additionally, of course, there are the unresolved questions of, *e.g.*, origin of neutrino masses, matter-antimatter asymmetry and of what constitutes dark matter. Regarding the latter, there are scenarios where dark matter can be explained by various elementary particles that do not couple strongly to the SM and do not change this picture very much [7] or actually even just interact with the SM gravitationally.

Currently, in the post-LHC era, the SM has been crowned as the very accurate quantum description

of the fundamental degrees of freedom of matter, but we actually have the indication that the new physics scale is somewhere far beyond the Planck scale, which means that actually a quantum theory of gravity would kick in much earlier. In the next subsection, we will briefly discuss the status of our understanding of gravity itself.

1.1.2 Status of General Relativity and its limits

Similarly to the SM, all astrophysical phenomena in the weak-field regime all well-described by GR [8] and its formalism is defined by the Einstein-Hilbert action over a spacetime with no boundary as

$$S_{\rm GR} = \frac{1}{16\pi G_{\rm N}} \int \mathrm{d}^4x\sqrt{-g}\,(R - 2\bar{\Lambda}) + S_m, \tag{1.1.1}$$

where $G_{\rm N} = 6.6743(15) \times 10^{-11} m^3/(kg \cdot s^2)$ is the CODATA recommended value [9] of the Newton constant that parameterizes the strength of gravitational self-interactions and also the coupling of gravity to matter, $\bar{\Lambda}$ is a small cosmological constant, $g = \det(g_{\mu\nu})$ and S_m is a "matter action" describing a source for non-gravitational fields[1]. We remark that the Einstein-Hilbert action is invariant under active [12] infinitesimal coordinate transformations ($x'^\mu = x^\mu - v^\mu$), or diffeomorphisms (*Diff*), acting on the metric field according to $g_{\mu\nu} \mapsto g_{\mu\nu} + \mathcal{L}_v g_{\mu\nu}$, with

$$\begin{aligned}\delta g_{\mu\nu} \equiv \mathcal{L}_v g_{\mu\nu} &= v^\rho \partial_\rho g_{\mu\nu} + (\partial_\mu v^\rho) g_{\rho\nu} + (\partial_\nu v^\rho) g_{\rho\mu} \\ &= g_{\rho\nu}\nabla_\mu v^\rho + g_{\mu\rho}\nabla_\nu v^\rho,\end{aligned} \tag{1.1.3}$$

where $\mathcal{L}_v$ is the Lie derivative along the generating vector field v^μ. The action (1.1.1) also provides the Einstein field equations,

$$G \equiv R_{\mu\nu} - \frac{1}{2} g_{\mu\nu} R + \bar{\Lambda} g_{\mu\nu} = 8\pi G_{\rm N} T_{\mu\nu}, \tag{1.1.4}$$

which encode how the dynamics of spacetime responds to the energy and momentum of the matter source given by the energy-momentum tensor

$$T_{\mu\nu} = \frac{2}{\sqrt{-g}} \frac{\delta S_m}{\delta g^{\mu\nu}}. \tag{1.1.5}$$

We adopt the conventions where the (Lorentzian) spacetime metric has signature $(-,+,+,+)$ with Riemann tensor defined by $R^\alpha{}_{\beta\mu\nu} = \partial_\mu \Gamma^\alpha{}_{\nu\beta} + \cdots$ and Ricci tensor defined by $R_{\alpha\beta} = R^\mu{}_{\alpha\mu\beta}$.

The Einstein-Hilbert action is a local and *Diff*-invariant action of the metric field tensor and the

[1] If our manifold were bounded by a closed hypersurface $\partial\mathcal{M}$, we would have to add to the Einstein-Hilbert action the Gibbons-Hawking-York boundary term [10, 11],

$$S_{\rm GHY} = -\frac{1}{8\pi G_{\rm N}} \int_{\partial\mathcal{M}} \mathrm{d}^3x\sqrt{\gamma}\,K, \tag{1.1.2}$$

where this integral is defined on the space-like boundary of a region $\mathcal{M}$ of the spacetime manifold, with γ being the determinant of the induced three-dimensional metric on the boundary and K is the trace of the extrinsic curvature (or second fundamental form).

Einstein field equations can be linearized to describe a unique propagating massless spin-2 field (see, *e.g.*, [13]).

Another formulation of gravity which is classically and kinematically equivalent to GR is the pure Einstein-Cartan theory [14–19]. It is characterized by two fundamental potentials: the vierbein (in four dimensions), $e^a{}_\mu$, associated to translations in the tangent space of the spacetime manifold and the spin-connection, $\omega^{ab}{}_\mu$, associated to local Lorentz transformations (*i.e.*, forming the Poincaré group). The presence of the vierbein ensures the strong equivalence principle: at every point in spacetime, it is always possible to find an orthonormal basis. The corresponding field strengths of the veirbein and spin-connection are the torsion and curvature. The torsion field vanishes outside matter and is non-propagating. In this case, we recover full GR where torsion is zero. Extensions with propagating torsion are straighforward to formulate by gauging the Poincaré group, leading to the Poincaré gauge gravity (see, *e.g.*, [20]). We will discuss in more details the Einstein-Cartan theory in Chapter 4.

There are still other alternative classically equivalent formulations of GR, but which exhibit invariance under a reduced set of transformations. One outstanding example is known as *unimodular gravity* [21–28]. In this symmetry-reduced version of GR, the determinant of the metric is non-dynamical and the cosmological constant is simply an external parameter, only appearing at the level of the equations of motion as an constant of integration. Its value can in principle be fit to the measured value $\Lambda_{\rm obs}$ from cosmological observations, which in some sense can elucidate the long-standing apparent mismatch between the observed cosmological constant and its anticipated value from estimates based on quantum field theory (also known as the *first cosmological constant problem* [29, 30]). The unimodular gravity formulation will be the subject of Chapter 5.

Despite GR being able to describe all current astrophysical phenomema in the weak-gravity regime, the last decade has witnessed exciting observations in the context of strong-field gravity with both indirect and direct probes of black holes, respectively through gravitational waves through the LIGO-Virgo Collaboration [31, 32] and through (supermassive) black hole shadows within the Event Horizon Telescope Collaboration [33–44]. Of course, these observations are very well compatible with GR predictions within quite systematic uncertainties. In this sense, these are not necessarily as precise tests of GR as for instance we have in the weak-field regime.

In Fig. 1.2, we see two ways of thinking about strong versus weak gravity: one of them is through the curvature scale (here represented by the Kretschmann scalar $\xi = (R^{\alpha\beta\mu\nu}R_{\alpha\beta\mu\nu})^{1/2}$) and the other is through the value of the gravitational potential of the system. Indeed, we see that gravity has been tested quite well in the regime where the gravitational potential is relatively low. This is exemplified by various Solar System tests and also by observing how the gravitational field acts on atoms (see, *e.g.*, [45] and references therein). The novelty are tests at high value of the gravitational potential which allow us to probe the strong-field gravity. The shadow images of supermassive black holes in the galactic center of the Messier 87 and the Milky Way and the gravitational waves from black holes and neutron-star binary mergers are the primary examples. With these, we observationally confirm that black holes do exist. Nevertheless, of course, theoretically we know that, if we go really deep into this strong-field regime and deeper into a black hole, at some point we will encounter the breakdown of GR through the

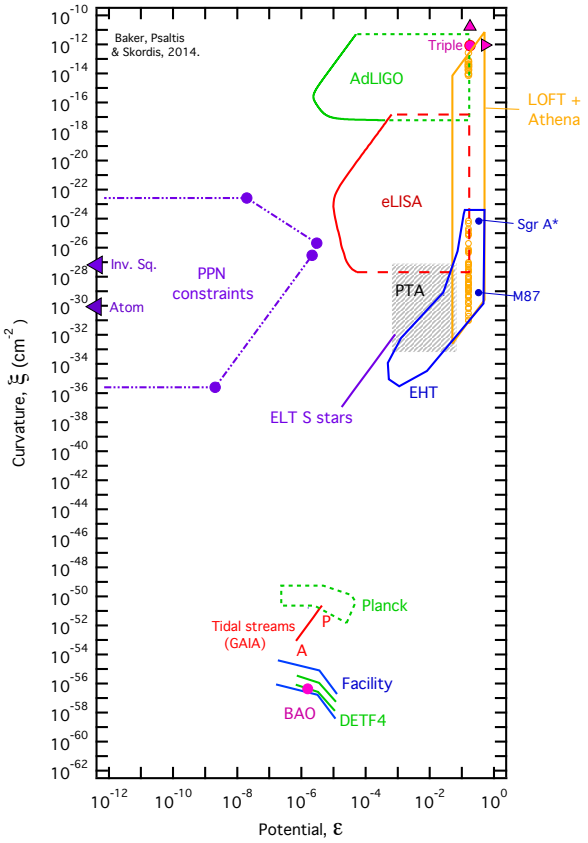

Figure 1.2: A landscape of regions of observational or experimental tests. The horinzontal axis indicates the characteristic gravitational potential of the system and the vertical axis indicates the typical curvature scale (given by the Kretschmann scalar $\xi = (R^{\alpha\beta\mu\nu}R_{\alpha\beta\mu\nu})^{1/2}$) probed by that system. Extracted from [45].

curvature singularity that GR black holes actually have, as dictated by the famous singularity theorems by Hawking and Penrose [46]. In this sense, even though currently the observations are compatible with GR predictions, the objects that we are observing fundamentally may not be black holes from GR.

From the agreement between observations and theory, we can exclude that there is a new physics scale that would predict strong modifications on the order of the curvature radius of a black hole, but we do not have a very clear indication for what scale of new physics is.

Overall, from the status of our understanding of the fundamental building blocks of Nature, we have an understanding that already reaches quite far and the indications that we have for the breakdown of GR and the Standard Model of particle physics is pointing us to new physics only setting in at or beyond the Planck scale, where quantum effects and gravity become important. There are, of course, open question in particle physics (*e.g.*, dark matter and matter-antimatter asymmetry), but there is no theoretical consideration that would uniquely motivate a particular scale of new physics where we would expect new particle physics to come in before the Planck scale. Therefore, this means that, if we want to make progress in understanding the fundamental building blocks of Nature, then the next atitude is to understand the quantum properties of gravity and then its interplay with matter as well.

1.2 Work plan

The present thesis is structured as follows: In Chapter 2, we discuss the general problem of perturbative quantum gravity and present the main ideas for the non-perturbative renormalization of gravity through the embodiment of the asymptotic safety program. Main results in the literature of the field are flashed out and an illustrative example of how to work with the functional Renormalization Group techniques are presented for the computation of the flow of a four-fermion coupling. This example will introduce some of the key concepts to be discussed in Chapter 4. Subsequently, in Chapter 3, we define the dark-matter-gravity models that we explore by introducing field content, interactions and symmetries. We provide an overview of the methodology to calculate beta functions and list the beta functions of our model in Appendix B. We close the chapter by providing the results and discussion of our analysis. In Chapter 4, we present the setup of our investigation in the form a Nambu-Jona-Lasinio system, which will be the center stage for the study of the mechanism of chiral symmetry breaking. We then introduce a flow equation for the effective potential, which we use as a tool to investigate torsion effects on chiral symmetry breaking. We close the chapter by presenting our main result, namely, the impact of a background torsion on the mechanism of chiral symmetry breaking. Technical aspects that are relevant to the computations but not essential for the understanding of the main content of the chapter are relegated to the Appendix C. Finally, in Chapter 5, we begin by giving an overview of classical unimodular gravity and providing a brief discussion of the background-field method, Faddeev-Popov quantization and functional Renormalization Group techniques for unimodular quantum gravity. We also discuss the two classes of polynomial projections of $f(R, R_{\mu\nu}R^{\mu\nu})$ and the extraction of beta functions. Results for the interacting gravitational fixed-point structure both for pure gravity and gravity-matter systems are then presented and discussed. Technical details and expressions for the anomalous dimensions used in this chapter are presented in the Appendix D. Throughout this thesis, we work in natural units $\hbar = c = 1$.

Chapter 2

An Asymptotically Safe View of Quantum Gravity

2.1 The problem of perturbative quantum gravity

A first attempt to approach the problem of quantum gravity perhaps would be by just considering the effects of quantum matter on a curved background. This approach is called the *semiclassical treatment of gravity*. Generally speaking, it can be described by replacing the classical energy-momentum tensor in (1.1.4) by the expectation value of the energy-momentum operator computed with respect to some quantum reference state Ψ,

$$R_{\mu\nu} - \frac{1}{2} g_{\mu\nu} R + \bar{\Lambda} g_{\mu\nu} = 8\pi G_{\mathrm{N}} \langle \Psi | \hat{T}_{\mu\nu} | \Psi \rangle \,. \tag{2.1.1}$$

However, this approach gets hampered by a proper treatment of regularization and renormalization of the right-hand side of (2.1.1). It is not our goal to discuss semiclassical gravity in this thesis any further. Therefore, for more details on its construction and problems, we refer the reader to, for instance, [47]. Instead, we will first pursue to review the construction of a full quantum theory of gravity by using the standard tools of perturbative quantization.

For this goal, our starting point for a quantum field theory of gravity is through the path integral over metric fluctuations for some classical (or microscopic) gravity action,

$$\mathcal{Z} = \int_{\Lambda_{\mathrm{UV}}} \mathcal{D}\hat{g}_{\mu\nu} \, \mathrm{e}^{iS_{\mathrm{grav}}[\hat{g}_{\mu\nu}]}, \tag{2.1.2}$$

where a hat denotes fields to be integrated over and Λ_{UV} denotes an ultraviolet (UV) cutoff in order to make the functional measure well-defined. In this sense, expectation value of any *Diff*-invariant observable $\mathcal{O}[g_{\mu\nu}]$ is computed from the integral over all metrics (modulo diffeomorphism) weighted with a quantum-mechanical phase factor, namely

$$\langle \mathcal{O}[\hat{g}_{\mu\nu}] \rangle = \frac{\int \mathcal{D}\hat{g}_{\mu\nu} \, \mathcal{O}[\hat{g}_{\mu\nu}] \, \mathrm{e}^{iS_{\mathrm{grav}}[\hat{g}_{\mu\nu}]}}{\int \mathcal{D}\hat{g}_{\mu\nu} \, \mathrm{e}^{iS_{\mathrm{grav}}[\hat{g}_{\mu\nu}]}}. \tag{2.1.3}$$

In this sense, field configurations of the metric either interfere destructively and are excluded from the path integral or interfere constructively and give a non-trivial contribution to observables. Our starting point for the perturbative quantization of gravity is the Einstein action,

$$S_{\rm EH} = \frac{1}{16\pi G_{\rm N}} \int {\rm d}^4x\sqrt{-g}\,(R - 2\bar{\Lambda}). \tag{2.1.4}$$

In d dimensions, the Newton coupling $G_{\rm N}$ and the cosmological constant $\bar{\Lambda}$ have canonical mass dimension $[G_{\rm N}] = 2-d$ and $[\bar{\Lambda}] = 2$, respectively. Next step is to perform a linear expansion of the metric around a classical background $\bar{g}_{\mu\nu}$,

$$\hat{g}_{\mu\nu} = \bar{g}_{\mu\nu} + \sqrt{32\pi G_{\rm N}}\,\hat{h}_{\mu\nu}, \tag{2.1.5}$$

where the (perturbatively small) fluctuations $\hat{h}_{\mu\nu}$ characterize the propagating spin-2 field, the massless excitations of which describe the two helicity modes of the *graviton*[1]. In this convention, the fluctuation $\hat{h}_{\mu\nu}$ has canonical mass dimension $[\hat{h}_{\mu\nu}] = 1$. In a perturbative approach, one would proceed by evaluating the classical contribution to an observable and then evaluate the quantum contributions in a loop expansion [48, 49]. Then, at 1-loop, UV divergencies[2] would already appear in the form of following operators

$$\sim \sqrt{-g}, \qquad \sim \sqrt{-g}\bar{R}, \qquad \sim \sqrt{-g}\bar{R}^2, \qquad \sqrt{-g}\bar{R}_{\mu\nu}\bar{R}^{\mu\nu}, \tag{2.1.6}$$

where a bar denotes quantities computed with the background metric. The first divergence is just related to determinant of the metric and it indicates the need to introduce a cosmological constant as a counterterm to the action. Then, there is a divergence that takes exactly the form as the initial action and this means that it can be absorbed in a renormalization of the Newton coupling. Furthermore, there are logarithmic divergencies[3] that have a four-derivative structure. These would indicate the need to introduce new counterterms that were not part of the initial action. However, at the 1-loop level, there is a way around this problem, at least for the pure gravity case without a cosmological constant and without matter. In this case, the classical equations of motion tell us that both $\bar{R}$ and $\bar{R}_{\mu\nu}$ are actually zero, and this means that on shell these two counterterms vanish in that setting[4]. Once matter and a cosmological constant are included, the logarithmic divergencies do not vanish, since in this case the equations of motion provide non-vanishing curvature-squared contributions [49, 53–60]. Nevertheless,

[1] Similarly to the photon in electromagnetism and the gluon in quantum chromodynamics, the quantum particle of the gravity responsible to mediate long-range (self-)interactions is the graviton, a massless bosonic particle.

[2] The 1-loop divergencies in Minkowskian signature can be straightforwardly computed using standard Schwinger-DeWitt method [50–52].

[3] In the first calculations of one 1-loop divergencies in quantum GR by 't Hooft and Veltman [48] for the case with no cosmological constant and then by Christensen and Duff [49] in the presence of the cosmological constant, a dimensional regularization was used. In this case, a logarithmic divergence is replaced by a simple pole $1/\epsilon$, where $\epsilon = 4 - d$.

[4] There is still another four-derivative invariant: $\bar{R}_{\mu\nu\alpha\beta}\bar{R}^{\mu\nu\alpha\beta}$, but this term is not independent from the Ricci scalar and the Ricci tensor. Indeed, they are related via the Gauss-Bonnet term, which reads $\int {\rm d}^4x\sqrt{-\bar{g}}(\bar{R}^2 - 4\bar{R}_{\mu\nu}\bar{R}^{\mu\nu} + \bar{R}_{\mu\nu\alpha\beta}\bar{R}^{\mu\nu\alpha\beta})$ and is a topological invariant in four dimensions, meaning that its variation with respect to the metric vanishes.

as we go to two-loops, there is a new divergence, the so-called Goroff-Sagnotti term [61–64],

$$\sim \sqrt{-g}\bar{R}^{\mu\nu}{}_{\lambda\rho}\bar{R}^{\lambda\rho}{}_{\alpha\beta}\bar{R}^{\alpha\beta}{}_{\mu\nu}, \tag{2.1.7}$$

and which is not of the form of the original action and so a new counterterm has to be introduced[5]. There is also no way to argue that this divergence can be set to zero because even the vacuum field equations do not provide a vanishing Riemann tensor. In fact, we could expect that this pattern to continue based on the superficial degree of divergence in perturbative gravity in a Minkowski background, $\bar{g}_{\mu\nu} = \eta_{\mu\nu}$, at loop order L in 4 dimensions[6], which is given by

$$\mathcal{D}_{\rm GR} = 2L + 2. \tag{2.1.9}$$

So, we expect that, whenever loop order L increases, the superficial degree of divergence of the diagrams goes up and that then ultimately implies that, at every loop order, there are new interactions. In this sense, at every loop order, there will be two more derivatives or another power of curvature tensor that comes into the counterterm that is needed to be introduced. Technically, this is known as **perturbative non-renormalizability**, but what that technical term really means is that the theory loses predictivity. This is because each of the counterterm with a coupling in front of them and that coupling is a free parameter and there is no way to determine it from theoretical considerations. Therefore, an experiment has to be performed in order to measure it and, consequently, the higher the loop order, the more experiments are actually needed in order to pin down the free parameters of the theory. Stated differently, if a prediction is made, for instance, for the scattering amplitude of gravitons at a given loop order, then likely going to next higher loop orders, there would be more counterterms that would contribute to the same observable and that would spoil the prediction, since they would come in with a new parameter that enters the prediction. That is really the problem of perturbative quantum gravity, and it does not, however, mean that GR and quantum physics cannot be reconciled, as one so often hears. Indeed, both formalisms can be reconciled as an effective field theory (EFT) [66].

The principle behind an EFT is naturalness, which basically means that all of the couplings that appear in all of the interactions in the theory can be written as a dimensionless coefficient that is of order one divided by some characteristic mass scale, which for gravity one would choose to be the Planck scale raised to an appropriate power. In the specific case of gravity, *Diff*-invariance dictates that an effective description is given by an expansion in terms of appropriate contractions of curvature

[5] Evanescent effects associated to evanescent operators such as the Gauss-Bonnet term can alter UV divergences as in the Goroff-Sagnotti divergence [65].

[6] Since the graviton propagator (which can be computed after a suitable gauge fixing [13]) and graviton self-interactions scale in the UV as $\sim p^{-2}$ and $\sim p^2$, respetively, then, generically, in d dimensions, a generic diagram containing in quantum GR with L-loops, I-internal propagators and V-vertices feature a momentum scaling of the form

$$\mathcal{I}_{\rm UV} = \int^{\Lambda_{\rm UV}} (\mathrm{d}^d p)^L \frac{1}{(p^2)^I}(p^2)^V \sim \Lambda_{\rm UV}^{d+(L-1)(d-2)}, \tag{2.1.8}$$

which generates a superficial degree of divergence $\mathcal{D}_{\rm GR} = dL - 2(L-1)$ if we make use of the topological relation $I - V = L - 1$.

tensors (symbolically denoted by $\mathcal{R}$) of the form

$$S_{\rm eff}[g] = S_{\rm EH}[g] + \sum_{n>1,m\geq 0} \int \mathrm{d}^4x\sqrt{-g}\,\frac{\alpha_{(n,m)}}{M_{\rm Planck}^{2(n+m)-4}}\nabla^{2m}\mathcal{R}^n, \tag{2.1.10}$$

where $[\alpha_{(n,m)}] = 0$ and $\alpha_{(n,m)} \sim \mathcal{O}(1)$. Within this assumption, higher-order interactions in the theory are subleading for processes that occur at energies $E \ll M_{\rm Planck}$. In this way, it is possible, for instance, to predict or calculate the quantum gravity corrections to the Newtonian potential between two non-relativistic point particles of masses M_1 and M_2 [67]

$$U(r) = -\frac{G_{\rm N}M_1M_2}{r}\left[1 + 3\frac{G_{\rm N}(M_1+M_2)}{rc^2} + \frac{41}{10\pi}\frac{G_{\rm N}\hbar}{r^2c^3} + \cdots\right], \tag{2.1.11}$$

where the first term is the usual Newtonian potential, the second term is the relativistic correction and the third term is the quantum gravity contribution coming from radiative corrections and we have reinstated the factors of $\hbar$ and c. Even though the third term is o genuine quantum nature, its effect is extremely hard to measure at any Earth-based laboratory. Considering even a tiny length scale as the Bohr radius, the third correction term would be of the order of 10^{-49} [68]. the take-home message of EFTs, and in particular in gravity, is that the an effective description is enough to capture and well-describe low-energy phenomena by the relevant degrees of freedom of the system.

It is worth mentioning that it is possible to construct quantum gravity theories that are perturbatively renormalizable at the cost of having to keep higher-order curvature invariants on top of the Einstein-Hilbert action. One famous example is the quadratic gravity action of Stelle [69],

$$S_{\rm Stelle}[g] = S_{\rm EH}[g] + \int \mathrm{d}^4x\sqrt{-g}\,(a\,R^2 + b\,C^2_{\mu\nu\alpha\beta}). \tag{2.1.12}$$

A third term proportional to the Gauss-Bonnet density is omitted due to its topological charater. Here, $C_{\mu\nu\alpha\beta}$ is the Weyl tensor and a and b are dimensionless couplings, rendering the theory renormalizable to all orders in perturbation theory and, under certain conditions, asymptotically free for all its couplings [70–72]. However, its spectrum contains negative norm states, *i.e.*, a massive *ghost*[7], which in principle can violate unitarity of the S-matrix[8] [69, 76, 77] (see also [78–85] for recent proposals to bypass the issue of unitarity violation, [86] for a recent review on quadratic gravity and [87] for settings of higher-order curvature terms.) Remarkably enough, recently, the asymptotically safe behavior that quadratic gravity can exhibit suggested to pursue an analogy with QCD [88–90] (see also [91]). In this analogy, in the trans-Planckian regime, quadratic gravity would be asymptotically safe with gravitons and ghost-like states in its asymptotic spectrum. For energies around the Planck scale, the theory would transition into a strongly-correlated regime. Finally, below the Planck scale, the effective low energy dynamics of the theory would be described by the Einstein-Hilbert action (as the leading-order

[7] Since this ghost comes from higher-derivative terms in the action, it can not be removed from the physical spectrum, in contrast to the Faddeev-Popov ghosts in gauge theories.

[8] At the classical level, higher-derivative terms can generate instabilities in the form of runaway solutions, known as Ostrogradsky instabilities [73, 74]. However, it has been shown recently that classical stable solutions can be computed for the nonlinear gravitational dynamics of quadratic gravity [75].

term), with the ghost-like states being eliminated from the spectrum due to a confinement-like phenomenom (se also [92] for a recent exploration of this analogy in the context of compatibility of light fermions in quantum gravity (see Section 4)).

However, if we want to understand quantum gravity in the most interesting regimes close to and above the Planck scale where quantum gravity effects are no longer small, without running into problems like unitarity violation, the problem then becomes that we truly have to confront the loss of predictivity. In this sense, there is no way around having to confront infinitely many free parameters and having to find a way to get rid of infinitely many of them, so that we can get back to a theory which has just a finite number of free parameters[9]. One may conclude that the problem resides in the deep Uv momentum modes and proceed to avoid a local QFT approach, as in the case of string theory. Alternatively, one pathway to a solution to restore predictivity and which does not necessarily lead to give up on local QFT techniques is to demand that the theory has more symmetry, which is the topic of our next discussion and will lead to the notion of **non-perturbative renormalizability** for quantum gravity.

2.2 Steps beyond perturbation theory: quantum scale symmetry

Imposing a symmetry on an action generically relates couplings to each other or just sets a set of couplings to zero and, thereby, reduces the number of free parameters of the theory. A very simple example is just a real scalar field theory with no internal symmetry. The allowed interactions in this case include all positive powers of the scalar field, parameterized in the form $\sum_i \lambda_i \phi^i$, with possible derivative interactions. If then it is required that an internal $\mathbb{Z}_2$ symmetry ($\phi \mapsto -\phi$) should be respected, then the infinitely number of allowed interactions with zero derivative is cut down by half, *i.e.*, $\sum_i \lambda_{2i} \phi^{2i}$, since now only even powers of the scalar field are allowed. Therefore, we need to think in a somewhat different way about symmetries in order to really restore predictive power to quantum gravity. And the way to do so is not by imposing that there is a symmetry at the classical level[10], as we usually do, but instead considering how a symmetry might emerge at the quantum level, and this will lead us to the idea of **asymptotic safety** and the symmetry that will be of uttermost importance here is **quantum scale symmetry** (see, *e.g.*, [94, 95] for a deep discussion of quantum scale invariance).

Scale symmetry basically states that, once the system is understood at one scale, it is understood at all scales, which means that the couplings of the theory do not change anymore with respect to an (external) energy scale. Just from this simple explanation, we can immediately see why this would be an attractive paradigm for quantum gravity. It would mean that, if we can make sense of quantum gravity, for instance, at the Planck scale, then we immediately understand gravity at higher energies or lower length scales. Thus, the hypothesis that will underpins the asymptotic safety approach for quantum gravity is that the quantum structure of spacetime is described by a theory that is scale-symmetric, but in a very particular fashion, namely by becoming asymptotically safe, which means

[9] In [93], it is shown that, in certain situations, quantum field theories characterized by infinitely many couplings can be studied at high energies perturbatively.

[10] And checking for possible anomalies after a quantization procedure is adopted.

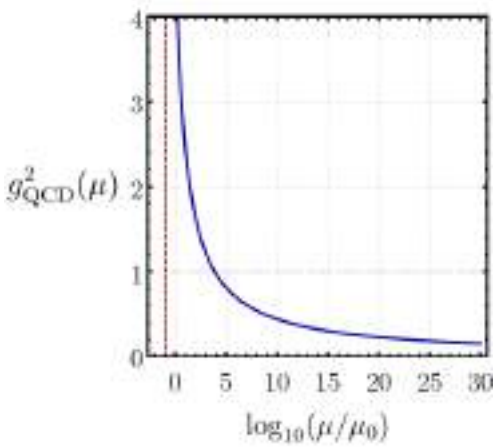

Figure 2.1: RG-running of QCD gauge coupling (in blue) at 1-loop approximation for the fermionic content of the Standard Model. The vertical-dashed line in red represents the Landau pole at the QCD scale $\Lambda_{\mathrm{QCD}} \approx 400$ MeV. We chose the IR initial condition $g^2_{\mathrm{QCD}}(\mu_0) = 1.17$ GeV [97] at the top mass $\mu_0 = 173$ GeV.

that scale symmetry only emerges at the quantum level a conjecture first explored by S. Weinberg [96].

Before we continue, it is worth mentioning that scale symmetry really is also a concept that is ubiquitous in science, making an appearance in mathematics in the context of self-similar systems, or fractals, and also in the context of phase transitions. At a second order or higher order phase transition, the correlation length in the system diverges and the system does not have a particular typical length scale anymore. A typical example is of the Ising model of many spins that can either point up or down. Lastly, scale symmetry is also important in particle physics. For instance, in the strong sector of the Standard Model, the scale dependence of the gauge coupling of quantum chromodynamics (QCD) at 1-loop approximation reads

$$g^2_{\mathrm{QCD}}(\mu) = \frac{g^2_{\mathrm{QCD}}(\mu_0)}{1 + \frac{7}{16\pi^2} g^2_{\mathrm{QCD}}(\mu_0) \log\left(\mu^2/\mu_0^2\right)}, \tag{2.2.1}$$

and asymptotes towards zero as we go to very high energies (cf. Fig. 2.1) for some reference energy scale μ_0 and initial condition $g_{\mathrm{QCD}}(\mu_0)$. Once it reaches zero, it also reaches a regime of scale invariance. Additionally, at low energies, the strong gauge coupling diverges at a Landau pole around the QCD scale Λ_{QCD}.

We are now ready to discuss how Weinberg originally characterized what an asymptotically safe theory is.

2.2.1 Weinberg's formulation of asymptotic safety

Weinberg's original formulation of what an asymptotically safe theory is concentrates on the absence of unphysical divergencies in measurable quantities, such as scattering cross-sections or reaction rates, when the cutoff scale $\Lambda_{\mathrm{UV}} \to \infty$. Observables measured at a characteristic energy scale E will depend on a set of essential[11] couplings g_i and a set of dimensionless kinematical variables X_n such as angles

[11] The nomenclature is due to the existence of inessential couplings ζ_i, which do not enter the expressions for observables and can be removed by a quasi-local field redefinition.

or additional energy ratios. Schematically, any observable quantity $\mathcal{O}$ associated to a physical process then can be written as

$$\mathcal{O} = \mu^{[\mathcal{O}]}\mathcal{F}\left(E/\mu, \tilde{g}_i(\mu), X_n\right), \tag{2.2.2}$$

where $[\mathcal{O}]$ is the total canonical mass dimension of the observable, μ is the renormalization scale and $\tilde{g}_i(\mu) = \mu^{-\Delta_i} g_i(\mu)$ are the dimensionless couplings with Δ_i being their canonical mass dimension. Since any observable should be independent of μ, we are free to choose $\mu = E$, which yields the scaling relation

$$\mathcal{O} = E^{[\mathcal{O}]}\mathcal{F}(1, \tilde{g}_i(E), X_n). \tag{2.2.3}$$

From the last equation it is straightforward to see that the limit $E \to \infty$ only exists if the dimensionless couplings $\tilde{g}_i(\mu)$ are finite as $\mu \to \infty$. If one or a subset of the dimensionless essential couplings diverge at some finite value of the characteristic energy $E = \Lambda_{\mathrm{UV}}$, then is is expected that the observable to also diverge at this energy scale. From the Callan-Symanzik-type RG-flow equations for the dimensionless couplings

$$\mu\frac{d}{d\mu}\tilde{g}_i(\mu) = \beta_i(\tilde{g}_i(\mu)), \tag{2.2.4}$$

we see that, if all the dimensionless couplings reach a UV fixed point, *i.e.*, $\lim_{\mu\to\infty} \tilde{g}_i(\mu) = \tilde{g}_i^*$, then

$$\lim_{E\to\infty} \mathcal{O} = E^{[\mathcal{O}]}\mathcal{F}(1, \tilde{g}_i^*, X_n) \tag{2.2.5}$$

and the theory reaches a quantum scale-invariant regime free from nonphysical UV divergences and we are left with an asymptotically safe theory. The existence of a fixed-point is equivalent to the existence of a root of the beta function of all the dimensionless couplings, *i.e.*, $\beta_i(\tilde{g}_i^*) = 0$, $\forall\, i$. In fact, in order to properly reach a UV scale-invariant regime, the dimensionless essential couplings that parameterize the theory space[12] should lie on a particular trajectory such that they asymptotically reach the fixed point via the renormalization group flow.

2.2.2 The predictive power of RG fixed points

In principle, the essential couplings that parameterize the theory space are infinite-dimensional, since there could an infinite number of operators compatible with the symmetries of theory. Therefore, if the QFT at hand exhibits an interacting UV fixed point $\tilde{g}^* = (\tilde{g}_1^*, \tilde{g}_2^*, \dots)$, one may wonder if it is necessary to provide infinitely many initial conditions to integrate the RG-flow which will produce RG-trajectories that will hit the fixed point. Fortunately, this is not what happens in general. To see

[12] The theory space consists of the space of action functionals, built from the field content of the theory, that are compatible with the symmetries that the system requires. This space can be parameterized then by the couplings of the field monomials.

this, it is instructive to study the linearized flow around the fixed point g^*, *i.e.*,

$$\begin{aligned}\mu\partial_\mu\tilde{g}_i &= \beta_i(\tilde{g}=\tilde{g}^*) + \sum_j \mathbf{M}_{ij}(\tilde{g}^*)(\tilde{g}_j - \tilde{g}_j^*) + \mathcal{O}\left((\tilde{g}-\tilde{g}^*)^2\right) \\ &= 0 + \sum_j \mathbf{M}_{ij}(\tilde{g}^*)(\tilde{g}_j - \tilde{g}_j^*) + \mathcal{O}\left((\tilde{g}-\tilde{g}^*)^2\right),\end{aligned} \tag{2.2.6}$$

for $i = 1, 2, \ldots$ and where we have defined the stability matrix

$$\mathbf{M}_{ij}(\tilde{g}^*) = \left.\frac{\partial\beta_i(\tilde{g})}{\partial\tilde{g}_j}\right|_{\tilde{g}=\tilde{g}^*}. \tag{2.2.7}$$

In terms of the critical exponents θ_l and the eigenvectors $V^{(l)}$, defined by the eigenvalue equation $\sum_j \mathbf{M}_{ij}(\tilde{g}^*)V_j^{(l)} = -\theta_l V_i^{(l)}$, the linearized flow (2.2.6) has a straightforward solution after a suitable diagonalization [13] and reads

$$\tilde{g}_i(\mu) = \tilde{g}_i^* + \sum_{l=1}^{\infty} C_l V_i^{(l)} (\mu/\mu_0)^{-\theta_l}, \qquad i = 1, 2, \ldots. \tag{2.2.8}$$

In this solution, μ_0 is an arbitrary reference scale, C_l denote integration constants, which can be determined by the initial conditions of the coupling $\tilde{g}_i$ at the reference scale μ_0:

$$\tilde{g}_i(\mu_0) = \tilde{g}_i^* + \sum_{l=1}^{\infty} C_l V_i^{(l)}, \qquad i = 1, 2, \ldots. \tag{2.2.9}$$

The apparent lack of predictivity given by the *a priori* infinite set $\{\tilde{g}_i(\mu_0)\}$ can be reconciled if there is a finite number of free parameters. This translates into a decomposition of the critical exponents into a finite set $\{\theta_1, \ldots, \theta_N\}$ such that $\mathrm{Re}(\theta_l) > 0$ and the remaining infinite set $\{\theta_{N+1}, \theta_{N+2}, \ldots\}$ with $\mathrm{Re}(\theta_l) < 0$, then the linearized flow (2.2.8) can be decomposed as

$$\tilde{g}_i(\mu) = \tilde{g}_i^* + \sum_{l=1}^{N} C_l V_i^{(l)} (\mu/\mu_0)^{-\theta_l} + \sum_{m=N+1}^{\infty} C_m V_i^{(m)} (\mu/\mu_0)^{-\theta_m}, \qquad i = 1, 2, \ldots. \tag{2.2.10}$$

Note that, in the UV limit $\mu \to \Lambda_{\mathrm{UV}} \to \infty$, the first terms in the sums vanishes, since $\mathrm{Re}(\theta_l) > 0$, moving the coupling towards the fixed point. Furthermore, at low energies, *i.e.*, $\mu \ll \mu_0$, the constants of integration C_l become important in evaluating the low-energy values of the couplings, being, thus, free parameters. In this case, the eigenvector associated are called **relevant directions** and are UV attractive/IR repulsive. Oppositely, for $\mathrm{Re}(\theta_l) < 0$, the terms in the second sum drives $\tilde{g}_i(\mu)$ away from the fixed point in the UV limit, unless the constants of integration are chosen as $C_l = 0$ for $l \geq N + 1$ and Eq. (2.2.9) turns into

$$\tilde{g}_i(\mu_0) = \tilde{g}_i^* + \sum_{l=1}^{N} C_l V_i^{(l)}, \qquad i = 1, 2, \ldots. \tag{2.2.11}$$

This puts a restriction on the set of allowed initial conditions $\{\tilde{g}_i(\mu_0)\}$. The eigenvector associated to $\mathrm{Re}(\theta_l) < 0$ are called **irrelevant directions** and are UV repulsive/IR attractive. For $\mu \ll \mu_0$, the term (μ/μ_0) shrinks away under the RG-flow, and so the C_l just take some arbitrary value and it will not

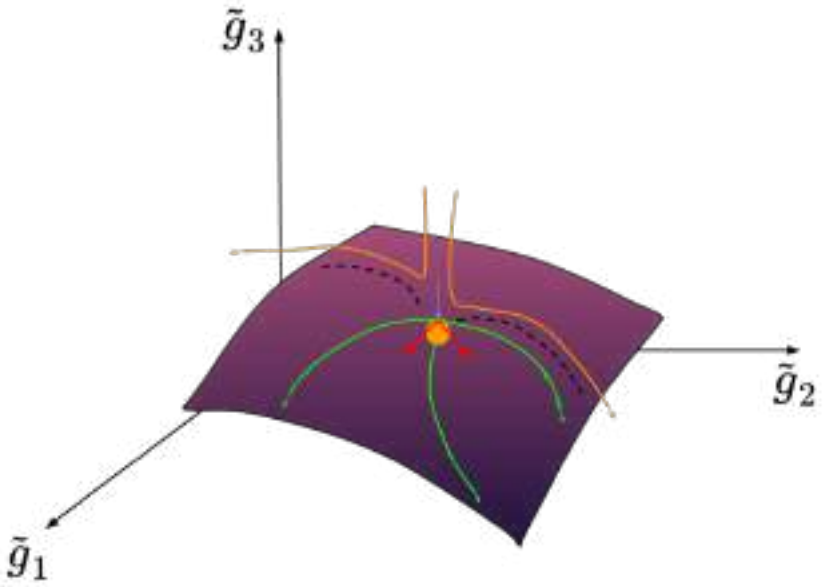

Figure 2.2: Pictorial representation of an interacting UV fixed point (yellow dot) and its associated UV critical hypersurface and it consists out of all the directions in which it is possible to depart from the fixed point. Orthogonal to this hypersurface, there is one irrelevant direction aligned with g_3 (light blue) which is attracted towards the fixed point and quantum fluctuations restore scale symmetry. The arrows point towards the IR.

enter the low-energy values of the couplings and, thus, there is no free parameter. From this point of view, predictivity gets restored as only a finite number of couplings need to be adjusted by experiments, while the remaining ones get predicted (or postdicted) by the RG-flow[13]. The finiteness in the number of relevant directions define in the theory space a hypersurface known as **critical hypersurface**. In Fig. 2.2, we show a schematic plot with an interacting UV fixed point (yellow dot) and its associated UV critical hypersurface. The tangent space of the hypersurface at the fixed point is spanned by the relevant directions which emanates from the fixed point. Moreover, we remark that beta functions are not universal, since they depend on various choices of scheme of calculation, but they do contain universal information which indeed is the same across all schemes and the critical exponents are one example of this [98].

But what actually determines whether a coupling is relevant or irrelevant? To answer this, let us discuss the counting of free parameters at free and interacting fixed points. Focusing first on the free fixed point (also known as Gaussian fixed point (GFP)), for a coupling g_i that is an eigendirection of the stability matrix $\mathbf{M}_{ij}$, the finite contributions to the critical exponent θ_i are given by

$$\theta_i = -\frac{\partial \beta_i}{\partial \tilde{g}_i}\bigg|_{\tilde{g}=0} = -\frac{\partial}{\partial \tilde{g}_i}\left(k\partial_k\left(g_i k^{-\Delta_i}\right)\right)\bigg|_{\tilde{g}=0} = \Delta_i. \tag{2.2.12}$$

[13]There is a third situation that, although rare, it is in principle possible to happen, which corresponds to $\mathrm{Re}(\theta_l) = 0$. In this case, the eigendirections are said to be **marginal** and one needs to go beyond the linearized flow in order to verify if indeed they correspond to a marginally relevant, marginally irrelevant or exactly marginal eigendirection.

This tells us that, whenever the coupling has a positive mass dimension, the associated critical exponent corresponds to a relevant direction or a free parameter. Whenever the coupling has a negative mass dimension, the critical exponent is negative, corresponding to an irrelevant direction and, thus, not a free parameter. The tricky cases are the couplings with vanishing mass dimension, since they can correspond either to a one marginally relevant or marginally irrelevant and one has to evaluate the leading-order term in the beta function beyond this canonical scaling contribution.

The situation is somewhat different at an interacting fixed point (also known as non-Gaussian fixed point (NGFP)), because it is not just the canonical term from canonical dimension that contributes to the critical exponent, but in general there is also a contribution that is linear or higher order in the couplings, *i.e.*,

$$\theta_i = -\frac{\partial \beta_i}{\partial \tilde{g}_i}\bigg|_{\tilde{g}=\tilde{g}^*} = -\frac{\partial}{\partial \tilde{g}_i}\left(k\partial_k\left(g_i k^{-\Delta_i}\right)\right)\bigg|_{\tilde{g}=\tilde{g}^*} = \Delta_i + \mathcal{O}(\tilde{g}_i^*). \tag{2.2.13}$$

Of course, this contribution can be of the same or of a different sign than the canonical mass dimension and, therefore, an interacting fixed point can be more or less predictive than the free fixed point. However, it also means that *a priori* there is no way to know the free parameters that a theory has and one has to do explicit calculations of the beta functions to do a count of the free parameters.

2.2.3 Mechanisms for asymptotic safety

In this subsection, we will briefly discuss the mechanisms for asymptotic safety, which will bring us towards asymptotic safety for gravity as well.

1-loop *versus* 2-loop effects

The first mechanism is when there is a balance between the 1-loop and the 2-loop effects in a perturbative beta function. So, for the beta function (we drop the tilde for dimensionless couplings from now on)

$$\beta_{g_i} = \beta_1 g_i^{\alpha_1} + \beta_2 g_i^{\alpha_2} + \cdots, \tag{2.2.14}$$

where β_1 and β_2 are the 1-loop and 2-loop coefficients respectively and the α's are the corresponding powers. The ellipsis represent higher-order terms. If one is able to achieve asymptotic safety in such a setting, *i.e.*, if the 1-loop term cancels the 2-loop term (or all the higher-order terms beyond this approximation), then the fixed-point value is at

$$g_i^* = \left(\frac{-\beta_1}{\beta_2}\right)^{\frac{1}{\alpha_2-\alpha_1}} \tag{2.2.15}$$

and the fixed point is only real for $\text{sign}(\beta_1) = -\text{sign}(\beta_2)$. A nice example of this scenario is the so-called Litim-Sannino models [99, 100], which consist of (gravity-free) non-Abelian SU(N_c) gauge-Yukawa theories in $d = 4$ with N_f flavors of Dirac fermions in the fundamental representation and

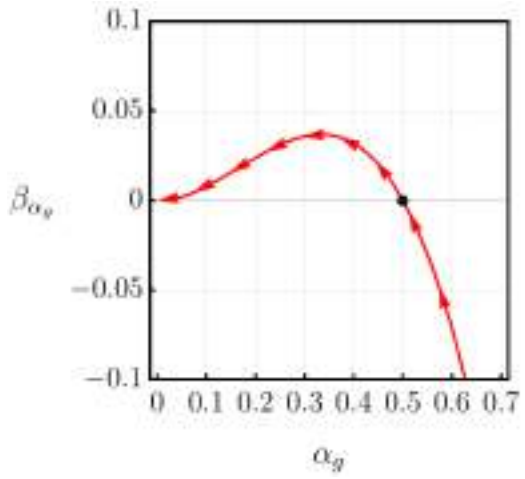

Figure 2.3: Beta function of the Litim-Sannino model with gauge coupling $\alpha_g = \frac{Ncg^2}{(4\pi)^2}$. The fixed point is found at $\alpha_g^* = 0.5$ (black dot) for the specific values $B = -1$ and $C = -2$. The arrows point towards the IR.

gauge coupling $\alpha_g = \frac{N_c g^2}{(4\pi)^2}$. The 2-loop beta function reads

$$\beta_{\alpha_g} = (-B + C\alpha_g)\alpha_g^2 + \mathcal{O}(\alpha_g^4). \tag{2.2.16}$$

In this model, an interacting fixed point is found at $\alpha_g^* = B/C$ for non-vanishing B and C. A related model but with an opposite UV-IR asymptotic behavior is the Banks-Zaks fixed-point in non-Abelian gauge theories [101].

Non-Abelian gauge theories can become asymptotically free if they do not contain too many matter fields in the fundamental representation. However, if we consider a setting with too many matter fields, then the 1-loop coefficient B can actually switch its sign, becoming negative and asymptotic freedom is lost. Asymptotic safety can be gained if the 2-loop coefficient C is also negative, which happens if Yukawa interactions are taken into account appropriately (cf. Fig. 2.3). Actually, asymptotic safety can be strictly proven in the so-called Veneziano limit, where the number of flavors and colors become large, but their ratio remains finite.

Canonical scaling vs quantum effects

There is another mechanism for couplings which have a non-vanishing mass dimension: a balance between the canonical scaling term and the quantum scaling term. Let us consider a theory that is asymptotically free in its critical dimension (the dimension in which the coupling is dimensionless) with the 1-loop beta function

$$\beta_{g_i}\Big|_{d=d_c} = c\beta_1 g_i^{\alpha}, \tag{2.2.17}$$

where $\beta_1 < 0$ and $\alpha = 2, 3$. We assume that we start in this critical dimension. Then, we go to $d = d_c + \epsilon$. The coupling then acquires a mass dimensionality $g_i = \bar{g}_i k^{c\epsilon}$, where $\bar{g}_i$ is dimensionful and $c > 0$. The beta function no longer starts with the 1-loop term, but with the term that depends on the canonical

dimension that the coupling has now acquired, namely

$$\beta_{g_i}\Big|_{d=d_c+\epsilon} = c\epsilon g_i + \beta_1 g_i^{\alpha}. \tag{2.2.18}$$

It is then possible these two terms balance each other out if $\beta_1 < 0$. If that is the case, then the theory has an interacting fixed point. An example for this is Yang-Mills theory in $d = 4 + \epsilon$ [102] and another one is gravity. For gravity, the critical canonical dimension is $d_c = 2$, where the Newton coupling is dimensionless and the theory is trivial, since the Einstein-Hilbert action is topological. The beta function for the dimensionless Newton coupling $G = G_N k^{d-2}$ can be computed in an ϵ-expansion around two dimensions, $d = 2 + \epsilon$ [96, 103, 104] and reads

$$\beta_G = \epsilon G - \frac{38}{3} G^2, \qquad \text{such that} \qquad G^* = \frac{3\epsilon}{38}. \tag{2.2.19}$$

We see that the leading-order term is positive, while the term from quantum fluctuations is negative, which provides asymptotic safety. Of course, it would be nice if we could set $\epsilon = 2$, but for that we would need a few more terms in the ϵ-expansion in order to do a reliable resummation. However, this result in the vicinity of the critical dimension already motivates that gravity in $d = 4$ might be asymptotically safe.

2.3 Non-perturbative renormalization to quantum gravity

The idea of asymptotic safety in gravity can be quite well explored and understood within the non-perturbative Wilsonian renormalization point of view of computing path integrals. In particular, we will adopt the more modern view of the Wilsonian renormalization which is known as the functional Renormalization Group (fRG). The tools of the fRG were applied to quantum gravity in a pioneering work by M. Reuter [105]. Before we delve into the details of functional renormalization for quantum gravity, it is worth mentioning that there are other tools used to probe asymptotic safety in gravity in four dimensions. One of them is lattice simulations in the framework of Euclidean and Causal Dynamical Triangulations (EDT/CDT) [106–112] where the spacetime is approximated by discrete building blocks and one searches for a point in the space of couplings where one can take the lattice spacing to zero[14]. Asymptotic safety actually allows us to take such a continuum limit because it demands a regime where gravity becomes scale invariant. In order for that to be realized, there has to be a second order phase transition in the phase diagram of these models. Indeed, in CDT, there is by now quite good evidence that there is a second order phase transition point [107] (see [111, 112, 114, 115] for recent results in EDT) and the question now becomes whether or not this point can be approached.

However, most of the results for asymptotic safety actually come from fRG techniques[15]. In the next subsections we will begin by defining a quantum-field theoretical formulation of metric gravity and

[14] Evidence for a suitable continuum limit in four dimensions was also obtained within quantum Regge calculus, a slightly different approach from Dynamical Triangulations, see, *e.g.*, [113].

[15] Recently, Dyson-Schwinger equations were also adapted to the context of quantum gravity in [116], opening up an alternative semi-analytical continuum field-theoretic path to probe the existence of a non-trivial fixed point.

shortly after define how to formulate a non-perturbative renormalization for quantum gravity using the fRG toolbox.

A comment is in order here: since, as we will see, the Wilsonian picture of renormalization (and the fRG techniques) will be based on the introduction of the notion of sorting of field modes in the path integral, there should be a notion of external cutoff scale. This can be easily achieved if we work with the Euclidean path integral, because then we can actually sort quantum fluctuations into high energy and low energy, or sort short wavelength and large wavelength, simply by looking at the Fourier modes of the Euclidean four-momentum. This solution comes with its own problem, since a clear definition of Wick-rotation from Lorentzian to Riemannian quantum gravity is still an open matter, as the time coordinate has no physical meaning. Therefore, from here on, we will work in the Euclidean setting (see Appendix A for conventions).

2.3.1 Asymptotic safety of metric gravity: key concepts

The starting point for defining asymptotic safety in gravity is the Euclidean version of the same path integral we started with in perturbation theory[16],

$$\mathcal{Z} = \int_{\Lambda_{\rm UV}} \mathcal{D}\hat{g}_{\mu\nu}\, \mathrm{e}^{-S_{\rm grav}[\hat{g}_{\mu\nu}]}, \tag{2.3.1}$$

but now the (bare) gravitational action is not composed just by the curvature and cosmological constant terms, but also include higher-order terms that are generated along the RG-flow and which are compatible with *Diff*-symmetry, *i.e.*,

$$S_{\rm grav}[\hat{g}_{\mu\nu}] = -\frac{1}{16\pi G_{\rm N}} \int \mathrm{d}^4x\sqrt{\hat{g}}\left(R(\hat{g}) - 2\bar{\Lambda}\right) + \sum_{n>1,m\geq 0} \int \mathrm{d}^4x\sqrt{\hat{g}}\,\alpha_{(n,m)}\nabla^{2m}\mathcal{R}^n, \tag{2.3.2}$$

where, as in the effective-field theoretical approach, $\mathcal{R}$ denotes appropriate contractions of curvature tensors. In the asymptotic safety approach, each one of these couplings depends on the renormalization group scale, which will be denoted by the Wilsonian scale k and will be driven by quantum fluctuations. The idea is that all these couplings assume an asymptotically-safe fixed point in the UV and the theory remains predictive at all scales through the mechanisms that were described.

Contrary to perturbation theory where contributions from quantum fluctuations are included at each loop order and the path integral of the generating functional is computed all at once, the Wilsonian renormalization computes the same path integral, but instead integrating over the field modes by following a momentum-shell-wise integration in flat spacetime. Each momentum shell contains field configurations with four-momentum $p = (p\cdot p)^{1/2}$ which slides in the range $[k-\delta, k+\delta]$ centered around the fiducial coarse-graining scale k and the path integral is completely computed once all field modes are

[16] We note that in the Euclidean version of the path integral the measure is weighted by a Boltzmann factor $\mathrm{e}^{-S_{\rm grav}}$, instead of a quantum phase $\mathrm{e}^{iS_{\rm grav}}$ of the corresponding Lorentzian configuration. This leads ultimately to a statistical field theory of space, instead of a truly quantum theory of spacetime. This has been the main setting for the asymptotic safety program, although recent attempts have been put forward at applying the fRG techniques to Lorentzian settings and at pursuing a Lorentzian formulation of asymptotic safety [117–123].

integrated[17]. At each integration step, the contributions of quantum fluctuations can be equivalently expressed in terms of the quantum effective action. Performing this procedure in a iterative way from $\Lambda_{\rm UV}$ down to zero should be tantamount to evaluating the full path integral at once.

Two immediate obstacles are faced when trying to apply the Wilsonian renormalization idea to gravity. Firstly, the classical gravitational interactions based on general relativity are mediated via the curvature of the spacetime, which implies that the spacetime itself is dynamical and, from a quantum point of view, also a fluctuating entity. In this sense, it serves as both the stage and the protagonist. This is in stark opposition to standard QFT where the flat spacetime is a fixed non-dynamical stage onto which only the quantum matter fields play their part. The dynamical character of the spacetime makes the task of defining a coarse-graining scale k difficult, since one would have to compare a momentum scale with respect to a reference scale that is not fixed, which would raise a lack of a notion of external scale which tells what is coarser or finer. Secondly, the underlying gravitational action is assumed to be *Diff*-invariant. However, this leads to redundancies in the path integral measure, since it sums over physically inequivalent field configurations. The standard way to solve this issue is to introduce a suitable gauge-fixing condition, along with Faddeev-Popov ghost terms. By construction, a gauge-fixing term breaks *Diff*-invariance, so it is expected the RG-flow will generate interaction field monomials which are obviously not gauge-invariant. However, the broken *Diff*-symmetry is recovered [124] by the so-called BRST (Becchi-Rouet-Stora-Tyutin) symmetry [125–127].

An easy way to overcome these challenges is to employ the background-field method [128, 129] (but see [130]), which amounts to splitting the metric field into a non-fluctuating background or reference metric $\bar{g}_{\mu\nu}$ and a (not necessarily small) fluctuation part $h_{\mu\nu} = \langle \hat{h}_{\mu\nu} \rangle$ such that $g_{\mu\nu} = \langle \hat{g}_{\mu\nu} \rangle = \bar{g}_{\mu\kappa} f(\bar{g}, h)^{\kappa}{}_{\nu}$, where f is an arbitrary function. In this thesis, two particular metric parameterizations or splits of the metric will be chosen, namely the linear and the exponential parameterizations, which are respectively defined by

$$g_{\mu\nu} = \bar{g}_{\mu\nu} + \kappa h_{\mu\nu}, \tag{2.3.3}$$

$$g_{\mu\nu} = \bar{g}_{\mu\alpha}[\exp(\kappa\, h^{\cdot}{}_{\cdot})]^{\alpha}{}_{\nu} = \bar{g}_{\mu\nu} + \kappa\, h_{\mu\nu} + \sum_{n=2}^{\infty} \frac{\kappa^n}{n!} h_{\mu\alpha_1} \cdots h^{\alpha_{n-1}}{}_{\nu}, \tag{2.3.4}$$

with $\kappa = (32\pi G_{\rm N})^{1/2}$. The indices are raised and lowered with the background metric, *i.e.*, $h^{\mu}{}_{\nu} = \bar{g}^{\mu\alpha} h_{\alpha\nu}$. Since the exponential of a matrix always possess positive definite eigenvalues, this implies that the signature of $g_{\mu\nu}$ is the same as that of $\bar{g}_{\mu\nu}$, a feature that does not happen for linear parameterization. This feature may be not so important for perturbative studies as they rely on small deviations from the background metric, but may be of relevance in the non-perturbative investigations. Additionally, we should warn that both parameterizations do not necessarily cover the same configuration space and the Jacobian arising from the path integral measure has to be taken into account. We refer the reader to references [124, 129] for a comprehensive discussion on those issues. System-

[17] Here we see explicitly the need of working in an Euclidean setting. If we were to adopt a Lorentzian four-momentum squared, $p^2 = p_0^2 - \vec{p}^2$, then the comparison of high energy ($p^2 > k^2$) and low energy ($p^2 < k^2$) field modes with respect to the coarse-graining scale k would be ill-defined.

atic studies employing more general parameterizations in *Diff*-invariant theories can be found in, e.g., [131–136] for perturbative quantum gravity and in [137–140] in the context of asymptotic safety. For specific calculations in this chapter, we will stick to the linear parameterization.

Having chosen a decomposition for the metric, with a compact background, a background covariant Laplacian is automatically defined, $\Delta_{\bar{g}} = -\bar{g}^{\mu\nu}\bar{\nabla}_\mu\bar{\nabla}_\nu$, where $\bar{\nabla}_\mu$ is computed with the background metric. The background covariant Laplacian acting on a field of spin s, $\Delta_{\bar{g}}\hat{\varphi}_s = \lambda_s\hat{\varphi}_s$, has eigenvalues which can be sorted into high-energy fluctuations ($\lambda_s \gtrsim k^2$) or into low-energy fluctuations ($\lambda_s \lesssim k^2$). Here, $\hat{\varphi}_s$ is a generic multiplet of fluctuation fields of spin s. If the background is chosen to be flat, *i.e.*, $\bar{g}_{\mu\nu} = \delta_{\mu\nu}$, then the eigenvalues will be the four-momentum squared, $\lambda_s = p^2$.

Next we turn to the problem of fixing the redundancies in the path integral measure. We recall that this issue arises due to the non-invariance of the measure under diffeomorphisms, which leads to an over-counting of field configurations. The linear split of the metric allows us to perform the diffeomorphism transformations (1.1.3) in two distinct ways that leave the gravitational action invariant. The first way is the so-called *quantum transformation*, which keeps the background $\bar{g}_{\mu\nu}$ invariant and attributes the gauge transformation of $g_{\mu\nu}$ to the fluctuation field, *i.e.*,

$$\delta_v^{(Q)}\bar{g}_{\mu\nu} = 0, \qquad \delta_v^{(Q)}h_{\mu\nu} = \mathcal{L}_v(\bar{g}_{\mu\nu} + h_{\mu\nu}). \tag{2.3.5}$$

This is somewhat motivated by the fact that observables should be *Diff*-invariant and background-independent. A second way is through a background-induced auxiliary transformation, known as *background transformation*, and consists to evenly split the diffeomorphism transformation between background and fluctuation, namely

$$\delta_v^{(B)}\bar{g}_{\mu\nu} = \mathcal{L}_v\bar{g}_{\mu\nu} = \bar{\nabla}_\mu v_\nu + \bar{\nabla}_\nu v_\mu, \tag{2.3.6}$$

$$\delta_v^{(B)}h_{\mu\nu} = \mathcal{L}_v h_{\mu\nu} = v^\alpha\bar{\nabla}_\alpha h_{\mu\nu} + h_{\alpha\nu}\bar{\nabla}_\mu v^\alpha + h_{\alpha\mu}\bar{\nabla}_\nu v^\alpha. \tag{2.3.7}$$

The quantum diffeomorphism must be broken by the gauge-fixing procedure, but can be recovered through BRST symmetry. Nonetheless, the background diffeomorphism is preserved by using a class of background covariant gauges. Next to that, we follow the usual Faddeev-Popov gauge-fixing procedure[18] and supplement the gravitational action by a gauge-fixing of the form

$$S_{\rm gf}[h,\bar{c},c;\bar{g}] = \frac{1}{2\alpha}\int \mathrm{d}^4x\sqrt{\bar{g}}\,\bar{g}^{\mu\nu}\mathcal{F}_\mu[h;\bar{g}]\mathcal{F}_\nu[h;\bar{g}] + \int \mathrm{d}^4x\sqrt{\bar{g}}\,\bar{c}^\mu\,\mathcal{M}_{\mu\nu}[h;\bar{g}]c^\nu, \tag{2.3.8}$$

where $\bar{c}_\mu$ and c^μ stand for the Faddeev-Popov ghosts. We choose a de-Donder-type linear gauge-fixing function of the form

$$\mathcal{F}_\mu[h;\bar{g}] = \left(\delta^\alpha_\mu\bar{g}^{\nu\beta} - \frac{1+\beta}{4}\delta^\nu_\mu\bar{g}^{\alpha\beta}\right)\bar{\nabla}_\nu h_{\alpha\beta}, \tag{2.3.9}$$

such that the gauge-fixing action is invariant under background transformations. Here α and β are gauge-fixing parameters. For practical calculations the limit $\beta \to \alpha \to 0$ will be used in the thesis. The

[18] We refer the reader to [13] for details on the Faddeev-Popov gauge-fixing procedure in quantum gravity.

Faddeev-Popov operator is computed according to the following relation

$$\begin{aligned}\mathcal{M}_{\mu\nu}[h;\bar{g}]c^{\nu} &= \frac{\delta\mathcal{F}_{\mu}[h;\bar{g}]}{\delta h_{\alpha\beta}}\delta_{c}^{(Q)}h_{\alpha\beta} \\ &= \bar{\nabla}^{\alpha}\left(g_{\mu\nu}\nabla_{\alpha}+g_{\alpha\nu}\nabla_{\mu}\right)c^{\nu}-\frac{1+\beta}{2}\bar{g}^{\alpha\beta}\left(\bar{\nabla}_{\mu}g_{\nu\beta}\nabla_{\alpha}\right)c^{\nu}.\end{aligned} \tag{2.3.10}$$

We note that the ghost part of the gauge-fixing action is linear in the fluctuation field $h_{\mu\nu}$, but contains vertices to all powers of the background metric $\bar{g}_{\mu\nu}$. This entails that gauge-fixing action depends on $\bar{g}_{\mu\nu}$ and $h_{\mu\nu}$ in a independent fashion. As the gauge-fixing action is added to the gravitational action, the full action of the theory does not respect the so-called *split symmetry*,

$$g_{\mu\nu}(\bar{g},h)\mapsto g_{\mu\nu}(\bar{g}+\delta_{\text{split}}\bar{g},h+\delta_{\text{split}}h)=g_{\mu\nu}(\bar{g},h). \tag{2.3.11}$$

This split transformation is tantamount to guaranteeing background independence (see [95, 101, 124] for a discussion in the context of the fRG approach). For the linear split of the metric[19], $g_{\mu\nu}=\bar{g}_{\mu\nu}+h_{\mu\nu}$, the split transformation is given by $\delta_{\text{split}}\bar{g}_{\mu\nu}=-\chi_{\mu\nu}$ and $\delta_{\text{split}}h_{\mu\nu}=\chi_{\mu\nu}$, with $\chi_{\mu\nu}=\chi_{\mu\nu}(x)$ being a local transformation parameter. For the non-linear exponential parameterization, more convenient for unimodular gravity, the explicit form of $\delta_{\text{split}}h_{\mu\nu}$ is not straightforward. In this case, we denote $\delta_{\text{split}}h_{\mu\nu}=\mathcal{N}^{\alpha\beta}_{\mu\nu}[\bar{g},h]\chi_{\alpha\beta}$, and its explicit form can be determined by an iterative procedure (see [141, 142]). At the quantum level, background independence is controlled by a functional Ward-Takahashi identity, called split-Ward identity, and encode the background independence of physical observables. Indeed, if we take the expectation value of a *Diff*-invariant operator with a gauge-fixed gravitational action,

$$\langle\mathcal{O}[\hat{g}_{\mu\nu}]\rangle=\frac{\int\mathcal{D}\hat{\phi}\,\mathrm{e}^{-S_{\text{gf}}[\bar{g},\hat{\phi}]}\,\mathcal{O}[\hat{g}_{\mu\nu}]\,\mathrm{e}^{-S_{\text{grav}}[\hat{g}_{\mu\nu}]}}{\int\mathcal{D}\hat{\phi}\,\mathrm{e}^{-S_{\text{gf}}[\bar{g},\hat{\phi}]}\,\mathrm{e}^{-S_{\text{grav}}[\hat{g}_{\mu\nu}]}}, \tag{2.3.12}$$

where $\hat{\phi}=\left(\hat{h}_{\mu\nu},\hat{c}^{\mu},\hat{\bar{c}}_{\mu},\hat{\phi}_{\text{mat}}\right)$ stands for the fluctuation operator including potential matter fields[20] $\hat{\phi}_{\text{mat}}$, we see that the right-hand side of (2.3.12) should be independent of the background metric, as the left-hand side is. In this way, by taking a $\bar{g}_{\mu\nu}$-derivative of (2.3.12) and subtracting from it the equivalent derivative with respect to $h_{\mu\nu}$, we arrive at

$$\left\langle\mathcal{O}[\hat{g}]\left(\frac{\delta}{\delta\bar{g}_{\mu\nu}}-\frac{\delta}{\delta h_{\mu\nu}}\right)S_{\text{gf}}[\bar{g},\hat{\phi}]\right\rangle=0. \tag{2.3.13}$$

This functional identity, in principle, must be verified when performing the path integral for generating functional of correlation functions. In the context of the fRG, the split symmetry is further violated by the regularization, but we postpone this discussion to Appendix D.5 of Chapter 5, where we discuss the fate of the split symmetry at the level of the effective (average) action.

We have all the ingredients to formulate the path integral of gauge-fixed quantum gravity with

[19] We omit the normalization factor at this point, since it is not relevant for this discussion.

[20] In this case, the gauge-fixing action may contain additional gauge-fixing conditions and Faddeev-Popov ghosts associated to the additional matter fields.

added sources,

$$\mathcal{Z}[\bar{g}, J] = \frac{1}{\mathcal{N}} \int \mathcal{D}\hat{\phi}\, \mathrm{e}^{-S_{\mathrm{grav}}[\bar{g}] - S_{\mathrm{gf}}[\bar{g},\hat{\phi}] + \int \mathrm{d}^4x \sqrt{-\bar{g}} J^a \hat{\phi}_a}, \tag{2.3.14}$$

from which correlation functions can be derived. Here, $J = (J_{\mu\nu}, J_{(c)\mu}, J_{(\bar{c})_\mu}, J_{\mathrm{mat}})$ and $\mathcal{N}$ is a normalization factor. We adopted a uniform notation where the field indices are raised and lowered with the metric γ^{ab}, where a represents Lorentz, gauge group and Dirac indices as well as species of the fields. The metric γ_{ab} is diagonal for bosons φ and symplectic for fermions $\psi, \bar{\psi}$, *i.e.*,

$$(\gamma_\varphi^{ab}) = \mathbb{I}, \qquad (\gamma_\psi^{ab}) = \begin{pmatrix} 0 & 1 \\ -1 & 0 \end{pmatrix}, \tag{2.3.15}$$

with the properties

$$\varphi^a = \gamma^{ab}\phi_b, \qquad \phi_a = \varphi^b \gamma_{ba}, \tag{2.3.16}$$

$$\gamma_b{}^a = \delta^a{}_b, \qquad (\gamma_\varphi)^a{}_b = \delta^a{}_b, \qquad (\gamma_\psi)^a{}_b = -\delta^a{}_b. \tag{2.3.17}$$

With these definitions, the contraction of the supercurrent and superfield reads explicitly

$$J^a \hat{\phi}_a = J^{\mu\nu}\hat{h}_{\mu\nu} + J_{(c),\mu}\hat{c}^\mu - \hat{\bar{c}}_\mu J^\mu_{(\bar{c})} + J_{\mathrm{mat}}\hat{\phi}_{\mathrm{mat}}. \tag{2.3.18}$$

Next, we define the Schwinger functional $\mathcal{W}[\bar{g}, J] = \log \mathcal{Z}[\bar{g}, J]$, which generates all the connected n-point correlation functions of the fluctuation fields of the underlying gravity-matter theory. Explicitly,

$$\frac{\delta^n \log \mathcal{Z}[\bar{g}, J]}{\delta J^{a_1} \cdots \delta J^{a_n}} = \left\langle \hat{\phi}_{a_1} \cdots \hat{\phi}_{a_n} \right\rangle_{\mathrm{conn}}. \tag{2.3.19}$$

We insert a factor $1/\sqrt{\bar{g}}$ in the convention for functional derivatives. Thus, for a tensor A of rank n, we have

$$\frac{\delta A_{\mu_1 \cdots \mu_n}(x)}{\delta A_{\nu_1 \cdots \nu_n}(y)} = \frac{1}{\sqrt{\bar{g}}} \delta(x-y) \delta^{(\nu_1}_{\mu_1} \cdots \delta^{\nu_n)}_{\mu_n}. \tag{2.3.20}$$

For the graviton field, this yields

$$\frac{\delta h_{\mu_1\mu_2}(x)}{\delta h_{\nu_1\nu_2}(y)} = \frac{1}{2\sqrt{\bar{g}}} \delta(x-y) \left(\delta^{\nu_1}_{\mu_1}\delta^{\nu_2}_{\mu_2} + \delta^{\nu_2}_{\mu_1}\delta^{\nu_1}_{\mu_2} \right). \tag{2.3.21}$$

Furthermore, we define the effective action, or the generating functional of 1-particle-irreducible (1PI) diagrams, $\Gamma = \Gamma_{\mathrm{1PI}}$, through the Legendre transform of the Schwinger functional,

$$\Gamma[\bar{g}, \phi] = \int \mathrm{d}^4x \sqrt{\bar{g}}\, J^a \phi_a - \mathcal{W}[\bar{g}, J], \tag{2.3.22}$$

which enables us to write

$$\mathrm{e}^{\Gamma[\bar{g},\phi]} = \frac{1}{\mathcal{N}} \int \mathcal{D}\hat{\phi}\, \mathrm{e}^{-S_{\mathrm{grav}}[\bar{g}] - S_{\mathrm{gf}}[\bar{g},\hat{\phi}] + \int \mathrm{d}^4x \sqrt{-\bar{g}} (\hat{\phi}_a - \phi_a) \frac{\delta\Gamma[\bar{g},J]}{\delta\phi_a}}. \tag{2.3.23}$$

Here, $\phi_a = \langle \hat{\phi}_a \rangle$ and we have used that

$$J^a[\bar{g}, \phi] = (-1)^{s_a} \frac{\delta \Gamma[\bar{g}, J]}{\delta \phi_a}, \tag{2.3.24}$$

with $s_a = 1$ for fermions and $s_a = 0$ for bosons.

2.3.2 Flow equation for gravity-matter systems

The fRG perspective implements the Wilsonian renormalization in a smooth fashion by the introduction of a mode-sorting term in the generating functional which suppresses quantum fluctuations with momentum below k. This can be achieved by augmenting the gravity-matter action with an IR-regulator function $R_k^{ab}[\Delta_{\bar{g}}](x, y)$ in the form of the regulator action

$$\Delta S_k[\bar{g}, \phi] = \frac{1}{2} \int_{\bar{x},\bar{y}} \phi_a(x) R^{ab}[\Delta_{\bar{g}}](x, y) \phi_b(y). \tag{2.3.25}$$

From here on, we use the shorthand notations for volume integrals of the full and background metrics, respectively, $\int_x = \int \mathrm{d}^4x \sqrt{g(x)})$ and $\int_{\bar{x}} = \int \mathrm{d}^4x \sqrt{\bar{g}(x)}$. The regulator matrix is given by

$$(R_k^{ab}) = \begin{pmatrix} R_h & 0 & 0 \\ 0 & 0 & R_c \\ 0 & -R_c & 0 \\ 0 & 0 & R_{\mathrm{mat}} \end{pmatrix}. \tag{2.3.26}$$

Since the regulator $R_k^{ab}[\Delta_{\bar{g}}](x, y)$ is a function of the covariant background Laplacian, it is then ultralocal in position space, *i.e.*, $R_k^{ab}[\Delta_{\bar{g}}](x, y) \propto \delta(x - y)$ and is such that it suppresses the propagation of field modes corresponding to eigenvalues $\lambda_s < k^2$ and allows the free propagation of field modes with eigenvalues $\lambda_s \gtrsim k^2$. By measuring the background covariant Laplacian in cutoff units, $z = \Delta_{\bar{g}}/k^2$, the regulator function $R_k^{ab}[z]$ should meet several requirements. The most important ones are: (i) for $z < 1$, $R_k^{ab}[z] > 0$ and (ii) $\lim_{z\to\infty} R_k^{ab}[z] = 0$. For more details on the properties, we refer the reader to [13].

The regulator action can be straightforwardly introduced in the path integral of the generating functional according to

$$\mathcal{Z}_k[\bar{g}, J] = \exp\left(- \int_{\bar{x},\bar{y}} \frac{\delta}{\delta J^a(x)} R_k^{ab}(x, y) \frac{\delta}{\delta J^b(y)} \right) \mathcal{Z}[\bar{g}, J]. \tag{2.3.27}$$

leading to the IR-regularized generating functional. If the generating functional $\mathcal{Z}[\bar{g}, J]$ is finite, then the IR-regularized generating functional $\mathcal{Z}_k[\bar{g}, J]$ is also finite. The Schwinger functional $\mathcal{W}_k[\bar{g}, J]$ has a flow equation once we take a scale-derivative $k\partial_k$ of (2.3.27), leading to (see, *e.g.*, [143] for details)

$$\partial_t \mathcal{W}_k[\bar{g}, J] = -\frac{1}{2} \mathrm{Tr} \left(\frac{\delta^2 \mathcal{W}_k}{\delta J^2} + \frac{\delta \mathcal{W}_k}{\delta J} \frac{\delta \mathcal{W}_k}{\delta J} \right) \partial R_k, \tag{2.3.28}$$

where all indices are omitted for simplicity and we have defined the RG-time $t = \ln(k/k_0)$, with k_0 being some fixed reference scale, so that $\partial_t = k\partial_k$. The trace contains a sum over Lorentz, position space and internal indices as well as possible species of fields, including the symplectic metric for fermionic fields. We note that the first term in the parenthesis is the connected part of the regularized two-point correlation functions, *i.e.*,

$$\frac{\delta^2 \mathcal{W}_k[\bar{g},\phi]}{\delta J(x)\delta J(y)} = G_k[\bar{g},\phi](x,y) = \left\langle \hat{\phi}(x)\hat{\phi}(y)\right\rangle - \phi(x)\phi(y), \tag{2.3.29}$$

and the second term is just the disconnected contribution, ϕ^2. The primary tool in fRG studies is the coarse-grained effective action, or effective average action (EAA), or simply flowing action, $\Gamma_k[\bar{g},\phi]$, which is given by the *modified* Legendre transform of the Schwinger functional,

$$\Gamma_k[\bar{g},\phi] = \int_{\bar{x}} J^a\phi_a - \mathcal{W}_k[\bar{g},J] - \frac{1}{2}\int_{\bar{x}} \phi_a R_k^{ab}\phi^b, \tag{2.3.30}$$

where the solution of the supercurrent is given by (2.3.24). The definition of the EAA is such that it reduces to the standard (1PI) effective action for $k = 0$ and provides the quantum equations of motion, at vanishing currents, for the expectation values of the quantum fields, *i.e.*, $\delta\Gamma_{1\text{PI}}[\bar{g},\phi]/\delta\phi = 0$. In terms of the EAA, the regulator function has the generic structure

$$R_k^{ab}[z] = \left(\Gamma_k^{(0,2)}[\bar{g},\phi]\right)^{ab} r_k(z), \tag{2.3.31}$$

where we have defined the shorthand notation for mixed functional derivatives (recall that a factor $1/\sqrt{\bar{g}}$ is included)

$$\Gamma_k^{(n,m)}[\bar{g},\phi] = \frac{\delta^{n+m}\Gamma_k[\bar{g},\phi]}{\delta\bar{g}^n\delta\phi^m} \tag{2.3.32}$$

and $r_k(z)$ is the regulator shape function. In this thesis, we will adopt the Litim and exponential shape functions, defined respectively by

$$r_k(z)\big|_{\text{Litim}} = \left(\frac{1}{z^\alpha} - 1\right)\theta(1-z)\,, \tag{2.3.33}$$

$$r_k(z)\big|_{\text{exp}} = \frac{z}{e^z - 1}\,, \tag{2.3.34}$$

with $\alpha = 1$ for bosonic fields and $\alpha = 1/2$ for spinor fields. From the flow equation for the Schwinger functional (2.3.28) and using that $\dfrac{\delta^2\mathcal{W}_k}{\delta J^2} = \left(\Gamma_k^{(0,2)} + R_k\right)^{-1}$, it is straighforward to derive the corresponding flow equation for the flowing action $\Gamma_k[\bar{g},\phi]$,

$$\partial_t\Gamma_k[\bar{g},\phi] = \frac{1}{2}\text{STr}\, G_k[\bar{g},\phi]\,\partial_t R_k = \frac{1}{2}$$ 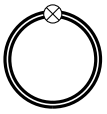 , (2.3.35)

where $G_k[\bar{g},\phi]$ is the full regularized propagator

$$G_k[\bar{g},\phi] = \frac{1}{\Gamma_k^{(0,2)}[\bar{g},\phi] + R_k}. \tag{2.3.36}$$

The notation STr for the supertrace is adopted to emphasize that the trace is over all indices and spacetime coordinates with appropriate sign/multiplicities in the case of complex/fermionic fields. The double line notation represents the full regularized propagators of the theory and the crossed circle in the loop stands for the regulator insertion $\partial_t R_k$. We emphasize that loop representation is not a perturbative loop as it relies on the *full* propagators (not the tree-level ones). The flow equation for $\Gamma_k[\bar{g},\phi]$ is also known as the Wetterich(-Ellwanger-Morris) equation [144–146].

Seen as a function of the coarse-graining scale, the flowing action interpolates between the microscopic (bare) action $\Gamma_{k\to\Lambda_{\rm UV}}$ when no quantum fluctuations are taken into account[21], and the 1PI effective action, $\Gamma_{\rm 1PI} = \Gamma_{k\to 0}$ when all quantum fluctuations are integrated out. The standard 1-loop expression for the effective action can be recovered if we substitute $\Gamma_k^{(0,2)}$ by the scale-independent second functional derivative of the classical action $S^{(0,2)}$ and perform the integration over the coarse-graining scale k from $k = \Lambda_{\rm UV}$ down to $k = 0$. This yields

$$\Gamma_{\rm 1PI}\big|_{\rm 1-loop}[\bar{g},\phi] \approx S_{\rm UV}[\bar{g},\phi] + \frac{1}{2}{\rm STr}\ln S^{(0,2)}[\bar{g},\phi], \tag{2.3.37}$$

with

$$S_{\rm UV}[\bar{g},\phi] = S[\bar{g},\phi] - \frac{1}{2}{\rm STr}\ln\left(S^{(0,2)}[\bar{g},\phi] + R_{\Lambda_{\rm UV}}\right). \tag{2.3.38}$$

The second term on (2.3.37) refers to the UV boundary condition for the RG flow.

In general, we can write the flowing action for a given field content Φ just as a sum of all possible interactions $\{\mathcal{O}^i\}$ in the theory in the form

$$\Gamma_k = \sum_i k^{-\Delta_i} g_i(k) \int {\rm d}^d x\, \mathcal{O}_i(\Phi,\nabla), \tag{2.3.39}$$

and the size of the interactions is parameterized by the dimensionless couplings $g_i(k)$ that carry the scale dependence. Here, Δ_i represents the canonical mass dimension of the operator $\mathcal{O}_i$. The operators $\mathcal{O}_i(\Phi,\nabla)$ are functions of the covariant derivative acting on the field Φ. In the case of gravity, the field content is composed of (Euclidean) spacetime metrics $g_{\mu\nu}$ and, for the Einstein-Hilbert action, the possible interactions are

$$\mathcal{O}_1(g) = \sqrt{g}, \qquad \mathcal{O}_2(g,\nabla) = \sqrt{g}R\,. \tag{2.3.40}$$

From the scale-derivative ∂_t of the flowing action, we get the RG beta functions, *i.e.*,

$$\partial_t\Gamma_k = \sum_i k^{-\Delta_i}(\partial_t g_i - \Delta_i g_i(k)) \int {\rm d}^d x\, \mathcal{O}_i(\Phi,\nabla). \tag{2.3.41}$$

The explicit expressions for the beta functions can thus be obtained by projecting the result from the flow equation into a functional space that contains only the operators that were already included in

[21] The problem of obtaining the microscopic action from the limit $\Gamma_{k\to\Lambda_{\rm UV}}$ is not so trivial and is known as the *reconstruction problem* [147–149].

the original truncation, *i.e.*,

$$\frac{1}{2}\mathrm{STr}\, G_k[\Phi]\, \partial_t R_k = \sum_i k^{-\Delta_i} \mathcal{B}_i(g(k)) \int \mathrm{d}^d x\, \mathcal{O}_i(\Phi, \nabla), \tag{2.3.42}$$

where the coefficients $\mathcal{B}_i(g(k))$ represents the quantum corrections. The matching of coefficients (2.3.41) with (2.3.42) yields the system of RG-flow equations

$$\partial_t g_i(k) = \Delta_i g_i(k) + \mathcal{B}_i(g(k)). \tag{2.3.43}$$

The key aspect about the method relying on the flow equation is that is provides a formally exact equation. However, it generates a tower of coupled equations for the beta functions of the different couplings. Since there are infinitely many couplings in the theory, it is an infinite tower, which in general is not something that one can actually meaningfully derive. Then, one has to resort to approximations, and thus the method loses its exactness. So, the strategy is to take into account only a finite set of equations or a finite set of interactions (or an infinite set of interactions, but of a very particular form). In such a truncation, one then searches for fixed-point solution. If one solution is found, the truncation is then enlarged, and step by step the results need to be checked for convergence or apparent convergence. If the results show apparent convergence, then the approximation can be trusted. Many successful examples of the application of this method and strategy in particle physics, statistical physics and condensed matter can be found in this recent review [150]. Additional systematic expansions of the flowing action may be employed in order to further reduce the level of complexity, leading to more practical or realizable truncations (see, *e.g.*, [124, 151, 152]).

2.3.3 Different flavors of running couplings

It is important to pause a bit to make some remarks about semantics. Throughout this chapter, the term "running coupling" has been used quite extensively to mean the change of a coupling according to an external energy scale. However, more fundamentally, there are three different notions of running couplings and the corresponding RG. We will follow closely the references [95, 153] for this discussion.

When particle physicists talk about running couplings, they define the coupling in terms of some scattering amplitude in some particular kinematical configuration characterized by a momentum scale $p = (p \cdot p)^{1/2}$. Once this scale is fixed to a particular renormalization scale, $p = \mu_R$, then what can be called **physical running** is the dependence of the coupling on μ_R. On the other hand, in perturbation theory, a parameter μ needs to be introduced in order to preserve dimensions, either in dimensional regularization (μ^{4-d}) or in cutoff regularization ($\log\left(\Lambda^2/\mu^2\right)$). The dependence of the coupling on this parameter can be called **μ-running**, and defines a less physical notion as the previous one, since it does not appear in the expressions of physical observables. The corresponding RG-flow equations can be computed by acting with a $\mu\frac{\partial}{\partial\mu}$ derivative on the coupling, or equivalently, with a $\Lambda\frac{\partial}{\partial\Lambda}$ derivative in cutoff regularization. Finally, in a non-perturbative context, one can define a RG as the dependence of the couplings in the effective action on some cutoff, which can be an UV cutoff in Wilson's definition

or an IR cutoff in fRG. This last notion can be dubbed **non-perturbative running**. These three notions of RG are different and it is important to see if and when they give the same results.

This question has been addressed in the literature (see, *e.g.*, [95, 154] for critical discussions and [153, 155] for more recent accounts), and we have a clearer understanding, although not fully complete, about the relation between these three notions.

One important difference between beta functions computed with the FRG in comparison with perturbative renormalization group schemes (*e.g.*, $\overline{\text{MS}}$-scheme) is that the structure $(\Gamma_k[\bar{g},\phi]+R_k)^{-1}$ in the flow equation (2.3.35) generically produces threshold contributions of the form $(1+\text{mass}^2)^{-\#}$, with $\#$ a positive number, when one integrates over massive fields. Such threshold effects automatically account for the decoupling of massive fields at RG scales below their mass scale. This is a significant contrast with perturbative schemes where the decoupling needs to be implemented "by hand".

At energies scales higher than the mass threshold of all masses, the leading- and the next-to-leading-order contributions to the perturbative beta functions can also be computed from the non-perturbative fRG-beta functions. The 1-loop contribution for the non-perturbative beta functions are straightforwardly obtained from (2.3.37). The 2-loop contributions are discussed in [156–162].

Finally, the physical running of couplings may be only defined in asymptotic regions and the non-perturbative running agrees in these regions. Indeed, this has been recently verified in [153] for a higher-derivative shift-invariant scalar toy-model of the type

$$\mathcal{L}=-\frac{Z_1}{2}\partial_\mu\phi\partial^\mu\phi-\frac{Z_1}{2m^2}-\frac{Z_1^2 g}{4m^4}(\partial_\mu\phi\partial^\mu)(\partial_\mu\phi\partial^\mu), \tag{2.3.44}$$

where Z_1 is the wave-function renormalization factor and m a mass. This model serves as a prototype of higher-derivative gravity theories. In this model, the effective-field theoretical physical beta functions for the higher-derivative coupling was seen to be zero, but the μ-beta function and fRG-beta function were non-vanishing. However, low-energy expansion in the fRG-beta function goes like $\beta_g\sim g^2k^4$, which indeed goes to zero in the limit $k\to 0$. Therefore, this quartic running can be thought of as being part of the threshold behavior. Whether the agreement between physical running and non-perturbative running in asymptotic regions is a general feature or not remains to be answered.

2.3.4 Illustrative example: RG-flow of a four-fermion interaction

As an illustrative example of how to work with the flow equation, we consider a purely fermionic massless system with only one fermion species ($N_{\text{F}}=1$) in $d=4$ Euclidean spacetime, characterized by a Nambu-Jona-Lasinio-type model, which shares many features of the strong interactions such as spontaneous symmetry breaking (see [163] for a review). This model is an effective theory that can be obtained from the one-flavor QCD dynamics after integrating out the gluonic degrees of freedom. We consider a zero-temperature setting (see, *e.g.*. [164, 165] and [166] for a review on the fRG-treatment of the finite temperature case). This example will also serve to introduce the main aspects of dynamical symmetry breaking in four-fermion models to be discussed in Chapter 4 in the context of gravitational catalysis.

Our truncation for the flowing action is composed of a scalar and pseudo-scalar interaction channels of the form

$$\Gamma_{k,\mathrm{NJL}}[\bar{\psi},\psi] = \int \mathrm{d}^4x \left\{ Z_\psi \bar{\psi} i\partial\!\!\!/ \psi + \frac{1}{2} Z_\psi^2 \bar{\lambda} \left[\left(\bar{\psi}\psi\right)^2 - \left(\bar{\psi}\gamma_5\psi\right) \right] \right\}, \tag{2.3.45}$$

where $\bar{\lambda}$ is the dimensionful four-fermion coupling and $Z_\psi(k)$ is the fermionic renormalization factor. The fermionic quartic self-coupling $\bar{\lambda}$ has canonical mass dimension $[\bar{\lambda}] = 2 - d$, which means that the theory is perturbatively non-renormalizable in four dimensions and we will define it with a fixed UV cutoff Λ_{UV}. The action (2.3.45) is invariant under phase transformations

$$\psi(x) \mapsto \mathrm{e}^{i\alpha}\psi(x), \qquad \bar{\psi}(x) \mapsto \bar{\psi}(x)\mathrm{e}^{-i\alpha}, \tag{2.3.46}$$

and under chiral U(1) transformations or axial transformations

$$\psi(x) \mapsto \mathrm{e}^{i\gamma_5\alpha}\psi(x), \qquad \bar{\psi}(x) \mapsto \bar{\psi}(x)\mathrm{e}^{i\gamma_5\alpha}, \tag{2.3.47}$$

with α being a real constant parameter. The chiral transformation prohibits an explicit mass term in the action, such as $m\bar{\psi}\psi$. As we will see, chiral symmetry can be spontaneously broken by quantum fluctuations, generating a finite fermionic condensate $\langle\bar{\psi}\psi\rangle$ in the ground state of the theory. This represents a dynamical generation of a mass term for the fermion, which would correspond to a constituent quark mass in low-energy QCD. The connection between the chiral symmetry breaking induced by quantum fluctuations and the strength of the quartic self-coupling can be mapped into mass terms for bound states through a Hubbard-Stratonobitch transformation [167, 168], which amounts to introducing an auxiliary scalar field in the theory. Schematically, this mapping reads $\bar{\lambda}(\bar{\psi}\psi) \mapsto \frac{1}{\bar{\lambda}}\phi^2 + \phi\bar{\psi}\psi$. Spontaneous chiral symmetry breaking is then signalled by a **diverging** four-fermion coupling where the mass term transitions from positive to negative values.

In momentum space, the effective action is given by

$$\begin{aligned}\Gamma_{k,\mathrm{NJL}}[\bar{\psi},\psi] = &- \int \frac{\mathrm{d}^4p}{(2\pi)^4} Z_\psi \bar{\psi}(p) p\!\!\!/ \psi(p) \\ &+ \frac{1}{2} Z_\psi^2 \bar{\lambda} \left(\prod_{i=1}^{3} \int \frac{\mathrm{d}^4p_i}{(2\pi)^4} \right) \bar{\psi}(p_1)\psi(p_2)\bar{\psi}(p_3)\psi(p_1 - p_2 + p_3) \\ &- \frac{1}{2} Z_\psi^2 \bar{\lambda} \left(\prod_{i=1}^{3} \int \frac{\mathrm{d}^4p_i}{(2\pi)^4} \right) \bar{\psi}(p_1)\gamma_5\psi(p_2)\bar{\psi}(p_3)\gamma_5\psi(p_1 - p_2 + p_3).\end{aligned} \tag{2.3.48}$$

Next, we need to compute the second functional derivatives of the flowing action with respect to the fields

$$\Phi(q) \equiv \begin{pmatrix} \psi(q) \\ \bar{\psi}^{\mathrm{T}}(-q) \end{pmatrix} \qquad \text{and} \qquad \Phi^{\mathrm{T}}(-q) = \left(\psi^{\mathrm{T}}(-q),\, \bar{\psi}(q)\right)^{\mathrm{T}}, \tag{2.3.49}$$

and evaluate it, for simplicity, for mean-field (constant) backgrounds $\bar{\Psi}$ and Ψ such that $\psi(p) =$

$\Psi(2\pi)^4\delta^{(4)}(p)$ and $\bar{\psi}(p) = \bar{\Psi}(2\pi)^4\delta^{(4)}(p)$. In this way, the so-called Hessian matrix is written as

$$\Gamma^{(2)}_{k,\mathrm{NJL}} = \frac{\delta^2\Gamma_{k,\mathrm{NJL}}}{\delta\Phi^{\mathrm{T}}(-p)\delta\Phi(p)} = \begin{pmatrix} \frac{\delta^2\Gamma_{k,\mathrm{NJL}}}{\delta\psi^{\mathrm{T}}(-p)\delta\psi(p)} & \frac{\delta^2\Gamma_{k,\mathrm{NJL}}}{\delta\psi^{\mathrm{T}}(-p)\delta\bar{\psi}^{\mathrm{T}}(-p)} \\ \frac{\delta^2\Gamma_{k,\mathrm{NJL}}}{\delta\bar{\psi}(p)\delta\psi(p)} & \frac{\delta^2\Gamma_{k,\mathrm{NJL}}}{\delta\bar{\psi}(p)\delta\bar{\psi}^{\mathrm{T}}(-p)} \end{pmatrix}. \tag{2.3.50}$$

In order to compute the flow of the four-fermion coupling, we can make use the so-called $\mathcal{PF}$-expansion [169]. In this approach, the inverse regularized propagator can be decomposed into an inverse regularized propagator matrix $\mathcal{P}_k = \Gamma^{(2)}_{k,\mathrm{NJL}}[\bar{\Psi} = 0 = \Psi] + \mathbf{R}_k$, which is field-independent, and a field-dependent fluctuation matrix $\mathcal{F}_k = \Gamma^{(2)}_{k,\mathrm{NJL}}[\bar{\Psi}, \Psi] - \Gamma^{(2)}_{k,\mathrm{NJL}}[\bar{\Psi} = 0 = \Psi]$, such that $\Gamma^{(2)}_{k,\mathrm{NJL}} + \mathbf{R}_k = \mathcal{P}_k + \mathcal{F}_k$. Adopting the following profile for the regulator matrix,

$$\mathbf{R}_k(p,p') = \begin{pmatrix} 0 & -Z_\psi \not{p}^{\mathrm{T}} r_\psi(\frac{p^2}{k^2}) \\ -Z_\psi \not{p} r_\psi(\frac{p^2}{k^2}) & 0 \end{pmatrix} (2\pi)^4\delta^{(4)}(p-p'), \tag{2.3.51}$$

where $r_\psi(p^2/k^2)$ is the fermionic shape function[22], there follow

$$\mathcal{P}_k(p,p') = \frac{\delta^2\Gamma_{k,\mathrm{NJL}}}{\delta\Phi^{\mathrm{T}}(p)\delta\Phi(p')} + \mathbf{R}_k(p,p') = \begin{pmatrix} 0 & -Z_\psi \not{p}^{\mathrm{T}}(1+r_\psi) \\ -Z_\psi \not{p}(1+r_\psi) & 0 \end{pmatrix} (2\pi)^4\delta^{(4)}(p-p') \tag{2.3.52}$$

and

$$\mathcal{F}_k(p,p') = \begin{pmatrix} \mathcal{F}_{11} & \mathcal{F}_{12} \\ \mathcal{F}_{21} & \mathcal{F}_{22} \end{pmatrix} (2\pi)^4\delta^{(4)}(p-p'). \tag{2.3.53}$$

where, respectively,

$$\begin{aligned} &\mathcal{F}_{11} = -\bar{\lambda}Z_\psi^2\left(\bar{\Psi}^{\mathrm{T}}\bar{\Psi} - \gamma_5\bar{\Psi}^{\mathrm{T}}\bar{\Psi}\gamma_5\right), \qquad \mathcal{F}_{12} = -\bar{\lambda}Z_\psi^2\left(\bar{\Psi}\Psi - \gamma_5(\bar{\Psi}\gamma_5\Psi) + \Psi\bar{\Psi} - \gamma_5\Psi\bar{\Psi}\gamma_5\right)^{\mathrm{T}} \\ &\mathcal{F}_{21} = -\mathcal{F}_{12}^{\mathrm{T}}, \quad \mathcal{F}_{22} = -\bar{\lambda}Z_\psi^2\left(\Psi\Psi^{\mathrm{T}} - \gamma_5\Psi\Psi^{\mathrm{T}}\gamma_5\right) \end{aligned} \tag{2.3.54}$$

The flow equation for fermions (with minus sign) can then be expanded in powers of the fields, ultimately representing a sum of 1-loop diagrams. The decomposition reads

$$\begin{aligned} \partial_t\Gamma_{k,\mathrm{NJL}} &= -\frac{1}{2}\mathrm{Tr}\frac{\partial_t\mathbf{R}_k}{\Gamma^{(2)}_{k,\mathrm{NJL}} + \mathbf{R}_k} \\ &= -\frac{1}{2}\mathrm{Tr}\tilde{\partial}_t \ln\left[\Gamma^{(2)}_{k,\mathrm{NJL}} + \mathbf{R}_k\right] \\ &= -\frac{1}{2}\mathrm{Tr}\tilde{\partial}_t \ln\left[\mathcal{P}_k + \mathcal{F}_k\right] \\ &= -\frac{1}{2}\mathrm{Tr}\tilde{\partial}_t \ln\mathcal{P}_k - \frac{1}{2}\sum_{n=1}^{\infty}\frac{(-1)^{n-1}}{n}\mathrm{Tr}\tilde{\partial}_t\left(\mathcal{P}_k^{-1}\mathcal{F}_k\right)^n, \end{aligned} \tag{2.3.55}$$

where we have introduced the formal scale-derivative $\tilde{\partial}_t$ which acts only on the k-dependence of the regulator function R_k, and not on $\Gamma^{(2)}_{k,\mathrm{NJL}}$ *i.e.*, formally $\tilde{\partial}_t = \int_q \partial_t R_k(q^2)\frac{\delta}{\delta R_k(q^2)}$. This expansion simply is an expansion with an increasing number of vertices of the theory. Here, $\mathcal{F}_k$ is quadratic in the Dirac

[22] At this stage, there is no need to specify the form of the regulator shape function.

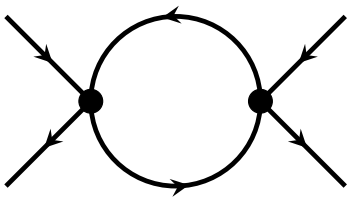

Figure 2.4: Diagram contributing to the running of the four-fermion coupling. The right-hand side of the flow equation is ultimately computed by acting with the formal scale-derivative $\tilde{\partial}_t$ on this diagram, which yields a corresponding regulator insertion $k\partial_k R_k$ on the internal propagators.

fields. Since we are interested in the RG-flow of the four-fermion coupling, it suffices to truncate the series and consider only the term $\mathrm{Tr}\left(\mathcal{P}_k^{-1}\mathcal{F}_k\right)^2$ as it is of fourth-order in the fields, *i.e.*, $\mathrm{Tr}\left(\mathcal{P}_k^{-1}\mathcal{F}_k\right)^2 \sim (\bar{\Psi}\Gamma_i\Psi)^2$, where Γ_i stands for some Dirac matrix or combination thereof. The first term is simply a vacuum contribution. The diagram contributing to the RG-flow of $\bar{\lambda}$ is displayed in Fig. 2.4. Explicitly,

$$\partial_t\Gamma_{k,\mathrm{NJL}}\big|_{(\bar{\Psi}\Gamma_i\Psi)^2} = \frac{1}{2}\mathrm{Tr}\tilde{\partial}_t\left(\mathcal{P}_{12}^{-1}\mathcal{F}_{22}\mathcal{P}_{21}^{-1}\mathcal{F}_{11}\right) + \frac{1}{2}\mathrm{Tr}\tilde{\partial}_t\left(\mathcal{P}_{12}^{-1}\mathcal{F}_{21}\mathcal{P}_{12}^{-1}\mathcal{F}_{21}\right), \tag{2.3.56}$$

where $\mathcal{P}_{ij}^{-1}$ and $\mathcal{F}_{ij}$ are the components of the regularized propagator and fluctuations matrices, respectively. The first term provides a vector-channel contribution of the form $(\bar{\Psi}\not{p}\Psi)^2$ and mixed-terms of the form $p^2\gamma_5(\bar{\Psi}\Psi)(\bar{\Psi}\gamma_5\Psi)$, which are terms generated along the flow, but they are not included in the original truncation of the flowing action. Therefore, they will be discarded. The second term provides non-trivial contributions which are part of the original truncation and reads

$$\begin{aligned}\frac{1}{2}\mathrm{Tr}\tilde{\partial}_t\left(\mathcal{P}_{12}^{-1}\mathcal{F}_{21}\mathcal{P}_{12}^{-1}\mathcal{F}_{21}\right) &= \frac{1}{2}\bar{\lambda}^2\int \mathrm{d}^4x\int\frac{\mathrm{d}^4p}{(2\pi)^4}\tilde{\partial}_t\frac{Z_\psi^2(1+r_\psi)^2}{\left[p^2(1+r_\psi)^2\right]^2}p^2\left[(\bar{\Psi}\Psi)^2-(\bar{\Psi}\gamma_5\Psi)^2\right]\\ &= \frac{1}{2}\bar{\lambda}^2\frac{\Omega_4}{(2\pi)^4}v_4k^2\left[(\bar{\Psi}\Psi)^2-(\bar{\Psi}\gamma_5\Psi)^2\right]\int_0^\infty \mathrm{d}z z^2\tilde{\partial}_t\left[\frac{Z_\psi^2(1+r_\psi)^2}{z^2(1+r_\psi)^4}\right],\end{aligned} \tag{2.3.57}$$

where we have defined the volume of d-sphere of unit radius $\Omega_d = \frac{2\pi^{d/2}}{\Gamma(d/2)}$ and v_4 stands for the volume of the four-dimensional spacetime. Again, a vector-channel contribution and mixed-terms are generated, which we disregard. The left-hand-side of the flow equation for our truncation, evaluated on constant background fields, is given by

$$\partial_t\Gamma_{k,\mathrm{NJL}} = \frac{1}{2}v_4\partial_t(Z_\psi^2\bar{\lambda})\left[(\bar{\Psi}\Psi)^2-(\bar{\Psi}\gamma_5\Psi)^2\right]. \tag{2.3.58}$$

The scale derivative hitting the wave-function renormalization factor term will produce the anomalous dimension $\eta_\psi = -\partial_t\ln Z_\psi$. Finally, we compare the coefficients of the four-fermion self-interactions terms on both sides of the flow equation to read the beta function for the four-fermion coupling $\bar{\lambda}$. By defining the dimensionless coupling $\lambda = k^2\bar{\lambda}$ and using the fermionic Litim shape function (2.3.33), we

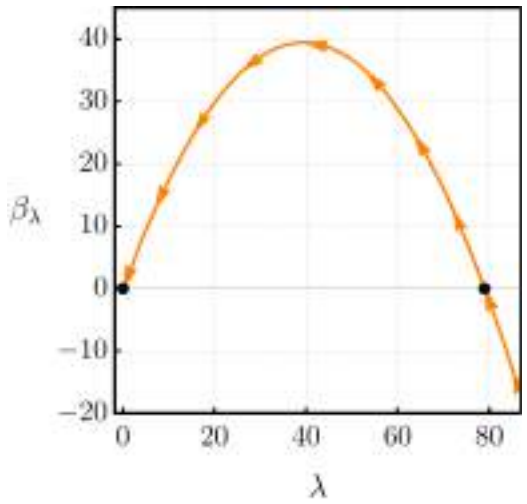

Figure 2.5: Plot of the β_λ for the dimensionless four-fermion self-coupling λ in the scalar-pseudoscalar channel as a function of the RG-scale k. The black dots indicate the fixed points.

are led to the 1-loop beta function

$$\beta_\lambda \equiv \partial_t \lambda = (2 + 2\eta_\psi)\lambda - \frac{1}{4\pi^2}\lambda^2. \tag{2.3.59}$$

In (2.3.59), the term $(2 + 2\eta_\psi)\lambda$ is the canonical scaling contribution and the other one comes from quantum corrections computed from the fermionic diagram in the flow. For this computation, we drop the anomalous dimension η_ψ coming from the regulator insertion $\partial_t R_k$ and only keep the corresponding contribution in η_ψ coming from the scaling term on the left-hand side of the flow equation. In Fig. 2.5, we show a sketch of the flow of the dimensionless four-fermion coupling λ. Apart from a free fixed point, the theory admits a non-Gaussian fixed point at $\lambda^* = 8\pi^2$ with critical exponent $\theta = -\frac{\partial \beta_\lambda}{\partial \lambda}\big|_{\lambda^*} = 2$, indicating that is a free parameter. The flow equation is a simple ordinary differential equation which can be straightforwardly solved analytically with boundary conditions at an IR-scale $k = k_{\rm IR}$ up to an UV-scale $k = \Lambda_{\rm UV}$ to yield

$$\lambda(k_{\rm IR}) = \frac{2\,(k_{\rm IR}/\Lambda_{\rm UV})^2\,\lambda_{\Lambda_{\rm UV}}}{2 - a\lambda_{\Lambda_{\rm UV}}(1 - (k_{\rm IR}/\Lambda_{\rm UV})^2)}, \tag{2.3.60}$$

where $a = 1/4\pi^2$. For initial condition $\lambda_{\Lambda_{\rm UV}} = \lambda^*$, the four-fermion coupling does not depende on the coarse-graining scale k: $\lambda(k_{\rm IR}) = \lambda^*$ (green-dashed line in Fig. 2.6). If the initial condition is chosen as $\lambda_{\Lambda_{\rm UV}} < \lambda^*$, then the four-fermion coupling decreases towards the IR, reaching a non-interacting regime (blue-dashed lines in Fig. 2.6). In this case, chiral symmetry remains unbroken. Finally, for $\lambda_{\Lambda_{\rm UV}} > \lambda^*$, the four-fermion coupling grows rapidly towards the IR, eventually diverging at a Landau pole (red-dashed lines in Fig. 2.6). As discussed previously, this behavior signals the breakdown of chiral symmetry in the ground state of the theory. In this way, the value of the fixed point can be regarded as an order parameter which separates the chirally symmetric phase from the broken chiral symmetry regime in the ground state.

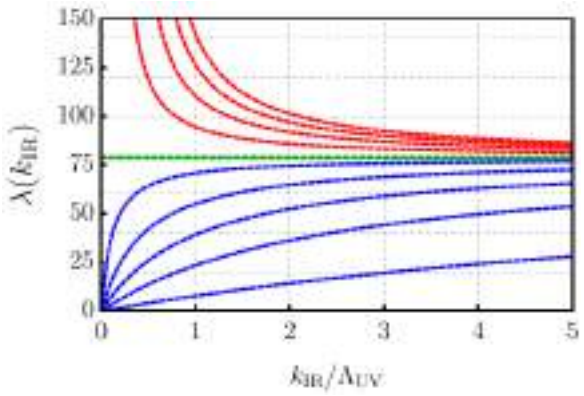

Figure 2.6: RG-flow of the four-fermion self-coupling λ. The green-dashed line indicates the RG-scale-independence of the coupling for $\lambda_{\Lambda_{\rm UV}} = \lambda^*$, the blue-dashed lines represent the RG-trajectories in which chiral symmetry is preserved in the IR for initial conditions $\lambda_{\Lambda_{\rm UV}} < \lambda^*$ and the red-dashed lines are RG-trajectories that signal chiral symmetry breaking for $\lambda_{\Lambda_{\rm UV}} > \lambda^*$.

2.4 Brief overview of results in asymptotic safety in gravity

Since the pioneering work by Reuter [105], a number of studies in asymptotic safety in gravity was put forth, providing more and more evidence for the existence of a non-trivial UV fixed point for gravity systems. In this section, we briefly review some important works.

The Einstein-Hilbert approximation

The fRG techniques were first applied in trying to quantize gravity by Reuter and Souma [105, 170] and subsequently by Reuter and Saueressig [171] in a simple truncation parametrized by the Einstein-Hilbert action

$$\Gamma_k[\bar{g};h] = \frac{k^{d-2}}{16\pi g_k}\int \mathrm{d}^d x\sqrt{g}\left(2k^2\lambda_k - R\right) + \text{classical gauge-fixing terms}, \tag{2.4.1}$$

where g_k and λ_k are the dimensionless Newton coupling and cosmologial constant. In Fig. 2.7, we show the phase diagram of the Newton coupling and the cosmological constant, exhibiting an asymptotically safe fixed point at[23] $g_k^* = 0.403$ and $\lambda_k^* = 0.330$. It is also possible to see that both couplings correspond to relevant directions, because there are many RG trajectories that reach many different values of g_k and λ_k starting from the fixed point. This can also be seen from the spiralling behavior of the flows from the complex conjugate pair of critical exponents $\theta_\pm = 1.941 \pm 3.147i$. In this way, both gravitational couplings correspond to free parameters.

The first non-trivial check of the theory is whether or not one can start at the fixed point and connect to a regime of classical gravity in the IR. For that, we need to see what characterized classical gravity. The classical regime is characterized by a constant dimensionfull Newton coupling, $G_{\rm N} = \text{const.}$, which means that in $d = 4$ the dimensionless Newton coupling scales like k^2, *i.e.*, $g_k = G_{\rm N}k^2 \sim k^2$. Similarly, in the classical regime the dimensionfull cosmological constant is constant, $\bar{\lambda} = \text{const.}$, which means that

[23] This calculation has been done [171] using a sharp regulator shape function, $r_k(z) = \frac{1}{\theta(z-1)} - 1$, within the so-called type-A scheme [13] and adopting the Feynman-'t Hooft gauge, $\alpha = 1$.

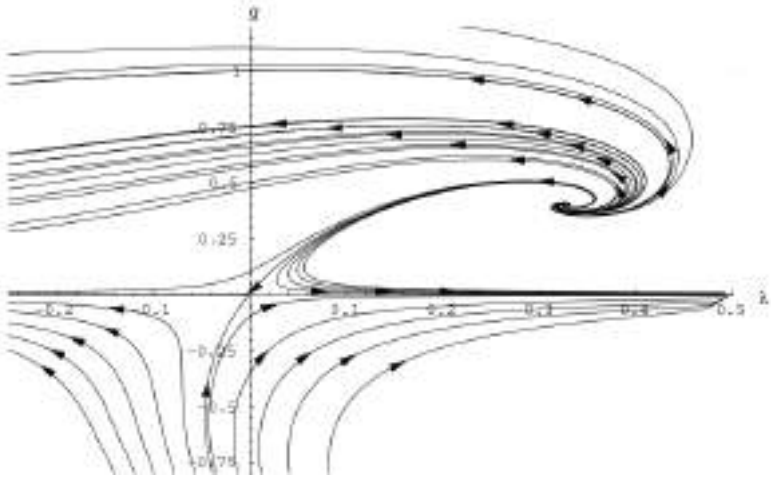

Figure 2.7: Phase portrait of the RG-flow for the Einstein-Hilbert action. The arrows point towards decreasing k, *i.e.*, towards the IR. Plot extracted from [171].

its dimensionless counterpart goes like k^{-2}, *i.e.*, $\lambda_k = \bar{\Lambda} k^{-2} \sim k^{-2}$. Combining these two implies that the product $g_k \lambda_k$ = const. in the classical gravity regime, which basically means that $g_k \sim 1/\lambda_k$. And this type of scaling is observed in Fig. 2.7 for trajectories that pass close to the origin. Among these RG trajectories, it is then possible to find one in particular that realizes the measured values of the Newton coupling and the cosmological constant with product $g_k \lambda_k = 0.14$, being then the RG trajectory "of our Universe". In references [171, 172], this product was computed using different schemes of regularization and choices of gauge, leading to the same number, which supports the idea that the product is regulator independent and, thus, has a universal meaning.

Curvature-squared results

Moving on with the first non-trivial order in curvature is the curvature-squared terms, which are the 1-loop counterterms of perturbative gravity. There are three terms at this level on top of the Einstein-Hilbert term, namely

$$\Gamma_{k,\mathrm{grav}}[g] = \frac{1}{16\pi G_{\mathrm{N}}} \int \mathrm{d}^4x \sqrt{g} \left[2\bar{\Lambda} - R + \bar{a} R_{\mu\nu}^2 + \bar{b} R^2 - \frac{1}{\bar{\rho}} E \right], \tag{2.4.2}$$

where $E = R^2 - 4R_{\mu\nu}R^{\mu\nu} + R_{\mu\nu\alpha\beta}R^{\mu\nu\alpha\beta}$ is the topological-invariant Gauss-Bonnet combination. The theory has four different (dimensionful) couplings of local terms and one of the topological term. It turns out that there is a fixed point [173, 174] which has three relevant directions, one irrelevant and one marginal. The marginal direction is connected to the topological term. But once again we start to see how asymptotic safety is predictive, because, in perturbation theory, there would be just four free parameters [70, 71, 175, 176] at this setting and in asymptotic safety one coupling does not correspond to a free parameter.

Again, we can wonder if we can use these three relevant directions to connect to our Universe. One scenario that one would want to connect to would be classical gravity plus Starobinsky inflation, which would be driven by the coupling $\bar{b} = k^{-2} b_k$ in the $b_k R^2$ term [177]. In Fig. 2.8, we display the

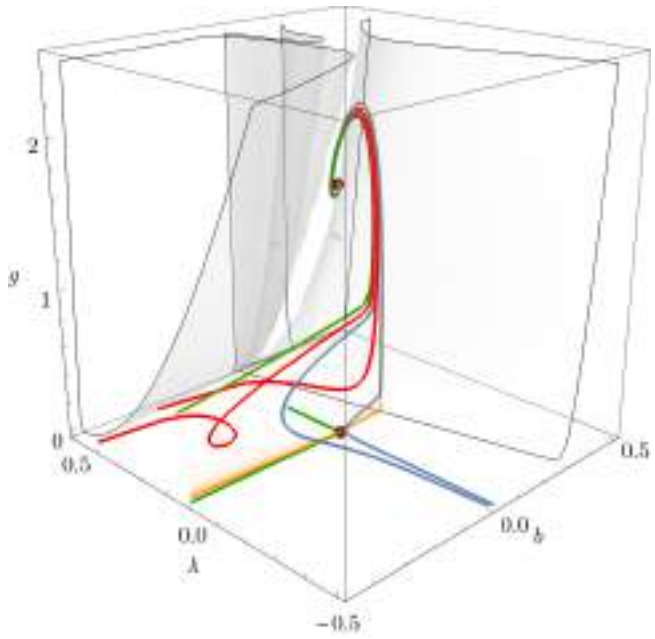

Figure 2.8: Phase portrait of selected RG trajectories in the space parametrized by g_k, λ_k and b_k. The fixed point is in red. Plot extracted from [177].

phase diagram of of selected RG trajectories in the space parametrized by g_k, λ_k and b_k. There is a non-trivial fixed point at $g_k^* = 1.59$, $\lambda_k^* = 0.133$ and $b_k^* = 0.119$ with critical exponents $\theta_\pm = 1.26 \pm 2.45i$ and 27.0. From this fixed point, there is a green trajectory that actually realizes both the classical values of G_N and $\bar{\Lambda}$ and also a value for b_k needed in order to drive Starobinsky inflation. The latter is not a must in the sense that, if it is possible to realize inflation in a different way or even to do without inflation entirely by just choosing different trajectories where b_k takes a lower value, so that one would not get into the inflationary regime.

Results in higher-order in curvature

Extended truncations in higher-order terms in curvature invariants have been addressed in the literature. We can cite, for instance, polynomial functions of the scalar curvature [178–183], $f(R)$, effective actions of both the forms $f_1(R_{\mu\nu}R^{\mu\nu}) + Rf_2(R_{\mu\nu}R^{\mu\nu})$ (which will explored in Chapter 5 in the context of unimodular gravity), where f_1 and f_2 are polynomial functions [184] and of general functions of the Riemman tensor and the inverse metric, $f(R_{\mu\nu\rho\sigma}, g^{\alpha\beta})$ [185], and truncations with the Einstein-Hilbert term plus the Goroff-Sagnotti counterterm $R^{\mu\nu}{}_{\rho\sigma}R^{\rho\sigma}{}_{\alpha\beta}R^{\alpha\beta}{}_{\mu\nu}$ [186]. For a complete list for extended higher-order in curvature truncations, see [95]. In all these investigations, a non-trivial UV fixed point with three relevant directions and higher-order irrelevant directions was observed. The higher order curvature-invariant terms are then predictions. Of course, these predictions are not necessarily easily testable, because we currently do not have a meaningfull access to values of higher-order curvature couplings even in the strong-gravity regime.

Results for gravity-matter systems

The asymptotic-safety paradigm has been extended to include the SM matter fields, see [187–189] for reviews. There is a robust evidence that gravity remains asymptotically safe with the inclusion of fluctuations of Standard Model fields [190–197]. The interplay of gravity with matter provides a mechanism that fixes couplings in the Standard Model from first principles [98, 198–207]. The interplay of asymptotic safety with scalars [208–218], fermions [219–226] and gauge fields [193, 199, 201, 227–229] has also been investigated separately. Extensions beyond the Standard Model have also been explored [230–247]. In Chapter 3, further extensions of the Standard Model will be studied with the inclusion of dark matter degrees of freedom coupled to quantum gravity.

Convergence of the results and the near-perturbative nature

So far, it seems that asymptotic safety in gravity has three free parameters and this emerges from, for instance, the studies of all the higher-order in Ricci scalar terms, but also from studies including the Goroff-Sagnotti term. Those type of studies indicate the existence of quite a lot of predictive power. In particular, in the studies of higher-order truncations in Ricci scalar, it is interesting to note that the values of these critical exponentes which feature $\mathrm{Re}(\theta) < 0$ are actually what is called **near-Gaussian**, since they are quite close to the canonical mass dimension. We recall that, if we were at the free fixed point, then the critical exponents would be exactly the canonical dimension. Therefore, if the values of the critical exponents are close to the canonical dimension, then this means that the fixed point is not quite non-perturbative, being actually called **near-perturbative**. This also means that there is a robust scheme of how to choose truncations for reliable calculations, which is according to the canonical power-counting. So, terms which have a canonical high mass dimension are very likely to be irrelevant, and then it is a matter of calculationg the critical exponents to check afterwards whether the initial assumption was correct, which is in general the case from the calculations cited.

In this way, despite the fact that with the fRG, one has to make approximations, there is by now a way of how to make these approximations quite robust. So, in summary, there is quite compelling evidence for asymptotic safety in a quantum theory of space, but not yet in a quantum theory of spacetime (but see the discussion below). Of course, moving beyond a pure theory about the building blocks of gravity, we can also by now have a lot to say about the predictive power of a theory about the building blocks of matter. It is fair to say that there is quite robust evidence for asymptotic safety in gravity-matter systems and a deep understanding what are the implications for particle physics.

2.5 Two open questions in brief

Unitarity

The conservation of probability is a fundamental principle in quantum mechanics. Extending to QFTs on a flat Euclidean background, conservation of probability is translated into a well-defined

scattering matrix (S-matrix), which connects asymptotic initial and final states. The results can then be converted to corresponding Lorentzian ones, as guaranteed by Osterwalder-Schrader axioms, which make use of the requirement of reflection positivity of the spectral function of the theory. In this way, the theory is guaranteed to possess an analytical continuation to a unitary QFT.

However, the situation is a lot complicated once we consider a general curved background $\bar{g}_{\mu\nu}$, as the generalization of the concept of an S-matrix is not trivial (but see [248, 249]) and a Wick-rotation gets further hampered by a dynamical metric. Around a flat background, higher-derivative gravity theories may contain negative-norm states in the asymptotic physical spectrum, featuring ghost-poles in the graviton propagator. In the context of an asymptotically safe theory of quantum gravity, the unitarity issue should be based on propagators extracted from the effective action $\Gamma_{k\to 0}$, since correlation functions derived from the flowing action Γ_k may contain artificial poles.

Aspects of non-perturbative unitarity in QFT and in QG were discussed in [250] where the possibility of ghost degrees of freedom in truncated effective actions could actually be fictitious was addressed. The results in [250] indicate that these "fake ghosts" would dissapear from the asymptotic spectrum of states once all possible operators compatible with the underlying symmetries are inclued in the effective action. In [251], criteria and conditions for the graviton propagator to be consistent with causality, unitarity and stability were presented.

Another indicator that ASQG could be unitarity comes from the cross-fertilization with other methods [252], such as CDT (see Section 2.3).

Euclidean *versus* Lorentzian signature

Related to the issue of unitarity in quantum gravity is the issue of having to perform asymptotic safety calculation in Euclidean settings. As discussed previously, this technical problem arises due to the need of sorting out modes in the path integral *à la* Wilson.

First studies aiming to address this problem came from trying to formulate asymptotic safety in spacetimes with a built-in foliation structure which naturally provides a direction of time, as in the Arnowitt-Deser-Misner formalism [192, 253–256](see also [231, 257–260]).

Fortunately, more recently, computations for ASQG could be directly performed within a Lorentzian signature. In [118–123], a direct fRG approach to Lorentzian (metric) quantum gravity was put forward, leading to the non-perturbative computation of the graviton spectral function. These results allow us to reach a stage in ASQG where we can have access to quantitative information for observables with Lorentzian signature.

Chapter 3

An Asymptotically Safe Road into the Darkness

3.1 Motivation for connecting quantum gravity and dark matter

Fundamental physics faces several profound challenges. One is to understand the quantum nature of gravity and another is to understand the true nature of the dark matter (DM). At a first glance, these challenges appear unrelated, because they are associated to very different energy scales. Quantum gravity is typically assumed to become dynamically important at energies of $E \approx M_{\text{Planck}} = 10^{19}\,\text{GeV}$. DM candidates span a huge range in masses [261–272], but most proposals focus on energy scales far below the Planck scale, with the typical mass scales for Weakly Interacting Massive Particles (WIMPs) in the GeV-TeV range [273]. In this chapter, we advocate that much can be learnt about both quantum gravity and DM, if we consider both challenges simultaneously. We support this claim by providing a concrete example.

The key idea underlying this chapter is that the interplay of quantum gravity with dark (and visible) matter[1] imprints structures on and constrains the couplings of the matter sector at the Planck scale, see [188] for a review. The renormalization group (RG) then acts as a lever arm that translates these structures at tiny length scales (high energies) to structures at large length scales (low energies). Thereby, two important goals are achieved: first, by generating predictions for the interaction structure of dark and visible matter, the quantum gravity theory becomes testable by current observations. Second, by predicting the interaction structure of the DM, the huge space of DM models is reduced and, as we will show, phenomenologically viable DM models are ruled out on theoretical grounds. Both goals – making quantum gravity testable and making DM models more predictive – are critical in order to make progress in our understanding of our Universe.

This chapter supports the idea that such progress can be made, if we overcome the division between quantum-gravity research and DM research, and consider quantum gravity and DM together in a multi-scale setup. In such a multi-scale setup, theoretical constraints at the Planck scale are combined with

[1] In this context, by matter we refer to all fields except the metric; *i.e.*, gauge fields are part of the matter sector.

phenomenological and observational constraints at lower scales and the resulting theory of DM and quantum gravity is significantly more predictive than a theory of DM on its own.

In the present chapter, we explore this general idea in the context of asymptotically safe quantum gravity (ASQG) and WIMP dark matter.

We have compelling evidence from cosmological and astrophysical observations ranging from the Cosmic Microwave Background (CMB) radiation to dwarf galaxies [274–276] that the majority of the matter density in the Universe is non-baryonic DM with no particle candidates in the Standard Model (SM) able to account for this DM content. This amount of evidence collected over the last eight decades suggest that DM consists of one or more particles. We are going to assume it is made of at least one new kind of particle. From these observations, a set of properties can be established on the DM content: first, it should be non-luminous, meaning that it should not have a large coupling[2] to $\mathrm{U}(1)_{\mathrm{EM}}$ gauge interactions and should not be charged under the strong gauge group[3] SU(3); second, it should be feebly interacting with itself and with visible particles of the SM; third, it should be a stable and long-lived particle with a lifetime longer than the age of the Universe ($t \gtrsim 14$ billion years); fourth, it should be non-relativistic (cold) at the time of cosmological structure formation and, finally, as a fifith requirement, it should be produced in the early Universe. A common assumption is that the DM particle is produced via the so-called *thermal freeze-out mechanism* and it works as follows: in the early Universe, the DM particle was in thermal equilibrium through interactions with the SM particles[4]. As the Universe expands and temperature decreases, the expansion rate becomes larger than the interaction rate for the DM production. Therefore, at some point, DM effectively decouples, creating the finite relic abundance of DM that is observed today [274].

The most studied DM particle candidate consistent with these properties has been the WIMP. However, the WIMP paradigm has become highly challenged by the absence of expected WIMP signals in DM particle search experiments – both direct, indirect and collider experiment [261, 280–284]. Therefore it is now highly motivated to study the remaining parts of the WIMP parameter space as well as alternatives to the WIMP paradigm and in particular new ways to constrain the vast parameter space of such alternative paradigms. Another promising candidate for cold dark matter is the QCD axion (see, *e.g.*, the review [285]). This is characterized by a light neutral scalar or pseudoscalar boson that couples weakly to the SM particles with a feeble decay constant parameter. The interest in this model is that it preserves the CP-symmetry of QCD via the so-called Peccei-Quinn (PQ) mechanism [286]. If the PQ is explicitly broken, either in the Langrangian or due to quantum effects such as anomalies, a small axion mass is generated, motivating its detection as DM in dedicated direct detection experiments (see, *e.g.*, the review [287] and references therein).

In the context of asymptotic safety, dark matter has for the first time been studied in [230], where it was discovered that the Higgs portal to a single, uncharged dark scalar must vanish, ruling out this

[2]The strength of the interaction should be less than the size of the interaction to electrons and protons, for instance.

[3]This is because DM particles are kinematically allowed to decay into neutral strongly-interacting particles, such as neutral pions, which, in turn, decay can into photons.

[4]Cosmological observations of the CMB radiation spectrum and of the light element abundance imply that the SM particles were also in thermal equilibrium in the early Universe [274, 277–279].

simplest WIMP candidate. Extended WIMP models have been considered in [232–235, 237, 243] and axion-like dark matter has been considered in [239]. In the present chapter, we start from a WIMP model that is phenomenologically viable, as explored in depth in [288], and investigate whether or not it is compatible with asymptotic safety.

3.2 Definition of the models

We consider two extensions of the SM coupled to gravity: $\mathrm{U}(1)_\mathrm{D}$ and $\mathrm{SU}(2)_\mathrm{D}$ hidden DM models with vector DM candidates and a new SM singlet scalar S that is charged under the dark gauge group. These models are particularly relevant since they are phenomenologically viable [288]. Schematically, the gauge-fixed flowing action for the gravity-matter dynamics reads

$$\Gamma_k = \Gamma_{k,\mathrm{grav}} + \Gamma^0_{k,\mathrm{SM}} + \Gamma_{k,\mathrm{DM}}. \tag{3.2.1}$$

For the SM subsystem, we consider the gauge interactions of the SM gauge group $\mathrm{U}(1)_\mathrm{Y} \times \mathrm{SU}(2)_\mathrm{L} \times \mathrm{SU}(3)_\mathrm{C}$ coupled to the quarks and leptons. In particular, for the Yukawa sector, we consider an approximation where only the top and bottom quarks have nonvanishing (real) Yukawa couplings. We denote by $\Gamma^0_{k,\mathrm{SM}}$ the SM action without the Higgs potential, and $g_\mathrm{Y} = \sqrt{\frac{3}{5}} g_1$, g_2 and g_3 are the respective SM gauge couplings, which are dimensionless in four dimensions. Explicitly, it reads

$$\begin{aligned}\Gamma^0_{k,\mathrm{SM}} = {} & \frac{1}{4}\int_x W^a_{\mu\nu} W^{a,\mu\nu} + \frac{1}{4}\int_x B_{\mu\nu} B^{\mu\nu} + S^{\mathrm{EW}}_{\mathrm{g.f.}} + S^{\mathrm{EW}}_{\mathrm{ghosts}} \\ & + \frac{1}{4}\int_x G^b_{\mu\nu} G^{b,\mu\nu} + S^{\mathrm{SU}(3)}_{\mathrm{g.f.}} + S^{\mathrm{SU}(3)}_{\mathrm{ghosts}} \\ & + \sum_{j=1,2,3} \int_x i\bar{\psi}^{\mathrm{L/R}}_{i,j} \not{D} \psi^{\mathrm{L/R}}_{i,j} + \int_x (D_\mu \Phi_i)^\dagger (D^\mu \Phi_i) + \Gamma_{k,\mathrm{Yukawa}}\,. \end{aligned} \tag{3.2.2}$$

Here B_μ is the $\mathrm{U}(1)_\mathrm{Y}$ hypercharge gauge field, W^a_μ are the $\mathrm{SU}(2)_\mathrm{L}$ weak gauge fields and A^a_μ are the gluon gauge fields of the color group $\mathrm{SU}(3)_\mathrm{C}$, with $B_{\mu\nu} = \partial_\mu B_\nu - \partial_\nu B_\mu$, $W^a_{\mu\nu} = \partial_\mu W^a_\nu - \partial_\nu W^a_\mu + g_2 \epsilon^{abc} W^b_\mu W^c_\nu$ and $G^a_{\mu\nu} = \partial_\mu A^a_\nu - \partial_\nu A^a_\mu + g_3 f^{abc} A^b_\mu A^c_\nu$ being their respective field-strengths. The fermionic fields $\psi_{i,j}$ represent general quark $q_{i,j}$ and lepton $l_{i,j}$ doublet fields with their respective chiralities, with i being the isospin index and j labeling the generation, ranging over the whole families of quarks and leptons of the SM. Compactly, we have $\psi_{i,j} = (q_{i,j}, l_{i,j})$. The covariant derivative of the fermionic fields reads

$$D_\mu \psi^I_{i,j} = \partial_\mu \psi^I_{i,j} + \omega_\mu \psi^I_{i,j} - i g_\mathrm{Y} Y B_\mu \psi^I_{i,j} - i g_2 W_{a,\mu} T^a_{ik} \psi^I_{k,j} + i g_3 A_{\mu,b} t^b_{IJ} \psi^J_{i,j}. \tag{3.2.3}$$

The quarks live in the fundamental representation of the color group $\mathrm{SU}(3)_\mathrm{C}$ with color indices $I, J = 1, 2, 3$. The matrices T^a and t^a are the generators of $\mathrm{SU}(2)_\mathrm{L}$ and $\mathrm{SU}(3)_\mathrm{C}$, respectively. The hypercharge values Y are assigned according to each quark and lepton generation and their respective chiralities. In this sense, right fermions do not couple to weak isospin. The coupling of the fermionic fields with gravity is via the so(4)-valued spin-connection ω_μ. Furthermore, the coupling of the Higgs

doublet with the EW gauge group is done via the covariant derivative

$$D_\mu \Phi_i = \partial_\mu \Phi_i - \frac{i}{2} g_{\rm Y} B_\mu \Phi_i - i g_2 W_{a,\mu} T^a_{ij} \Phi_j . \tag{3.2.4}$$

The gauge-fixing and the associated Faddeev-Popov ghost action for the EW and QCD sectors are, respectively,

$$\begin{aligned} S^{\rm EW}_{\rm g.f.} + S^{\rm EW}_{\rm ghosts} = {} & \frac{1}{2\xi_{\rm W}} \int_{\bar{x}} (\partial_\mu W^{a,\mu})^2 + \frac{1}{2\xi_{\rm B}} \int_{\bar{x}} (\partial_\alpha B^\alpha)^2 \\ & + \int_{\bar{x}} \left(\bar{c}^{(2)}_a \partial_\mu \partial^\mu c^{(2)}_a - g_2 \epsilon^{abc} \bar{c}^{(2)}_a \partial_\alpha \left(W_c{}^\alpha c^{(2)}_b \right) \right), \end{aligned} \tag{3.2.5}$$

$$S^{\rm SU(3)}_{\rm g.f.} + S^{\rm SU(3)}_{\rm ghosts} = \frac{1}{2\xi_{\rm A}} \int_{\bar{x}} (\partial_\mu A^{a,\mu})^2 \int_{\bar{x}} \left(\bar{c}^{(3)}_a \partial_\mu \partial^\mu c^{(3)}_a - g_3 f^{abc} \bar{c}^{(3)}_a \partial_\alpha \left(A_c{}^\alpha c^{(3)}_b \right) \right), \tag{3.2.6}$$

For the Yukawa sector, we consider an approximation where only the top and bottom quarks have nonvanishing (real) Yukawa couplings. The explicit action reads

$$\Gamma_{k,\rm Yukawa} = \int_x y_t \left(\bar{q}^{\rm L}_{i,3} \Phi^i q^{\rm R}_{1,3} + \bar{q}^{\rm R}_{1,3} \Phi^{\dagger i} q^{\rm L}_{i,3} \right) + \int_x y_b \left(\bar{q}^{\rm L}_{i,3} \tilde{\Phi}^i q^{\rm R}_{2,3} + \bar{q}^{\rm R}_{2,3} \tilde{\Phi}^{\dagger i} q^{\rm L}_{i,3} \right), \tag{3.2.7}$$

where the spinorial and color indices are omitted and $\tilde{\Phi}^i = i\sigma_2^{ij} \Phi^\dagger_j$ with σ_2 being the second Pauli matrix. The third generation of the right chirality $\mathrm{SU}(2)_{\rm L}$ quark doublet is explicitly given by $q^{\rm R}_{i,3} = (t^{\rm R}, b^{\rm R})^{\rm T}$. Moreover, all the SM and beyond SM fields, including ghosts, are augmented by wave-function renormalization factors, *i.e.*, $\phi_{\rm SM} \mapsto Z^{1/2}_{\rm SM} \phi_{\rm SM}$ and $\phi_{\rm DM} \mapsto Z^{1/2}_{\rm DM} \phi_{\rm DM}$, which encode the running of all the respective attached fields, leading to the anomalous dimensions $\eta_{\rm SM} = -\partial_t \log Z_{\rm SM}$ and $\eta_{\rm DM} = -\partial_t \log Z_{\rm DM}$.

The gauge-fixed pure gravity sector of our truncated flowing action is given by the Einstein-Hilbert action

$$\Gamma_{k,\rm grav} = \frac{1}{16\pi G_{\rm N}} \int_x \left(2\bar{\Lambda} - R(g) \right) + \frac{1}{2\alpha} \int_{\bar{x}} \bar{g}^{\mu\nu} \mathcal{F}_\mu[h;\bar{g}] \mathcal{F}_\nu[h;\bar{g}] + \int_{\bar{x}} \bar{C}^\mu \mathcal{M}_{\mu\nu}[h;\bar{g}] C^\nu , \tag{3.2.8}$$

where R is the Ricci scalar, $G_{\rm N}$ and $\bar{\Lambda}$ are the scale-dependent dimensionful Newton coupling and cosmological constant, respectively, and C^μ and $\bar{C}_\mu$ denote the Faddeev-Popov ghosts. Their dimensionless counterparts are obtained through $G_{\rm N}(k) = k^{-2} G(k)$ and $\bar{\Lambda}(k) = k^2 \Lambda(k)$. The (full) metric is expanded into an Euclidean background $\bar{g}_{\mu\nu} = \delta_{\mu\nu}$ and a dynamical (not necessarily small) fluctuation piece $h_{\mu\nu}$ as

$$g_{\mu\nu} = \delta_{\mu\nu} + Z_h^{1/2} (32\pi k^{-2} G(k))^{1/2} h_{\mu\nu} \tag{3.2.9}$$

where Z_h is the wave-function renormalization factor for the graviton $h_{\mu\nu}$. The choice of a flat background is sufficient in order to compute the RG-flow of curvature-independent, matter couplings. The

linear gauge-fixing function is

$$\mathcal{F}_\mu[h;\bar{g}] = \sqrt{2}Z_h^{1/2}\left(\delta^\alpha_\mu \bar{g}^{\nu\beta} - \frac{1+\beta}{4}\delta^\nu_\mu \bar{g}^{\alpha\beta}\right)\bar{\nabla}_\nu h_{\alpha\beta}, \tag{3.2.10}$$

where α and β are gauge-fixing parameters. Here, $\bar{\nabla}_\mu$ stands for the spacetime covariant derivative defined with respect to the background metric. The Landau-gauge limit, $\alpha \to 0$, is adopted. The corresponding Faddeev-Popov operator is computed from the gauge-fixing function $\mathcal{F}_\mu[h;\bar{g}]$ and reads

$$\mathcal{M}_{\mu\nu}[h;\bar{g}] = \sqrt{2}Z_h^{1/2}\left[\bar{\nabla}^\alpha\left(g_{\mu\nu}\nabla_\alpha + g_{\alpha\nu}\nabla_\mu\right) - 2\frac{1+\beta}{4}\bar{g}^{\alpha\beta}\left(\bar{\nabla}_\mu g_{\nu\beta}\nabla_\alpha\right)\right]. \tag{3.2.11}$$

Extensions

We first extend the Standard Model by a dark complex scalar S charged under a $\mathrm{U}(1)_\mathrm{D}$ gauge symmetry with gauge boson V_μ. Explicitly, the gauge-fixed action reads [289]

$$S_\mathrm{DM}^{\mathrm{U}(1)_\mathrm{D}} = \int_x \left[\frac{1}{4}V_{\mu\nu}V^{\mu\nu} + (D_\mu S)^*(D^\mu S) + V(\Phi,S)\right] + \frac{1}{2\xi_\mathrm{D}}\int_{\bar{x}}(\partial_\alpha V^\alpha)^2\,, \tag{3.2.12}$$

where $V_{\mu\nu} = \partial_\mu V_\nu - \partial_\nu V_\mu$ is the field-strength tensor for the $\mathrm{U}(1)_\mathrm{D}$ gauge field and

$$D_\mu S = \partial_\mu S - i g_\mathrm{D} V_\mu S, \tag{3.2.13}$$

in which g_D is the $\mathrm{U}(1)_\mathrm{D}$ gauge coupling and Φ is the $\mathrm{SU}(2)_\mathrm{L}$ Higgs doublet. For explicit computations, we adopt the Landau-gauge limit, *i.e.*, $\xi_\mathrm{D} \to 0$ and the corresponding Faddeev-Popov ghosts only contribute to the flow of the gravitational couplings. An additional unbroken $\mathbb{Z}_2$ symmetry is present, under which the dark vector boson transforms as

$$V_\mu \mapsto -V_\mu, \tag{3.2.14}$$

while all other fields are even. This symmetry ensures the stability of the dark sector and prohibits a kinetic mixing between the dark vector V_μ and the gauge field of the hypercharge sector of the SM, *i.e.*, a term of the form $V_{\mu\nu}B^{\mu\nu}$, where $B_{\mu\nu} = \partial_\mu B_\nu - \partial_\nu B_\mu$.

The scalar potential supplemented by a portal interaction with the Higgs doublet is given by [288]

$$V(\Phi,S) = m_\mathrm{H}^2\Phi_i^\dagger\Phi_i + \frac{\lambda_\mathrm{H}}{6}(\Phi_i^\dagger\Phi_i)^2 + m_\mathrm{S}^2 S^*S + \frac{\lambda_\mathrm{S}}{6}(S^*S)^2 + 2\lambda_\mathrm{p}(\Phi_i^\dagger\Phi_i)(S^*S), \tag{3.2.15}$$

where the quartic couplings λ_H, λ_S and λ_p are dimensionless in four dimensions.

The second model to be considered is the non-Abelian $\mathrm{SU}(2)_\mathrm{D}$ extension. In this model, the DM candidate comprises a $\mathrm{SU}(2)_\mathrm{D}$ vector triplet V_μ^a with $a = 1,2,3$, alongside a complex $\mathrm{SU}(2)_\mathrm{D}$ doublet

S_i with $i = 1, 2$. Explicitly, the gauge-fixed action is given, in this case, by [290]

$$S_{\rm DM}^{{\rm SU}(2)_{\rm D}} = \int_x \left[\frac{1}{4} V^a_{\mu\nu} V^{a,\mu\nu} + (D_\mu S_i)^\dagger (D^\mu S_i) + V(\Phi, S) \right] + S_{\rm g.f.}^{{\rm SU}(2)_{\rm D}} + S_{\rm ghosts}^{{\rm SU}(2)_{\rm D}}, \tag{3.2.16}$$

where $V^a_{\mu\nu} = \partial_\mu V^a_\nu - \partial_\nu V^a_\mu + g_{\rm D} \epsilon^a{}_{bc} V^b_\mu V^c_\nu$ is the field-strength of the ${\rm SU}(2)_{\rm D}$ gauge field and

$$D_\mu S_i = \partial_\mu S_i - i g_{\rm D} V_{a,\mu} T^a_{ij} S_j, \tag{3.2.17}$$

where we use the same notation for the non-Abelian dark gauge coupling as in the Abelian case. These couplings should be distinguished by the context. The matrices T^a are the generators of the ${\rm SU}(2)_{\rm D}$ dark gauge group. Gauge symmetry forbids kinetic mixing of the DM vector triplet V^i_μ with SM gauge fields. For this non-Abelian case, Faddeev-Popov ghosts do not decouple in the matter sector. In this way, the proper gauge-fixing action along with the associated Faddeev-Popov ghost term are given by

$$S_{\rm g.f.}^{{\rm SU}(2)_{\rm D}} + S_{\rm ghosts}^{{\rm SU}(2)_{\rm D}} = \frac{1}{2\xi_{\rm D}} \int_{\bar{x}} (\partial_\mu V^{a,\mu})^2 + \int_{\bar{x}} \left(\bar{c}^{({\rm D})}_a \partial_\mu \partial^\mu c^{({\rm D})}_a - g_{\rm D} \epsilon^{abc} \bar{c}^{({\rm D})}_a \partial_\alpha \left(V_c{}^\alpha c^{({\rm D})}_b \right) \right). \tag{3.2.18}$$

The Landau-gauge limit is also chosen here. Similarly to the Abelian case, the potential is chosen with the normalization

$$V(\Phi, S) = m^2_{\rm H} \Phi^\dagger_i \Phi_i + \frac{\lambda_{\rm H}}{6} (\Phi^\dagger_i \Phi_i)^2 + m^2_{\rm S} S^\dagger_i S_i + \frac{\lambda_{\rm S}}{6} (S^\dagger_i S_i)^2 + 2\lambda_{\rm p} (\Phi^\dagger_i \Phi_i)(S^\dagger_i S_i). \tag{3.2.19}$$

These truncations are motivated by previous results that asymptotically safe gravity can induce a near-perturbative UV completion for matter models, see, e.g., [188] and references therein. In such a near-perturbative setting, the above truncations are likely to capture all relevant terms and are thus sufficient for a first study.

We can proceed by using the FRG machinery to compute the beta functions of SM and DM couplings including contributions due to gravitational fluctuations. Explicit expressions for the beta functions are displayed in the Appendix B.

3.3 Approximations for the beta functions

In our analysis of the system of beta functions, we have considered the following approximations:

- We set $m^2_{\rm H}$ and $m^2_{\rm S}$ to zero in the beta functions of the gauge and Yukawa couplings. This approximation allows us to integrate the flow of the gauge and Yukawa couplings independently of the quartic couplings and mass parameters.

- We work within the 1-loop approximation: since the regulator function is typically chosen to be proportional to the wave-function renormalization factors, their scale-derivative coming from the right-hand-side of the flow equation generates further anomalous dimensions contributions. Once these contributions are expressed in terms of the couplings, they lead to higher-order con-

tributions in the couplings for the beta functions. Generally, from FRG-extracted beta functions, the universal 1-loop results can be recovered for perturbatively renormalizable couplings by simply neglecting the additional anomalous dimensions contributuions coming from the regulator insertions.

- We parametrize the flow of the dimensionless gravitational couplings G and Λ with a Heaviside function according to

$$G(k) = G_* \, \theta(k - M_{\rm Pl}) \;\text{ and }\; \Lambda(k) = \Lambda_* \, \theta(k - M_{\rm Pl}) \,, \tag{3.3.1}$$

where G_* and Λ_* denote their fixed-point values, corresponding to the zero of the gravitational beta functions in [202]. This parameterization is a good approximation of the flow resulting from the integration of the beta functions in [202]. In particular, it implements the decoupling of the gravitational contributions below the Planck scale. We note that this decoupling is not due to true massive threshold effects, but due to the fact that the (dimensionful) Newton coupling is approximately constant below the Planck scale, *i.e.*, it is due to gravity transitioning into the classical-gravity regime.

3.4 Results

3.4.1 Constraints from direct detection experiments

There are several ways of constraining DM models in the IR including via direct and indirect detection, hidden decays and from requiring the correct relic density. We focus here on constraints coming direct detection Earth-based experiments. In this type of experiment, the DM candidate from *e.g.* the Milky Way scatters off the nucleon of a noble gas element such as Xenon in the XENON1T experiment [291]. One would then measure the recoil of the nucleon and from that deduce the mass of the DM particle which hit it. Currently, the experiments that provide the most stringent constraints on DM are the XENONnT [292], LUX-ZEPLIN (LZ) [293] and PandaX-4T [294] experiments. We assume that the presented models account for all of dark matter. We, thus, require a relic density of $\Omega_c h^2 = 0.120 \pm 0.001$ [274]. This requirement is satisfied on a single line in the coupling-mass parameter space for both $U(1)_{\rm D}$ and $\mathrm{SU}(2)_{\rm D}$ models, as displayed in Fig. 3.1.

An overview of the constraints of the $\mathrm{U}(1)_{\rm D}$ model can be found in [288], which focuses on DM masses $M_V < \mathcal{O}(10)$ TeV (cf. Fig. 3.1). Then, the DM mass is constrained to around 1 TeV with a coupling $0.66 \leq g_{\rm D} \leq 0.7$.

In the following section we will investigate three points in parameter space to illustrate the general situation. Besides one point in the phenomenologically viable area, we also investigate two points at lower values of the coupling, $g_{\rm D} = 0.1$ and $g_{\rm D} = 0.25$. Despite being excluded due to an overproduction of the DM relic density from thermal freeze-out according to [288], we include them in our study to

[5] The neutrino floor denotes a theoretical limit on WIMP-like DM models that could be discovered in direct detection experiments. Usually it is interpreted as the point at which DM signals are hidden underneath a similar-shaped neutrino background, since the recoil signatures of neutrinos and DM can be very much alike.

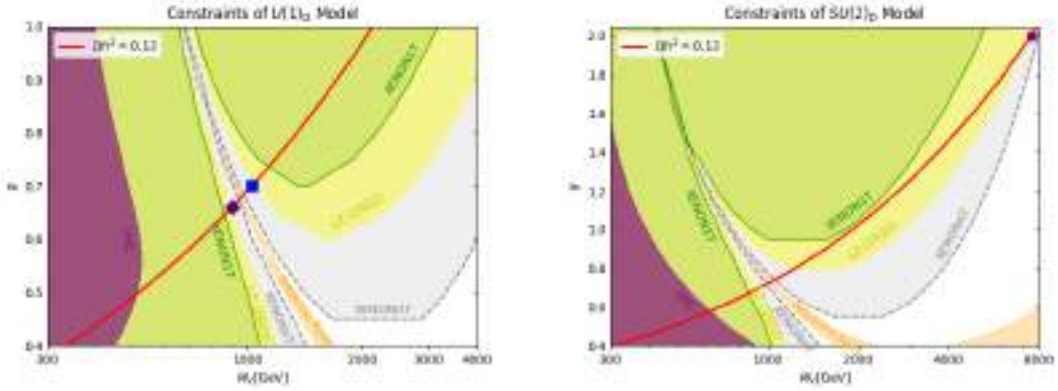

Figure 3.1: The red line indicates the correct relic abundance, $\Omega h^2 = 0.12$ [274]. The yellow region represents the excluded region by the LZ experiment [293], the green region indicates the XENON1T experiment [291], the purple region indicates the LHC constraint for Higgs decay into two dark scalars [295, 296], the orange region indicates the neutrino floor[5] [297] and the gray region is the projected 90% confidence level exclusion limit constraint from the XENONnT experiment [292]. Plots extracted from [288].

illustrate the exclusion mechanism from asymptotic safety. Furthermore, assuming a mass of $M_V = 911\,\text{GeV}$ for the vector DM candidate, these parameter points are also excluded by direct detection experiments such as XENON1T and LZ [298, 299].

For the $\text{SU}(2)_\text{D}$ model, there is a small unconstrained region similar to the $\text{U}(1)_\text{D}$ model for $0.7 \leq g_\text{D} \leq 0.8$ (cf. Fig. 3.1). Alternatively, one can consider the case where the coupling is $g_\text{D} \geq 2$, where the model generally escapes constraints from direct detection. Arguably this comes at the price of departing from the perturbative regime. Depending on how heavy a DM mass one considers, the larger the mass, the larger the coupling [288].

3.4.2 Constraints from asymptotic safety on $\text{U}(1)_\text{D}$ dark matter

In this section, we explore asymptotically safe RG-trajectories emanating from UV fixed points obtained from the beta functions presented in Appendix B. Here, we focus on the $\text{U}(1)_\text{D}$ DM model to discover whether asymptotically safe constraints are compatible with the phenomenological constraints from direct detection experiments reviewed above.

We focus on fixed-point solutions with vanishing non-Abelian gauge and bottom Yukawa couplings, *i.e.*,

$$g_{2,*} = 0\,, \quad g_{3,*} = 0 \quad \text{and} \quad y_{b,*} = 0\,. \tag{3.4.1}$$

This choice is motivated by: i) the fact that g_2 and g_3 are asymptotically free even without gravity; ii) previous studies in ASQG indicating that one can accommodate the IR-measured value of y_b on an RG-trajectory starting from $y_{b,*} = 0$ [202], whereas a nonzero fixed-point value of y_b results in a prediction of the ratio of the top and bottom mass [204] that is not our focus here.

Using the beta functions for the gravitational couplings reported in [202] to compute their fixed-point values, we find

$$G_* = 2.78 \quad \text{and} \quad \Lambda_* = -3.58\,, \tag{3.4.2}$$

FP	$g_{\mathrm{D},*}$	$g_{\mathrm{Y},*}$	$g_{2,*}$	$g_{3,*}$	$y_{t,*}$	$y_{b,*}$	Stable $V_*(\Phi,S)$?
i	0, rel	0, rel	0, rel	0, rel	0, rel	0, rel	Yes (Flat)
ii	0, rel	> 0, irrel	0, rel	0, rel	> 0, irrel	0, rel	Yes
iii	0, rel	0, rel	0, rel	0, rel	> 0, irrel	0, rel	Yes
iv	0, rel	> 0, irrel	0, rel	0, rel	0, rel	0, rel	No
v	> 0, irrel	0, rel	0, rel	0, rel	0, rel	0, rel	No
vi	> 0, irrel	> 0, irrel	0, rel	0, rel	0, rel	0, rel	No
vii	> 0, irrel	0, rel	0, rel	0, rel	> 0, irrel	0, rel	No
viii	> 0, irrel	> 0, irrel	0, rel	0, rel	> 0, irrel	0, rel	No

Table 3.1: Classification of fixed-point solutions for the gauge-Higgs-top-bottom system with $\mathrm{U}(1)_\mathrm{D}$ DM sector with gravity. Herein, "rel" stands for relevant directions and "irrel" denotes irrelevant directions. $V_*(\Phi,S)$ stands for the scalar potential evaluated at the fixed-point values of the mass parameters and quartic couplings. We note that the fixed point (i) has a flat scalar potential, *i.e.* $V_*(\Phi,S)=0$

which are obtained by setting the matter content to that of the SM plus the $\mathrm{U}(1)_\mathrm{D}$ DM model.

In total, there are eight fixed-point candidates compatible with Eq. (3.4.1) and Eq. (3.4.2). In Tab. 3.1, we classify the different fixed points in terms of the signs and (ir)relevance of gauge and Yukawa couplings.

First, we note that the fixed points with non-vanishing gauge coupling g_D (FP's (v)-(viii), cf. Tab. 3.1) lead to a negative (unstable) scalar potential in the fixed-point regime, *i.e.*, at least the dark quartic scalar coupling λ_S is negative at the fixed point. This is a consequence of the signs of the g_D^4 and g_D^2 contributions to $\beta_{\lambda_\mathrm{S}}$ and $\beta_{m_\mathrm{S}^2}$, respectively, cf. Eq. (B.0.11) and Eq. (B.0.17). That these terms can trigger negative quartic couplings is a generic result and holds whenever the gravitational contribution is not too large, see Tab. 1 in [300].

Similarly, the fixed point with $g_{\mathrm{Y},*}>0$ and $y_{t,*}=0$ (FP (iv), cf. Tab. 3.1) leads to negative fixed-point values for λ_H and m_H^2 through a similar type of terms in the respective beta functions.

In our study, we stay within a near-perturbative regime and therefore assume that the quadratic and quartic terms in the potential are sufficient. We further assume that the fixed-point potential should be stable in order to yield a well-defined path integral. Thus, we will not investigate RG-trajectories emanating from fixed-point candidates with negative values of quartic couplings.

Second, we also disregard the fixed point (ii) in Tab. 3.1. This is motivated by previous studies in ASQG indicating that a fixed point with $g_{\mathrm{Y},*}>0$ leads to a prediction of the IR value of the hypercharge gauge coupling that is approximately 35% larger than the measured value [203]. The fixed-point value here is different than in [203], because it is affected by the dark degrees of freedom which change the gravitational fixed-point values and therefore the fixed-point values of matter couplings. Nevertheless, the change is not sufficient to produce the correct value of the gauge coupling in the IR. The fixed-point value of the hypercharge gauge coupling with DM degrees of freedom is $g_{\mathrm{Y},*}=1.143$, whereas its Planck-scale value in the Standard Model is significantly smaller.

The remaining viable fixed points are the candidates (i) and (iii) in Tab. 3.1. We focus on the fixed point (iii), which is the most predictive among the viable options. In particular, we note that the top Yukawa coupling corresponds to an irrelevant direction at the fixed point (iii), which means that one can predict its IR value as a function of the relevant couplings. At the same time, this prediction

IR values at $k = 173$ GeV			
Coupling	$g_D = 0.10$	$g_D = 0.25$	$g_D = 0.66$
g_Y (free par.)	0.35	0.35	0.35
g_2 (free par.)	0.65	0.65	0.65
g_3 (free par.)	1.17	1.17	1.17
y_t (pred.)	0.665	0.664	0.665
λ_H (pred.)	$-3.88 \cdot 10^{-2}$	$-4.15 \cdot 10^{-2}$	$-3.87 \cdot 10^{-2}$
λ_S (pred.)	$-9.77 \cdot 10^{-4}$	$-4.27 \cdot 10^{-2}$	$-4.63 \cdot 10^{7}$
λ_p (pred.)	$-3.13 \cdot 10^{-7}$	$-2.16 \cdot 10^{-6}$	-1.86
m_H^2 (free par.)	-0.005	-0.005	-0.005
m_S^2 (free par.)	-0.5	-0.5	-0.5

Table 3.2: We show IR values of various couplings in the $U(1)_D$ DM model evaluated at $k = 173$ GeV for different IR values of g_D. The label "free par." indicates that the RG-flow allows us to choose the IR value of the corresponding coupling, since it is a free parameter. In contrast, the label "pred." indicates that the IR value is a prediction of an RG-trajectory with asymptotically safe boundary condition.

corresponds to an upper bound on values of the top Yukawa coupling achievable from fixed point (i). Due to this property, we will see that by ruling out fixed point (iii), we simultaneously rule out fixed point (i).

The quartic couplings λ_H, λ_S and λ_p are also irrelevant at this fixed point. Thus, their IR values are predictions of the RG-trajectories emanating from such a fixed point. Explicitly, the fixed point (iii) is located at

$$\begin{aligned} &g_{Y,*} = 0\,, \qquad g_{2,*} = 0\,, \qquad g_{3,*} = 0\,, \qquad g_{D,*} = 0, \\ &y_{t,*} = 0.20\,, \qquad y_{b,*} = 0, \\ &\lambda_{H,*} = 5.56 \cdot 10^{-3}, \qquad \lambda_{S,*} = 0, \qquad \lambda_{p,*} = 0, \\ &(m_H^2)_* = 7.59 \cdot 10^{-4}, \qquad (m_S^2)_* = 0\,. \end{aligned} \tag{3.4.3}$$

Note that the scalar potential at this fixed point is flat in the dark scalar direction.

We obtain RG-trajectories by integrating the system of beta functions reported in Appendix B with boundary conditions corresponding to the fixed point in (3.4.3). In the integration process, we select the RG-trajectories to match the appropriate IR values for relevant couplings g_Y, g_2, g_3 and y_b. In particular, we use their reference one-loop values at $k_{IR} = 173\,\text{GeV}$ [6]. We decouple the bottom Yukawa coupling by approximating $y_b \approx 0$. In Tab. 3.2, we summarize the IR values of the various couplings at 173 GeV.

We investigate the three benchmark values for the $U(1)_D$ dark gauge coupling,

$$g_D(M_V = 911\ \text{GeV}) = 0.10, 0.25, 0.66\,, \tag{3.4.4}$$

fixed at a phenomenologically relevant mass scale. The latter matches the phenomenologically viable point explored in [288] (cf. Fig. 3.1).

In Fig. 3.2, we plot the RG-trajectories for various couplings in our model. In the first row, we show the gauge and Yukawa couplings, which show a SM-like behavior for the SM gauge couplings. The dark gauge coupling is asymptotically free (which is a crucial difference to the setting without gravity) and decreases very slowly in the IR. The top Yukawa coupling increases towards the IR from its fixed-point

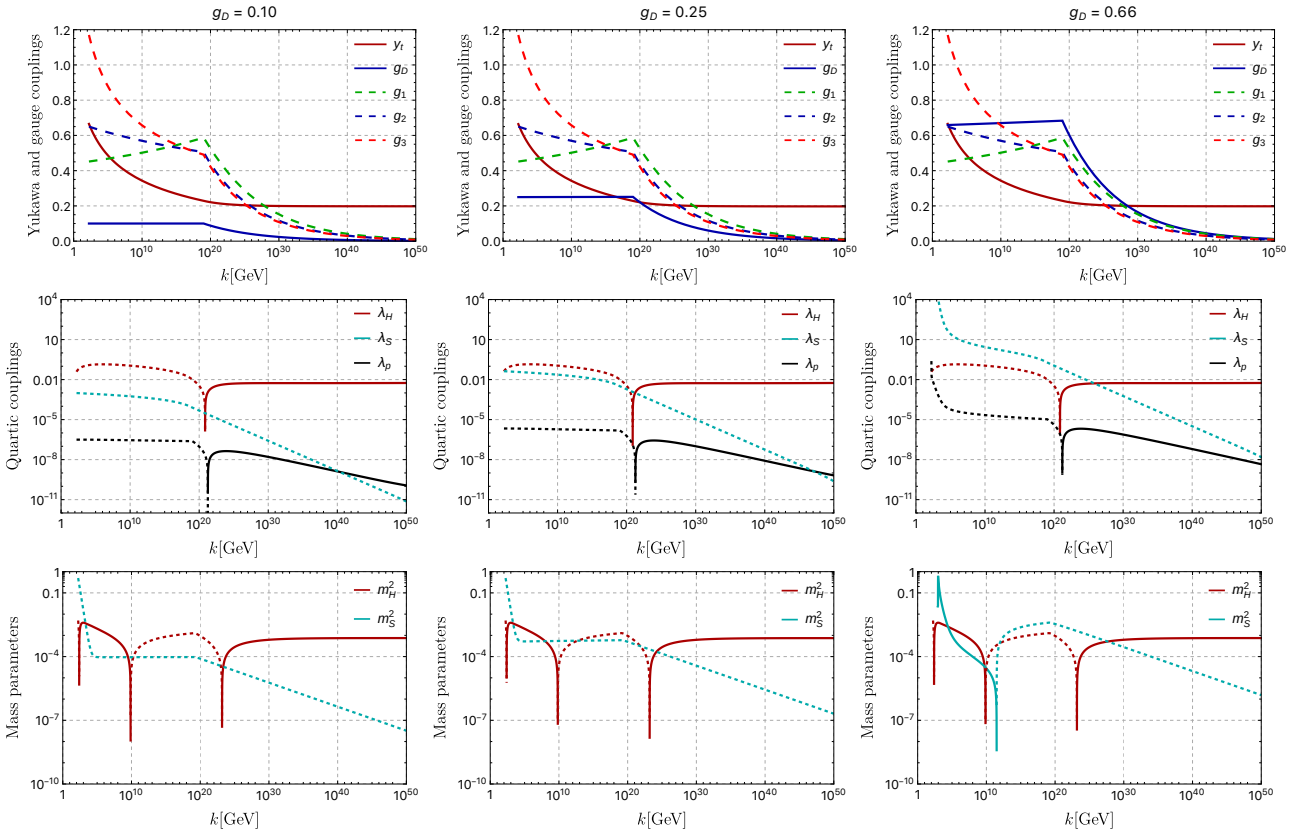

Figure 3.2: RG-trajectories of various couplings in the $U(1)_D$ DM model for different IR values of the dark gauge coupling, $g_D(M_V = 911\ \text{GeV}) = 0.10$ (left), 0.25 (middle) and 0.66 (right panels). The top panels depict top Yukawa and gauge couplings, where the RG-flow of the bottom Yukawa coupling is omitted and we employ the normalization $g_1 = \sqrt{5/3}g_Y$. The middle panels illustrate scalar couplings, with negative values (dashed lines) indicating unstable potential in both the Higgs and dark scalar directions, posing a challenge to asymptotic safety. Finally, the bottom panels display the dimensionless mass parameters of the Higgs and the dark scalar.

value. Its predicted value in the IR is too low compared to measurements [301, 302]. This is different from the result in [202], where the predicted value was compatible with the experimentally determined value. The difference between the two settings are the dark sector degrees of freedom. These impact the top Yukawa coupling indirectly: they change the gravitational fixed-point values, which in turn change the top Yukawa fixed-point value.

In the second row of Fig. 3.2, we show RG-trajectories corresponding to the quartic couplings λ_H, λ_S and λ_p. All quartic couplings become negative in the IR. This is caused by gauge field fluctuations, encoded in the g_D^4-term in the beta function β_{λ_S}. Since the term proportional to g_D^4 has a positive coefficient, it drives the quartic coupling towards negative values in the IR. In the beta functions for λ_H and λ_p, there is a competition between positive and negative terms. In the UV, the negative terms dominate, such that λ_H and λ_p flow towards positive values. Further in the IR, the positive terms in λ_H and λ_p start to dominate over the negative ones, thus pushing λ_H and λ_p towards negative values. The transition from positive to negative values of λ_H and λ_p happens around $k = 10^{21}$ GeV. All quartic couplings remain negative below this scale.

Furthermore, we have verified that the Higgs and dark quartic couplings flow towards negative IR values even when the mass parameters are excluded from the system of RG equations. The main

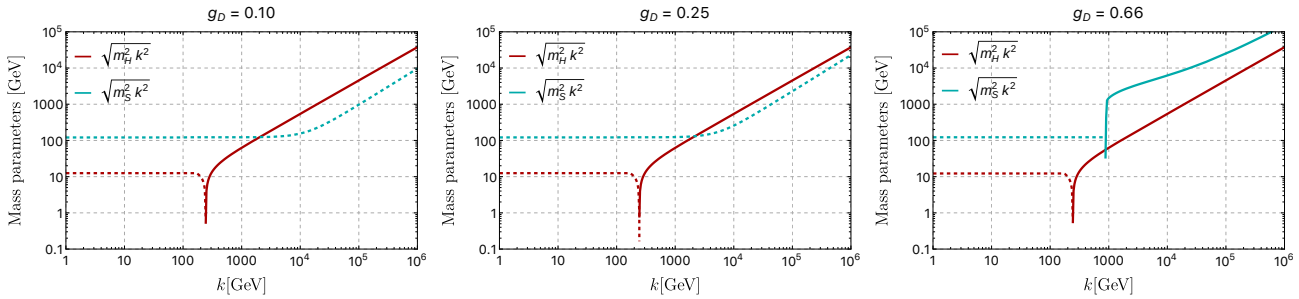

Figure 3.3: RG-trajectories of the dimensionful mass parameters ($\sqrt{m_i^2 k^2}$ with $i = \mathrm{H}, \mathrm{S}$) for various IR values of the dark gauge coupling, $g_\mathrm{D}(M_V = 911\ \mathrm{GeV}) = 0.10$ (left), 0.25 (middle) and 0.66 (right panel).

difference is that, in this case, the portal coupling vanishes along the entire RG-trajectory.

In the third row of Fig. 3.2, we plot the RG-trajectories for the dimensionless (squared) mass parameters m_H^2 and m_S^2 (see also Fig. 3.3 for RG-trajectories of the dimensionful mass parameters ($\sqrt{m_i^2 k^2}$ with $i = \mathrm{H}, \mathrm{S}$) in the IR region). For the Higgs mass parameter, we obtain the same behavior for all the benchmark values of the dark gauge coupling g_D. As we see, the running of m_H^2 oscillates between positive and negative values. We select its IR value according to Tab. 3.2 as an attempt to obtain spontaneous symmetry-breaking in the IR. The dark mass parameter departs from its fixed-point value $(m_\mathrm{S}^2)_* = 0$ in the UV towards negative values. It remains negative all the way to the deep IR for the benchmark values $g_\mathrm{D}(k = 911\,\mathrm{GeV}) = 0.10$ and $g_\mathrm{D}(k = 911\,\mathrm{GeV}) = 0.25$. For $g_\mathrm{D}(k = 911\,\mathrm{GeV}) = 0.66$, m_S^2 becomes positive in the IR.

The overall picture we obtain is this: starting from an asymptotically safe transplanckian regime one can connect the gauge couplings to phenomenologically viable values in the IR. There are, however, two problems with other couplings. First, the top quark Yukawa coupling is predicted to be significantly smaller than the measured value. Because this prediction also serves as an upper bound for top-Yukawa-values of fixed point (i), it also puts fixed point (i) in tension with experiment. Second, the quartic scalar couplings run towards negative IR values, which results in a perturbatively unstable scalar potential.[6] This is a strong indication that the $\mathrm{U}(1)_\mathrm{D}$ DM model explored in [288] is incompatible with ASQG. We emphasize that this conclusion is not just a consequence of the specific benchmark values used in our analysis. The instability of the scalar potential is a general consequence of the positive contribution involving gauge couplings to the 4^{th} power in the beta functions for the quartic couplings. Therefore, different benchmark values of $g_D(k = 911\,\mathrm{GeV})$ can change quantitative details, but without changing our qualitative results.

3.4.3 Constraints from asymptotic safety on $\mathrm{SU}(2)_\mathrm{D}$ dark matter

The RG flow obtained with the $\mathrm{SU}(2)_\mathrm{D}$ DM model shares many of the features with the $\mathrm{U}(1)_\mathrm{D}$ model discussed in the previous section. Nevertheless, there are important differences:

- First, the non-Abelian dark gauge coupling g_D is asymptotically free even in the absence of

[6] In our setting, we cannot exlude that a non-perturbative IR setting may be phenomenologically viable and feature a stable potential in the presence of higher-order terms.

gravity. This reduces the number of fixed-point candidates, as $g_{\mathrm{D},*} = 0$ is the only possibility of UV completion for the non-Abelian dark gauge coupling. In this case, the possible fixed-point candidates share the same feature as the candidates (i)-(iv) in Tab. 3.1.

- Second, using the matter content of $\mathrm{SU}(2)_{\mathrm{D}}$ DM model, one obtains the fixed-point values $G_* = 1.88$ and $\Lambda_* = -2.19$. At this fixed point, the value for the cosmological constant lies outside the viable region for UV completion of Yukawa couplings ($\Lambda \lesssim -3.3$ [202]), *i.e.*, the Yukawa couplings vanish at the Planck scale.

In principle, one can argue that the last point already indicates the incompatibility between the $\mathrm{SU}(2)_{\mathrm{D}}$ DM model with ASQG. However, the fixed-point values of the gravitational couplings are subject to large systematic uncertainties, and it is interesting to explore the qualitative features of the RG-flow independently of specific values of G_* and Λ_*.

We thus explored RG-trajectories obtained by integrating the flow with benchmark values for G_* and Λ_* lying inside the viable region for UV completion in the Yukawa sector. We focused on trajectories with boundary conditions corresponding to a UV fixed point with similar features as the fixed-point candidate (iii) in Tab. 3.1. The resulting trajectories are similar to the ones obtained in the previous subsection.

In particular, the RG-flow drives the quartic scalar couplings to negative values in the IR, resulting in a perturbatively unstable scalar potential. Again, this is a consequence of positive contributions to the beta functions of the quartic scalar couplings that are proportional to the gauge couplings. This result constitutes a strong indication of the incompatibility between the $\mathrm{SU}(2)_{\mathrm{D}}$ DM model and ASQG. We refer the reader to [188] for an up-to-date status of DM models which have indications of being compatible with ASQG.

Chapter 4

Fate of Chiral Symmetry in Riemann-Cartan Spaces

4.1 Light fermions

In the Standard Model, the masses of all quarks and leptons, that constitute our visible Universe, are very much light as compared to the Planck scale. The generation of masses for fermions is related to the breaking of chiral symmetry. This symmetry merely rotates the left- and right-handed chiralities of a Dirac fermion field, $\psi_{\rm L}$ and $\psi_{\rm R}$[1], into each other independently, prohibiting the formation of a mass term $m_\psi\bar{\psi}\psi = m_\psi(\bar{\psi}_R\psi_{\rm L} + \bar{\psi}_{\rm L}\psi_{\rm R})$, see also Subsection (4.2.1). At two distinct energy scales, there are two independent mechanisms in the Standard Model that underpin the generation of fermion masses. First, at the Fermi scale (or electroweak scale), characterized by the vacuum expectation value (VEV) of the Higgs field, $v_{\rm EM} \approx 246$ GeV, the Englert-Brout-Higgs-Guralnik-Hagen-Kibble mechanism[2] generates *current* masses for the quarks and charged leptons[3] triggered by the Higgs-Yukawa couplings [303–306]. Below this, at the QCD scale $\Lambda_{\rm QCD} = \mathcal{O}(100)$ MeV, the masses of the nucleons (protons and neutrons) are lifted dynamically through the interactions of quarks with gluons, leading to the *constituent-quark masses*.

For instance, focusing on the light quark sector of the SM, comprised of the up and down quarks, the *current-quark masses* of the light u and d quarks are of order of a couple of MeV, $(m_{u/d})_{\rm cur} \approx 3-5$ MeV, which are two orders of magnitude smaller than the constituent-quark masses, $(m_{u/d})_{\rm con} \approx 300-400$ MeV. Since the proton is made up of three quarks (uud), this explains why about 99% of the mass of the proton (which is ≈ 938 MeV) is dynamically produced in QCD. This mechanism is also called *dynamical chiral symmetry breaking* (DχSB), which is a nonperturbative effect as it is rooted in the low-energy regime of QCD, where notably the strong coupling $\alpha_{\rm QCD}$ is large.

On the other hand, it is conceivable that the attractive nature of gravity could induce genera-

[1] The left- and right-handed chiralities of a Dirac fermion field is defined through the chiral projectors, $P_{\rm R,L} = \frac{1}{2}(\mathbf{1}\pm\gamma_5)$, with $\psi_{\rm R,L} = P_{\rm R,L}\psi$.

[2] For brevity, from now on, we will only refer to it as "the Higgs mechanism".

[3] The Higgs mechanism also generates masses for the gauge bosons of the weak interactions, *i.e.*, the $W^\pm$ and Z^0 vector bosons.

tion of nontrivial fermionic bound states in a nonperturbative regime due to metric fluctuations and, consequently, breaking chiral symmetry. In this scenario, the mass spectrum of all fermions in our Universe would be of the order of the Planck mass, being thus incompatible with observations. In this sense, one could conceive of a number of mechanisms that could break chiral symmetry in quantum gravity. Here, we focus on three mechanisms. The first is due to induced graviton fluctuations. This has been investigated in the context of asymptotically safe quantum gravity and no induced interaction terms that could violate chiral symmetry were observed thus far [222, 225]. A regulator function that explicitly violates chiral symmetry could change this conclusion.

Nevertheless, graviton fluctuations induce fermions (self-)interactions [200, 219, 221, 223, 307], being the second mechanism considered. The class of interactions induced by gravity belongs to the chirally-symmetric four-fermion interactions of the Nambu-Jona-Lasinio type, which are characterized by dimension-six operators of the form

$$S_{\text{Induced}-4\text{F}} = \frac{1}{16\pi G_{\text{N}}} \int_x \sqrt{\det g} \left(\bar{\lambda}_+ \left(\mathcal{V} + \mathcal{A} \right) + \bar{\lambda}_- \left(\mathcal{V} - \mathcal{A} \right) \right), \tag{4.1.1}$$

with the local four-fermion operators for N_{F} flavors

$$\mathcal{V} = (\bar{\psi}^i \gamma_\mu \psi^i)(\bar{\psi}^j \gamma^\mu \psi^j), \qquad \mathcal{A} = (\bar{\psi}^i i\gamma_\mu \gamma_5 \psi^i)(\bar{\psi}^j i\gamma^\mu \gamma_5 \psi^j), \tag{4.1.2}$$

where $i, j \in \{1, \ldots, N_{\text{F}}\}$ and the sum over the indices $i, j, \cdots$ is implied. This class of induced four-fermion interactions has also been investigated within the asymptotic safety framework of quantum gravity [200, 219, 221]. In particular, the combination of Abelian gauge and metric fluctuations leads to a lower bound on the number of charged fermions in order for chiral symmetry to be intact [307]. However, in a QCD-gravity system, topology-changing fluctuations induced by gravitational instantons possibly lead to anomalous spontaneous chiral-symmetry-breaking at the Planck scale [308].

The third aspect of the interplay between gravity and chiral symmetry breaking is the mechanism of *gravitational catalysis*, which is already operative on classical geometries [168, 309–336]. In this case, a negative spacetime curvature, which encodes the effects of the gravitational background field, generates an effective mass term for fermionic systems. In this sense, an anti-de Sitter geometry *catalyses* nontrivial bound-state formation. In particular, this phenomenom is a consequence of an effective dimensional reduction in the spectrum of the Dirac Laplacian. The mechanism of gravitational catalysis resembles the magnetic catalysis of chiral symmetry breaking for (2+1)-dimensional fermionic systems placed in a magnetic background field [337–340].

In [334], the mechanism of gravitational catalysis was used in conjunction with the effects of metric fluctuations in ASQG to establish a bound on the curvature of local patches of spacetime by demanding long-range chiral symmetry to remain intact. As pointed out in [334], the mechanism of gravitational catalysis produces an upper bound on the number of fermions that are compatible with chiral symmetry. This result was later extended to include thermal effects [335].

So far, studies of the phenomenon of gravitational catalysis are mostly restricted to formulations of gravity where the spacetime geometry is fully characterized by the metric. However, there are other

proposals of gravitational theories that give rise to richer geometric structures. For example, the general class of metric-affine theories [19, 341, 342] treats the spacetime metric and the affine connection as independent objects. In contrast to the metric formulation, where the spacetime geometry can be entirely specified by the curvature tensor, in the metric-affine formulation, the spacetime geometry also depends on information about the nonmetricity and the torsion tensors. The general class of metric-affine theories includes Palatini [343–345] and teleparallel [346–348] theories as special cases.

Within metric-affine theories, we can also describe gravity in such a way that the metric and the affine connection are built in terms of more fundamental (and independent) objects, namely, the vierbein and the spin connection. A particular case is the so-called Einstein-Cartan theory, see [14–19]. In general, the spacetime geometry encoded in the Einstein-Cartan formalism is characterized by curvature and torsion. The Einstein-Cartan formulation has the appealing feature of bringing gravity to a language that is closer to the other fundamental interactions. The spin connection is the gauge field associated with local Lorentz symmetry, thus playing a similar role to the gauge bosons in Yang-Mills theories.

The Einstein-Cartan formalism is naturally related to some approaches to quantum gravity, such as loop quantum gravity and spin foams [349, 350]. In this context, spin foam models formulated in terms of BF-theories exhibit a correspondence to the Einstein-Cartan action augmented with the Holst term. The Holst action was also investigated in the context of ASQG, pointing toward the viability of an asymptotically safe theory formulated in terms of Einstein-Cartan formalism [351].

The Einstein-Cartan theory is classically equivalent to the Einstein-Hilbert theory in the absence of fermions. In the presence of fermions, torsion is naturally sourced and metric and torsion (or more naturally, metric and affine connection) are independent fundamental variables. Indeed, in this case, torsion is, on-shell, expressed in terms of fermionic bilinears. Once it is plugged back into the original action, it gives rise to a metric theory with additional dimension-six operators accounting for the interaction of fermionic axial[4] currents [354–356]. In this scenario, phenomenological implications for inflation and dark matter production were investigated in [353, 357]. At the quantum level, it is expected that the Einstein-Cartan theory is not equivalent to the quantum Einstein-Hilbert formalism. Thus, in the search for a theory of quantum gravity, it would be helpful to have a classification of the degrees of freedom we should account for in the quantization process.

In this chapter, we explore the possibility of using the interplay between chiral symmetry breaking and gravity to gain some insights on the allowed geometric structures in a gravitational theory due to its coupling to matter degrees of freedom. We focus on the Einstein-Cartan theory, where the spacetime geometry can exhibit nonvanishing torsion. Focusing on a fermionic system coupled to a gravitational background with nonvanishing torsion, we study the impact of the background torsion on the dynamics of four-fermion interactions. In particular, our goal is to understand whether torsion acts in favor or against chiral symmetry breaking, and whether torsion can also act as a gravitational

[4]The presence of torsion allows for nonminimal Dirac kinetic terms (see, *e.g.*, [352, 353]), which then generate interactions of parity-violating axial-vector currents and vector-vector currents. In this work, we leave out the possibility of considering these nonminimal interactions.

catalyzer. Our findings suggest that spacetime torsion acts in favor of chiral symmetry breaking, but not enough to engender gravitational catalysis.

4.2 Chiral symmetry breaking mechanism in Riemann-Cartan background

4.2.1 Setup

In this section, the general setup for the investigation is presented. In this first part, we give a brief detour on the main features of the Riemann-Cartan geometry, which forms the basis for the Einstein-Cartan formulation, or otherwise generically known as the first order formalism of gravity [358]. In the second part, we present the fermionic system chosen to probe the fate of chiral symmetry in the presence of both curvature and torsion.

Overview of Riemann-Cartan geometry

In Riemann-Cartan geometry, the spacetime geometry is characterized by the tetrad/vierbein 1-form $e^a(x) = e^a{}_\mu(x)\,\mathrm{d}x^\mu$ and the spin connection 1-form $\omega^{ab}(x) = \omega^{ab}{}_\mu(x)\,\mathrm{d}x^\mu$, with x being a arbitrary spacetime point over a four-dimensional[5] differentiable manifold $\mathcal{M}$. The spin-connection $\omega^{ab}(x)$ defines the notion of parallel transport of tensors on $\mathcal{M}$ as it is deeply connected with the affine connection (see discussion below). Here and hereafter, the Latin *frame indices* $a, b, c, \ldots$ refer to coordinates in the tangent space $T_x(\mathcal{M})$ of the manifold, while Greek *world indices* $\mu, \nu, \alpha, \ldots$ refer to local spacetime coordinates in a given chart. Throughout this chapter, the quantum fields are written within Euclidean signature, since functional renormalization group methods will be employed[6]. In this way, $T_x(\mathcal{M})$ corresponds to Euclidean flat space of flat metric $\delta_{ab} = \mathrm{diag}(+,+,+,+)$. Nevertheless, the term spacetime will still be used to refer to the background space where quantum fields are defined.

For every spacetime point $x \in \mathcal{M}$, a coordinate system x^μ is related to a local inertial frame x^a in the tangent space by means of the isomorphism $\mathrm{d}x^a = e^a{}_\mu(x)\mathrm{d}x^\mu$ and $dx^\mu = e_a{}^\mu(x)dx^a$, with $e_a{}^\mu(x)$ being the inverse of the vierbein field [12, 360]. In this sense, the isomorphism relations ensure the metric field arises as a composite field built from the vierbein as $g_{\mu\nu}(x) = e^a{}_\mu(x)e^b{}_\nu(x)\delta_{ab}$. An infinite number of inertial frames are connected to each other by means of an SO(4) transformation, leaving the metric field invariant. For this Euclidean orthonormal frame, these local frame rotations form the

[5] In d dimensions, $e^a{}_\mu(x)$ is called the *vielbein*, while for specific dimensions, one has *zweibein, dreibein, vierbein* and so on for, respectively, $2, 3, 4, \ldots$.

[6] See [117, 118, 121, 122, 253–256, 359] for recent developments on Lorentzian formulation of the functional renormalization group with a direct or indirect focus toward a quantum field theory of gravity or general quantum fields on curved backgrounds.

isometry group of the Euclidean spacetime.[7]

We define the covariant derivative acting on objects with frame (implicit) and world indices by the following rule

$$D_\mu A_{\nu_1 \dots \nu_k} = (\partial_\mu + \omega_\mu) A_{\nu_1 \dots \nu_k} - \sum_{i=1}^{k} \Gamma^\lambda_{\mu \nu_i} A_{\nu_1 \dots \nu_{i-1} \lambda \nu_{i+1} \dots \nu_k}, \tag{4.2.1}$$

where $\omega_\mu = \frac{1}{2}\omega^{ab}{}_\mu \Sigma_{ab}$, with Σ_{ab} being the generators of the orthogonal group. Both $\omega^{ab}{}_\mu$ and Σ_{ab} are antisymmetric in the tangent space indices, *i.e.*, $\omega^{ab}{}_\mu = -\omega^{ba}{}_\mu$ and $\Sigma_{ab} = -\Sigma_{ba}$. The compatibility conditions on both the vierbein and the metric are assumed, which are expressed by $D_\mu e^a{}_\nu = 0$ (vierbein postulate) and $D_\mu g_{\nu\lambda} = \nabla_\mu g_{\nu\lambda} = 0$, where ∇_μ is the standard covariant derivative that acts on objects containing only world indices, thus depending only on the affine connection $\Gamma^\alpha_{\mu\nu}$. The compatibility conditions ultimately ensure that the nonmetricity tensor, $Q_{\mu\nu\lambda} = \nabla_\mu g_{\nu\lambda}$, vanishes[8] and allow us to establish a relation between the spin connection and the affine connection, namely

$$\Gamma^\lambda_{\mu\nu} = e_a{}^\lambda (\partial_\nu e^a{}_\mu + \omega^a{}_{b\nu} e^b{}_\mu). \tag{4.2.2}$$

Equation (4.2.2) implies that the affine connection $\Gamma^\alpha_{\mu\nu}$ is not necessarily symmetric in its two lower indices. The antisymmetric contribution of the connection $\Gamma^\alpha_{\mu\nu}$ defines the torsion tensor $T^\lambda{}_{\mu\nu} = e_a{}^\lambda T^a{}_{\mu\nu} = \Gamma^\lambda_{\mu\nu} - \Gamma^\lambda_{\nu\mu}$, which can be written as the field strength of the vierbein, *i.e.*,

$$T^a{}_{\mu\nu} = \partial_\mu e^a{}_\nu - \partial_\nu e^a{}_\mu + \omega^a{}_{c\mu} e^c{}_\nu - \omega^a{}_{c\nu} e^c{}_\mu. \tag{4.2.3}$$

In the case of vanishing torsion tensor, the affine connection is symmetric in its lower indices, being thus given by the Levi-Civita connection and GR is recovered.

Additionally, the field strength of the spin connection defines the Riemann-Cartan curvature tensor[9]. Its components in the dual basis reads

$$R^{ab}{}_{\mu\nu} = \partial_\mu \omega^{ab}{}_\nu - \partial_\nu \omega^{ab}{}_\mu + \omega^a{}_{c\mu} \omega^{cb}{}_\nu - \omega^a{}_{c\nu} \omega^{cb}{}_\mu. \tag{4.2.4}$$

The vierbein can be used to recast local indices in favor of world indices, namely $R^\alpha_{\beta\mu\nu} = e^\alpha_a \, e_{\beta b} R^{ab}{}_{\mu\nu}$, which is the usual Riemann tensor related to the affine connection $\Gamma^\alpha_{\mu\nu}$.

[7] For a Minkowski flat tangent space, the local inertial coordinate system enforces the strong equivalence principle [360], which states that at every point in spacetime, it is always possible to find an orthonormal basis (excluding thus the effects of gravity). In this sense, for local spacetime regions, the laws of special relativity hold. Put differently, tangent spaces of flat Minkowskian metric are equivalent to freely falling local reference frames. In this case, locally there are infinite equivalent tangent spaces connected by local Lorentz transformations via $e'^a{}_\mu(x) = \Lambda^a{}_b(x) e^b{}_\mu(x)$, with $\Lambda^a{}_b(x) \in \mathrm{SO}(1,3)$, and the isometry group of the Minkowski space is given by the Lorentz group.

[8] Geometrically, if the nonmetricity tensor does not vanish, then the norm of a vector is not preserved under parallel transport. For metric-affine Langrangians under suitable conditions, *a priori* a nonvanishing nonmetricity tensor would imply the propagation of a *potentially* dangerous free massless spin-3 particle [342, 361, 362].

[9] The geometrical interpretation of curvature and torsion is quite simple. The curvature tensor carries information on the failure of the parallelogram rule of vector addition. In other words, it describes how the orientation of a vector gets modified by a parallel transport around a closed path. If, additionally, torsion is present, then the parallelogram formed by the parallel transport of any two vectors will not close.

One can solve Eq. (4.2.3) for the spin connection, resulting in the following expression

$$\omega^{ab}{}_{\mu} = \mathring{\omega}^{ab}{}_{\mu}(e) + K^{ab}{}_{\mu}(e,T). \tag{4.2.5}$$

The first term is the so-called Levi-Civita spin connection and encodes the torsion-independent part of $\omega^{ab}{}_{\mu}$. One can express the Levi-Civita spin connection solely in terms of the vierbein, namely

$$\mathring{\omega}^{ab}{}_{\mu}(e) = \frac{1}{2} e_{c\mu} \left(\Omega^{abc} + \Omega^{bca} - \Omega^{cab} \right), \tag{4.2.6}$$

where $\Omega^{abc} = e^{a\nu} e^{b\lambda} \left(\partial_\nu e^c{}_\lambda - \partial_\lambda e^c{}_\nu \right)$. Throughout this chapter, a circle on top of geometrical objects indicates association with the torsionless part of the underlying geometry. The second term in (4.2.5) is the contorsion tensor defined by

$$K^{ab}{}_{\nu} = \frac{1}{2} \Big(e^{a\lambda} e^{b\mu} - e^{b\lambda} e^{a\mu} \Big) (T_{\lambda\mu\nu} - T_{\mu\nu\lambda} + T_{\nu\lambda\mu}). \tag{4.2.7}$$

Note that this tensor is antisymmetric in its first two indices. Moreover, Eqs. (4.2.4) and (4.2.5) allow us to write the relation

$$R^{\alpha}{}_{\beta\mu\nu} = \mathring{R}^{\alpha}{}_{\beta\mu\nu} + \mathring{\nabla}_\mu K^{\alpha}{}_{\beta\nu} - \mathring{\nabla}_\nu K^{\alpha}{}_{\beta\mu} + K^{\alpha}{}_{\lambda\mu} K^{\lambda}{}_{\beta\nu} - K^{\alpha}{}_{\lambda\nu} K^{\lambda}{}_{\beta\mu}, \tag{4.2.8}$$

where $\mathring{\nabla}_\mu$ and $\mathring{R}^{\lambda}{}_{\rho\mu\nu}$ denote, respectively, the covariant derivative and Riemann curvature tensor associated with the (torsionless) Levi-Civita connection $\mathring{\Gamma}^{\alpha}_{\mu\nu}$ (Christoffel symbols). We emphasize that the Riemann-Cartan curvature tensor $R^{\alpha}{}_{\beta\mu\nu}$ is no longer symmetric under simultaneous change of pair of indices. Due to this missing symmetry, the Ricci tensor constructed from the Riemann-Cartan curvature tensor, $R_{\mu\nu} = R^{\alpha}{}_{\beta\alpha\nu}$, is no longer symmetric ($R_{\mu\nu} \neq R_{\nu\mu}$). For completeness, the corresponding Ricci scalar for the connections $\Gamma^{\lambda}{}_{\mu\nu}$ is the unique contraction $R = R^{\mu\nu}{}_{\mu\nu}$ and it is written in terms of the torsion tensor as

$$R = \mathring{R} + \frac{1}{4} T_{\alpha\beta\lambda} T^{\alpha\beta\lambda} + \frac{1}{2} T_{\alpha\beta\lambda} T^{\beta\alpha\lambda} + T^{\alpha}{}_{\alpha}{}^{\beta} T^{\lambda}{}_{\beta\lambda} - 2\mathring{\nabla}_\beta T^{\alpha}{}_{\alpha}{}^{\beta}. \tag{4.2.9}$$

Note that the last term $\propto 2\mathring{\nabla}_\beta T^{\alpha}{}_{\alpha}{}^{\beta}$ can be disregarded. In manifolds with boundary, this term would give rise to a surface contribution.

Four-fermion interactions in a Riemann-Cartan framework

We aim to study the impact of torsion on the fate of chiral symmetry. For this purpose, we consider the NJL model [163, 363] for a system with N_{F} Dirac fermions in a curved background with nonvanishing torsion. The starting point is a chirally symmetric (Euclidean) action comprising the $(\mathcal{V}+\mathcal{A})$-channel of four-fermion interactions

$$S[\psi, \bar{\psi}; e] = \int_x \left(\frac{i}{2} \big(\bar{\psi}^i \gamma^\mu D_\mu \psi^i - D_\mu \bar{\psi}^i \gamma^\mu \psi^i \big) - \frac{\lambda}{4} (\mathcal{V} + \mathcal{A}) \right), \tag{4.2.10}$$

with local (dimension-six) four-fermion operators[10] of the form of (4.1.2). Herein, we adopt the shorthand notation $\int_x = \int \mathrm{d}^4x\,|e|$ for the integral over the four-dimensional spacetime with $|e| = \det(e^a{}_\mu) = \sqrt{\det g}$. The Dirac gamma matrices in a curved background are connected to their tangent/flat space counterparts via the vierbein, *i.e.*, $\gamma_\mu = e^a{}_\mu \gamma_a$, and satisfy the (Euclidean) Clifford algebra $\{\gamma_\mu, \gamma_\nu\} = 2g_{\mu\nu}\mathbf{1}_4$ and $\gamma_5 = \gamma^0\gamma^1\gamma^2\gamma^3$ (see App. (A) for more details on Euclidean conventions). The covariant derivative acts on Dirac fermions according to

$$D_\mu \psi = \partial_\mu \psi + \frac{1}{8}\,\omega^{ab}{}_\mu [\gamma_a, \gamma_b]\,\psi\,, \tag{4.2.11}$$

$$D_\mu \bar{\psi} = \partial_\mu \bar{\psi} - \frac{1}{8}\omega^{ab}{}_\mu\,\bar{\psi}\,[\gamma_a, \gamma_b]\,. \tag{4.2.12}$$

The action (4.2.10) is symmetric under the global chiral group $\mathrm{SU(N_F)_L \times SU(N_F)_R}$, which corresponds to transformations of the form

$$\psi_i \mapsto \psi_i' = (U_\mathrm{R})_{ij}\, P_\mathrm{R}\psi_j + (U_\mathrm{L})_{ij}\, P_\mathrm{L}\psi_j\,, \tag{4.2.13}$$

$$\bar{\psi}_i \mapsto \bar{\psi}_i' = \bar{\psi}_j P_\mathrm{L}\,(U_\mathrm{R}^\dagger)_{ji} + \bar{\psi}_j P_\mathrm{R}\,(U_\mathrm{L}^\dagger)_{ji}\,, \tag{4.2.14}$$

where $U_{\mathrm{R,L}}^\dagger U_{\mathrm{R,L}} = U_{\mathrm{R,L}} U_{\mathrm{R,L}}^\dagger = 1$ with $P_{\mathrm{R,L}} = \frac{1}{2}(\mathbf{1} \pm \gamma_5)$. Such symmetry is spontaneously broken if a finite condensate $\langle \bar{\psi}\psi \rangle$ is generated. As discussed in the introduction, a four-fermion operator of the form $(\mathcal{V} - \mathcal{A})$ is also allowed by chiral symmetry. However, our analysis is restricted to the $(\mathcal{V} + \mathcal{A})$-channel, which is the channel related to chiral symmetry breaking [11].

By using the technique of Fierz rearrangements (see App. (A.2)), the $(\mathcal{V}+\mathcal{A})$-channel can be recast in terms of scalar and pseudoscalar channels, according to

$$\mathcal{V} + \mathcal{A} = -2\left[(\bar{\psi}^i\psi^j)(\bar{\psi}^j\psi^i) - (\bar{\psi}^i\gamma_5\psi^j)(\bar{\psi}^j\gamma_5\psi^i)\right]. \tag{4.2.15}$$

Equation (4.2.15) can be further rewritten in terms of the chiral components, $\psi^i = \psi^i_\mathrm{R} + \psi^i_\mathrm{L}$ (with $\psi^i_{\mathrm{R,L}} = P_{\mathrm{R,L}}\psi^i$), as

$$\mathcal{V} + \mathcal{A} = -8(\bar{\psi}^i_\mathrm{L}\psi^j_\mathrm{R})(\bar{\psi}^j_\mathrm{R}\psi^i_\mathrm{L}). \tag{4.2.16}$$

Thus, the action (4.2.10) turns into

$$S[\psi, \bar{\psi}; g] = \int_x \left(\frac{i}{2}\left(\bar{\psi}^i\gamma^\mu D_\mu\psi^i - D_\mu\bar{\psi}^i\,\gamma^\mu\psi^i\right) + 2\lambda\,(\bar{\psi}^i_\mathrm{L}\psi^j_\mathrm{R})(\bar{\psi}^j_\mathrm{R}\psi^i_\mathrm{L}) \right). \tag{4.2.17}$$

The investigation on the fate of chiral symmetry becomes easier if we consider a partially bosonized version of the four-fermion model in (4.2.17), which can be achieved by a Hubbard-Stratonovich transformation [167, 168]. In this way, the four-fermion interaction can be translated into a Yukawa-like interaction with new scalar degrees of freedom. The bosonized formulation of the action (4.2.17) can

[10] The reader should be cautious with the use of Latin indices for both tangent space indices and internal labels for fermionic fields. Letters from the beginning of the alphabet are used to denote tangent space indices, while lettes from the middle of the alphabet are devoted to internal labels of Dirac fermions.

[11] The $(\mathcal{V} - \mathcal{A})$-channel might be associated to the generation of a vector condensate [167].

be written as

$$S_{\mathrm{B}} = \int_x \left(\frac{i}{2}\big(\bar{\psi}^i \gamma^\mu D_\mu \psi^i - D_\mu \bar{\psi}^i \gamma^\mu \psi^i\big) + \frac{1}{2\lambda}\,\mathrm{tr}\big(\phi^\dagger \phi\big) + i\bar{\psi}^i \left[P_{\mathrm{L}}(\phi^\dagger)_{ij} + P_{\mathrm{R}}\phi_{ij}\right]\psi^j \right), \tag{4.2.18}$$

where we have introduced a conjugate pair of matrix-valued fields ϕ and $\phi^\dagger$, both of which are scalars under Lorentz transformations. The action (4.2.17) can be recovered by integrating out ϕ and $\phi^\dagger$ in the path integral or, equivalently, plugging in (4.2.18) the composite scalar fields,

$$\phi_{ij} = -2i\lambda \bar{\psi}^j P_{\mathrm{L}} \psi^i, \qquad \phi^*_{ji} = -2i\lambda \bar{\psi}^i P_{\mathrm{R}} \psi^j, \tag{4.2.19}$$

derived from the equations of motion. The Yukawa-like interaction now forces ϕ to transform according to

$$\phi \mapsto \phi' = U_{\mathrm{R}}\, \phi\, U_{\mathrm{L}}^\dagger\,, \tag{4.2.20}$$

$$\phi^\dagger \mapsto \phi'^\dagger = U_{\mathrm{L}}\, \phi^\dagger\, U_{\mathrm{R}}^\dagger\,, \tag{4.2.21}$$

so that the partially bosonized action continues to be chirally symmetric [167].

In this scenario, the spontaneous breaking of chiral symmetry translates into a finite and positive expectation value $\langle\phi\rangle$, leading to a mass term for the fermion. Thus, the expectation value of the field ϕ can be seen as an order parameter. To determine whether or not ϕ has a nonvanishing expectation value, we analyze the structure of minima of the effective potential $V_{\mathrm{eff}}(\phi, \phi^\dagger)$ obtained by integrating out fermionic fluctuations.

Since we are interested in the effects of the background torsion on the mechanism of chiral symmetry breaking, it is useful to rewrite (4.2.18) in such a way that we can make the torsion contribution explicit. Using Eqs. (4.2.5) and (4.2.11), one can write

$$D_\mu \psi = \mathring{D}_\mu \psi + K_\mu \psi, \tag{4.2.22}$$

$$D_\mu \bar{\psi} = \mathring{D}_\mu \bar{\psi} - \bar{\psi} K_\mu, \tag{4.2.23}$$

with $\mathring{D}_\mu$ being the Dirac covariant derivative built with the torsionless spin connection and $K_\mu = \frac{1}{8} K^{ab}{}_\mu [\gamma_a, \gamma_b]$ is the so(4)-valued contorsion, which, using the relation (4.2.7), reads

$$K_\mu = \frac{1}{16}\big[\gamma^\alpha, \gamma^\beta\big](T_{\alpha\beta\mu} - T_{\beta\alpha\mu} - T_{\mu\alpha\beta})\,. \tag{4.2.24}$$

Upon integration by parts, the Dirac term can be expressed as

$$S_{\mathrm{Dirac}} = \int_x \frac{i}{2}\big(\bar{\psi}^i \gamma^\mu D_\mu \psi^i - D_\mu \bar{\psi}^i \gamma^\mu \psi^i\big) = \int_x \left(i\bar{\psi}^i \mathring{\not{D}} \psi^i + \frac{i}{2}\bar{\psi}^i \big\{\gamma^\mu, K_\mu\big\}\psi^i \right). \tag{4.2.25}$$

At this point, it is convenient to decompose the torsion tensor in terms of its irreducible components T_μ (vector component), A_μ (axial-vector component)[12] and $q_{\mu\nu\rho}$ (irreducible rank-3 component) [352,

[12] These names are due to their behaviour under time reversal and space inversion (parity transformation).

364, 365]. Explicitly,

$$T^{\lambda}{}_{\mu\nu} = \frac{1}{3}(\delta^{\lambda}_{\nu}T_{\mu} - \delta^{\lambda}_{\mu}T_{\nu}) + \frac{1}{6}\epsilon^{\lambda}{}_{\mu\nu\sigma}A^{\sigma} + q^{\lambda}{}_{\mu\nu}, \tag{4.2.26}$$

with $q^{\lambda}{}_{\mu\lambda} = 0$, $\epsilon^{\mu\nu\rho\sigma}q_{\nu\rho\sigma} = 0$ and $q^{\lambda}{}_{\mu\nu} = -q^{\lambda}{}_{\nu\mu}$. Furthermore, $T_{\mu} = T^{\lambda}{}_{\mu\lambda}$ is the trace of the torsion tensor and $A^{\rho} = \epsilon_{\lambda}{}^{\mu\nu\rho}T^{\lambda}{}_{\mu\nu}$ is the axial-trace vector[13]. Using Eqs. (4.2.24) and (4.2.26), together with the identity $\{\gamma^{\mu}, [\gamma^{\alpha}, \gamma^{\beta}]\} = 4\epsilon^{\mu\alpha\beta\rho}\gamma_5\gamma_{\rho}$, yields

$$\{\gamma^{\mu}, K_{\mu}\} = \frac{1}{4}\gamma_5 \not{A}. \tag{4.2.27}$$

Thus, the Dirac action finally turns into

$$S_{\text{Dirac}} = \int_x \left(i\bar{\psi}^i \not{\mathcal{D}}\psi^i + \frac{i}{8}\bar{\psi}^i\gamma_5 \not{A}\psi^i \right) = \int_x i\bar{\psi}^i \not{\mathcal{D}}\psi^i \,, \tag{4.2.28}$$

where we have introduced a new derivative operator defined by

$$\mathcal{D}_{\mu}\psi = \mathring{D}_{\mu}\psi - \frac{1}{8}\gamma_5 A_{\mu}\psi \,, \tag{4.2.29}$$

$$\mathcal{D}_{\mu}\bar{\psi} = \mathring{D}_{\mu}\bar{\psi} + \frac{1}{8}\bar{\psi}\gamma_5 A_{\mu} \,. \tag{4.2.30}$$

Thus, the minimal coupling of Dirac fermions with gravity in the presence of nonvanishing torsion is equivalent to fermions minimally coupled to a torsionless curved background, plus an axial interaction through A_{μ} [367, 368]. The torsion-dependent term $\bar{\psi}^i\gamma_5 \not{A}\psi^i$ has certain similarities with parity-violating terms investigated in the context of theories with Lorentz- and CPT-symmetry violations [369–371].

The onset of chiral symmetry breaking is signalled by a nonvanishing vacuum expection value of ϕ. For simplicity, we choose an homogeneous breaking pattern $\phi_{ij} = \phi_0\delta_{ij}$, with ϕ_0 being a constant. This vacuum configuration breaks the $\mathrm{SU(N_F)_L \times SU(N_F)_R}$ down to the diagonal subgroup $\mathrm{SU(N_F)_V}$. In this way, the bosonized action (4.2.18) can be expressed as

$$S_{\text{B}}[\psi, \bar{\psi}; \phi_0] = \int_x \left[i\bar{\psi}^i \not{\mathcal{D}}\psi^i + i\phi_0\bar{\psi}^i\psi^i + \frac{N_{\text{F}}}{2\lambda}\phi_0^2 \right]. \tag{4.2.31}$$

We are now ready to analyze the effective potential associated with (4.2.31).

4.2.2 Effective potential and its flow equation

The fermions appear as bilinears in the bosonized action (4.2.31) and, once inserted in the Boltzmann weight of the generating functional, they can be readily integrated out. This ultimately provides an expression for a purely bosonic quantum effective action. The associated effective potential $\tilde{V}_{\text{eff}}(\phi_0)$

[13] A spin-parity decomposition of the torsion tensor, inspired by the York decomposition of symmetric rank-2 tensors, is given in [366] and is tailored-made for 1-loop computations involving the torsion tensor in arbitrary dimensions.

is given by (see, *e.g.*, [167] for details)

$$\begin{aligned}\tilde{V}_{\text{eff}}(\phi_0) &= \frac{N_{\text{F}}}{2\lambda}\phi_0^2 - \frac{N_{\text{F}}}{v_4}\log\big[\text{Det}\big(\not{\mathcal{D}} + \phi_0\big)\big] \\ &= \frac{N_{\text{F}}}{2\lambda}\phi_0^2 - \frac{N_{\text{F}}}{2v_4}\text{Tr}\big[\log\big(-\not{\mathcal{D}}^2 + \phi_0^2\big)\big].\end{aligned} \tag{4.2.32}$$

The factor v_4 stands for the 4-dimensional spacetime volume[14].

Our goal is to explore how local patches of the spacetime geometry influence the mechanism of chiral symmetry breaking. Therefore, instead of computing the effective potential taking into account all modes of the fermionic field, we perform a coarse-grained analysis in terms of a scale-dependent effective potential. The idea is to introduce a momentum scale k that acts as an infrared regulator, such that the effective potential associated with a scale k (denoted as $\tilde{V}_k(\phi_0)$) only includes effects of fermionic modes with "momentum"[15] larger than k. In this sense, the scale-dependent effective potential $\tilde{V}_k(\phi_0)$ probes the effects of local patches of geometry with a characteristic length scale of order $\sim 1/k$.

To define the scale-dependent effective potential we follow a strategy inspired by the regularization scheme used in the framework of the functional Renormalization Group [13, 150, 372] (see also Sect. 2.3).[16] Here, we regularize (4.2.32) by the replacement

$$\log\big(-\not{\mathcal{D}}^2 + \phi_0^2\big) \mapsto \log\big(-\not{\mathcal{D}}^2 + R_k(-\not{\mathcal{D}}^2) + \phi_0^2\big)\,, \tag{4.2.33}$$

where $R_k(-\not{\mathcal{D}}^2)$ is the FRG regulator function. As discussed in Sect. 2.3, the regulator function $R_k(-\not{\mathcal{D}}^2)$ is defined[17] such that it suppresses quantum fermionic fluctuation contributions based on the spectrum of the effective Dirac operator $-\not{\mathcal{D}}^2$, *i.e.*, $R_k(-\not{\mathcal{D}}^2)$ suppresses modes with eigenvalues lower than k^2. In general, in the limit $k \to 0$ the regulator $R_k(-\not{\mathcal{D}}^2)$ should vanish, implying that $\tilde{V}_{k=0}(\phi_0) = \tilde{V}_{\text{eff}}(\phi_0)$. Throughout this chapter, we use the notation $R_k(-\not{\mathcal{D}}^2) = k^2 r(y)$ (with $y = -\not{\mathcal{D}}^2/k^2$), and we explore the Litim [374] and exponential shape functions, respectively defined by (c.f. Sect. 2.3.2)

$$\text{Litim:} \qquad r(y) = (1-y)\theta(1-y)\,, \tag{4.2.34}$$

$$\text{Exponential:} \qquad r(y) = \frac{y}{e^y - 1}\,. \tag{4.2.35}$$

[14] In the case of a noncompact manifold, an appropriate regularization must be employed.

[15] More precisely, we define the coarse-graining procedure in terms of the differential operator $-\not{\mathcal{D}}^2$. Thus, the scale-dependent potential $\tilde{V}_k(\phi_0)$ includes fermionic fluctuations associated with eigenvalues of $-\not{\mathcal{D}}^2$ that are larger than k^2.

[16] Alternatively, one can also define a scale-dependent potential using the proper-time regularization scheme as done in [334, 335] in the study of gravitational catalysis in Riemannian geometries.

[17] Following [373], we adopt the so-called type-II regularization, in which the argument of the regulator function is the full Dirac operator squared. This choice is motivated by [220], where the authors argued that the type-II regulator is more appropriate for the treatment of fermions in a curved background. See also [225, 226].

Based on this FRG regularization scheme, we define the scale-dependent effective potential as

$$\tilde{V}_k(\phi_0) = \frac{N_{\rm F}}{2\lambda}\phi_0^2 - \frac{N_{\rm F}}{2v_4}\mathrm{Tr}\big[\log\big(-\not{\mathcal{D}}^2 + R_k(-\not{\mathcal{D}}^2) + \phi_0^2\big)\big]\,. \tag{4.2.36}$$

We define the flow of $\tilde{V}_k(\phi_0)$ by acting on (4.2.36) with a scale-derivative operator $k\partial_k$, such that

$$k\partial_k\tilde{V}_k(\phi_0) = -\frac{N_{\rm F}}{2v_4}\mathrm{Tr}\Big[\Big(-\not{\mathcal{D}}^2 + R_k(-\not{\mathcal{D}}^2) + \phi_0^2\Big)^{-1} k\partial_k R_k(-\not{\mathcal{D}}^2)\Big]\,. \tag{4.2.37}$$

The right-hand side of (4.2.37) is both ultraviolet- and infrared-finite, as long as $R_k(-\not{\mathcal{D}}^2)$ satisfies all the standard properties of an fRG-regulator (c.f. Sect. 2.3.2). To compute the effective potential at a given scale $k_{\rm IR}$, we integrate the flow equation (4.2.37), resulting in[18]

$$\begin{aligned}\tilde{V}_{k_{\rm IR}}(\phi) &= \frac{N_{\rm F}}{2\lambda_\Lambda}\phi^2 - \int_{k_{\rm IR}}^{\Lambda}\frac{\mathrm{d}k}{k}k\partial_k V_k(\phi)\\ &= \frac{N_{\rm F}}{2\lambda_\Lambda}\phi^2 + \frac{N_{\rm F}}{2v_4}\int_{k_{\rm IR}}^{\Lambda}\frac{\mathrm{d}k}{k}\mathrm{Tr}\Big[\Big(-\not{\mathcal{D}}^2 + R_k(-\not{\mathcal{D}}^2) + \phi^2\Big)^{-1} k\partial_k R_k(-\not{\mathcal{D}}^2)\Big]\,,\end{aligned} \tag{4.2.38}$$

where Λ is an ultraviolet cutoff scale, and we used the boundary condition $\tilde{V}_\Lambda(\phi) = N_{\rm F}\,\phi^2/(2\lambda_\Lambda)$, with $\lambda_\Lambda = \lambda$. Since field-independent contributions in $\tilde{V}_{k_{\rm IR}}(\phi)$ are irrelevant for the analysis of chiral symmetry breaking, it is convenient to define

$$V_{k_{\rm IR}}(\phi) = \tilde{V}_{k_{\rm IR}}(\phi) - \tilde{V}_{k_{\rm IR}}(0)\,, \tag{4.2.39}$$

which automatically removes divergences that are proportional to Λ^4.

Before discussing the impact of torsion on the mechanism of chiral symmetry breaking, let us briefly review how to identify chiral symmetry breaking from $V_{k_{\rm IR}}(\phi)$. To simplify the discussion, we first consider the case of flat spacetime. In this case, we can compute the trace in (4.2.38) in Fourier space. Computing $V_{k_{\rm IR}}(\phi)$ in a polynomial expansion around $\phi = 0$, we find[19]

$$\begin{aligned}V_{k_{\rm IR}}(\phi) &= \frac{N_{\rm F}}{2\lambda_\Lambda}\phi^2 + \frac{N_{\rm F}}{8\pi^2}\int_{k_{\rm IR}}^{\Lambda}\frac{\mathrm{d}k}{k}\left(\frac{k^6}{k^2+\phi^2} - k^4\right)\\ &= \frac{N_{\rm F}}{2\lambda_\Lambda}\phi^2 + \frac{N_{\rm F}}{16\pi^2}(k_{\rm IR}^2 - \Lambda^2)\phi^2 + \mathcal{O}(\phi^4)\\ &= \frac{N_{\rm F}}{2}\left(\frac{1}{\lambda_\Lambda} - \frac{1}{\lambda_{\rm cr}} + \frac{1}{8\pi^2}k_{\rm IR}^2\right)\phi^2 + \mathcal{O}(\phi^4)\,,\end{aligned} \tag{4.2.40}$$

where $\lambda_{\rm cr} = 8\pi^2\Lambda^{-2}$. We are interested in determining if $\phi = 0$ is a local minimum or a local maximum of $V_{k_{\rm IR}}(\phi)$. If $\phi = 0$ is a local maximum, the structure of $V_{k_{\rm IR}}(\phi)$ implies the existence of at least two degenerate minima with nonvanishing ϕ,[20] thus implying chiral symmetry breaking.

Since $V'_{k_{\rm IR}}(0) = 0$, $\phi = 0$ is an extremum of $V_{k_{\rm IR}}(\phi)$. Thus, to determine if $\phi = 0$ is a local minimum

[18] From now on, we omit the subscript on ϕ_0 and we write simply ϕ for constant field configurations.

[19] In this example, we use the Litim regulator defined in (2.3.33).

[20] Assuming that the effective potential is bounded from below (which is necessary for stability reasons), it implies that, if $\phi = 0$ is a local maximum, the potential $V_{k_{\rm IR}}(\phi)$ has at least two local minima with nonvanishing ϕ.

or a local maximum, we need to investigate the sign of

$$V''_{k_{\rm IR}}(0) = N_{\rm F}\left(\frac{1}{\lambda_\Lambda} - \frac{1}{\lambda_{\rm cr}} + \frac{1}{8\pi^2}k_{\rm IR}^2\right). \tag{4.2.41}$$

If $\lambda_\Lambda < \lambda_{\rm cr}$, then the sign of $V''_{k_{\rm IR}}(0)$ is positive for all values of $k_{\rm IR}$, implying that $\phi = 0$ is a local minimum of $V_{k_{\rm IR}}(\phi)$ for all $k_{\rm IR}$. However, if $\lambda_\Lambda > \lambda_{\rm cr}$, then the sign of $V''_{k_{\rm IR}}(0)$ becomes negative for $k_{\rm IR} < k_{\chi{\rm SB}}$ (where $k^2_{\chi{\rm SB}} = 8\pi^2(\lambda_\Lambda - \lambda_{\rm cr})/(\lambda_\Lambda\lambda_{\rm cr})$), implying that $\phi = 0$ is a local maximum of $V_{k_{\rm IR}}(\phi)$ for $k_{\rm IR} < k_{\chi{\rm SB}}$. Thus, for $\lambda_\Lambda > \lambda_{\rm cr}$, the potential $V_{k_{\rm IR}}(\phi)$ has nontrivial minima for $k_{\rm IR} < k_{\chi{\rm SB}}$, indicating that quantum fluctuation can trigger chiral symmetry breaking.

From the discussion above, we see that the sign of $V''_{k_{\rm IR}}(0)$ plays a key role in determining whether or not the system exhibits chiral symmetry breaking. Using Eq. (4.2.38), we can write

$$V''_{k_{\rm IR}}(0) = \frac{N_{\rm F}}{\lambda_\Lambda} - \frac{N_{\rm F}}{v_4}\int_{k_{\rm IR}}^{\Lambda}\frac{{\rm d}k}{k}{\rm Tr}\Big[\Big(-\not{\mathcal{D}}^2 + R_k(-\not{\mathcal{D}}^2)\Big)^{-2} k\partial_k R_k(-\not{\mathcal{D}}^2)\Big]. \tag{4.2.42}$$

In the next section, we use this equation to study the impact of a nontrivial background geometry on $V''_{k_{\rm IR}}(0)$.

4.2.3 The impact of torsion on the fate of chiral symmetry

In this section we investigate the impact of the background torsion on the mechanism of chiral symmetry breaking. Our analysis entails the evaluation of the trace on the right-hand side of (4.2.42). In general, it requires the knowledge of the spectral properties of the nonminimal operator $-\not{\mathcal{D}}^2$ (c.f., Eq. (4.2.48)), thus leading to a complicated problem of spectral geometry. To simplify the analysis, we focus on two different regimes:

- $|\mathring{R}|/k^2_{\rm IR} \ll 1$ and $A^2/k^2_{\rm IR} \ll 1$: In this regime, we can use early-time heat kernel expansion to evaluate the trace in (4.2.42). This approximation allows us to carry the combined effect of background curvature and torsion. However, it is not applicable in the infrared regime.
- $\mathring{R}_{\mu\nu\alpha\beta} \approx 0$ and A^2 is approximately homogeneous: In this regime, we can evaluate the trace in (4.2.42) without employing the early-time heat kernel expansion. Therefore, this approximation allows us to investigate the impact of background torsion in the deep infrared regime.

Effects of background curvature and torsion

Now, we investigate the regime where $\mathring{R}$ and A^2 are small in comparison with the cutoff scale $k^2_{\rm IR}$. In this regime, we can evaluate the trace in (4.2.42) using standard heat kernel methods based on early-time expansion.

For a generic function of the square of the Dirac operator $\mathcal{W}(-\not{\mathcal{D}}^2)$, the heat kernel expansion reads

[13, 367, 372, 375]

$$\mathrm{Tr}\mathcal{W}(-\not{\mathcal{D}}^2) = \frac{1}{(4\pi)^2}\sum_{n=0}^{\infty}\int_x \mathcal{Q}_{2-n}[\mathcal{W}]\ \mathrm{tr}\left[b_{2n}(-\not{\mathcal{D}}^2)\right], \tag{4.2.43}$$

where $b_{2n}(-\not{\mathcal{D}}^2)$ denotes the nonintegrated heat kernel coefficients for the operator $-\not{\mathcal{D}}^2$. The $\mathcal{Q}$-functionals are defined as

$$\mathcal{Q}_n[\mathcal{W}] = \frac{(-1)^p}{\Gamma(n+p)}\int_0^\infty \mathrm{d}z\, z^{n+p-1}\frac{\mathrm{d}^p\mathcal{W}(z)}{\mathrm{d}z^p}, \tag{4.2.44}$$

where p denotes some arbitrary positive integer satisfying the restriction $n+p>0$. In particular, if n is positive, then $p=0$. Here, tr denotes the trace over the internal and spacetime indices.

For the trace that we are interested in computing (see Eq. (4.2.42)), we can identify the function

$$\mathcal{W}(z) = \frac{k\partial_k R_k(z)}{\left(z+R_k(z)\right)^2}, \tag{4.2.45}$$

leading to

$$\mathcal{Q}_n[\mathcal{W}] = \frac{1}{\Gamma(n)}\int_0^\infty \mathrm{d}z\, z^{n-1}\frac{k\partial_k R_k(z)}{\left(z+R_k(z)\right)^2} = 2\,k^{2(n-1)}\mathcal{I}_n[r]\,. \tag{4.2.46}$$

We have introduced the dimensionless threshold integral $\mathcal{I}_n[r]$, which one defines in terms of the shape function $r(y)$ according to

$$\mathcal{I}_n[r] = \frac{1}{\Gamma(n)}\int_0^\infty \mathrm{d}y\, y^{n-1}\,\frac{r(y)-y\,r'(y)}{\left(y+r(y)\right)^2}\,. \tag{4.2.47}$$

The numerical value of $\mathcal{I}_n[r]$ depends on the explicit form of the shape function $r(y)$, except in the case $n=1$ where one can show that $\mathcal{I}_1[r]=1$ for all suitable choices of regulator (see, *e.g.*, [13, 372]). Since we are interested in the regime where $|\mathring{R}|/k_{\mathrm{IR}}^2 \ll 1$ and $A^2/k_{\mathrm{IR}}^2 \ll 1$, we will only keep terms that are at most linear in $\mathring{R}$ and A^2. In such case, we just need to evaluate $\mathcal{I}_2[r]$, which results in $\mathcal{I}_2[r]=1/2$ for the Litim regulator and $\mathcal{I}_2[r]=1$ for the exponential regulator.

In order to use the (nonintegrated) heat-kernel coefficients b_{2n} available in the literature, it is useful to rewrite the Dirac operator $-\not{\mathcal{D}}^2$ in a minimal form. In fact,

$$-\not{\mathcal{D}}^2 = -\mathring{D}^2 + \hat{B}^\mu\mathring{D}_\mu + \hat{X}\,, \tag{4.2.48}$$

where the operators $\hat{B}^\mu$ and $\hat{X}$ are defined as follows

$$\hat{B}^\mu = -\frac{i}{4}\gamma_5\sigma^{\mu\nu}A_\nu\,, \tag{4.2.49}$$

$$\hat{X} = \frac{1}{4}\left(\mathring{R}+\frac{1}{16}A^2\right)\mathbf{1} + \frac{1}{8}(\mathring{\nabla}\cdot A - i\sigma^{\mu\nu}\mathring{\nabla}_\mu A_\nu)\gamma_5\,, \tag{4.2.50}$$

where $\sigma^{\mu\nu} = \frac{i}{2}[\gamma^\mu,\gamma^\nu]$. The heat-kernel coefficients for this class of operators are available, *e.g.*, in

[376–378]. In our analysis, we use

$$\mathrm{tr}\left[b_0(-\not{\mathcal{D}}^2)\right] = 4\,, \tag{4.2.51}$$

$$\mathrm{tr}\left[b_2(-\not{\mathcal{D}}^2)\right] = \frac{2}{3}\mathring{R} + \frac{1}{2}\,\mathrm{tr}\left(\mathring{\nabla}_\mu \hat{B}^\mu\right) - \frac{1}{4}\,\mathrm{tr}\left(\hat{B}_\mu \hat{B}^\mu\right) - \mathrm{tr}\left(\hat{X}\right). \tag{4.2.52}$$

From the definition of $\hat{B}^\mu$ and $\hat{X}$, one can show that $\mathrm{tr}\left(\mathring{\nabla}_\mu \hat{B}^\mu\right) = 0$, $\mathrm{tr}\left(\hat{B}_\mu \hat{B}^\mu\right) = -\frac{3}{4}A^2$, and $\mathrm{tr}\left(\hat{X}\right) = \mathring{R} + \frac{1}{16}A^2$, resulting in

$$\mathrm{tr}\left[b_2(-\not{\mathcal{D}}^2)\right] = -\frac{1}{3}\mathring{R} + \frac{1}{8}A^2\,. \tag{4.2.53}$$

Plugging those results in Eq. (4.2.42) leads to

$$V''_{k_{\mathrm{IR}}}(0) = N_{\mathrm{F}}\left(\frac{1}{\lambda_\Lambda} - \frac{1}{\lambda_{\mathrm{cr}}}\right) + \frac{N_{\mathrm{F}}}{4\pi^2}\mathcal{I}_2[r]k_{\mathrm{IR}}^2 + \frac{N_{\mathrm{F}}}{16\pi^2}\left(\frac{1}{3}\langle\mathring{R}\rangle - \frac{1}{8}\langle A^2\rangle\right)\log\left(\Lambda^2/k_{\mathrm{IR}}^2\right), \tag{4.2.54}$$

where we have defined spacetime averaged quantities as $\langle(\cdots)\rangle = \frac{1}{v_4}\int_x(\cdots)$. Here, we also use the critical coupling λ_{cr} defined as

$$\frac{1}{\lambda_{\mathrm{cr}}} = \frac{\Lambda^2}{4\pi^2}\mathcal{I}_2[r]. \tag{4.2.55}$$

In order to absorb the logarithmic divergence in the last term of (4.2.54), we add the following counterterm to the original action

$$\delta S[\phi] = \frac{N_{\mathrm{F}}\,\xi_\Lambda}{3}\int_x \left(R - T_{\alpha\beta\mu}T^{\alpha\beta\mu} + T_{\alpha\beta\mu}T^{\beta\alpha\mu} + T^{\mu}_{\ \mu\alpha}T^{\nu\alpha}_{\ \ \ \nu} + 2\,\nabla^\mu T^{\nu}_{\ \ \nu\mu}\right)\phi^2\,, \tag{4.2.56}$$

where all geometrical objects are defined with respect to the full affine connection $\Gamma^\alpha_{\mu\nu}$. Such counterterm leads to the following contribution to the scale-dependent effective potential

$$\delta V_{k_{\mathrm{IR}}}(\phi) = N_{\mathrm{F}}\,\xi_\Lambda\left(\frac{1}{3}\langle\mathring{R}\rangle - \frac{1}{8}\langle A^2\rangle\right)\phi^2\,. \tag{4.2.57}$$

Thus, we define a renormalized effective potential such that

$$V''_{k_{\mathrm{IR}}}(0) = N_{\mathrm{F}}\left(\frac{1}{\lambda_\Lambda} - \frac{1}{\lambda_{\mathrm{cr}}}\right) + \frac{N_{\mathrm{F}}}{4\pi^2}\mathcal{I}_2[r]k_{\mathrm{IR}}^2 + N_{\mathrm{F}}\,\xi_{\mathrm{IR}}\left(\frac{2}{3}\langle\mathring{R}\rangle - \frac{1}{4}\langle A^2\rangle\right), \tag{4.2.58}$$

where we have introduced the renormalized coupling

$$\xi_{\mathrm{IR}} = \xi_\Lambda + \frac{1}{32\pi^2}\log\left(\Lambda^2/k_{\mathrm{IR}}^2\right). \tag{4.2.59}$$

In principle, ξ_{IR} needs to be fixed by experiments. In our analysis, we leave ξ_{IR} as a free parameter.

As discussed in the previous section, the analysis of chiral symmetry breaking relies on the sign of $N_{\mathrm{F}}^{-1}V''_{k_{\mathrm{IR}}}(0)$. If chiral symmetry breaking is present and a bound-state formation occurs, there must

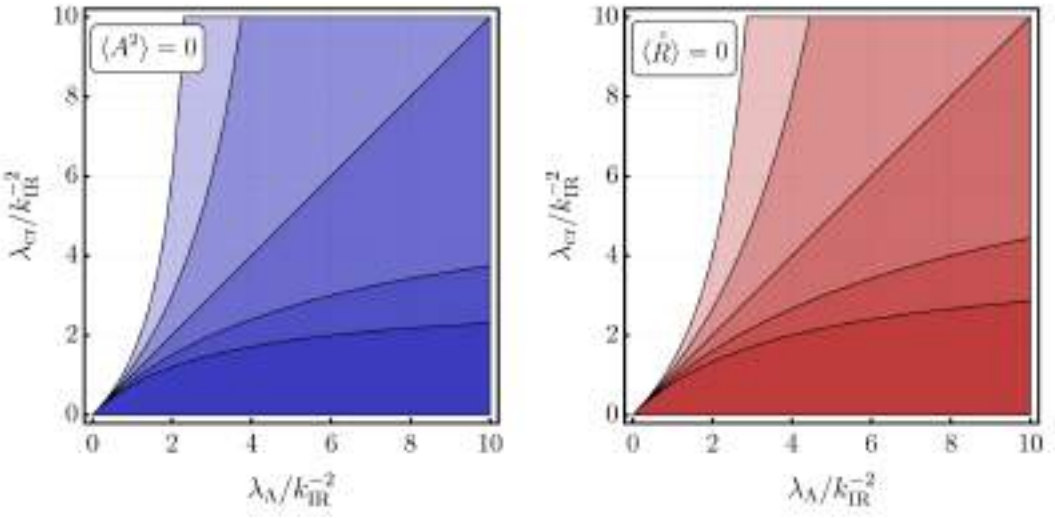

Figure 4.1: Regions in the parameter space $\lambda_\Lambda \times \lambda_{\rm cr}$ where chiral symmetry breaking is triggered by quantum fluctuations in the presence of curvature or torsion. Left panel: we have set $\langle A^2\rangle = 0$ and we have probed the range $\xi_{\rm IR} k_{\rm IR}^{-2}\langle \mathring{R}\rangle = -1/2\,, -1/4\,, 0\,, 1/4\,, 1/2$ from lighter to darker regions. Right panel: we have set $\langle \mathring{R}\rangle = 0$ and from darker to lighter we have probed the range $\xi_{\rm IR} k_{\rm IR}^{-2}\langle A^2\rangle = -1\,, -1/2\,, 0\,, 1/2\,, 1$.

be a transition scale $k_{\rm tr}$ such that $V''_{k_{\rm tr}}(0) = 0$. From (4.2.58), we find the transition scale

$$k_{\rm tr}^2 = \frac{4\pi^2}{\mathcal{I}_2[r]}\left(\frac{1}{\lambda_{\rm cr}} - \frac{1}{\lambda_\Lambda} - \frac{2}{3}\xi_{\rm IR}\langle \mathring{R}\rangle + \frac{1}{4}\xi_{\rm IR}\langle A^2\rangle\right). \tag{4.2.60}$$

For vanishing curvature and torsion, such transition scale only makes sense if $\lambda_\Lambda \geq \lambda_{\rm cr}$. For nonvanishing curvature and/or torsion, the viability of chiral symmetry breaking depends on the inequality

$$\frac{1}{\lambda_{\rm cr}} - \frac{1}{\lambda_\Lambda} - \frac{2}{3}\xi_{\rm IR}\langle \mathring{R}\rangle + \frac{1}{4}\xi_{\rm IR}\langle A^2\rangle \geq 0. \tag{4.2.61}$$

For $\xi_{\rm IR} > 0$, we find that positive (negative) values of $\langle \mathring{R}\rangle$ act against (in favor of) chiral symmetry breaking, while the axial-torsion term $\langle A^2\rangle$ acts exclusively in favor of chiral symmetry breaking. For $\xi_{\rm IR} < 0$, the term $\langle \mathring{R}\rangle$ can still act in favor of or against chiral symmetry breaking (depending on its sign), while the axial-torsion term only acts toward the preservation of chiral symmetry. A comment is in order: due to our use of an Euclidean setting, the sign of A^2 is positive definite. In a Lorentzian framework, this is not necessarily true, and a spacetime average can be rather misleading quantity in order to make concrete statements. In such a quantum-field theoretic on a fixed background setting, one can choose specific backgrounds where one can compute quantities beyond their averages. In Fig. 4.1, we show the regions in the parameter space $\lambda_\Lambda \times \lambda_{\rm cr}$ where chiral symmetry breaking is triggered by quantum fluctuations in the presence of curvature or torsion.

Since the results presented in this section were based on the early-time heat kernel truncated at the first order in $|\mathring{R}|/k_{\rm IR}^2$ and $A^2/k_{\rm IR}^2$, our results do not allow us to extract information concerning the deep infrared regime. In the deep infrared, higher order terms in $|\mathring{R}|$ and A^2 would come with inverse powers of the infrared scale $k_{\rm IR}$, which would dominate over the first order contributions. It is of great

importance then to determine whether or not there is a mechanism of gravitational catalysis related to a nontrivial background structure. For Riemannian manifolds (*i.e.*, without torsion), the mechanism of gravitational catalysis was investigated, *e.g.*, in [334]. If we take such infrared contributions into account, we expect the inequality (4.2.61) to have an extra term, namely

$$\frac{1}{\lambda_{\rm cr}} - \frac{1}{\lambda_\Lambda} - \frac{2}{3}\xi_{\rm IR}\langle \mathring{R}\rangle + \frac{1}{4}\xi_{\rm IR}\langle A^2\rangle + \mathcal{F}_{k_{\rm IR}}(A_\mu, \mathring{R}_{\mu\nu\alpha\beta}) \geq 0\,, \tag{4.2.62}$$

where $\mathcal{F}_{k_{\rm IR}}$ is a function of invariants built from A_μ and $\mathring{R}_{\mu\nu\beta\alpha}$ (and their derivatives), and it encodes the contributions beyond the early-time heat kernel expansion. We expect that $\mathcal{F}_{k_{\rm IR}}$ acts as the dominant contribution in the infrared. Thus, if $\mathcal{F}_{k_{\rm IR}} > 0$, it would necessarily trigger chiral symmetry breaking. Determining the form of $\mathcal{F}_{k_{\rm IR}}$ associated with the operator $-\not{\mathcal{D}}^2$ (see Eq. (4.2.48)) in the presence of curvature and torsion is a complicated problem of spectral geometry lying outside the scope of this work. In the next section, we show that $\mathcal{F}_{k_{\rm IR}} = 0$ if we neglect curvature effects and restrict the axial-torsion component to be homogeneous.

Is there a torsion-based catalysis?

In this section, we study the regime of homogeneous axial-torsion A_μ and vanishing Riemannian curvature $\mathring{R}_{\mu\nu\alpha\beta} = 0$. Our goal is to derive the contribution of A_μ to $V''_{k_{\rm IR}}(0)$ beyond the early-time heat kernel approximation, aiming at an understanding if torsion can be a source of gravitational catalysis.

Within the approximation where $\mathring{R}_{\mu\nu\alpha\beta} = 0$ and A_μ is homogeneous, the differential operator $-\not{\mathcal{D}}^2$ reduces to

$$-\not{\mathcal{D}}^2 = \left(-\partial^2 + \frac{1}{64}A^2\right)\mathbf{1} - \frac{i}{4}\gamma_5\sigma^{\mu\nu}A_\nu\partial_\mu\,. \tag{4.2.63}$$

This approximation is useful because it allows us to evaluate the full heat-kernel trace (see Appendix C for more details), resulting in the following expression

$$\mathrm{Tr}\left[\exp\left(-\tau\not{\mathcal{D}}^2\right)\right] = \frac{1}{16\pi^2\tau^2}\left(4 + \frac{\tau}{8}A^2\right). \tag{4.2.64}$$

Surprisingly, the axial-torsion contributes at most up to linear order in A^2. This result implies that we can determine all the heat kernel coefficients b_n associated with the operator in (4.2.63), leading to

$$\mathrm{tr}\left[b_n(-\not{\mathcal{D}}^2)\right] = 4\delta_{n,0} + \frac{1}{8}A^2\delta_{n,2}\,. \tag{4.2.65}$$

Thus, only b_0 and b_2 lead to nonvanishing contributions to the trace in (4.2.43). In other words, we can truncate the series in (4.2.43) at $n = 1$ without resorting to any form of early-time approximation. Based on these results, we find

$$V''_{k_{\rm IR}}(0) = N_{\rm F}\left(\frac{1}{\lambda_\Lambda} - \frac{1}{\lambda_{\rm cr}}\right) + \frac{N_{\rm F}}{4\pi^2}\mathcal{I}_2[r]k^2_{\rm IR} - \frac{1}{4}N_{\rm F}\,\xi_{\rm IR}\langle A^2\rangle\,, \tag{4.2.66}$$

which correspond exactly to the limit $\mathring{R} \to 0$ of (4.2.58). However, the current result is exact and not restricted to small values of $A^2/k_{\rm IR}^2$.

The most striking feature of Eq. (4.2.66) is the absence of torsion-dependent contributions related to the deep infrared regime. On physical grounds, a background torsion would affect the mechanism of chiral symmetry breaking by deforming the region in the parameter space of $\lambda_\Lambda \times \lambda_{k_{\rm IR}}$ where we can flip the sign of $V''_{k_{\rm IR}}(0)$. However, our results show no indication of a mechanism of gravitational catalysis based on a background torsion. If λ_Λ is sufficiently small, then $V''_{k_{\rm IR}}(0)$ remains positive in the deep infrared, thus avoiding chiral symmetry breaking. This is different from the mechanism of curvature-based gravitational catalysis investigated in [334], where chiral symmetry breaking might be triggered even for arbitrarily small values of λ_Λ.

This conclusion may change if we drop the assumptions we considered in this section. It is possible that by combining the effects of curvature and torsion, a more sophisticated geometric-driven mechanism could lead to gravitational catalysis. It is also conceivable that a nonhomogeneous A_μ could change our conclusion. The analysis in this direction, however, goes beyond the scope of this work.

Comments on the teleparallel theory

Manifolds with torsion play an important role in the formulation of teleparallel theories of gravity [346–348] (see also [379–381] for reviews). This class of theories is a particular case of the general class of metric-affine gravity (MAG) [19, 341], and they are known to be classically equivalent to general relativity [342].

The teleparallel formulation is characterized by vanishing curvature and nonmetricity tensors, such that spacetime degrees of freedom are entirely encoded in the torsion tensor. In this framework, there is a special spin connection configuration $\dot{\omega}^{ab}{}_\mu$, called the Weitzenböck spin connection, that ensures that $\dot{R}^\rho{}_{\lambda\mu\nu} = 0$, with

$$\dot{\omega}^{ab}{}_\mu = \mathring{\omega}^{ab}{}_\mu + \dot{K}^{ab}{}_\mu. \tag{4.2.67}$$

Here, we use a filled ring to indicate that the geometric quantities are computed with the Weitzenböck spin connection.

In the following, we briefly discuss the mechanism of chiral symmetry breaking (due to background effects) in the context of teleparallel theories. The key point for such discussion is to identify the prescription of minimal coupling between fermions and gravity in teleparallel theories. Following Refs. [382, 383], in the context of teleparallel theories, fermions couple to gravity according to

$$\partial_\mu\psi \mapsto \partial_\mu\psi + \frac{1}{8}(\dot{\omega}^{ab}{}_\mu - \dot{K}^{ab}{}_\mu)[\gamma_a, \gamma_b]\psi. \tag{4.2.68}$$

Using condition (4.2.67) we recover the usual Levi-Civita covariant derivative and no torsion contribution appears. Therefore, the mechanism of chiral symmetry breaking in the context of teleparallel theories is equivalent to the case of Riemannian manifolds explored in [334].

Chapter 5

Exploring New Corners in Asymptotically Safe Unimodular Quantum Gravity

5.1 Introduction

Still to these days, the apparent mismatch between the observed value of the cosmological constant ($\Lambda_{\rm obs}$) and its anticipated value ($\Lambda_{\rm QFT}$) from estimates based on quantum field theory is a concern that brings together efforts from particle physicists and cosmologists to try to solve it. Whether there is really a conflict between the Standard Model's vacuum condensates and the phenomenological value of the cosmological constant has remained elusive. Since more than 30 years ago, Weinberg published a very thorough review on the so-called *cosmological constant problem* [29], where the related questions are precisely formulated, but still lack a generally accepted answer.

In the ΛCDM model, see, *e.g.*, Sections. 22 to 29 of the Review of Particle Physics [384], one attributes the cosmological constant to the density of the dark energy (DE), $\rho_{\rm DE} = \Lambda_{\rm obs} M^2_{\rm Planck}$, where $M_{\rm Planck} = 1/\sqrt{8\pi G_{\rm N}}$ is the reduced Planck mass. Furthermore, the parameter fit of the ΛCDM model allows that $\rho_{\rm DE}$ is equivalent to the energy density of the vacuum, which in turn is then assumed to be the case. The cosmological constant problem can be now quantified such that $\rho_{\rm DE}$ has, with respect to the Standard Model's scales, a very tiny parameter fit value of $\rho_{\rm DE} \approx (\text{meV})^4$ [385].

On the other hand, a possible way of getting a predicted value for the cosmological constant comes from a number of contributions from particle physics. According to the Weinberg-Salam electroweak theory, our current Universe is in the low-temperature symmetry-broken phase, leading to a contribution to the vacuum energy density of $\rho_{\rm EW} \approx (200\ \text{GeV})^4$. If one resorts to the QCD dynamics and, in particular, to the fact that light quarks undergo dynamical chiral symmetry breaking (DχSB), the vaccum energy density gets an extra contribution. One effective quantity to describe the magnitude of the QCD-related DχSB is the so-called quark condensate. For the two lightest quark flavors $q(x) = (u(x), d(x))^{\rm T}$, this quantity is given by[1] $\langle 0|\, \bar{q}(x) q(x)\, |0\rangle \simeq -(0.23 \pm 0.03\,\text{GeV})^3$. Then, D$\chi$SB

[1] From the point of view of the RG, one should note that the quark condensate is both RG scheme and RG scale dependent, and its typical size, for the two light quarks, is computed at a renormalization scale of order 1 GeV and within the MOM scheme [386].

leads to a vacuum energy density $\rho_{\mathrm{D}\chi\mathrm{SB}} \approx (0.2\,\mathrm{GeV})^4$. However, if we extend our quantum field theory calculations all the way up to the Planck scale, a contribution of $\rho_{\mathrm{Planck}} \approx (10^{18}\ \mathrm{GeV})^4$ would arise. Solely, the ratio of this contribution to the observed parameter fit of the ΛCDM model gives rise to the famous 10^{120} discrepancy. In this sense, if particle physics were to contribute to the cosmological constant up to the Planck scale, then the scale atributed to the theoretical vaccum energy density would be in glaring mismatch as in comparison with the parameter fit of the ΛCDM model.

In Weinberg's review [29], among five different approaches to the cosmological problem, one that stood the test of time as a firm contender is the idea of considering a transverse-diffeomorphism-invariant version of General Relativity in which the cosmological constant appears only at the level of the equations of motion as a constant of integration. In this way, such a constant would simply be fixed by an initial boundary condition, then most conveniently chosen as the measured value (Λ_{obs}). This symmetry-reduced version, which has the same classical dynamics as GR, is usually dubbed *unimodular gravity* (UG) [21–28]. From a quantum-gravity perspective, alternative theories of the gravitational field based on different symmetry principles will, very likely, define different quantum theories. However, in the case of UG, this issue becomes subtle, since it is based on a different symmetry principle in comparison to GR, but feature the same classical dynamics. Hence, it is an immediate question whether dynamical equivalence remains true in the quantum realm.

In particular, with a view towards asymptotic safety, the theory space defined by *Diff*-invariant operators is different from the one associated with *TDiff*. This is due to the treatment of the cosmological constant. In GR, it corresponds to a parameter which is fixed from the beginning and added by hand, as a coupling constant. It is, generically, subject to quantum corrections. In UG, the cosmological constant arises as an integration constant and, therefore, must be fixed by initial conditions. However, as such, it does not enter the classical action of the theory invariant under *TDiff* since the measure term is just a fixed scalar density. Thus, in the former case, the cosmological constant defines a direction in the theory space while in the latter, it does not. This can indicate that, if asymptotically safe, *Diff*- and *TDiff*-invariant theories might not be equivalent. However, as pointed out in [30, 142, 387], this discussion is more subtle than it sounds and this is still not completely understood.

In a standard perturbative quantization of GR within the background-field method, the dynamical structure of vertices and propagators will contain infinitely powers of the fluctuation field. The situation is completely different for a perturbative quantization of UG, since the metric determinant is fixed and various Feynman diagrams will be structurally modified. Thus, once again, there is no strong reason to believe that GR and UG will describe equivalent quantum theories. In this regard, both theories might be described by distinct quantum theories, but featuring the same classical limit.

The question of the quantum (in)equivalence was probed in [388, 389], where the computation of tree-level (on-shell) amplitudes for the scattering of three, four and five gravitons suggests that GR and UG produce coincident results, despite the considerable differences in the overall structure of propagators and vertices. By incorporating quantum effects, in [387], the one-loop effective action of UG was shown to be the same as that of GR, a result which is in agreement with the conclusions of [390, 391] for fully *Diff*-invariant versions of UG (but see [392] for a conflicting result within a

Hamiltonian analysis). For an updated review on perturbative computations of scattering amplitudes in UG, see [393].

The quantum (in)equivalence was latter revisited in [394] for the case of *TDiff* and later extended for the case of *WTDiff* in [393], both in the Euclidean setting. In [394], a formal proof at the level of path integrals was put forward for a general *Diff*-invariant action $S_{Diff}[g(\bar{g};h)]$ within the background-field method approach. By gauge-fixing the longitudinal diffeomorphisms (*LDiff*), followed by an appropriate definition of the functional measure, it was shown that the path integral of the *Diff*-invariant action over the fluctuation field was equivalent to that of its unimodular version. Thus, showing that there is a quantization scheme where both quantum theories are equivalent.

In this chapter, we leave aside this discussion and take *TDiff* as the fundamental symmetry of the would-be theory of quantum gravity and look for further hints for the existence of a non-trivial UV fixed point. For simplicity, we call the hypothetical asymptotically safe theory as unimodular quantum gravity (UQG), although it does not mean that our starting point for the quantization is the unimodular version of the Einstein-Hilbert action. Earlier results on asymptotic safety and unimodular gravity can be found in [395–398], where a non-trivial fixed point was obtained within truncations of the flowing action Γ_k. We provide a systematic analysis of fixed points within certain classes of truncations of Γ_k by taking into account the following refinements: We take Γ_k to be a function of the Ricci scalar and the quadratic contraction of Ricci tensors, i.e.,

$$\Gamma_k = \int \mathrm{d}^d x\, \omega\, f_k(R, R^{\mu\nu}R_{\mu\nu})\,. \tag{5.1.1}$$

For concreteness, we subdivide the analysis in two classes, the first being the so-called $f(R)$-truncations, i.e., $f_k(R, R^{\mu\nu}R_{\mu\nu}) = f_k(R)$ and the second is defined by $f_k(R, R^{\mu\nu}R_{\mu\nu}) = F_k(R^2_{\mu\nu}) + RZ_k(R^2_{\mu\nu})$, where $F_k(R^2_{\mu\nu})$ and $Z_k(R^2_{\mu\nu})$ are arbitrary functions. The second class of truncations was introduced in [399]. For both classes, we restrict the analysis to polynomial expansions of the curvatures on a spherical background, for technical simplicity. The other improvement that we implement in this chapter is that we employ the modified flow equation for UQG introduced in [142] due to the properties of the functional measure of UQG discussed in [30, 387]. Moreover, we treat the anomalous dimensions of the elementary fields in different approximations as discussed in the context of UG in [142]. Finally, we minimally couple matter fields and analyse the impact they play on the gravitational couplings.

5.2 Executive summary

The results obtained in the future sections of this chapter can be summarized in the following way:

- We considered extended truncations for a general Langragian $f_k(R, R^2_{\mu\nu})$. For this, flow equations have been derived, in a spherical background, for particular polynomial projections for the sub-classes $f_k(R)$ and $F_k(R^2_{\mu\nu}) + RZ_k(R^2_{\mu\nu})$ for two choices of the endomorphism parameter in the regulator function. For both choices, we have observed stable qualitative results in both polynomial truncations, where the fixed point features two relevant directions.

- We found that the modification in the flow equation for UQG due to the proper treatment of the functional measure does not seem to change the qualitative properties of the fixed-point structure in comparison with previous works in the literature.

- Finally, we also investigated the impact of matter fields on fixed-point candidates in the unimodular theory space. The minimal requirement for a viable scenario of asymptotically safe UQG coupled to matter is that it should accommodate the matter content associated with the SM, *i.e.*, $N_s = 4$, $N_v = 12$ and $N_f = 22.5$. The results in Table 5.1 fo Section 5.7.2 indicate that such matter content is compatible with an asymptotically safe scenario. We also find indications of suitable fixed-point candidates for UG coupled to the matter content $N_s = 4$, $N_v = 12$ and $N_f = 24$, which corresponds to a SM extension where we add three right-handed neutrinos. For the matter content corresponding to beyond SM scenarios of *minimal supersymmetric standard model* (MSSM) and SU(5) *grand unified theories* (GUT), there is no suitable fixed-point candidate. For the matter content corresponding to SO(10) GUT, we do not find suitable fixed-point candidates at the level of the unimodular Einstein-Hilbert truncation, but we find fixed-point candidates for higher-order truncations. In general, our results for asymptotically safe UQG show a qualitative agreement with investigations based on the "standard" scenario for ASQG.

5.3 Unimodular gravity: The classical theory

The name *unimodular gravity* stems from constraining gravity to obey $\sqrt{|g|} = 1$. Interestingly, this version of UG was first explored by Einstein himself (see [400] for the English version of the manuscript.) However, behind this specific condition is a predetermined choice of coordinate systems with dimensions of length. Moving away from this restriction, we will adopt a more general definition of UG by requiring that the square root of the determinant of the metric is taken to be some prescribed fixed function $\omega(x)$, which is a scalar density of weight one. Hence, the so-called unimodularity condition reads[2]

$$\sqrt{|g(x)|} = \omega(x)\,. \tag{5.3.1}$$

The symmetry group is reduced from the group of diffeomorphisms (*Diff*) to the subgroup of transverse diffeomorphisms (*TDiff*), *i.e.*, volume-preserving coordinate transformations[3]. Such a group is generated by transverse vectors ϵ^α_T, which satisfy $\nabla_\alpha \epsilon^\alpha_T = 0$, where the covariant derivative is defined with respect to the unimodular metric $g_{\mu\nu}$. This can be seen by looking at the variation of the determinant of the metric under *TDiff* transformations $\delta_{\epsilon_T} g_{\mu\nu} = g_{\nu\alpha}\nabla_\mu \epsilon^\alpha_T + g_{\mu\alpha}\nabla_\nu \epsilon^\alpha_T$, namely

$$\delta_{\epsilon_T}(\det g_{\mu\nu}) = g^{\alpha\beta}\delta_{\epsilon_T} g_{\alpha\beta} \det g_{\mu\nu} = 2\det g_{\mu\nu}\,(\nabla_\alpha \epsilon^\alpha_T) = 0\,. \tag{5.3.2}$$

[2]For the discussion on the classical theory of UG, there is no need to stick to an Euclidean signature and we come back *momentarily* to the Lorentzian setting.

[3]We remark that UG is different from the so-called *TDiff*-gravity [401]. Despite the fact that both theories share the symmetry-reduced group of *TDiff* transformations, in *TDiff*-gravity no restriction is imposed on the determinant of the metric, and, as a consequence, an extra propagating mode is present in the theory in comparison to UG. Additionally, *TDiff*-gravity theories are generally equivalent to scalar-tensor theories under a specific gauge-fixing [401, 402].

The unimodular version of a general gravity-matter action $S_{\rm UG}[g;\Phi]$ is constructed by replacing $\sqrt{|g(x)|}$ by the fixed, non-dynamical scalar function $\omega(x)$ in the volume form. Here, Φ denotes a generic matter field multiplet. Since the determinant of the metric is a fixed function, any arbitrary unimodular-preserving functional variation of the metric is subject to the tracelessness condition

$$g^{\mu\nu}\tilde{\delta}g_{\mu\nu} = 0, \tag{5.3.3}$$

where the tilde notation defines variation which satisfies the condition (5.3.1). Relation (5.3.3) allows us to express $\tilde{\delta}g_{\mu\nu}$ in terms of the traceless part of $\delta g_{\mu\nu}$ in d dimensions, namely

$$\tilde{\delta}g_{\mu\nu} = \left(\delta^{\alpha\beta}_{\mu\nu} - \frac{1}{d}g_{\mu\nu}g^{\alpha\beta}\right)\delta g_{\alpha\beta}, \tag{5.3.4}$$

where $\delta^{\alpha\beta}_{\mu\nu} = \frac{1}{2}(\delta^{\alpha}_{\mu}\delta^{\beta}_{\nu} + \delta^{\beta}_{\mu}\delta^{\alpha}_{\nu})$ is the symmetric identity. The unimodular-preserving functional variation of the gravity-matter action, $\tilde{\delta}S_{\rm UG}[g;\Phi]$, leads to the trace-free form of Einstein's field equations (see, *e.g.*, [30, 393]). For the case of the Einstein-Hilbert action plus a generic matter action[4],

$$S_{\rm UG}[g;\Phi] = -\frac{1}{16\pi G_{\rm N}}\int \mathrm{d}^d x\,\omega\,R(g) + S_m[g;\Phi], \tag{5.3.5}$$

with $G_{\rm N}$ being the gravitational Newton constant, the trace-free equations read

$$R^{\mu\nu} - \frac{1}{d}g^{\mu\nu}R = 8\pi G_{\rm N}\left(T^{\mu\nu}_{\rm UG} - \frac{1}{d}g^{\mu\nu}T_{\rm UG}\right), \tag{5.3.6}$$

where we have defined the symmetric rank-two tensor $T^{\mu\nu}_{\rm UG} = \dfrac{2}{\omega}\dfrac{\delta S_m}{\delta g_{\mu\nu}}$. However, we should not fall into the temptation to call this quantity an energy-momentum tensor for two reasons. First, the underlying symmetry with respect to *TDiff* is not sufficient to guarantee that $T^{\mu\nu}_{\rm UG}$ is conserved. Second, the quantity $T^{\mu\nu}_{\rm UG}$ leads to a dynamical different structure with respect to the corresponding energy-momentum tensor in GR. For instance, if we consider a scalar field coupled to gravity in the unimodular setting,

$$S_\phi = \int \mathrm{d}^d x\,\omega\left(-\frac{1}{2}g^{\mu\nu}\nabla_\mu\phi\nabla_\nu\phi - V(\phi)\right) = \int \mathrm{d}^d x\,\omega\,\mathcal{L}_m(g;\phi), \tag{5.3.7}$$

we would get $T^{\mu\nu}_{\rm UG} = \nabla^\mu\phi\nabla^\nu\phi$. This is not the same as $T^{\mu\nu}_{\rm GR} = \nabla^\mu\phi\nabla^\nu\phi - g^{\mu\nu}\left(\frac{1}{2}\nabla^\alpha\phi\nabla_\alpha\phi + V(\phi)\right)$, which would be the energy-momentum tensor for a scalar field coupled to GR. In particular, we see that $T^{\mu\nu}_{\rm UG}$ does not recover the correct flat-field limit that one would obtain from $T^{\mu\nu}_{\rm GR}$.

However, by demanding the matter part of the action to be *TDiff*-invariant, there follows the

[4]Notice that, since the metric determinant is a fixed scalar density, a vacuum energy contribution such as a cosmological constant automatically decouples and we can omit such a a term in the action from the beginning. Thus, it is usually said that the vaccum energy does not "gravitate" in UG.

weaker condition[5] [30]

$$\nabla_\mu T^{\mu\nu}_{\rm UG} = \nabla^\nu \Sigma(x) \to \nabla_\mu (T^{\mu\nu}_{\rm UG} - g^{\mu\nu}\Sigma) = 0, \tag{5.3.9}$$

where we can define a new tensor which is covariantly conserved with the help of an arbitrary scalar function $\Sigma(x)$. This implies that the rank-two tensor extracted from the constrained variation can be improved to the one extracted from standard GR. In this regard, the usual statement of energy-momentum conservation is seen as a subsidiary condition in UG. Moreover, the modified conserved tensor $T^{\mu\nu}_{\rm UG} - g^{\mu\nu}\Sigma$ matches $T_{\rm GR}$ if one identifies the arbitrary auxiliary scalar function with (minus) the matter Lagrangian, *i.e.*, $\Sigma = -\mathcal{L}_m$.

We highlight that, in many works (see, *e.g.*, the status report [393] and references therein), it is invoked a conservation of the tensor $T^{\mu\nu}_{\rm UG}$ obtained from the constrained variation. In particular, it is said that this is an essential condition in order to regain Einstein's field equations from the trace-free unimodular equations. However, as we saw, this is an over-constraining condition, since $T^{\mu\nu}_{\rm UG}$ is not necessarily conserved if one works out with an explicit example.

Furthermore, the trace-free unimodular field equations (5.3.6) are invariant under the redefinition $T^{\mu\nu}_{\rm UG} \mapsto T^{\mu\nu}_{\rm GR} = T^{\mu\nu}_{\rm UG} - g^{\mu\nu}\Sigma$. Therefore, using this freedom, the trace-free unimodular field equations read

$$R^{\mu\nu} - \frac{1}{d} g^{\mu\nu} R = 8\pi G_{\rm N} \left(T^{\mu\nu}_{\rm GR} - \frac{1}{d} g^{\mu\nu} T_{\rm GR} \right). \tag{5.3.10}$$

Finally, taking the four-divergence of Eq. (5.3.10), making use of energy-momentum conservation and employing the Bianchi identities, one obtains

$$\nabla^\nu \left(\frac{d-2}{2} R - 8\pi G_{\rm N} T_{\rm GR} \right) = 0, \tag{5.3.11}$$

which can be straightforwardly integrated, resulting in

$$\frac{d-2}{2} R - 8\pi G_{\rm N} T_{\rm GR} = d\,\Lambda_0, \tag{5.3.12}$$

where Λ_0 denotes an integration constant (the multiplicative factor of d has been introduced for further convenience). By plugging this result back into Eq. (5.3.10), one regains the Einstein's field equations for standard GR,

$$R^{\mu\nu} - \frac{1}{2} g^{\mu\nu} R + g^{\mu\nu}\Lambda_0 = 8\pi G_{\rm N} T^{\mu\nu}_{\rm GR} \tag{5.3.13}$$

and the classical equivalence between GR and UG is complete. Therefore, locally, UG provides the same equations of motion as GR, and the cosmological constant appears as an integration constant, which must be determined by initial boundary conditions. However, if the manifold has a well-defined volume V, then the integration of the local unimodularity condition $\sqrt{|g(x)|} = \omega(x)$ amounts to fixing

[5] Indeed, this weaker condition fulfills the invariance of the matter action under *TDiff* transformations according to

$$\begin{aligned} \delta_{\epsilon_{\rm T}} S_m &= \int {\rm d}^d x \frac{\delta S_m}{\delta g_{\mu\nu}} \delta_{\epsilon_{\rm T}} g_{\mu\nu} = \frac{1}{2} \int {\rm d}^d x\, \omega \tilde{T}^{\mu\nu} (2 g_{\mu\alpha} \nabla_\nu \epsilon^\alpha_{\rm T}) \\ &= - \int {\rm d}^d x\, \omega (\nabla_\mu \tilde{T}^{\mu\nu}) \epsilon_{{\rm T},\nu} = - \int {\rm d}^d x\, \omega (\nabla^\nu \Sigma) \epsilon_{{\rm T},\nu} = \int {\rm d}^d x\, \omega \Sigma (\nabla_\mu \epsilon^\mu_{\rm T}) = 0. \end{aligned} \tag{5.3.8}$$

the volume form, which imposes a global physical restriction, *i.e.*,

$$\int \mathrm{d}^d x \sqrt{|g(x)|} = \int \mathrm{d}^d x \, \omega(x) = V. \tag{5.3.14}$$

In this sense, there is a single global degree of freedom associated to the spacetime total volume (and thus to the cosmological constant), playing a different role in GR and UG.

Finally, we note that if the tensor $T^{\mu\nu}_{\mathrm{UG}}$ had not been redefined, there would be an extra term associated to $\Sigma(x)$ in the field equations (5.3.13) which could be associated to some kind of diffusion process, which, in turn, would hamper the GR-UG classical equivalence, but allowing for interesting applications in astrophysics and cosmology [403–407].

5.4 Unimodular quantum gravity: Method and model

5.4.1 UG and the background-field method

For the purposes of this chapter, it is highly convenient to choose the exponential parameterizationor split of the metric. We recall its definition:

$$g_{\mu\nu} = \bar{g}_{\mu\alpha}[\exp(\kappa\, h^{\cdot}_{\cdot})]^{\alpha}_{\ \nu} = \bar{g}_{\mu\nu} + \kappa\, h_{\mu\nu} + \sum_{n=2}^{\infty} \frac{\kappa^n}{n!} h_{\mu\alpha_1} \cdots h^{\alpha_{n-1}}_{\ \ \ \nu}, \tag{5.4.1}$$

with $\kappa = (32\pi G_{\mathrm{N}})^{1/2}$. The unimodularity condition $\det g_{\mu\nu} = \omega^2(x)$ can be easily implemented in Eq. (5.4.1) by choosing a unimodular background $\det \bar{g}_{\mu\nu} = \omega^2(x)$ and traceless fluctuations $\bar{g}^{\mu\nu} h_{\mu\nu} \equiv h^{\mathrm{tr}} = 0$. This allows to write the transversality condition in terms of the background covariant derivative:

$$0 = \nabla_\mu \epsilon^\mu_{\mathrm{T}} = \frac{1}{\sqrt{g}} \partial_\mu (\sqrt{g} \epsilon^\mu_{\mathrm{T}}) = \frac{1}{\sqrt{\bar{g}}} \partial_\mu (\sqrt{\bar{g}} \epsilon^\mu_{\mathrm{T}}) = \bar{\nabla}_\mu \epsilon^\mu_{\mathrm{T}}. \tag{5.4.2}$$

In a path-integral formulation, the restriction to traceless fluctuations around a unimodular background in the exponential parameterization automatically restricts the configuration space to unimodular metrics. It must be emphasized that the tracelessness of the fluctuation field is not taken as a gauge condition but rather as a constraint from the very definition of such a field. Such a formulation of the unimodularity condition is called as "minimal version" and was put forward in [30, 387, 395, 397, 398]. This is one particular way to implement the unimodularity condition in the path integral and it is the one we adopt in this chapter. Different strategies to implement such a condition may bring different conclusions with respect to those reported here. See, e.g., [396, 408, 409] for different perspectives on how to implement the unimodularity condition in the path integral.

5.4.2 Digression on the Faddeev-Popov quantization in UG

The Euclidean path integral of UQG is performed over trace-free fluctuations in the exponential parameterization as discussed in Subsect. 5.4.1 and can be written formally as

$$\mathcal{Z}_{\rm UQG} = \int \frac{\mathcal{D}h_{\mu\nu}^{\text{tr-free}}}{V_{\rm TDiff}} \, \mathrm{e}^{-S_{\rm UG}[h;\bar{g}]}, \tag{5.4.3}$$

where $V_{\rm TDiff}$ stands for the volume of the *TDiff* group and the classical unimodular action $S_{\rm UG}[h;\bar{g}]$ is invariant under *TDiff* - but does not need to coincide with the unimodular version of the Einstein-Hilbert action. Applying the standard Faddeev-Popov procedure[6], one inserts in the functional integral a formal identity as

$$\mathcal{Z}_{\rm UQG} = \int \frac{\mathcal{D}h_{\mu\nu}^{\text{tr-free}}}{V_{\rm TDiff}} \left(\int \mathcal{D}\epsilon^{\rm T} \Delta_{\rm FP} \, \delta(F^{\rm T}) \right) \mathrm{e}^{-S_{\rm UG}[h;\bar{g}]}, \tag{5.4.4}$$

where $\Delta_{\rm FP}$ corresponds to the Faddeev-Popov determinant and $F_\mu^{\rm T}[h;\bar{g}] = 0$ corresponds to a transverse gauge-fixing condition, which respects the transversality of the diffeomorphisms. The Faddeev-Popov unity is obtained by the integration over transverse contravariant vectors $\epsilon^{{\rm T}\mu}$. In addition, we assume that the integration measures are invariant under *TDiff*.

Differently from the standard situation in the Faddeev-Popov prescription, one cannot factor out the integral over the transverse vectors $\epsilon^{{\rm T}\mu}$ and associate it with the $V_{\rm TDiff}$. The main reason is that the transverse vector is metric-dependent. Following [30, 387], the volume of *TDiff* is defined as

$$V_{\rm TDiff} = \int \mathcal{D}\epsilon \, \delta(\bar{\nabla}_\mu \epsilon^\mu) \, , \tag{5.4.5}$$

where it is used that for unimodular metrics, $\nabla_\mu \epsilon^\mu = \bar{\nabla}_\mu \epsilon^\mu$. Decomposing ϵ^μ in terms of transverse and longitudinal parts, i.e., $\epsilon^\mu = \epsilon^{{\rm T}\mu} + \bar{\nabla}^\mu \varphi$, it is straightforward to find that

$$V_{\rm TDiff} = \mathrm{Det}^{-1/2}(-\bar{\nabla}^2) \int \mathcal{D}\epsilon^{\rm T} \, , \tag{5.4.6}$$

as a proper representation of the volume of the *TDiff* group. Therefore, the final expression of the path integral of unimodular quantum gravity is represented as

$$\mathcal{Z}_{\rm UQG} = \int \mathcal{D}h_{\mu\nu}^{\text{tr-free}} \mathcal{D}\bar{C}_\alpha \mathcal{D}C^\beta \, \mathrm{Det}^{1/2}(-\bar{\nabla}^2) \, \mathrm{e}^{-S_{\rm UG}[h;\bar{g}] - S_{\rm g.f.+gh.}[h,\bar{C},C;\bar{g}]}, \tag{5.4.7}$$

where $S_{\rm g.f.+gh.}[h,\bar{C},C;\bar{g}]$ corresponds to a gauge-fixing action along with Faddeev-Popov ghosts $\bar{C}_\alpha$ and C^β term. In summary, Eq. (5.4.7) is the proper formal definition of the Euclidean functional integral of UG (in its minimal version) and the starting point for applying fRG techniques.

[6] See [30, 142, 387] for further details about the Faddeev-Popov procedure in UG in its minimal version.

5.4.3 Functional Renormalization Group for UG

In order to search for a fixed point in the renormalization group flow, we employ functional renormalization techniques, broadly discussed in Section 2.3. One can formally define a scale-dependent path integral for a metric formulation of UQG by introducing a regulator action in the Boltzmann factor. This yields

$$\mathcal{Z}_{\mathrm{UQG,k}}[J,\eta,\bar{\eta};\bar{g}] = \int \mathcal{D}h^{\text{tr-free}}_{\mu\nu}\mathcal{D}\bar{C}_{\alpha}\mathcal{D}C^{\beta}\,\mathrm{Det}^{1/2}(-\bar{\nabla}^2)\,\exp\Bigg(-S_{\mathrm{UG}}[h;\bar{g}] - S_{\text{g.f.+gh.}}[h,C,\bar{C};\bar{g}] \\ - \Delta S_k[h,C,\bar{C};\bar{g}] + \int \mathrm{d}^d x\,\sqrt{\bar{g}}\left(J^{\mu\nu}h_{\mu\nu} + \bar{\eta}_{\mu}C^{\mu} - \bar{C}_{\mu}\eta^{\mu}\right)\Bigg), \tag{5.4.8}$$

where, $(J^{\mu\nu},\eta^{\mu},\bar{\eta}_{\mu})$ are external classical sources. Following the discussion in Section 2.3, it is straightforward to derive the Wetterich equation for UQG. The flow equation now receives an extra contribution coming from the extra determinant in (5.4.7). Regularizing the extra determinant as $\mathrm{Det}(-\bar{\nabla}^2) \mapsto \mathrm{Det}(P_k(-\bar{\nabla}^2))$, where $P_k(z) = z + R_k(z)$, the flow equation for Γ_k becomes

$$\partial_t\Gamma_k = \frac{1}{2}\mathrm{STr}\left[\left(\Gamma_k^{(2)} + \mathbf{R}_k\right)^{-1}\partial_t\mathbf{R}_k\right] - \frac{1}{2}\mathrm{Tr}\left(\frac{\partial_t R_k(-\bar{\nabla}^2)}{P_k(-\bar{\nabla}^2)}\right). \tag{5.4.9}$$

Note that, according to the procedure adopted earlier, the extra determinant does not generate additional fluctuation vertices and it arises from a proper application of the Faddeev-Popov procedure in UG. As a consequence, it contributes only to the "background flow" $\partial_t\Gamma_k[0;\bar{g}]$.

5.4.4 Setting the truncation for unimodular gravity-matter systems

In this chapter, the key strategy to obtain information about the fixed-point structure is based on a mixed approach which combines the background-field approximation, vertex, and derivative expansion, similarly to what has been done in [142, 190, 212, 410–414]. On the one hand, in the background approximation the extraction of the beta functions of the dimensionless gravitational background couplings is obtained from the flow equation by turning off all the fluctuating fields after the computation of the Hessian. Moreover, the anomalous dimension of the graviton is identified with the running of the background Newton coupling. The ghost and matter anomalous dimensions are set to zero. On the other hand, a simultaneous vertex and derivative expansion generate one-loop-structure diagrams as corrections to the flow of the two-point function of the fields and allow to unambiguously derive independent anomalous dimensions of all fluctuating fields. In this sense, the extra functional trace associated with the path integral measure only contributes to the background flow, since it only depends on the background metric. Furthermore, as an approximation, the different avatars of the Newton coupling (see, *e.g.*, [195, 213]) in the vertices and graviton propagator are identified with its background value.

We consider a truncation for the flowing action Γ_k in the unimodular setting containing an arbitrary

number of massless Gaussian matter fields[7], namely scalar, Abelian vector and Dirac fields, minimally coupled to gravity in four-dimensional Euclidean spacetime. Throughout the chapter, we investigate a truncation of the form

$$\Gamma_k = \Gamma_k^{\text{gravity}} + \Gamma_k^{\text{matter}} + \Gamma_k^{\text{g.f.}} + \Gamma_k^{\text{gh.}}\,, \tag{5.4.10}$$

where we follow [136, 399] and write the gravitational sector as

$$\Gamma_k^{\text{gravity}}[g_{\mu\nu}] = \frac{1}{16\pi G_{\text{N},k}} \int_x \omega\, f_k(R, R^2_{\mu\nu})\,, \tag{5.4.11}$$

where $G_{\text{N},k}$ is the dimensionful Newton coupling, f_k is an arbitrary function of the Ricci scalar and the square of the Ricci tensor, $R^2_{\mu\nu} = R_{\mu\nu}R^{\mu\nu}$. The k-dependence comes from the scale-dependent renormalization factors and couplings of curvature invariants. The matter sector of the effective average action is composed of N_ϕ scalar fields, N_A Abelian vector fields and N_ψ Dirac spinors. Its complete action is given by

$$\begin{aligned}\Gamma_k^{\text{matter}}[g,\phi,\bar\psi,\psi,A] = \frac{1}{2}\sum_{i=1}^{N_\phi}\int_x \omega\, g^{\mu\nu}\partial_\mu\phi_i\partial_\nu\phi_i + \sum_{i=1}^{N_\psi}\int_x \omega\, i\bar\psi_i \not{\nabla}\psi_i \\ + \frac{1}{4}\sum_{i=1}^{N_A}\int_x \omega\, g^{\mu\alpha}g^{\nu\beta}F_{i,\mu\nu}F_{i,\alpha\beta}\,,\end{aligned} \tag{5.4.12}$$

where the summation index i runs over the particle species and $F_{i,\mu\nu}$ is the field-strength of the Abelian gauge field $A_{i,\mu}$. We do not consider the running of wave-function renormalization factors of the matter fields as they do not lead to self-consistent results within the hybrid approximation adopted in this chapter (see Subsect. 5.7.1 for details). The covariant Dirac operator $\not{\nabla} = e_a{}^\mu\gamma^a\nabla_\mu$ satisfies the Lichnerowicz relation

$$\Delta_{\text{L}\frac{1}{2}}\psi_i = -\not{\nabla}^2\psi_i = \left(-\nabla^2 + \frac{R}{4}\right)\psi_i\,. \tag{5.4.13}$$

The fermion-gravity interaction is achieved through the vierbein and spin connection. In a spacetime manifold with vanishing torsion, these are not independent fields and can both be expressed in terms of $h_{\mu\nu}$ adapted to the exponential decomposition once the local $O(4)$ gauge invariance is gauge-fixed by a Lorentz symmetric condition (see App. B in Ref. [205])[8]. Moreover, due to the relation $g_{\mu\nu} = e^a{}_\mu e^b{}_\nu\eta_{ab}$, the vierbein also obeys the unimodularity condition, i.e., $\det e^a_{\ \mu} = \omega$. Besides featuring a $\mathbb{Z}_2$ symmetry for the scalar sector under which $\phi_i \mapsto -\phi_i$, this toy model also features a shift symmetry $\phi_i \mapsto \phi_i + \text{const.}$, which prevents a scalar mass term. Additionally, an axial U(1) symmetry, i.e., $\psi_i \to e^{i\alpha\gamma_5}\psi_i$, $\bar\psi_i \to \bar\psi_i e^{i\alpha\gamma_5}$, prohibits a Dirac mass term. In this model the scalars and "chiral" fermions are uncharged, not leading to gauge interactions.

The gauge-fixing action for the *TDiff* and the Abelian gauge symmetry is given by [30, 205, 387, 395, 397]

$$\Gamma_k^{\text{g.f.}}[h,A;\bar g] = \frac{1}{2a}\int_x \omega\,\bar g^{\mu\nu}F^{\text{T}}_\mu[h;\bar g]F^{\text{T}}_\nu[h;\bar g] + \frac{1}{2\zeta}\sum_{i=1}^{N_A}\int_x \omega\,(\bar g^{\mu\nu}\bar\nabla_\mu A_{i,\nu})^2, \tag{5.4.14}$$

[7] Meaning that we do not consider matter self-interactions.

[8] Alternatively, for the Dirac covariant operator $\not{\nabla}$, one could use the spin-base formalism [415–417] expressed in accordance with the exponential parameterization. Both prescriptions are equivalent at the level of our computations.

where a and ζ represent gauge parameters for the gravitational and Abelian sectors, respectively. Using the transverse projector with respect to the background metric $(\mathcal{P}_{\mathrm{T}})_{\mu\nu} = \bar{g}_{\mu\nu} - \bar{\nabla}_\mu(\bar{\nabla}^2)^{-1}\bar{\nabla}_\nu$, we define the transverse gauge-fixing function as $F^{\mathrm{T}}_\mu[h;\bar{g}] = \sqrt{2}\,(\mathcal{P}_{\mathrm{T}})_\mu{}^\nu\,\bar{\nabla}^\alpha h_{\nu\alpha}$. This particular prescription of the gauge-fixing function is necessary, since only the transverse diffeomorphism sector should be fixed. In this chapter, we adopt the Landau gauge for both gravitational and Abelian sectors, i.e., $a \to 0$ and $\zeta \to 0$. The introduction of the transverse projector makes the gauge fixing for *TDiff* a non-local functional. This could be avoided by allowing a higher-derivative operator in the gauge-fixing, see, e.g., [398].

Accompanying the gauge-fixing term there is the action for the Faddeev-Popov ghosts[9] which reads

$$\Gamma^{\mathrm{gh.}}_k[h,\bar{C},C,\bar{c},c;\bar{g}] = \int_x \omega\,\bar{C}_\mu\,\bar{g}^{\mu\nu}\frac{\delta F^{\mathrm{T}}_\nu[h;\bar{g}]}{\delta h_{\alpha\beta}}\delta^Q_C h_{\alpha\beta} + \sum_{i=1}^{N_A}\int_x \omega\,\bar{c}_i(-\bar{\nabla}^2)c_i, \tag{5.4.15}$$

where $C^\mu\,(\bar{C}_\mu)$ and $c_i\,(\bar{c}_i)$ are ghost and anti-ghost for the gravitational and Abelian sectors, respectively. In the unimodular setting, the Faddeev-Popov ghost for the gravitational sector is constrained by the transversality condition $\nabla_\mu C^\mu = \bar{\nabla}_\mu(g^{\mu\nu}C_\nu) = 0$ as a consequence of the transverse nature of the *TDiff* generator. Furthermore, $\delta^Q_C h_{\alpha\beta}$ corresponds to the "quantum" transformation of the fluctuation field with generator being the ghost field C^μ. The explicit implementation of the gravitational ghost sector suitable for the exponential split of the metric is discussed in [141, 142].

A minimal and diagonal Hessian together with an exact inversion of the kinetic operators can be achieved following two steps: first, going to a spherical background, characterized by

$$\bar{R}_{\mu\nu\alpha\beta} = \frac{1}{12}(\bar{g}_{\mu\alpha}\bar{g}_{\nu\beta} - \bar{g}_{\mu\beta}\bar{g}_{\nu\alpha})\bar{R}, \qquad \text{and} \qquad \bar{R}_{\mu\nu} = \frac{1}{4}\bar{g}_{\mu\nu}\bar{R}, \tag{5.4.16}$$

and, second, by decomposing the fluctuation field $h_{\mu\nu}$ into the York basis [421], namely,

$$h_{\mu\nu} = h^{\mathrm{TT}}_{\mu\nu} + 2\bar{\nabla}_{(\mu}\xi_{\nu)} + \Big(\bar{\nabla}_\mu\bar{\nabla}_\nu - \frac{1}{4}\bar{g}_{\mu\nu}\bar{\nabla}^2\Big)\sigma. \tag{5.4.17}$$

We emphasize the absence of the trace mode in the decomposition due to the unimodularity condition. No non-local field redefinitions are performed and, as a consequence, the Jacobians arising from the change of variables are taken into account in the flow equation by a suitable regularization of the resulting determinants. Furthermore, appropriate wave-function renormalization factors are introduced for the gravitational ghost fields and for each spin sector of the gravitational fluctuation according to

$$h^{\mathrm{TT}}_{\mu\nu} \mapsto \mathcal{Z}^{1/2}_{k,\mathrm{TT}}\,h^{\mathrm{TT}}_{\mu\nu}\,, \qquad \xi_\mu \mapsto \mathcal{Z}^{1/2}_{k,\xi}\,\xi_\mu, \qquad \sigma \mapsto \mathcal{Z}^{1/2}_{k,\sigma}\,\sigma, \tag{5.4.18a}$$

$$C^\mu \mapsto \mathcal{Z}^{1/2}_{k,C}\,C^\mu, \qquad \bar{C}_\mu \mapsto \mathcal{Z}^{1/2}_{k,C}\,\bar{C}_\mu. \tag{5.4.18b}$$

[9] Alternatively, the gauge-fixing and ghost terms for different formulations of unimodular gravity can be derived through BRST transformations, see [408, 418]. See also [419, 420] for a discussion of the BRST implementation of the unimodular gauge.

The wave-function renormalization factors $\mathcal{Z}_{k,\Phi}$ with $\Phi = (\mathrm{TT}, \xi, \sigma, C, \bar{C})$ generate anomalous dimensions $\eta_\Phi = -\partial_t \ln \mathcal{Z}_{k,\Phi}$ and contribute to the system of beta functions of Newton and higher curvature couplings.

The Abelian gauge potentials are also decomposed into its transverse and longitudinal parts,

$$A_{i,\mu} = A^{\mathrm{T}}_{i,\mu} + \bar{\nabla}_\mu \big[(-\bar{\nabla}^2)^{-1/2} A^{\mathrm{L}}_i\big], \qquad \bar{\nabla}_\mu A^{\mathrm{T}\mu}_i = 0. \tag{5.4.19}$$

Contrary to the fluctuation field decomposition, herein we chose to insert an inverse square root of the Bochner Laplacian, $-\bar{\nabla}^2$, so that the Jacobian associated with this field redefinition is a simple identity.

5.5 Setting the flow equation

At the practical level, the right-hand side of the flow equation is expanded on the same basis as the one chosen for the truncation such that a suitable projection rule selects the beta functions associated to each coupling. The beta functions of the background gravitational couplings can be read off at zeroth order in the fluctuating fields and the elements of the Hessian[10] employed in such a computation are listed in the App. D.2. The entries of the regulator function $\mathbf{R}_k$ are built from the following prescription [180]

$$\mathbf{R}_{k,\varphi_i\varphi_j}(\Delta) = \Gamma^{(2)}_{k,\varphi_i\varphi_j}(\Delta)\Big|_{\Delta \mapsto \Delta + R_k(\Delta)} - \Gamma^{(2)}_{k,\varphi_i\varphi_j}(\Delta)\,, \tag{5.5.2}$$

where Δ is an appropriate coarse-graining operator and $\Gamma^{(2)}_{k,\varphi_i\varphi_j}$ denotes the second functional derivative of Γ_k with respect to the fields φ_i and φ_j. For the regulator kernel (i.e., for the shape function that enters the regulator) we choose the Litim-type cutoff (2.3.33)

$$R_k(\Delta) = (k^2 - \Delta)\theta(k^2 - \Delta)\,. \tag{5.5.3}$$

In particular, we adopt two types of regularization schemes distinguished by two common choices of coarse-graining operators [180] namely, the Bochner-Laplacian, $-\bar{\nabla}^2$ (Type I), and the Lichnerowicz-Laplacians, $\Delta_{\mathrm{L}s}$ (Type II), which are connected by the Lichnerowicz relations on a four-dimensional maximally symmetric Euclidean background

$$\Delta_{\mathrm{L}_2} = -\bar{\nabla}^2 + \frac{2}{3}\bar{R}\,, \qquad \Delta_{\mathrm{L}_1} = -\bar{\nabla}^2 + \frac{1}{4}\bar{R}\,, \qquad \Delta_{\mathrm{L}_0} = -\bar{\nabla}^2\,. \tag{5.5.4}$$

[10] The elements $\Gamma^{(0,2)}_k[x, y; \bar{g}, h]$ of the Hessian can be extracted after expanding the flowing action up to second order in the fluctuation field. Schematically, this reads

$$\begin{aligned}\Gamma_k = \bar{\Gamma}_k &+ \int \mathrm{d}^4x\, \omega(x) \Gamma^{(0,1)}_{k,A}[x; \bar{g}, h]\varphi^A(x) \\ &+ \frac{1}{2}\int \mathrm{d}^4x \int \mathrm{d}^4y\, \omega(x)\omega(y)\varphi^A(x)\Gamma^{(0,2)}_{k,AB}[x, y; \bar{g}, h]\varphi^B(y) + \mathcal{O}(\varphi^3),\end{aligned} \tag{5.5.1}$$

where $\varphi = (h_{\mu\nu}, C_\mu, \bar{C}^\mu)$.

Inspired by [190, 194, 422, 423], in order to accommodate both regularization prescriptions, we define the "interpolating" coarse-graining operator for each spin-s sector as $\Delta_s = \Delta_{\mathrm{L}s} - \gamma_s \bar{R}$, where the endomorphism parameters were introduced such that the choice $\gamma_0 = \gamma_{\frac{1}{2}} = \gamma_1 = \gamma_2 = 0$ implements the Lichnerowicz-Laplacians and $\gamma_0 = 0$, $\gamma_{\frac{1}{2}} = 1/4$, $\gamma_1 = 1/4$ and $\gamma_2 = 2/3$ result in the Bochner-Laplacian. According to [220], in order to account for a correct sign for the fermionic contributions to the Newton coupling constant, a Type II regularization must be adopted. The fermionic regulator function then is written as

$$\mathbf{R}_{k,\psi\psi}(z) = i\Big[\sqrt{1 + (k^2/z - 1)\theta(k^2/z - 1)} - 1\Big]\not{\nabla}, \tag{5.5.5}$$

where $z = \Delta_{\mathrm{L}_{\frac{1}{2}}}$. Furthermore, since for massless scalar fields both types of regularizations are equal, we adopt for simplicity the Type II regularization prescription for the gauge fields as well [190]. Henceforth, we explore in this chapter both types of coarse-graining operators only in the gravitational sector.

For the truncation (5.4.10), the running of the dimensionless gravitational couplings can be read off, at zeroth order in the fields, from the following flow equation written in the Landau gauge, i.e., $a = 0$,

$$\begin{aligned}
\partial_t \Gamma_k = {} & \frac{1}{2}\mathrm{Tr}_{(2)}\Big[\mathbf{G}_{\mathrm{TT}}\,\partial_t \mathbf{R}_{k,\mathrm{TT}}\Big] + \frac{1}{2}\mathrm{Tr}'_{(1)}\Big[\mathbf{G}_{\xi\xi}\,\partial_t \mathbf{R}_{k,\xi\xi}\Big] + \frac{1}{2}\mathrm{Tr}''_{(0)}\Big[\mathbf{G}_{\sigma\sigma}\,\partial_t \mathbf{R}_{k,\sigma\sigma}\Big] - \mathrm{Tr}_{(1)}\Big[\mathbf{G}_{C\bar{C}}\,\partial_t \mathbf{R}_{k,C\bar{C}}\Big] \\
& - \frac{1}{2}\mathrm{Tr}'_{(0)}\Big[\left(\Delta_0 + R_k(\Delta_0)\right)^{-1}\partial_t R_k(\Delta_0)\Big] + \frac{N_\phi}{2}\mathrm{Tr}_{(0)}\Big[\mathbf{G}_{\phi\phi}\,\partial_t \mathbf{R}_{k,\phi\phi}\Big] - N_\psi \mathrm{Tr}_{(1/2)}\Big[\mathbf{G}_{\psi\psi}\,\partial_t \mathbf{R}_{k,\psi\psi}\Big] \\
& + \frac{N_A}{2}\mathrm{Tr}_{(1)}\Big[\mathbf{G}_{A^{\mathrm{T}}A^{\mathrm{T}}}\,\partial_t \mathbf{R}_{k,A^{\mathrm{T}}A^{\mathrm{T}}}\Big] + \frac{N_A}{2}\mathrm{Tr}'_{(0)}\Big[\mathbf{G}_{A^{\mathrm{L}}A^{\mathrm{L}}}\,\partial_t \mathbf{R}_{k,A^{\mathrm{L}}A^{\mathrm{L}}}\Big] - N_A \mathrm{Tr}_{(0)}\Big[\mathbf{G}_{c\bar{c}}\,\partial_t \mathbf{R}_{k,c\bar{c}}\Big] \\
& + \mathcal{T}^{\mathrm{Jacob.}}_{(1)} + \mathcal{T}^{\mathrm{Jacob.}}_{(0)},
\end{aligned} \tag{5.5.6}$$

with $\mathbf{G}_{ij} = \Big[\big(\Gamma_k^{(2)} + \mathbf{R}_k\big)^{-1}\Big]_{ij}$ for every pair (i, j). The first term in the second line corresponds to the extra determinant accounting for an appropriate treatment of the volume of the *TDiff* group. The last two terms in the fourth line denote additional contributions coming from the Jacobian associated with the change of variables $h_{\mu\nu} \mapsto \{h^{\mathrm{TT}}_{\mu\nu}, \xi_\mu, \sigma\}$. Upon regularization $\Delta_s \mapsto \Delta_s + R_k(\Delta_s)$, these contributions manifest themselves as the following additional traces

$$\mathcal{T}^{\mathrm{Jacob.}}_{(1)} = -\frac{1}{2}\mathrm{Tr}'\left[\left(\Delta_1 + R_k(\Delta_1) + \frac{2\gamma_1 - 1}{2}\bar{R}\right)^{-1}\partial_t R_k(\Delta_1)\right], \tag{5.5.7a}$$

$$\begin{aligned}
\mathcal{T}^{\mathrm{Jacob.}}_{(0)} = {} & -\frac{1}{2}\mathrm{Tr}''\left[\left(\Delta_0 + R_k(\Delta_0) - \frac{1}{3}\bar{R}\right)^{-1}\partial_t R_k(\Delta_0)\right] \\
& - \frac{1}{2}\mathrm{Tr}''\Big[\left(\Delta_0 + R_k(\Delta_0)\right)^{-1}\partial_t R_k(\Delta_0)\Big].
\end{aligned} \tag{5.5.7b}$$

The computation of the traces in the fRG equation is performed with standard heat kernel techniques. All the necessary technical tools and notation are collected in App. D.3. In general, the result of the trace computation leads to very long expressions and, therefore, we shall not report explicit results here. The anomalous dimensions can be computed by acting with two functional derivatives with respect to the fields on the flow equation (5.5.6) and expanding the full scale-dependent effective

action in powers of the fields on a flat background. Their extraction is then obtained by means of suitable projection rules. We follow the same strategy as in [142, 205]. The explicit expressions for the anomalous dimensions used in this chapter are reported in App. D.4.

5.6 $f(R, R_{\mu\nu}R^{\mu\nu})$ projections and extraction of beta functions

In this section, we discuss the extraction of beta functions from two different types of polynomial projections of the $f_k(R, R_{\mu\nu}R^{\mu\nu})$-truncation minimally coupled with Gaussian matter degrees of freedom in the unimodular setting.

To extract the beta functions of the background gravitational couplings from the fRG equation, we can adopt a projection which consists in setting to zero all fluctuation fields. Within the background approximation, the truncation (5.4.10), inserted in the left-hand side of (5.5.6), leads to a flow equation of the form

$$\frac{1}{16\pi G_{\mathrm{N},k}}\Big[-\eta_{\mathrm{N}} f_k\left(\bar{R}, \bar{R}^2_{\mu\nu}\right) + \partial_t f_k\left(\bar{R}, \bar{R}^2_{\mu\nu}\right)\Big] = \mathcal{F}\left(f_k, f_k^{(m,n)}, \eta_i, \partial_t f_k, \partial_t f_k^{(m,n)}, N_\Psi\right), \tag{5.6.1}$$

where the left-hand side of (5.6.1) features the "background anomalous dimension" $\eta_{\mathrm{N}} = -\partial_t \ln \mathcal{Z}_{\mathrm{N}}$ with $\mathcal{Z}_{\mathrm{N}} = (16\pi G_{\mathrm{N},k})^{-1}$ and $N_\Psi = (N_\phi, N_A, N_\psi)$. The dependence on $\vec{\eta} = (\eta_{\mathrm{TT}}, \eta_\xi, \eta_\sigma, \eta_c)$ on the right-hand side of (5.6.1) comes from the regulator insertion $\partial_t \mathbf{R}_k$ associated with each field sector. Moreover, we adopt the compact notation

$$f_k^{(m,n)} = \frac{\partial^{m+n} f_k(\bar{R}, \bar{X})}{\partial \bar{R}^m \partial \bar{X}^n}, \tag{5.6.2}$$

with $\bar{X} = \bar{R}^2_{\mu\nu}$. In order to obtain concrete results, we resort to polynomial truncations. In principle, had we performed all calculations in a generic background, the most general polynomial expansion (within the class of the $f_k(R, R^2_{\mu\nu})$-truncation) would be of the form

$$f_k(R, R^2_{\mu\nu}) = \sum_{n_1,n_2} \bar{\alpha}_k^{(n_1,n_2)} R^{n_1} \left(R_{\mu\nu}R^{\mu\nu}\right)^{n_2} \tag{5.6.3}$$

where $\bar{\alpha}_k^{(n_1,n_2)}$ denotes the scale-dependent couplings. The running of the couplings $\bar{\alpha}_k^{(n_1,n_2)}$ can be extracted by expanding both sides of the flow equation (5.6.1) in powers of $\bar{R}$ and $\bar{R}_{\mu\nu}$ and comparing the coefficients of the same curvature invariants on both sides order by order. Unfortunately, this procedure carries an ambiguity for a spherical background as the invariant $\bar{R}^2_{\mu\nu}$ collapses to $\frac{1}{4}\bar{R}^2$. As a consequence, the running of any two couplings $\bar{\alpha}_k^{(p_1,p_2)}$ and $\bar{\alpha}_k^{(q_1,q_2)}$ can no longer be disentangled for all pairs (p_1, p_2) and (q_1, q_2) satisfying the relation $p_1 + 2p_2 = q_1 + 2q_2$. A way to bypass this ambiguity, without appealing to a generic background, is to impose some restriction on the function $f_k(R, R^2_{\mu\nu})$.

5.6.1 $f(R)$ polynomial projection

In this subsection, we consider the particular case corresponding to the $f(R)$-approximation, which can be directly obtained by neglecting the $R^2_{\mu\nu}$-dependence in our truncation. For practical computations, we focus on the polynomial approximation

$$f_k(R) = -R + \sum_{n=2}^{N} k^{2-2n}\alpha_{k,n}R^n\,, \tag{5.6.4}$$

where $\alpha_{k,n}$ corresponds to scale-dependent dimensionless couplings and the parameter N stands for a positive integer number that fixes the maximal degree of the polynomial truncation. This truncation was largely explored in the context of "standard" asymptotic safety. See, *e.g.*, [178–183, 194, 399, 422–435]. The coefficient of the first term is normalized to -1 in order to recover the unimodular Einstein-Hilbert truncation once higher-order powers of the curvature scalar are neglected. Furthermore, the zeroth-order term, which would be proportional to the cosmological constant, is absent since we are dealing with a unimodular theory space[11].

We extract the system of beta functions associated with the dimensionless Newton coupling G_k and the set of dimensionless couplings $\{\alpha_{k,n}\}_{n=2,\cdots,N}$ by plugging Eq. (5.6.4) into the flow equation (5.6.1) and expanding both sides of it up to order $\bar{R}^N$. In this case, the flow equation leads to the following structure

$$\frac{\eta_{\rm N}}{16\pi G_k}k^2\bar{R} + \frac{1}{16\pi G_k}\sum_{n=2}^{N}\Big((2-2n-\eta_{\rm N})\alpha_{k,n} + \beta_\alpha^{(n)}\Big)k^{4-2n}\bar{R}^n \equiv \sum_{n=1}^{N}\mathcal{H}_n\left(\alpha_k, N_\Psi, \vec{\eta}, \beta_\alpha^{(m)}\right), \tag{5.6.5}$$

where $G_k = k^2\,G_{{\rm N},k}$ is the dimensionless Newton coupling and we have defined $\beta_\alpha^{(n)} = \partial_t\alpha_{k,n}$. The function $\mathcal{H}_n$ has the general schematic form

$$\mathcal{H}_n\left(\alpha_k, N_\Psi, \vec{\eta}, \beta_\alpha^{(m)}\right) \equiv \mathcal{A}_n(\alpha_k) + \tilde{\mathcal{A}}_n(N_\Psi) + \sum_{j=1}^{4}\mathcal{B}_{n,j}(\alpha_k)\eta_j + \sum_{m=2}^{N}\mathcal{M}_{n,m}(\alpha_k)\beta_\alpha^{(m)}\,. \tag{5.6.6}$$

The coefficients $\mathcal{A}_n$, $\tilde{\mathcal{A}}_n$, $\mathcal{B}_{n,j}$ and $\mathcal{M}_{n,m}$ are scheme-dependent quantities and can be computed analytically for the Litim's cutoff. By matching contributions according to the power of scalar curvature, we arrive at the RG equations

$$\beta_G = 2G_k\left[1 + 8\pi G_k\,\mathcal{H}_1\left(\alpha_k, N_\Psi, \vec{\eta}, \beta_\alpha^{(m)}\right)\right], \tag{5.6.7a}$$

$$\beta_\alpha^{(n)} = (\eta_{\rm N} + 2n - 2)\alpha_{k,n} + 16\pi G_k\,\mathcal{H}_n\left(\alpha_k, N_\Psi, \vec{\eta}, \beta_\alpha^{(m)}\right), \tag{5.6.7b}$$

with $n = 2, \ldots, N$. In Eq. (5.6.7a) we have used $\eta_{\rm N} = G_k^{-1}\beta_G - 2$. We highlight that the system of

[11] It is important to emphasize that, since the introduction of the regulator breaks BRST invariance, mass-like terms for the graviton can be generated and mimick the effect of the cosmological constant [142]. Nevertheless, such terms arise as a symmetry-breaking effect due to the regulator and are not present in the background approximation.

RG equations defined by (5.6.7a) and (5.6.7b) provides only implicit results for the beta functions β_G and $\beta_\alpha^{(n)}$. Furthermore, the system is not closed because of the presence of the anomalous dimensions $(\eta_{\rm TT}, \eta_\xi, \eta_\sigma, \eta_c)$. In principle, this system can be solved analytically in order to extract explicit results for β_G and $\beta_\alpha^{(n)}$ once a prescription to obtain the anomalous dimensions is adopted. In Sect. 5.7.1, we will consider two types of prescriptions: the standard "RG-improvement" approximation[12] and a hybrid semi-perturbative approximation based on an independent calculation of the anomalous dimensions using the derivative expansion around a flat background. We emphasize that the latter prescription is somewhat not self-consistent since it glues together results obtained under different schemes and backgrounds. Nonetheless, we take this tentative choice to obtain results beyond the background approximation. As usual in functional methods, the use of hybrid schemes might be justified *a posteriori* if the underlying results find good convergence properties. Nevertheless, the final expressions for the system of RG equations are very lengthy and not worth being reported here.

The so-called non-trivial or non-Gaussian fixed-point (NGFP) solutions (denoted as G^* and α_n^*) may be obtained in terms of the following equations

$$2G^*\left[1 + 8\pi G^*\,\mathcal{H}_1\left(\alpha^*, N_\Psi, \vec{\eta}\,\big|_*, 0\right)\right] = 0, \tag{5.6.8a}$$

$$(2n-4)\alpha_n^* + 16\pi G^*\,\mathcal{H}_n\left(\alpha^*, N_\Psi, \vec{\eta}\,\big|_*, 0\right) = 0. \tag{5.6.8b}$$

The notation $(\cdots)\big|_*$ indicates that the quantity in parenthesis is evaluated at the fixed-point solution. In Sect. 5.7.1, we report numerical evidence for interacting fixed-point solutions associated with various choices of N.

5.6.2 $F(R_{\mu\nu}R^{\mu\nu}) + R\,Z(R_{\mu\nu}R^{\mu\nu})$ polynomial projection

Another way of bypassing the technical problem of distinguishing the invariants R^2 and $R_{\mu\nu}^2$ on a spherical background is to consider an alternative class of truncation, which is characterized by the following decomposition[13]

$$f_k(R, R_{\mu\nu}^2) = F_k(R_{\mu\nu}^2) + R\,Z_k(R_{\mu\nu}^2), \tag{5.6.9}$$

where $F_k(R_{\mu\nu}^2)$ and $Z_k(R_{\mu\nu}^2)$ denote scale-dependent arbitrary functions of the invariant $R_{\mu\nu}^2$. This class of truncation was first investigated in [399] as an approach to include effects beyond the tensor structure of the Ricci scalar. For practical calculations, we restrict our analysis to polynomial truncations defined by

$$F_k(R_{\mu\nu}R^{\mu\nu}) = \sum_{n=1}^{N_F} k^{2-4n}\rho_{k,2n}(R_{\mu\nu}R^{\mu\nu})^n\,, \tag{5.6.10a}$$

[12] In Appendix D.5, the reader can find more details about the identification of the background anomalous dimension with the one derived from the second derivative of the flowing action with respect to fluctuations.

[13] Hereafter we refer to such decomposition as FZ-truncation.

$$Z_k(R_{\mu\nu}R^{\mu\nu}) = -1 + \sum_{n=1}^{N_Z} k^{-4n}\rho_{k,2n+1}(R_{\mu\nu}R^{\mu\nu})^n\,, \tag{5.6.10b}$$

where $N_F = \lfloor N/2 \rfloor$ and $N_Z = \lfloor (N-1)/2 \rfloor$, with $\lfloor \cdots \rfloor$ representing the floor function. We denote as $\{\rho_{k,n}\}_{n=2,\cdots,N}$ the set of scale-dependent dimensionless couplings. This particular decomposition allows us to unambiguously extract the beta functions associated with the set of higher-curvature couplings $\{\rho_{k,n}\}_{n=2,\cdots,N}$ even in a spherical background. This follows from the fact that $F_k(R_{\mu\nu}R^{\mu\nu})$ and $R\,Z_k(R_{\mu\nu}R^{\mu\nu})$ contribute to the left-hand side of the flow equation with even and odd powers of $\bar{R}$, respectively, when projected onto a spherical background. Following the same procedure outlined in the $f(R)$-approximation, we extract the system of RG equations associated with the dimensionless couplings G_k and $\{\rho_{k,n}\}_{n=2,\cdots,N}$ by plugging (5.6.10a) and (5.6.10b) into both left-hand side and right-hand side of Eq. (5.6.1) to obtain the following expressions

$$\begin{aligned}
&\frac{1}{16\pi G_{\mathrm{N},k}}\left[-\eta_{\mathrm{N}} f_k\left(\bar{R}, \bar{R}^2_{\mu\nu}\right) + \partial_t f_k\left(\bar{R}, \bar{R}^2_{\mu\nu}\right)\right]\Big|_{S^4} = \\
&\qquad = \frac{\eta_{\mathrm{N}}}{16\pi G_k}k^2\bar{R} + \frac{1}{16\pi G_k}\sum_{n=1}^{N_F}\frac{k^{4-4n}}{4^n}\left(\beta_\rho^{(2n)} + (2-4n-\eta_{\mathrm{N}})\rho_{k,2n}\right)\bar{R}^{2n} \\
&\qquad + \frac{1}{16\pi G_k}\sum_{n=1}^{N_Z}\frac{k^{2-4n}}{4^n}\left(\beta_\rho^{(2n+1)} - (4n+\eta_{\mathrm{N}})\rho_{k,2n+1}\right)\bar{R}^{2n+1}\,,
\end{aligned} \tag{5.6.11a}$$

for the right-hand side of the flow equation and

$$\begin{aligned}
&\mathcal{F}\left(f_k, f_k^{(m,n)}, \eta_i, \partial_t f_k, \partial_t f_k^{(m,n)}, N_\Psi\right)\Big|_{S^4} = \\
&= \sum_{n=1}^{N}\left(\mathcal{A}_n(\rho_k) + \tilde{\mathcal{A}}_n(N_\Psi) + \sum_{j=1}^{4}\mathcal{B}_{n,j}(\rho_k)\eta_j + \sum_{m=2}^{N}\mathcal{M}_{n,m}(\rho_k)\beta_\rho^{(m)}\right),
\end{aligned} \tag{5.6.11b}$$

for the left-hand side of the flow equation. The notation $(\cdots)\big|_{S^4}$ denotes the projection on the spherical background. Performing an order by order comparison in the curvature scalar $\bar{R}$, one easily obtains the system of RG equations for the FZ-truncation and the equations for the fixed-point solutions G^* and $\{\rho_n^*\}_{n=2\cdots N}$. The final expressions are quite similar to the condensed expressions in (5.6.7a) and (5.6.7b) for the flow equations and (5.6.8a) and (5.6.8b) for the fixed-point equations, respectively. Nevertheless, the explicit form of the coefficients $\mathcal{A}_n$, $\tilde{\mathcal{A}}_n$, $\mathcal{B}_{n,j}$ and $\mathcal{M}_{n,m}$ obtained within the FZ-truncation differs considerably from the ones extracted via $f(R)$-approximation.

5.7 Results for the interacting gravitational fixed-point structure

5.7.1 Pure gravity systems

In the following, we present our results regarding the fixed-point structure extracted within the two previously defined polynomial truncations, focusing on the case without matter fields, i.e., by setting $N_\phi = N_A = N_\psi = 0$. The analysis including matter contributions is reported in Sect. 5.7.2.

The fixed-point equations for both truncations are considerably complicated so that we resort to a numerical recursive solution of the fixed-point equations for the higher-order couplings in terms of the two lowest ones and adopt a bootstrap search strategy [181, 182] to select suitable fixed-point solutions and critical exponents. Within the background approximation, a canonical choice of closure for the system of RG equations is obtained with the RG-improved anomalous dimensions (see, e.g., [413]) $\eta_{\mathrm{TT}} = \eta_\sigma = G_k^{-1}\partial_t G_k - 2$ and $\eta_\xi = \eta_c = 0$. Alternatively, a hybrid closure is obtained by improving the background approximation with anomalous dimensions computed in an independent way via the vertex expansion (see, e.g., [142, 412, 413]).

For the $f(R)$-approximation within the RG-improved closure, we have performed the search for fixed-point candidates at each order of the approximation from $N = 1$ to $N = 20$. It is worth mentioning that, in the case of standard ASQG, i.e., where the theory space is defined by all *Diff*-invariant operators, the fixed-point analysis has been performed within polynomial expansions involving terms up to R^{70} [183].

In Fig. 5.1, we show the results of the fixed-point values for some of the dimensionless couplings (up to α_6^*), defined in the polynomial $f(R)$-decomposition - see Eq. (5.6.4), as functions of the order of approximation N. For higher-order couplings ($\alpha_7^*, \cdots, \alpha_{20}^*$), the fixed-point coordinates are of order $|\alpha_n^*| < 10^{-4}$. In each plot, the results computed with the Bochner-Laplacian (Type I) as a coarse-graining operator are represented by a blue circle, whereas the ones computed employing the Lichnerowicz-Laplacians (Type II) are distinguished by a red square. We observe that the fixed-point values stabilize against the inclusion of higher-order operators. Albeit quantitatively different, the fixed-point structure is similar for both coarse-graining operators and, in particular, it displays an apparent stabilization for sufficiently large truncation.

In order to provide a better visualization of the stabilization pattern against higher-order extensions for both regularization schemes, we consider in Fig. 5.2 a convenient normalization for the fixed-point couplings. Following [182, 183, 399], we define the set of normalized fixed points $\{\lambda_n\}_{n=1,\cdots,N}$ according to

$$\lambda_1(N) = \frac{G^*(N)}{G^*(N_{\max})} + 1 \qquad \text{and} \qquad \lambda_n(N) = \frac{\alpha_n^*(N)}{\alpha_n^*(N_{\max})} + n, \tag{5.7.1}$$

where $G^*(N)$ and $\alpha_n^*(N)$ represent the fixed-point values of the dimensionless couplings computed at order N. The couplings λ_n are normalized in units of the fixed-point values computed at the largest approximation order, which in the present case is $N_{\max} = 20$, and are shifted by n. Fig. 5.2 gives evidence for the rapid apparent stabilization of the fixed points.

Fig. 5.3 displays the corresponding critical exponents for both types of coarse-graining operators as functions of N and gives evidence for a non-increasing number of relevant directions. This indicates that the dimensionality of the UV critical hypersurface does not grow up to the dimension of the truncated unimodular theory space, which is a crucial feature for the asymptotic safety program. As occurred for the fixed-point values, higher-order additional invariant operators do not seem to spoil the stabilization of the critical exponents. In particular, for the critical exponents computed within the Type I regularization, i.e., Bochner-Laplacian as a coarse-graining operator. Fig. 5.3 (left) indicates

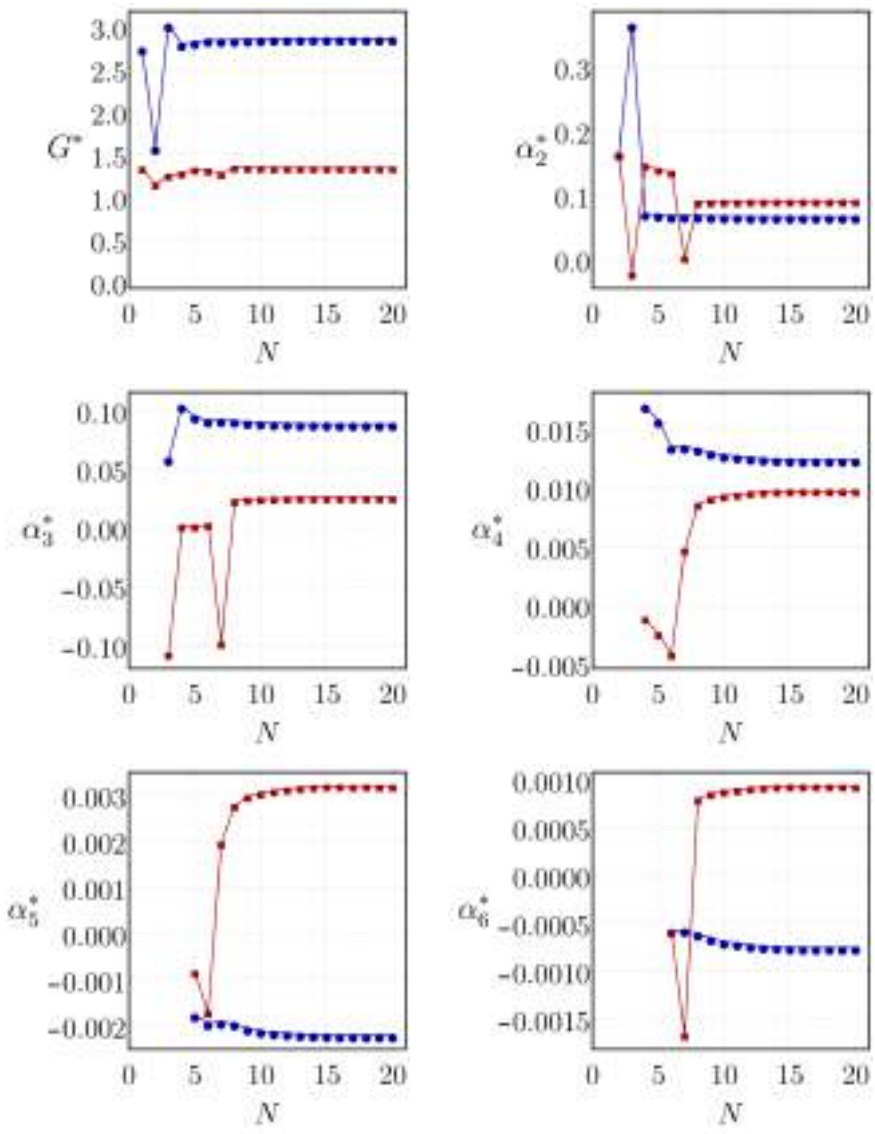

Figure 5.1: Fixed-point values of the couplings G_k, $\alpha_{k,2}$, $\alpha_{k,3}$, $\alpha_{k,4}$, $\alpha_{k,5}$ and $\alpha_{k,6}$ in the $f(R)$-truncation. The blue circle indicates the Type I regularization (Bochner-Laplacian), whereas the red square indicates the Type II regularization (Lichnerowicz-Laplacians). All plots are computed within the RG-improved prescription.

that the number of relevant directions saturates at two (except obviously for $N = 1$). For the Type II regularization, characterized by the Lichnerowicz-Laplacians (right), the analysis is a bit more subtle. In this case, we observe a small oscillation in the neighborhood of positive values for lower-order truncations ($N < 6$). In spite of that, the inclusion of additional invariant operators drives the number of relevant directions to stabilize at two as well.

An interesting feature also displayed in Fig. 5.3 is the near-canonical character of the critical exponents , *i.e.*, a small deviation of the critical exponents in comparison with the canonical scaling of the operators appearing in our truncation. Indeed, the critical exponents computed within the $f(R)$-expansion behave like $\theta_n \sim \Delta_n$, where $\Delta_n = 4 - 2n$ is the canonical scaling dimension of an invariant of the form $\bar{R}^n$. The two positive critical exponents appear as exceptions, since they deviate from the corresponding canonical scaling dimension by a greater gap. The near-canonical character of the

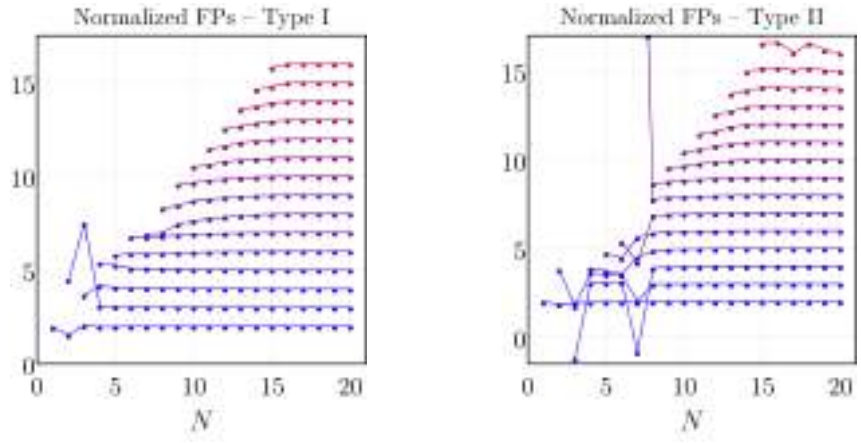

Figure 5.2: Normalized fixed points in the $f(R)$-truncation. The convergence pattern is exhibited with the normalization $\lambda_1(N) = \frac{G^*(N)}{G^*(N_{\max})} + 1$ and $\lambda_n(N) = \frac{\alpha_n^*(N)}{\alpha_n^*(N_{\max})} + n$ (for $n > 1$). From bottom to top, we display $\lambda_n(N)$ for $n = 1, \cdots, 15$ in the $N_{\max} = 20$ truncation (see main text). The left panel shows the normalized fixed-points values associated with the Type I regularization scheme, while the right panel corresponds to results obtained via the Type II regularization scheme. Both schemes of calculation are closed with the RG-improved prescription.

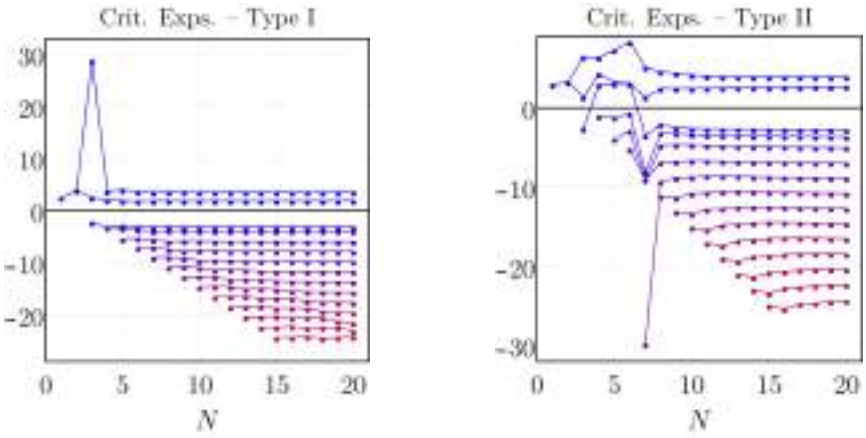

Figure 5.3: Critical exponents associated with the fixed-point structure in the $f(R)$-approximation for the range $n = 1, \cdots, 15$ in the $N_{\max} = 20$ truncation within the RG-improved closure. The left panel corresponds to results obtained under the Type I regularization, while the right panel displays the results obtained under the Type II regularization.

critical exponents was already observed in a unimodular setting based on a polynomial expansion of $f(R)$ up to $\bar{R}^{10}$ [397]. Additionally, it is worth mentioning that a near-canonical spectrum of critical exponents has been investigated in detail within standard ASQG [181–184, 195, 213, 399]. In particular, such a property suggests that power-counting can be a good guiding principle in the construction of truncations of the flowing effective action.

As stated earlier, as an attempt to go beyond the RG-improvement prescription, the anomalous dimensions of the fluctuating metric and ghost fields may be independently computed through a simultaneous vertex and derivative expansion of the effective average action in the same fashion as discussed previously in the unimodular setting [142] (see also [412, 413]). This provides a second way of closing the system of RG equations by combining the background-field approximation for the couplings with independent anomalous dimensions for fluctuating fields in a hybrid approach, as in [190, 411, 413, 414].

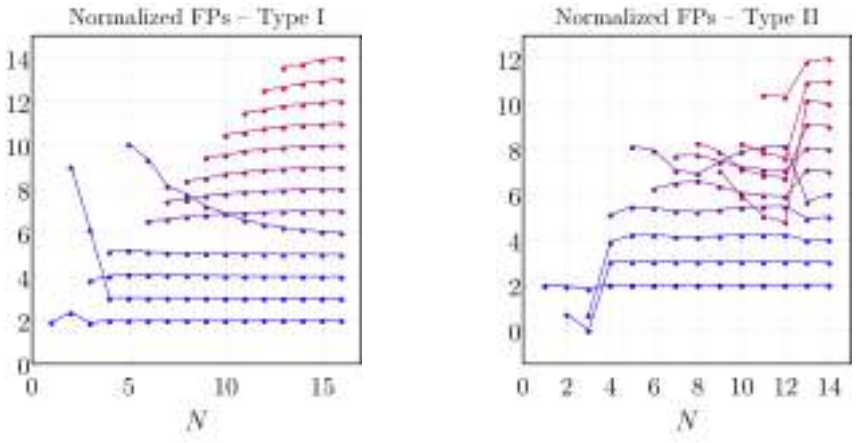

Figure 5.4: Plots of the convergence pattern for the normalized fixed-point values of the couplings $\lambda_n(N)$ for the $f(R)$-approximation evaluated within the hybrid semi-perturbative closure. The left plot exhibits the convergence pattern for the the range $n = 1, \cdots, 13$ in the $N_{\max} = 16$ truncation under the Type I regularization, while the right plot displays the convergence pattern for the range $n = 1, \cdots, 11$ in the $N_{\max} = 14$ truncation under the Type II regularization. All couplings follow the same normalization convention as defined previously. The truncations are smaller with respect to previous results and different for different coarse-graining operators due to numerical instabilities.

Our setup for the generation of the interaction proper vertices employs the same ansatz (5.4.10). In order to capture higher-curvature effects, the Lagrangian $f(R, R^2_{\mu\nu})$ is decomposed into an Einstein-Hilbert term supplemented by quadratic-curvature invariants such that the gravitational sector is in the form

$$\Gamma_k^{\text{gravity}}[g_{\mu\nu}] = \frac{k^2}{16\pi G_k} \int_x \omega \left(-R + k^{-2}\alpha_{k,2} R^2 + k^{-2}\rho_{k,2} R_{\mu\nu} R^{\mu\nu} \right), \tag{5.7.2}$$

with $\alpha_{k,2}$ and $\rho_{k,2}$ being the same dimensionless couplings as in (5.6.4) and (5.6.10a), respectively. In particular, for computational simplicity, curvature-squared contributions to the vertices are neglected. We emphasize that this is an additional approximation that should be refined in a future investigation. After expanding the gravitational action in powers of the fluctuation field $h_{\mu\nu}$, we set $\bar{g}_{\mu\nu} = \delta_{\mu\nu}$. This setup allows us to obtain the anomalous dimensions in the form $\eta_i = \eta_i(G_k, \alpha_{k,2}, \rho_{k,2}, \beta_\alpha, \beta_\rho, N_\Psi)$. The explicit expressions are given in App. D.4 within a semi-perturbative approximation[14] and, when inserted in the RG equations for the $f(R)$-truncation, the coupling $\rho_{k,2}$ and its beta function are set to zero, since the $f(R)$-approximation does not contain any $R^2_{\mu\nu}$-dependence. Similarly, when treating the system of RG equations for the FZ-truncation, the coupling $\alpha_{k,2}$ and its beta function are not considered.

To avoid a proliferation of similar plots, we refrain from showing the plots of convergence of individual fixed-point values and only exhibit results for the normalized fixed points and the critical exponents in Fig. 5.4 and Fig. 5.5.

As argued in [191], for a generic class of regulators proportional to the two-point functions, the imposition that the regulators must diverge in the UV leads to the constraint $\vec{\eta}\big|_* < 2$. Since our regulators fall in this class, we have selected, within the hybrid semi-perturbative prescription, fixed-

[14]The semi-perturbative approximation consists in setting to zero all the η's that would arise from the RG-scale derivative on the regulator function. This amounts to neglecting the η's on the right-hand side of the expressions for the anomalous dimensions [141, 142, 190, 203, 212, 223, 228].

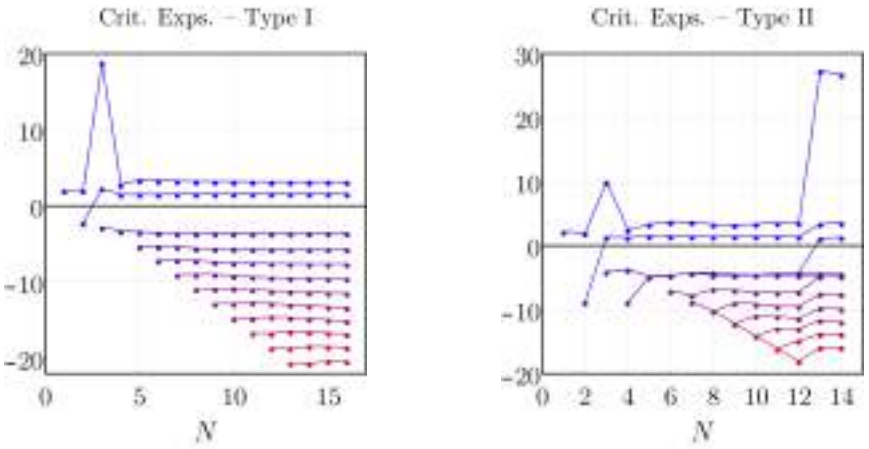

Figure 5.5: Critical exponents associated with the fixed-point structure in the $f(R)$-approximation within the hybrid semi-perturbative closure. The left panel corresponds to results for the range $n = 1, \cdots, 13$ in the $N_{\max} = 16$ truncation under the Type I regularization. In particular, only the third and fourth set of critical exponents, under this regularization, are complex conjugate pairs and, consequently, the lines representing their real parts fall on top of each other. The right plot exhibits the results for the range $n = 1, \cdots, 11$ in the $N_{\max} = 14$ truncation under the Type II regularization. Clearly, in the latter case, the truncation needs to be further extended in order to verify if apparent convergence is restored for the critical exponents.

point values for G^* and α_2^* which respect the bound[15] $\vec{\eta}\big|_* < 2$. The convergence pattern of the normalized fixed-point values $\lambda_n(N)$ for the $f(R)$-approximation are displayed in Fig. 5.4 for both types of regularization schemes. Considering the non-linear character of the expressions for the anomalous dimensions given by (D.4.1a), (D.4.1b), (D.4.2), as opposed to the RG-improved case, we managed to find suitable fixed-point solutions for the polynomial truncation up to $N_{\max} = 16$ for the Type I regularization and up to $N_{\max} = 14$ for Type II. As in the case of the RG-improved prescription, the Type I regularization leads to stable fixed-point solutions, apart from a late stabilization of the normalized coupling associated with the invariant $\bar{R}^5$. However, the Type II regularization only leads to a clear apparent stabilization for the first four lower-order operators and seems to be sensitive against the inclusion of higher-order invariants. This behavior is again evident in the plots of the critical exponents in Fig. 5.5. In order to tell if this behavior is a truncation artifact due to the independently-computed anomalous dimensions or simply reflects a limitation in our search method, an investigation of higher-order truncations would be needed. Interestingly though, the near-canonical character of the critical exponents is still manifest for both types of regularization schemes within this hybrid semi-perturbative approximation. This indicates that quantum fluctuations encoded in the anomalous dimensions provide a mild contribution to all invariant operators.

We move on to discuss the fixed-point structure of the polynomial FZ-truncation. The more complicated nature of this truncation naturally leads to larger expressions in contrast with the $f(R)$-truncation, thus demanding additional computational capacity. As a consequence, within the RG-improved prescription, we limit ourselves to explore the fixed-point equations within a truncation where the highest-order invariant operator corresponds to $R(R_{\mu\nu}R^{\mu\nu})^7$ (i.e., $N_{\max} = 15$). As in the

[15]The constraint verified in this chapter is subjected to the approximations made here. In particular, for η_σ the range of fixed-point values may be more restrict if one considers the effects of symmetry-breaking graviton mass terms (and full closure), as discussed in [142].

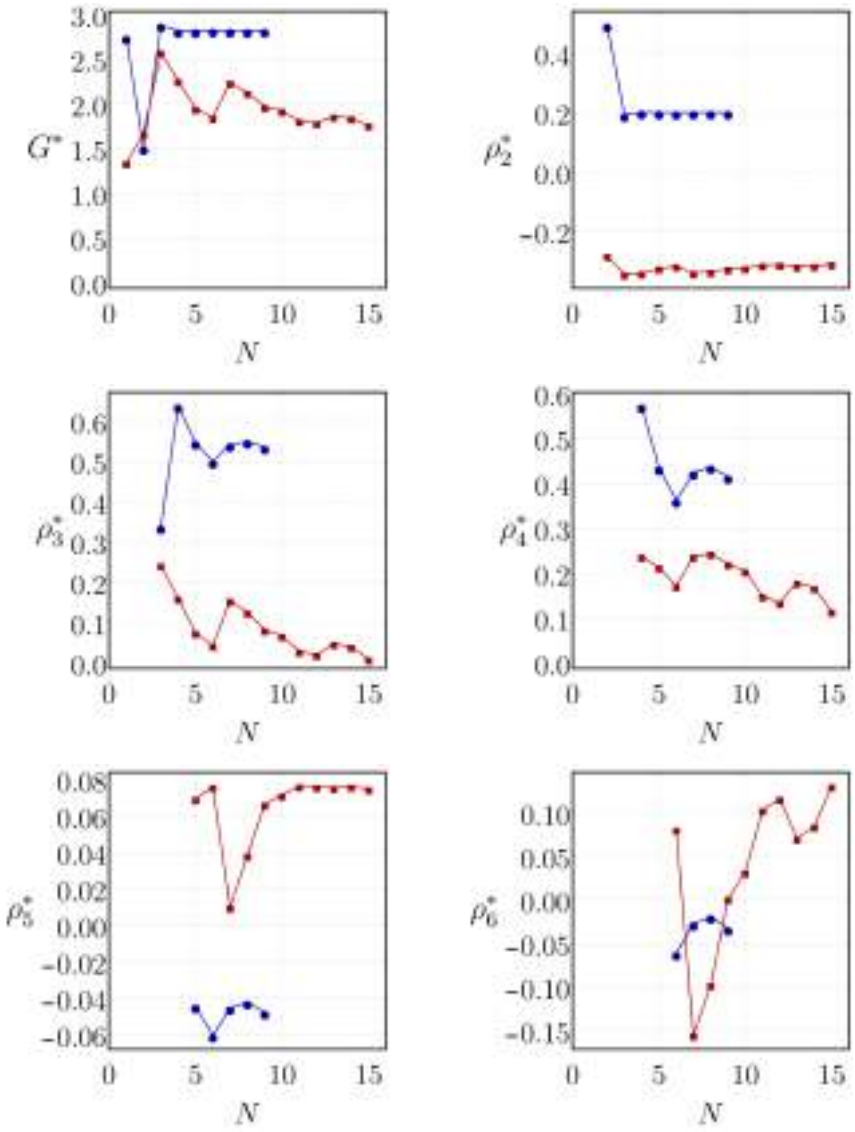

Figure 5.6: Fixed-point values of the couplings G_k, $\rho_{k,2}$, $\rho_{k,3}$, $\rho_{k,4}$, $\rho_{k,5}$ and $\rho_{k,6}$ in the FZ-truncation. The blue circle indicates the Type I regularization (Bochner-Laplacian), whereas the red square indicates the Type II regularization (Lichnerowicz-Laplacians). All plots are computed within the RG-improved prescription.

$f(R)$ case, a numerical recursive solution of the fixed-point equations is implemented alongside a bootstrap search method.

In Fig. 5.6, we display our findings of the fixed-point values of the dimensionless couplings up to $\rho_{k,6}$ as functions of N extracted from the FZ-truncation for both types of coarse-graining operators. We adopt the same convention for the plot markers as in the $f(R)$-truncation. Additionally, in Fig. 5.7, we display the convergence pattern of the normalized fixed-point values of the couplings $\lambda_n(N)$ defined in terms of $(G_k, \rho_{k,n})$. As one can notice from Figs. 5.6 and 5.7, for the regularization employed by the Lichnerowicz-Laplacians (red squares in 5.6 and right panel in 5.7), we managed to find suitable NGFP solutions for the polynomial truncation until $N_{\max} = 15$, exhibiting mild oscillations for higher-order operator invariants (with the exception of wild oscillations at the approximation orders $N = 3$ and $N = 8$). Contrarily, the regularization based on the Bochner-Laplacian (blue circles in 5.6 and left

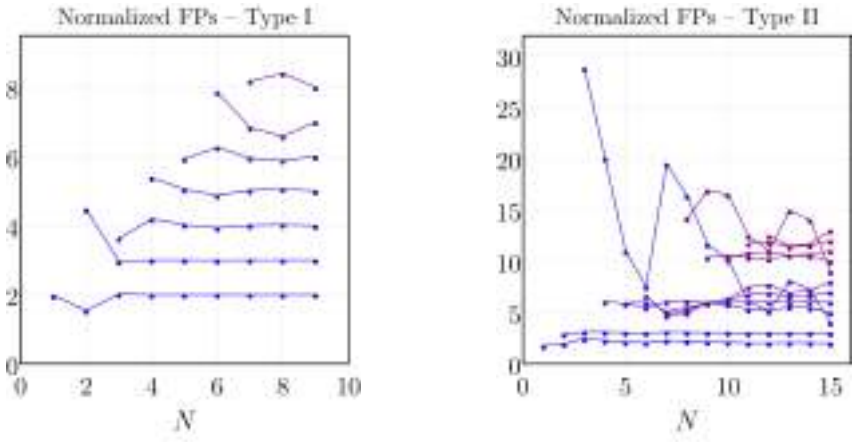

Figure 5.7: Plots of the convergence pattern of the normalized fixed-point values of the couplings $\lambda_n(N)$ (now given in terms of $(G_k, \rho_{k,n})$) for the FZ-truncation evaluated within the RG-improved prescription. The left plot exhibits the convergence pattern for the range $n = 1, \cdots, 7$ in the $N_{\max} = 9$ truncation under the Type I regularization, while the right plot displays the convergence pattern for the range $n = 1, \cdots, 12$ in the $N_{\max} = 15$ truncation under the Type II regularization. All couplings follow the same normalization convention as in the $f(R)$ case.

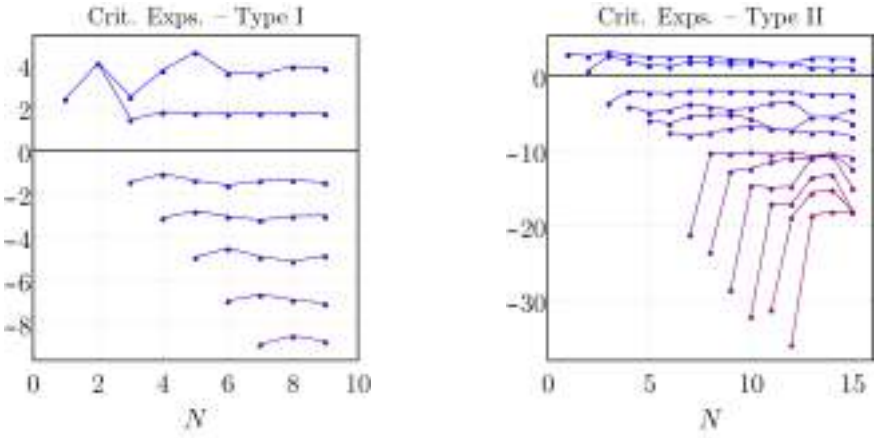

Figure 5.8: Critical exponents associated with the fixed-point structure in the FZ-truncation within the RG-improved closure. The left panel corresponds to results for the range $n = 1, \cdots, 7$ in the $N_{\max} = 9$ truncation obtained under the Type I regularization, while the right plot displays the results for the range $n = 1, \cdots, 12$ in the $N_{\max} = 15$ truncation obtained under the Type II regularization.

panel in 5.7) leads to suitable, apparently stabler, NGFP solutions only up to $N_{\max} = 9$. This feature is attributed to a limitation in our numerical method implemented to generate fixed-point solutions.

According to the critical exponents illustrated in Fig. 5.8, our findings for the FZ-truncation still indicate that the UV critical hypersurface is characterized by two relevant directions for both types of coarse-graining operators. Despite the stabilization of the number of relevant directions, the numerical values for the critical exponents undergo the same unstable behavior as the fixed-point values depicted in Fig. 5.6. Albeit the difficulties in extending our analysis to truncations higher than $N = 9$ for the Type I regularization scheme, the results shown in Fig. 5.8 (left) indicate that the critical exponents share the same near-canonical character as in the case of the $f(R)$-approximation. However, such a behavior is less apparent in the case of Type II coarse-graining operators. Here, as one can see from Fig. 5.8 (right), some critical exponents behave according to the near-canonical scaling. Nevertheless,

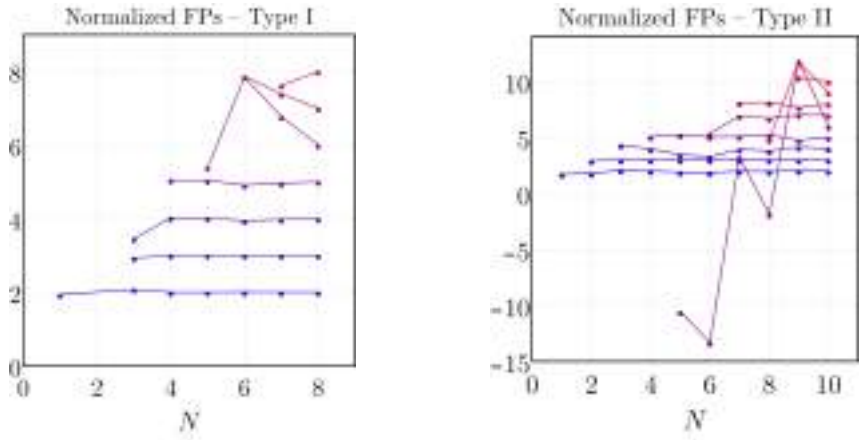

Figure 5.9: Plots of the convergence pattern for the normalized fixed-point values of the couplings $\lambda_n(N)$ (given in terms of $(G_k, \rho_{k,n})$) for the FZ-truncation evaluated within the semi-perturbative prescription. The left plot exhibits the convergence pattern for the range $n = 1, \cdots, 7$ in the $N_{\max} = 8$ truncation under the Type I regularization, while the right plot displays the convergence pattern for the range $n = 1, \cdots, 9$ in the $N_{\max} = 10$ truncation under the Type II regularization. All couplings follow the same normalization convention as in the $f(R)$ case.

for assorted choices of N there are points which exhibit appreciable deviations from the canonical scaling of invariant operators within the truncation.

To conclude this section, we display in Figs. 5.9 and 5.10 the results for the normalized fixed-point values and critical exponents in the FZ-truncation when the semi-perturbative prescription is adopted. For the regularization employed by the Lichnerowicz-Laplacians (right panel in Fig. 5.9), suitable NGFP solutions were found for polynomial truncation until $N_{\max} = 10$, with improved stabilization of the fixed-point coordinates, apart from a severe oscillation at order $N = 5$. These are better results in comparison with the previous case (given the simplicity of our truncation). Regarding the Bochner-Laplacian operator (left panel in Fig. 5.9), stable results were achieved only up to $N_{\max} = 8$. A similar limitation was observed in the previous analysis. Moreover, at order $N = 2$, we have disregarded the only would-be suitable NGFP solution for the pair (G^*, ρ_2^*), since one of the two corresponding critical exponents is ~ 110 and may be regarded as a truncation artifact. Conclusive statements regarding the stability of the fixed point requires an extensive analysis of more sophisticated truncations.

As in the RG-improved case, the dimensionality of the UV critical hypersurface is still two for both regularization schemes. However, for the Type II case, the two positive critical exponents exhibit mild oscillations and, as opposed to the corresponding RG-improved result, the gap controlling their near-canonical scaling is severely reduced by the anomalous dimensions contributions when higher-order invariant operators are included. Nevertheless, in contrast with the RG-improved analysis, the critical exponents do not exhibit appreciable deviations from canonical scaling for several choices of the approximation order N.

Notably, our findings suggest that in the unimodular version of the FZ-truncation the search for fixed-point candidates gets hampered by difficulties in extending the approximation order beyond $N = 16$ (which is the case considering Lichnerowicz-Laplacians within the RG-improvement prescription) in comparison with the fixed-point analysis in the unimodular version of the $f(R)$-approximation.

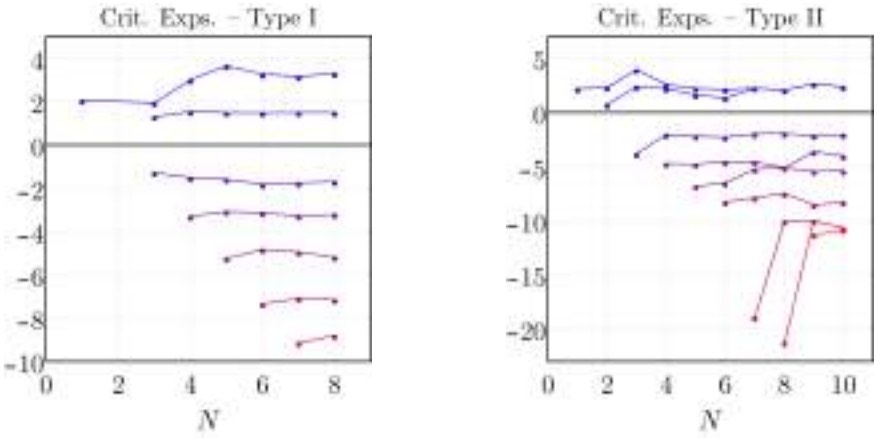

Figure 5.10: Critical exponents associated with the fixed-point structure in the FZ-truncation within the semi-perturbative closure. The left panel corresponds to results for the range $n = 1, \cdots, 7$ in the $N_{\max} = 8$ truncation obtained under the Type I regularization, while the right plot displays the results for the range $n = 1, \cdots, 9$ in the $N_{\max} = 10$ truncation obtained under the Type II regularization.

The possibility of extension gets more restricted when independent anomalous dimensions are adopted. As a consequence, the FZ-truncation in the unimodular setting generates less stable solutions than its $f(R)$ relative overall. This characteristic is opposed to considerations previously made in the standard ASQG setting. In particular, the systematic investigation carried out in [399] reveals that the FZ-truncation presents a faster stabilization, including higher-order extensions, than the $f(R)$-approximation. Considering the approximations we have used, our findings reveals the opposite behavior in the unimodular version.

5.7.2 Gravity-matter systems

Several works in standard ASQG provide strong hints for the existence of a NGFP in the RG flow within different truncations, ranging from the Einstein-Hilbert approximation to more sophisticated ones [138, 139, 151, 170, 171, 174, 178–184, 186, 253, 255, 399, 410–413, 422–432, 434–450]. On top of that, a growing number of investigations provide compelling evidence for the persistence of the NGFP against the introduction of a large class of matter fields, such as the field content corresponding to the SM of particle physics and some beyond SM (bSM) extensions, see [141, 190–196, 198, 200–204, 208, 209, 211–213, 219–223, 225, 230, 232, 233, 307, 414, 433, 435, 451–458, 458–462, 462, 463]. In this section, we explore the impact of matter degrees of freedom on the interacting gravitational fixed-point structure in the unimodular setting for both $f(R)$ and $F(R^2_{\mu\nu}) + RZ(R^2_{\mu\nu})$ polynomial truncations. By varying the number of matter fields, we can probe the compatibility of non-trivial fixed-point solutions in the unimodular theory space coupled to the field content corresponding to the SM of particle physics as well as to some bSM extensions.

Following the same strategy employed in the pure gravity case, a numerical recursive solution and a bootstrap search method were adopted for the selection of suitable fixed-point candidates. For both $f(R)$- and FZ-truncations we have limited our search to fixed-point solutions within polynomial approximations ranging from $N = 1$ to $N = 10$. The results reported in the case of gravity-matter

Stability of NGFP for some specific matter models							
Model	Matter content			Type I		Type II	
	N_ϕ	N_A	N_ψ	$f(R)$	$F(R^2_{\mu\nu}) + RZ(R^2_{\mu\nu})$	$f(R)$	$F(R^2_{\mu\nu}) + RZ(R^2_{\mu\nu})$
SM	4	12	45/2	✓(2)	✓(2)	✓(2)	✓(2)
SM + $3\nu_{\rm R}$	4	12	24	✓(2)	✓(3)	✓(2)	✓(2)
MSSM	49	12	61/2	✖	✖	✖	✖
SU(5) GUT	124	24	24	✖	✖	✖	✖
SO(10) GUT	97	45	24	✓*(2)	✓*(3)	✓*(2)	✓*(2)

Table 5.1: Collection of the results on the stability of NGFPs arising from the matter content of the Standard Model and some of its commonly studied extensions for both $f(R)$ and $F(R^2_{\mu\nu}) + RZ(R^2_{\mu\nu})$ polynomial projections in the unimodular setting. The RG-improved closure is adopted. The symbols go as follows: check-marks ✓ indicate the underlying setup possesses a suitable NGFP which converges for increasing order of approximation N. The number between parenthesis indicates the number of relevant directions observed. An asterisk simply indicates that there is no NGFP at the level of the Einstein-Hilbert truncation ($N = 1$), converging afterwards towards a suitable NGFP. Finally, an ✖ means that there is no NGFP at all orders of approximation, except for one appearance at only one power of curvature.

systems are restricted to the RG-improved treatment for the anomalous dimensions, i.e., using a prescription that relates $\eta_{\rm TT}$ and η_σ to the beta function of the Newton coupling, while setting all other anomalous dimensions to zero. The other prescription considered in the pure gravity case, with anomalous dimensions computed via derivative expansion, will not be reported here. The reason is related to the existence of certain bounds on the anomalous dimensions, as it was pointed out in [191], appearing as a consistency requirement for an appropriate behavior of the fRG regulator at $k \to \infty$. For gravity-matter systems we have found fixed-point values that violate such bounds and we can argue that these results are not self-consistent.

In Table 5.1 we exhibit a summary of the results concerning the stability of NGFPs for specific matter contents for both $f(R)$ and $F(R^2_{\mu\nu}) + RZ(R^2_{\mu\nu})$ approximations. In this case, we just report the main qualitative features, i.e., in which cases we find evidence for fixed-point solutions and the corresponding number of relevant directions. In all cases, we have investigated polynomial truncations including operators up to $\mathcal{O}(R^{10})$.

The minimal requirement for a phenomenological viable fixed-point solution is its compatibility with the matter content of the SM, i.e., $N_\phi = 4$, $N_A = 12$ and $N_\psi = 45/2$. As we can observe in Table 5.1, our result points towards the existence of this fixed point for both truncations under investigation and for both types of regulators employed in the coarse-graining procedure. The fixed-point solution corresponding to the SM matter content exhibits similarities with the results observed for pure gravity. In both truncations and regularization schemes, we have found evidence for two-dimensional UV critical surfaces. Furthermore, the numerical values for the fixed-point solutions, as well as for the critical exponents, seem to stabilize for truncations characterized by $N \gtrsim 6$. The exception is the FZ-approximation with Type I regulator, which presents a mild deviation from the "convergence" pattern at $N = 9$ and $N = 10$.

To complement our analysis, we also have considered the matter content associated with some bSM

scenarios. The first extension, which is motivated by the necessity to accommodate neutrino masses, corresponds to the choice $(N_\phi = 4, N_A = 12, N_\psi = 24)$, i.e., including 3/2 additional Dirac fermions (or 3 Weyl fermions), accounting for 3 right-handed neutrinos. In this case, our results also point towards the existence of UV fixed-point solutions. The main difference in comparison with the SM matter content is the appearance of an extra relevant direction in the FZ-truncation with Type I regularization. For the other approximations/schemes, our results indicate two relevant directions.

It is also interesting to consider matter content corresponding to bSM scenarios characterized by larger symmetry groups, e.g., supersymmetric models and grand unified theories (GUTs). In Table 5.1, we report our findings for matter content associated with the minimally supersymmetric Standard Model (MSSM), SU(5) and SO(10) GUTs. Among these options, only the SO(10) GUT ($N_\phi = 97$, $N_A = 45$ and $N_\psi = 24$) exhibits suitable fixed-point solutions. In this case, most of the schemes under investigation leads to UV fixed-points characterized by two relevant directions. The exception, once again, is the FZ-truncation with Type I regulator, where we have found three relevant directions. It is also interesting to emphasize that, in the case of matter content corresponding to SO(10) GUT, the fixed-point solutions do not appear at the level of the lowest truncation, i.e., $N = 1$.

For the matter content corresponding to the MSSM and SU(5) GUT, we do not find evidence for the existence of suitable fixed-point solutions within the aforementioned truncations. Our findings show a qualitative agreement with the results for non-unimodular settings reported in [190, 194]. As it was pointed out in [190], the absence of suitable UV fixed-points for gravity-matters systems with field content corresponding to the MSSM and SU(5) GUT can be explained by the inclusion of too many scalars and fermions, without being compensated by the inclusion of extra vector fields. It is important to emphasize that this explanation is restricted to the calculations based on the background-field approximation. It is worth mentioning that results from the fluctuation approach, see [124], for ASQG indicate that the inclusion of too many scalars pushes the scalar anomalous dimension to a regime that violates certain regulator bounds [191].

The upshot is that, apart from the global degree of freedom and the status of the cosmological constant at the level of field equations, no substantial differences have been found between UQG and its Diff-invariant version, even when matter is included.

Chapter 6

Concluding Remarks and Outlook

In this thesis, we investigated the interplay of quantum fluctuations of matter with different incarnations of gravity. In particular, both quantum properties of the background spacetime and its fluctuations were put to the test in order to provide constraints on dark matter models, on the fate of chiral symmetry for fermions and on kinematically classical siblings of gravity itself.

Non-perturbative renormalization techniques in the context of the functional Renormalization Group were the main tools for the three investigations, and, in particular, to probe the existence of a suitable UV fixed point for quantum gravity-matter systems within the asymptotic safety perspective.

Our first endeavor was to put to the test the predictive power of asymptotic safety in testing concrete (vector) dark matter models, which are phenomenological not excluded. There are a priori several ways in which asymptotic safety can be incompatible with a given phenomenological model.

First, there might not be any asymptotically safe fixed point in the model together with quantum gravity. This is not the case of Chapter 3, where, in fact, there are several fixed points at which different subsets of the couplings are nonzero.

Second, a fixed point can have irrelevant directions. Each irrelevant direction generates a prediction for a coupling (or combination of couplings) in the infrared. These predictions may disagree with phenomenologically allowed or experimentally measured values. This is the case here, where the top quark Yukawa coupling is predicted for some fixed points (and bounded from above by others) and comes out smaller than the value inferred from experiment. There is, however, a caveat to ruling out a model in this way and that caveat is due to systematic uncertainties. These arise from the use of a truncation (and thus the neglecting of higher-order interactions which are generically present at an asymptotically safe fixed point and impact the beta functions within the truncation), but also from the use of Euclidean signature in the RG calculations. Although attempts can be made [202, 207], these systematic uncertainties are difficult to estimate. If we are very conservative about the size of systematic uncertainties, ruling out the model robustly based on the too-low value of the top quark mass may not be possible. If we are somewhat more optimistic about the size of systematic uncertainties, the present work provides an explicit example of the idea put forward in [202]: dark degrees of freedom change gravitational fixed-point values and thus result in changes of all predicted SM couplings, even if the

corresponding degree of freedom (here, the top quark) is not coupled to the dark sector. Furthermore, we emphasize that the DM models considered in this paper are only ruled out in the near-perturbative regime and it is in principle not excluded that a very different strongly coupled UV completion exists once we go beyond the approximations adopted.

Third, a model may rely on a dynamical mechanism, with spontaneous symmetry breaking as one important example. Whereas spontaneous symmetry breaking in phenomenological models is usually built in by fiat by making assumptions about the scalar potential, this is no longer an option in an asymptotically safe setting. There, the scalar potential at low energies arises as a combination of the UV initial conditions from asymptotic safety with the effect of quantum fluctuations at all scales down to the IR. The UV initial conditions are subject to the free-parameter count from asymptotic safety and typically only the mass parameters remain as free parameters. At all scales below, the contribution that arises from quantum fluctuations is completely fixed in terms of the other couplings in the model. In our case, these restrictions are sufficient to rule the model out, because most fixed points result in either perturbatively unstable or symmetry-broken potentials in the UV. At the remaining fixed points, gauge fluctuations in the dark sector drive the quartic coupling towards negative values. Because there are no free parameters in the scalar potential that could offset this effect, the resulting potential is not bounded from below within the perturbative regime. We stress that this last criterion, in contrast to the second one, is a *qualitative*, not a *quantitative* one. Thus, it is less sensitive to the systematic uncertainties of our study, because it only relies on well-established, universal *signs* of terms in beta functions.

Because of the qualitative and general nature of the criterion that rules out these particular DM models, we conjecture that vector DM models with only vectors and scalars in the dark sector are generally not viable in asymptotic safety in a near-perturbative regime. If fermions are added with a large enough Yukawa coupling, they may stabilize the scalar potential (see [232] in the context of DM and [247] for work in the context of cosmic strings). We highlight that exploring vector dark models beyond the perturbative regime, where additional, canonically irrelevant, interactions may be relevant, is an interesting subject for further studies.

This result adds further to the evidence that models with a Higgs portal to the dark sector are either strongly constrained [233, 235] or fully ruled out [230] in asymptotic safety, depending on the matter and interaction content of the dark sector. This motivates to look elsewhere for viable DM models. It is already known that axion-like particles are also constrained [239], putting another popular DM candidate under (theoretical) pressure.

We thus propose that a way towards finding viable models of DM in asymptotic safety is to follow up on results which show which interaction structures are generically viable in asymptotic safety. A promising candidate could be strongly coupled fermionic sectors in which symmetry breaking triggers the formation of massive bound states. Such composite models with dark sectors may fit into the asymptotic safety paradigm [464], because it is known that i) gravity does not trigger bound-state formation, so that bound states less massive than the Planck scale may be viable [200, 219, 221, 307], ii) gravity generates non-vanishing four-fermion interactions which may then be driven to criticality by

a non-Abelian gauge interaction [465] and iii) the fermion mass parameter generically remains a free parameter [222] so that even in non-chiral fermion systems bound-state formation may be achieved. If indeed composite models with dark sectors are viable in asymptotic safety, then a dark gauge interaction is present, but, unlike in the setting of this work, does not supply the dark-matter candidate itself.

Our second endeavor was to investigate the impact of a non-trivial spacetime background on the fate of chiral symmetry. In particular, we focused on the impact of background torsion. Our analysis was based on the evaluation of a scale-dependent effective potential in the bosonized version of the NJL model on a Riemann-Cartan manifold. Within this setting, we used fRG-inspired tools to define a coarse-grained effective potential.

We have analyzed the impact of torsion in two different situations. First, in the approximation where $|\mathring{R}|/k_{\mathrm{IR}}^2 \ll 1$ and $A^2/k_{\mathrm{IR}}^2 \ll 1$, we investigated the combined impact of torsion and curvature. In this case, torsion may contribute toward or against chiral symmetry breaking, depending on the infrared value of the renormalized nonminimal coupling ξ_{IR}. In fact, for a given sign of the nonminimal coupling ξ_{IR}, the torsion contribution plays the analog role of negative curvature, *i.e.*, favors chiral symmetry breaking for positive nonminimal coupling and prevents it for negative coupling. The analysis with $|\mathring{R}|/k_{\mathrm{IR}}^2$ and A^2/k_{IR}^2 does not capture the deep infrared regime. Thus, it does not allow us to investigate a possible torsion-based gravitational catalysis.

The second analysis we performed was in the regime of vanishing curvature and homogeneous torsion. Although this analysis does not capture the combined effects of curvature and torsion, it allows us to investigate the impact of torsion on the mechanism of chiral symmetry breaking in the deep infrared. Surprisingly, in this regime, the only contribution of torsion to $V''_{k_{\mathrm{IR}}}(0)$ comes from the leading order correction in A^2 in an early-time heat kernel expansion. In physical terms, we have found no indication of a torsion-based gravitational catalysis mechanism.

To our knowledge, this is the first paper investigating the effect of non-Riemannian structures on the mechanism of gravitational catalysis. The results presented here are in agreement with the very recent account [466], where the possibility of chiral symmetry breaking was also investigated in a background with curvature and torsion, but computing the effective action from the anomaly-induced vacuum effective action in non-Riemannian spacetimes probed in [467]. Furthermore, the results presented here were restricted to a nondynamical background. As a next step, we aim to investigate the impact of torsion fluctuations on the mechanism of chiral symmetry breaking. In particular, one can investigate the compatibility of light fermions [219] with quantum gravity scenarios with fluctuating torsion field. We hope to report on this soon.

Torsion effects can also play a role in low-energy physics. For instance, effects of torsion can be emulated in condensed matter systems [468–470]. In the context of the geometric theory of defects, the appearance of torsion and curvature in solids are associated with topological defects known as dislocations and disclinations, respectively. Crystalline structures are then viewed as a manifold endowed with a Riemman-Cartan-like geometry. The methods used in this paper can, in principle, be adapted to the study of chiral symmetry breaking in low-energy systems that emulate torsion effects. This path could pave the road to the experimental realization of the results presented in this paper by means of

analog gravity systems.

Our final investigation was with regards to unimodular quantum gravity. In Chapter 5, the renormalization group flow of unimodular quantum gravity was analyzed. This was motivated by the possibility of such a quantum theory to be asymptotically safe and, thus, well defined up to arbitrarily short distances. We have explored larger theory spaces with respect to previous analyses, by considering truncations which involve the tensorial structure of Ricci-tensor invariants and anomalous dimensions which are computed from the running of the two-point function of gravitons and Faddeev-Popov ghosts. Moreover, in the background approximation, we have used the background-dependent correction to the flow equation discussed in [142]. Such improvements enabled us to confront previous results [395, 397] with truncations enlargements and, apart from quantitative differences which follows from truncation-induced effects, we have found evidence for the persistence of the fixed point.

Technically, we have also tested how the underlying fixed-point structure is affected by different choices of the endomorphism parameter in the regulator function. In particular, we discussed results obtained for Bochner and Lichnerowicz coarse-graining operators. As expected, different choices of such operators, in the background approximation, directly affect the projection onto curvature invariants in the flow equation and can lead to substantial different qualitative results such as the number of relevant directions (see, e.g., [434, 471]). For this discrete choice of the endomorphism parameter, we have observed stable qualitative results both in the $f(R)$ and FZ truncations, where the fixed point features two relevant directions. Nevertheless, different classes of truncations lead to different computational subtleties and we have verified that in this setup, the $f(R)$ truncation has better (apparent) convergence properties. More efficient methods must be employed for the FZ-truncation in order to probe whether the fixed point structure stabilize for larger truncations. In any case, it is remarkable that by changing the endomorphism parameter and the anomalous dimension prescription in each class leads to a fixed point which features the same qualitative features, leading to the expectation that this is a consequence of the near-perturbative nature of the fixed point (which is reflected in the near-canonical scaling).

Finally, we have considered the interaction of unimodular quantum gravity with matter degrees of freedom. Intuitively, matter fluctuations will affect the running of the gravitational couplings and since we aim at describing a realistic theory of quantum gravity, the fixed point must exist in the presence of matter fields. As a first approximation, we have included scalars, spinors and vectors without self-interactions coupled to the unimodular gravitational field. As discussed, the matter content of the SM and of some of its extensions does not destroy the fixed point, leading to evidence for the existence of a complete theory of quantum gravity and matter. However, as pointed out, for some extensions of the SM, the matter content is “too big" and destroys the fixed point, i.e., they act against scale invariance in the UV. Hence, it is a concrete realization that even for truncated theory spaces, one might indeed find systems which do not feature a fixed point.

The investigation of Chapter 5 suggests several different ways of improving the truncations of unimodular quantum gravity and matter systems. In particular, a promising and necessary direction is the consideration of approximations that go beyond the background one. In this work we have performed a purely background approximation and a hybrid one. However, it is necessary to investigate

momentum-dependent correlation functions in unimodular quantum gravity and compare the results with our present findings. We hope to report on this soon.

Lastly, there is the discussion about the equivalence of unimodular quantum gravity and standard quantum gravity. Conceptually, from the point of view of asymptotically safe quantum gravity, this is still an important puzzle to be resolved. Different symmetry groups define, in principle, different theory spaces and hence, a different set of essential couplings that should reach a non-trivial fixed point. In the unimodular setting, there is no room for a cosmological constant as an essential coupling while in standard gravity, it is usually treated as an essential coupling (but see [472]) and it is required to reach a fixed point in the asymptotic safety program. However, it is far from clear if this necessarily leads to incompatible pictures. In standard gravity, the cosmological constant corresponds to a relevant direction and, thus, a free parameter that should be fixed by "experiments". In unimodular gravity, the cosmological constant appears as a constant of integration which is also fixed by initial conditions. In the end, it remains to be understood if such theories share the same observables or not.

Appendix A

Euclidean Spacetime Conventions

In this appendix, we outline the procedure for Wick rotation and we fix our conventions for objects defined directly with the four-dimensional Euclidean signature. These conventions will be used throughout this thesis, unless explicitly stated otherwise (see Chapter [CITE]). All the expressions written in terms of Lorentzian objects were defined with the metric signature $\eta_{\mu\nu} = \mathrm{diag}(+,-,-,-)$.

A.1 Minkowski to Euclidean Spacetime

A.1.1 Wick Rotation

The Wick rotation is defined by

$$x^0|_{\mathrm{L}} = -ix_0|_{\mathrm{E}}, \quad x^1|_{\mathrm{L}} = x_1|_{\mathrm{E}}, \quad x^2|_{\mathrm{L}} = x_2|_{\mathrm{E}}, \quad x^3|_{\mathrm{L}} = x_3|_{\mathrm{E}}, \tag{A.1.1}$$

which is valid for Lorentzian coordinates with upper indices. For Lorentzian coordinates with lower indices, we have

$$x_0|_{\mathrm{L}} = -ix_0|_{\mathrm{E}}, \quad x_1|_{\mathrm{L}} = -x_1|_{\mathrm{E}}, \quad x_2|_{\mathrm{L}} = -x_2|_{\mathrm{E}}, \quad x_3|_{\mathrm{L}} = -x_3|_{\mathrm{E}}. \tag{A.1.2}$$

The Euclidean version of the scalar product of the coordinates follows if we define the Euclidean metric $\delta_{\mu\nu} = \mathrm{diag}(+,\ldots,+)$, such that

$$\eta_{\mu\nu}x^\mu|_{\mathrm{L}}x^\nu|_{\mathrm{L}} = -\delta_{\mu\nu}x_\mu|_{\mathrm{E}}x_\nu|_{\mathrm{E}}. \tag{A.1.3}$$

Under Wick rotation, the derivative ∂_μ transforms according to

$$\partial_0|_{\mathrm{L}} = i\partial_0|_{\mathrm{E}}, \quad \partial_1|_{\mathrm{L}} = \partial_1|_{\mathrm{E}}, \quad \partial_2|_{\mathrm{L}} = \partial_2|_{\mathrm{E}}. \quad \partial_3|_{\mathrm{L}} = \partial_3|_{\mathrm{E}}. \tag{A.1.4}$$

A.1.2 Fourier Transforms

In this subsection, we summarize our conventions for Fourier transforms in four-dimensional Euclidean spacetime. For bosonic fields, we employ

$$\Phi(x) = \int \frac{d^4p}{(2\pi)^4}\Phi(p)\mathrm{e}^{ip_\mu x_\mu}. \tag{A.1.5}$$

For fields which are complex or Grassmaniann in nature, the conjugate pair carries an additional minus sign in the exponential factor. So, for fermionic fields our conventions read

$$\psi(x) = \int \frac{d^4p}{(2\pi)^4}\psi(p)\mathrm{e}^{ip_\mu x_\mu}, \tag{A.1.6}$$

$$\bar{\psi}(x) = \int \frac{d^4p}{(2\pi)^4}\bar{\psi}(p)\mathrm{e}^{-ip_\mu x_\mu}, \tag{A.1.7}$$

where, by self-consistency, the dual Euclidean spinor carries an imaginary factor, namely, $\bar{\psi} = (i\psi)^\dagger\gamma_0$. ψ and $\bar{\psi}$ should be considered as independent anti-commuting Grassmann fields. We refer to App. (A.2) for our conventions on Euclidean gamma matrices.

A.2 Euclidean Clifford Algebra and Fierz Identities

Fermions form a great part of this thesis, so it is justified to properly state our conventions for the Euclidean Clifford algebra and the Fierz rearrangement identities.

Euclidean Clifford Algebra

The Clifford algebra in Euclidean signature reads[1]

$$\{\gamma_\mu, \gamma_\nu\} = \gamma_\mu\gamma_\nu + \gamma_\nu\gamma_\mu = 2\delta_{\mu\nu}\mathbb{I}, \tag{A.2.1}$$

$$\gamma_\mu^\dagger = \gamma_\mu, \tag{A.2.2}$$

$$\gamma_5 = \gamma_0\gamma_1\gamma_2\gamma_3 = \frac{1}{4!}\epsilon_{\mu\nu\alpha\beta}\gamma^\mu\gamma^\nu\gamma^\alpha\gamma^\beta \quad \text{with} \quad \gamma_5^\dagger = \gamma_5, \tag{A.2.3}$$

$$\sigma_{\mu\nu} = \frac{i}{2}[\gamma_\mu, \gamma_\nu] = \frac{i}{2}\left(\gamma_\mu\gamma_\nu - \gamma_\nu\gamma_\mu\right). \tag{A.2.4}$$

The explicit form of the gamma matrices in the Weyl representation reads

$$\gamma_0 = \begin{pmatrix} 0 & \mathbb{I}_2 \\ \mathbb{I}_2 & 0 \end{pmatrix}, \quad \gamma_j = \begin{pmatrix} 0 & -i\sigma_j \\ i\sigma_j & 0 \end{pmatrix}, \quad \gamma_5 = \begin{pmatrix} -\mathbb{I}_2 & 0 \\ 0 & \mathbb{I}_2 \end{pmatrix}, \tag{A.2.5}$$

where σ_j are the usual Pauli matrices.

[1] Check the definition of the (densitized) Levi-Civita later.

Fierz Rearrangement Identities

In some chapters of this thesis we will be interested in four-fermion interactions of the form

$$\mathcal{I}_{\mathrm{X}} = \left(\bar{\psi}^i \mathcal{O}_{\mathrm{X}} \psi^i\right)\left(\bar{\psi}^j \mathcal{O}_{\mathrm{X}} \psi^j\right), \tag{A.2.6}$$

with $i, j \in \{1, \ldots, N_{\mathrm{F}}\}$, where N_{F} is the number of Dirac fermions. Different choices for $\mathcal{O}_{\mathrm{X}}$ correspond to different four-fermion channels. We consider $\mathrm{X} \in \{\mathrm{S}, \mathrm{V}, \mathrm{T}, \mathrm{A}, \mathcal{P}\}$, so that

$$\mathcal{O}_{\mathrm{S}} = \mathbb{I}, \quad \mathcal{O}_{\mathrm{V}} = \gamma_\mu, \quad \mathcal{O}_{\mathrm{T}} = \frac{1}{\sqrt{2}}\sigma_{\mu\nu} \quad \mathcal{O}_{\mathrm{A}} = i\gamma_\mu\gamma_5, \quad \mathcal{O}_{\mathcal{P}} = \gamma_5. \tag{A.2.7}$$

Our aim is to show that

$$\left(\bar{\psi}^i \mathcal{O}_{\mathrm{X}} \psi^i\right)\left(\bar{\psi}^j \mathcal{O}_{\mathrm{X}} \psi^j\right) = \sum_{\mathrm{Y}} \mathrm{C}_{\mathrm{XY}} \left(\bar{\psi}^i \mathcal{O}_{\mathrm{Y}} \psi^j\right)\left(\bar{\psi}^j \mathcal{O}_{\mathrm{Y}} \psi^i\right), \tag{A.2.8}$$

with $\mathrm{Y} \in \{\mathrm{S}, \mathrm{V}, \mathrm{T}, \mathrm{A}, \mathcal{P}\}$ and for an appropriate choice of C_{XY}.

In order to achieve this, let us consider the following basis for the Euclidean Clifford algebra:

$$\{\Gamma^{(\mathrm{A})}\} = \{\mathbb{I}, \gamma_\mu, \frac{1}{\sqrt{2}}\sigma_{\mu\nu}, i\gamma_\mu\gamma_5, \gamma_5\}, \tag{A.2.9}$$

which obey the property

$$\mathrm{tr}\Big(\Gamma^{(\mathrm{A})}\Gamma^{(\mathrm{B})}\Big) = 4\,\delta^{\mathrm{AB}} \tag{A.2.10}$$

along with the completeness relation

$$\frac{1}{4}\sum_{\mathrm{A}} (\Gamma_{(\mathrm{A})})_{\alpha\beta} (\Gamma^{(\mathrm{A})})_{\tilde{\alpha}\tilde{\beta}} = \delta_{\alpha\tilde{\beta}}\delta_{\beta\tilde{\alpha}}. \tag{A.2.11}$$

Therefore, any pair of matrices $\mathrm{M}^{(1)}_{\alpha\beta}$ and $\mathrm{M}^{(2)}_{\rho\sigma}$ in the Clifford algebra can be expanded as

$$\begin{aligned} \mathrm{M}^{(1)}_{\alpha\rho}\mathrm{M}^{(2)}_{\sigma\beta} &= \delta_{\alpha\tilde{\beta}}\delta_{\beta\tilde{\alpha}}\mathrm{M}^{(2)}_{\sigma\tilde{\alpha}}\mathrm{M}^{(1)}_{\tilde{\beta}\rho} \\ &= \frac{1}{4}\sum_{\mathrm{A}} (\Gamma_{(\mathrm{A})})_{\alpha\beta}\mathrm{M}^{(2)}_{\sigma\tilde{\alpha}} (\Gamma^{(\mathrm{A})})_{\tilde{\alpha}\tilde{\beta}}\mathrm{M}^{(1)}_{\tilde{\beta}\rho}. \end{aligned} \tag{A.2.12}$$

Written in matrix notation, we get

$$\mathbf{M}^{(1)}\mathbf{M}^{(2)} = \frac{1}{4}\sum_{\mathrm{A}} \Gamma_{(\mathrm{A})}\mathbf{M}^{(2)}\Gamma^{(\mathrm{A})}\mathbf{M}^{(1)}. \tag{A.2.13}$$

Using the last identity, we can rewrite $\mathcal{I}_{\rm X}$ according to

$$\begin{aligned}\mathcal{I}_{\rm X} &= \left(\bar{\psi}^i_\alpha(\mathcal{O}_{\rm X})_{\alpha\rho}\psi^i_\rho\right)\left(\bar{\psi}^j_\sigma(\mathcal{O}_{\rm X})_{\sigma\beta}\psi^j_\beta\right)\\ &= (\mathcal{O}_{\rm X})_{\alpha\rho}(\mathcal{O}_{\rm X})_{\sigma\beta}\bar{\psi}^i_\alpha\psi^i_\rho\bar{\psi}^j_\sigma\psi^j_\beta\\ &= -\frac{1}{4}\sum_{\rm A}(\Gamma_{\rm (A)})_{\alpha\beta}\left(\mathcal{O}_{\rm X}\Gamma^{\rm (A)}\mathcal{O}_{\rm X}\right)_{\sigma\rho}\bar{\psi}^i_\alpha\psi^j_\beta\bar{\psi}^j_\sigma\psi^i_\rho\\ &= -\frac{1}{4}\sum_{\rm A}\left(\bar{\psi}^i\Gamma_{\rm (A)}\psi^j\right)\left(\bar{\psi}^j\mathcal{O}_{\rm X}\Gamma^{\rm (A)}\mathcal{O}_{\rm X}\psi^i\right),\end{aligned} \tag{A.2.14}$$

where $(\alpha,\beta,\dots)$ denote spinorial indices. From Eq. (A.2.14), it follows then that

$$\mathcal{I}_{\rm X} = -\frac{1}{4}\sum_{\rm Y}\left(\bar{\psi}^i\mathcal{O}_{\rm Y}\psi^j\right)\left(\bar{\psi}^j\mathcal{O}_{\rm X}\mathcal{O}_{\rm Y}\mathcal{O}_{\rm X}\psi^i\right), \tag{A.2.15}$$

such that $\mathcal{O}_{\rm X}\mathcal{O}_{\rm Y}\mathcal{O}_{\rm X} = -4{\rm C}_{\rm XY}\mathcal{O}_{\rm Y}$, with ${\rm C}_{\rm XY}$ having the matrix form

$${\rm C}_{\rm XY} = -\frac{1}{4}\begin{pmatrix}1 & 1 & 1 & 1 & 1\\ 4 & -2 & 0 & 2 & -4\\ 6 & 0 & -2 & 0 & 6\\ 4 & 2 & 0 & -2 & -4\\ 1 & -1 & 1 & -1 & 1\end{pmatrix}. \tag{A.2.16}$$

Thus, we achieve the so-called Fierz identities for rearranging four-fermion interactions:

$$\left(\bar{\psi}^i\mathcal{O}_{\rm X}\psi^i\right)\left(\bar{\psi}^j\mathcal{O}_{\rm X}\psi^j\right) = \sum_{\rm Y}{\rm C}_{\rm XY}\left(\bar{\psi}^i\mathcal{O}_{\rm Y}\psi^j\right)\left(\bar{\psi}^j\mathcal{O}_{\rm Y}\psi^i\right). \tag{A.2.17}$$

$(\mathcal{V}+\mathcal{A})$ and $(\mathcal{V}-\mathcal{A})$ channels

Let us exemplify the Fierz rearrangement identities for the particular cases of the $(\mathcal{V}+\mathcal{A})$ and $(\mathcal{V}-\mathcal{A})$ channels:

$$(\mathcal{V}\pm\mathcal{A}) = \underbrace{\left(\bar{\psi}^i\mathcal{O}_{\rm V}\psi^i\right)^2}_{\mathcal{I}_{\rm V}} \pm \underbrace{\left(\bar{\psi}^i O_{\rm A}\psi^i\right)^2}_{\mathcal{I}_{\rm A}}, \tag{A.2.18}$$

where $\mathcal{I}_{\rm V} = \left(\bar{\psi}^i\gamma_\mu\psi^i\right)\left(\bar{\psi}^j\gamma^\mu\psi^j\right)$ and $\mathcal{I}_{\rm A} = \left(\bar{\psi}^i\gamma_\mu\gamma_5\psi^i\right)\left(\bar{\psi}^j\gamma^\mu\gamma_5\psi^j\right)$. Let us define

$$\rho^{ij} = \bar{\psi}^i\mathcal{O}_{\rm S}\psi^j = \bar{\psi}^i\psi^j, \tag{A.2.19}$$

$$\rho_5^{ij} = \bar{\psi}^i\mathcal{O}_{\mathcal{P}}\psi^j = \bar{\psi}^i\gamma_5\psi^j, \tag{A.2.20}$$

$$(J^{ij})^\mu = \bar{\psi}^i\mathcal{O}_{\rm V}\psi^j = \bar{\psi}^i\gamma^\mu\psi^j, \tag{A.2.21}$$

$$(J_5^{ij})^\mu = \bar{\psi}^i\mathcal{O}_{\rm A}\psi^j = \bar{\psi}^j i\gamma^\mu\gamma_5\psi^j, \tag{A.2.22}$$

$$(\tau^{ij})^{\mu\nu} = \bar{\psi}^i\mathcal{O}_{\rm T}\psi^j = \frac{1}{\sqrt{2}}\bar{\psi}^i\sigma^{\mu\nu}\psi^j. \tag{A.2.23}$$

Using the Fierz identities, we obtain

$$\mathcal{I}_{\mathrm{V}} = -\rho^{ij}\rho^{ji} + \rho_5^{ij}\rho_5^{ji} + \frac{1}{2}J^{ij}\cdot J^{ji} - \frac{1}{2}J_5^{ij}J_5^{ji}, \tag{A.2.24}$$

$$\mathcal{I}_{\mathrm{A}} = -\rho^{ij}\rho^{ji} + \rho_5^{ij}\rho_5^{ji} - \frac{1}{2}J^{ij}\cdot J^{ji} + \frac{1}{2}J_5^{ij}J_5^{ji}. \tag{A.2.25}$$

Therefore, we can recast the $(\mathcal{V}+\mathcal{A})$ and $(\mathcal{V}-\mathcal{A})$ channels in terms of scalar/pseudoscalar and vector/axial-vector interactions, respectively, as

$$(\mathcal{V}+\mathcal{A}) = -2\left(\rho^{ij}\rho^{ji} - \rho_5^{ij}\rho_5^{ji}\right) = -2\left(\bar{\psi}^i\psi^j\bar{\psi}^j\psi^i - \bar{\psi}^i\gamma_5\psi^j\bar{\psi}^j\gamma_5\psi^i\right) \tag{A.2.26}$$

$$(\mathcal{V}-\mathcal{A}) = J^{ij}\cdot J^{ji} - J_5^{ij}J_5^{ji} = \bar{\psi}^j\gamma_\mu\psi^j\bar{\psi}^j\gamma^\mu\psi^i - \bar{\psi}^i i\gamma_\mu\gamma_5\psi^j\bar{\psi}^j i\gamma^\mu\gamma_5\psi^i. \tag{A.2.27}$$

Appendix B

Beta Functions for SM and DM Couplings with Gravity Threshold Effects

Using the FRG, we computed the beta functions of SM and DM couplings including contributions due to gravitational fluctuations. In this appendix, we present explicit expressions for the beta function used in our analysis.

For compactness, we define the effective Newton coupling

$$G^n_{(m_1,m_2)} = \frac{G^n}{(1-2\Lambda)^{m_1}(1-4\Lambda/3)^{m_2}}, \tag{B.0.1}$$

where G and Λ are the dimensionless versions of the scale-dependent Newton coupling and cosmological constant, respectively. For $n = 1$, we use the notation $G_{(m_1,m_2)} = G^1_{(m_1,m_2)}$. Some of the beta functions also depend on a parameter ζ, which allows us to unify the results obtained with $\mathrm{U}(1)_\mathrm{D}$ ($\zeta = 0$) and $\mathrm{SU}(2)_\mathrm{D}$ ($\zeta = 1$) vector DM models.

For the SM (non-)Abelian gauge couplings, we find

$$\beta_{g_\mathrm{Y}} = -f_g\, g_\mathrm{Y} + \frac{5\, g_\mathrm{Y}^3}{12\pi^2} + \frac{g_\mathrm{Y}^3}{96\pi^2(1+m_\mathrm{H}^2)^4}, \tag{B.0.2}$$

$$\beta_{g_2} = -f_g\, g_2 - \frac{5\, g_2^3}{24\pi^2} + \frac{g_2^3}{96\pi^2(1+m_\mathrm{H}^2)^4}, \tag{B.0.3}$$

$$\beta_{g_3} = -f_g\, g_3 - \frac{7\, g_3^3}{16\pi^2}, \tag{B.0.4}$$

where f_g is the gravitational contribution to the flow of gauge couplings (see [98, 193, 199, 201, 203, 205, 227–229, 473, 474])

$$f_g = \frac{5\, G_{(1,0)}}{9\pi} - \frac{5\, G_{(2,0)}}{18\pi}. \tag{B.0.5}$$

We note that f_g is the same for all gauge couplings, which is a consequence of gravity being "blind" to internal symmetries.

For the gauge coupling in the dark sector, we find

$$\beta_{g_D} = -f_g\, g_D + \frac{(1-\zeta/2)\, g_D^3}{48\pi^2(1+m_S^2)^4} - \frac{11\,\zeta\, g_D^3}{24\pi^2}\,. \tag{B.0.6}$$

In the Yukawa sector of the SM, we focus on the top and bottom Yukawa couplings. The other flavors have subleading effects in our analysis. The resulting beta functions are

$$\begin{aligned}\beta_{y_t} = &-f_y\, y_t + \frac{3\, y_t^3}{16\pi^2} + \frac{3\, y_t^3}{32\pi^2(1+m_H^2)^2} + \frac{3\, y_b^2 y_t}{16\pi^2} - \frac{y_b^2 y_t}{16\pi^2(1+m_H^2)} - \frac{y_b^2 y_t}{32\pi^2(1+m_H^2)^2} - \frac{g_3^2\, y_t}{2\pi^2} \\ &- \frac{g_Y^2\, y_t}{24\pi^2} - \frac{3\, g_Y^2\, y_t}{128\pi^2(1+m_H^2)} - \frac{3\, g_Y^2\, y_t}{128\pi^2(1+m_H^2)^2} - \frac{9\, g_2^2\, y_t}{128\pi^2(1+m_H^2)} - \frac{9\, g_2^2\, y_t}{128\pi^2(1+m_H^2)^2}\,,\end{aligned} \tag{B.0.7}$$

and

$$\begin{aligned}\beta_{y_b} = &-f_y\, y_b + \frac{3\, y_b^3}{16\pi^2} + \frac{3\, y_b^3}{32\pi^2(1+m_H^2)^2} + \frac{3\, y_t^2 y_b}{16\pi^2} - \frac{y_t^2 y_b}{16\pi^2(1+m_H^2)} - \frac{y_t^2 y_b}{32\pi^2(1+m_H^2)^2} - \frac{g_3^2\, y_b}{2\pi^2} \\ &+ \frac{g_Y^2\, y_b}{48\pi^2} - \frac{3\, g_Y^2\, y_b}{128\pi^2(1+m_H^2)} - \frac{3\, g_Y^2\, y_b}{128\pi^2(1+m_H^2)^2} - \frac{9\, g_2^2\, y_b}{128\pi^2(1+m_H^2)} - \frac{9\, g_2^2\, y_b}{128\pi^2(1+m_H^2)^2}\,,\end{aligned} \tag{B.0.8}$$

with the flavor-independent gravitational contribution (see [98, 200, 205, 209, 233, 456])

$$\begin{aligned}f_y = &-\frac{15\, G_{(2,0)}}{16\pi} + \frac{G_{(0,1)}}{8\pi} - \frac{G_{(0,2)}}{48\pi} + \frac{2\, G_{(0,2)}\, m_H^4}{3\pi(1+m_H^2)^2} - \frac{2\, G_{(0,1)}\, m_H^2}{5\pi(1+m_H^2)} + \frac{8\, G_{(0,1)}\, m_H^2}{15\pi(1+m_H^2)^2} \\ &- \frac{2\, G_{(0,2)}\, m_H^2}{15\pi(1+m_H^2)} - \frac{G_{(0,1)}}{36\pi(1+m_H^2)^2} - \frac{G_{(0,2)}}{36\pi(1+m_H^2)}\,.\end{aligned} \tag{B.0.9}$$

For the Higgs and dark quartic scalar couplings, we find

$$\begin{aligned}\beta_{\lambda_H} = &-f_{\lambda_H}\, \lambda_H + \frac{\lambda_H^2}{4\pi^2(1+m_H^2)^3} - \frac{9\, g_2^2\, \lambda_H}{32\pi^2(1+m_H^2)} - \frac{9\, g_2^2\, \lambda_H}{32\pi^2(1+m_H^2)^2} \\ &- \frac{3\, g_Y^2\, \lambda_H}{32\pi^2(1+m_H^2)} - \frac{3\, g_Y^2\, \lambda_H}{32\pi^2(1+m_H^2)^2} + \frac{3\,(1+\zeta)\, \lambda_p^2}{2\pi^2(1+m_S^2)^3} + \frac{3\, \lambda_H\, y_b^2}{4\pi^2} + \frac{3\, \lambda_H\, y_t^2}{4\pi^2} \\ &+ \frac{9\, g_2^2\, g_Y^2}{32\pi^2} + \frac{27\, g_2^4}{64\pi^2} + \frac{9 g_Y^4}{64\pi^2} - \frac{9\, y_b^4}{4\pi^2} - \frac{9\, y_t^4}{4\pi^2}\,,\end{aligned} \tag{B.0.10}$$

and

$$\begin{aligned}\beta_{\lambda_S} = &-f_{\lambda_S}\, \lambda_S + \frac{5\,(1+\zeta/5)\, \lambda_S^2}{24\pi^2(1+m_S^2)^3} + \frac{3\, \lambda_p^2}{\pi^2(1+m_H^2)^3} - \frac{3\,(1-\zeta/4)\, g_D^2\, \lambda_S}{8\pi^2(1+m_S^2)^2} - \frac{3\,(1-\zeta/4)\, g_D^2\, \lambda_S}{8\pi^2(1+m_S^2)} \\ &+ \frac{9\,(1-13\,\zeta/16)\, g_D^4}{4\pi^2}\,.\end{aligned} \tag{B.0.11}$$

The gravitational contributions to the quartic scalar couplings are (see, e.g., [208, 230, 233, 460, 462])

$$f_{\lambda_{H/S}} = -\frac{5\, G_{(2,0)}}{2\pi} - \frac{G_{(0,2)}}{3\pi} + F_{\lambda_{H/S}}(m_{H/S}^2)\,, \tag{B.0.12}$$

with

$$
\begin{aligned}
F_\lambda(m^2) = &-\frac{16\,G_{(0,1)}\,m^4}{\pi(1+m^2)^3} - \frac{16\,G_{(0,2)}\,m^4}{3\pi(1+m^2)^2} + \frac{16\,G_{(0,1)}\,m^2}{3\pi(1+m^2)^2} + \frac{8\,G_{(0,2)}\,m^2}{3\pi(1+m^2)} \\
&- \frac{G_{(0,1)}}{9\pi(1+m^2)^2} - \frac{G_{(0,2)}}{9\pi(1+m^2)} + \lambda^{-1}\left(\frac{64\,m^4}{3}G^2_{(0,3)} + 240\,m^4\,G^2_{(3,0)}\right. \\
&\left. - \frac{256\,m^6\,G^2_{(0,2)}}{3\,(1+m^2)^2} + \frac{1024\,m^8\,G^2_{(0,2)}}{3\,(1+m^2)^3} + \frac{1024\,m^8\,G^2_{(0,3)}}{3\,(1+m^2)^2} - \frac{512\,m^6\,G^2_{(0,3)}}{3\,(1+m^2)}\right).
\end{aligned}
\tag{B.0.13}
$$

As in the gravitational contribution to the flow of the SM gauge couplings, we note that these contributions are the same for both quartic couplings, *i.e.*, the gravitational contribution is "blind" to internal symmetries. For the scalar portal coupling, we find

$$
\begin{aligned}
\beta_{\lambda_\mathrm{p}} = &-f_{\lambda_\mathrm{p}}\,\lambda_\mathrm{p} + \frac{\lambda_\mathrm{p}^2}{4\pi^2(1+m_\mathrm{H}^2)^2(1+m_\mathrm{S}^2)} + \frac{\lambda_\mathrm{p}^2}{4\pi^2(1+m_\mathrm{H}^2)(1+m_\mathrm{S}^2)^2} - \frac{9\,g_2^2\,\lambda_\mathrm{p}}{64\pi^2(1+m_\mathrm{H}^2)} \\
&- \frac{9\,g_2^2\,\lambda_\mathrm{p}}{64\pi^2(1+m_\mathrm{H}^2)^2} - \frac{3\,(1-\zeta/4)\,g_\mathrm{D}^2\,\lambda_\mathrm{p}}{16\pi^2(1+m_\mathrm{S}^2)} - \frac{3\,(1-\zeta/4)\,g_\mathrm{D}^2\,\lambda_\mathrm{p}}{16\pi^2(1+m_\mathrm{S}^2)^2} - \frac{3\,g_\mathrm{Y}^2\,\lambda_\mathrm{p}}{64\pi^2(1+m_\mathrm{H}^2)} \\
&- \frac{3\,g_\mathrm{Y}^2\,\lambda_\mathrm{p}}{64\pi^2(1+m_\mathrm{H}^2)^2} + \frac{\lambda_\mathrm{H}\,\lambda_\mathrm{p}}{8\pi^2(1+m_\mathrm{H}^2)^3} + \frac{(1+\zeta/2)\,\lambda_\mathrm{p}\,\lambda_\mathrm{S}}{12\pi^2(1+m_\mathrm{S}^2)^3} + \frac{3\,\lambda_\mathrm{p}\,y_b^2}{8\pi^2} + \frac{3\,\lambda_\mathrm{p}\,y_t^2}{8\pi^2}\,,
\end{aligned}
\tag{B.0.14}
$$

with gravitational contribution (see [230, 233])

$$
\begin{aligned}
f_{\lambda_\mathrm{p}} = &-\frac{5\,G_{(2,0)}}{2\pi} - \frac{G_{(0,2)}}{3\pi} - \frac{8\,G_{(0,1)}\,m_\mathrm{H}^4}{3\pi(1+m_\mathrm{H}^2)^3} \\
&- \frac{16\,G_{(0,1)}\,m_\mathrm{H}^2 m_\mathrm{S}^2}{3\pi(1+m_\mathrm{H}^2)^2(1+m_\mathrm{S}^2)} - \frac{16\,G_{(0,1)}\,m_\mathrm{H}^2 m_\mathrm{S}^2}{3\pi(1+m_\mathrm{H}^2)(1+m_\mathrm{S}^2)^2} \\
&+ \frac{4\,G_{(0,2)}\,m_\mathrm{H}^2}{3\pi(1+m_\mathrm{H}^2)} - \frac{G_{(0,1)}}{18\pi(1+m_\mathrm{H}^2)^2} - \frac{G_{(0,2)}}{18\pi(1+m_\mathrm{H}^2)} \\
&- \frac{8\,G_{(0,1)}\,m_\mathrm{S}^4}{3\pi(1+m_\mathrm{S}^2)^3} + \frac{8\,G_{(0,1)}\,m_\mathrm{S}^2}{3\pi(1+m_\mathrm{S}^2)^2} - \frac{G_{(0,1)}}{18\pi(1+m_\mathrm{S}^2)^2} \\
&- \frac{16\,G_{(0,2)}\,m_\mathrm{H}^2 m_\mathrm{S}^2}{3\pi(1+m_\mathrm{H}^2)(1+m_\mathrm{S}^2)} + \frac{8\,G_{(0,1)}\,m_\mathrm{H}^2}{3\pi(1+m_\mathrm{H}^2)^2} \\
&+ \frac{4\,G_{(0,2)}\,m_\mathrm{S}^2}{3\pi(1+m_\mathrm{S}^2)} - \frac{G_{(0,2)}}{18\pi(1+m_\mathrm{S}^2)} \\
&+ \lambda_\mathrm{p}^{-1}\left(+\frac{32\,G^2_{(0,3)}\,m_\mathrm{H}^2\,m_\mathrm{S}^2}{9} + 40\,G^2_{(3,0)}\,m_\mathrm{H}^2\,m_\mathrm{S}^2\right. \\
&- \frac{128\,G^2_{(0,3)}\,m_\mathrm{H}^4\,m_\mathrm{S}^2}{9\left(1+m_\mathrm{H}^2\right)} - \frac{64\,G^2_{(0,2)}\,m_\mathrm{H}^4\,m_\mathrm{S}^2}{9\left(1+m_\mathrm{H}^2\right)^2} \\
&+ \frac{512\,G^2_{(0,3)}\,m_\mathrm{H}^4\,m_\mathrm{S}^4}{9\left(1+m_\mathrm{H}^2\right)\left(1+m_\mathrm{S}^2\right)} + \frac{256\,G^2_{(0,2)}\,m_\mathrm{H}^4\,m_\mathrm{S}^4}{9\left(1+m_\mathrm{H}^2\right)^2\left(1+m_\mathrm{S}^2\right)} \\
&\left. + \frac{256\,G^2_{(0,2)}\,m_\mathrm{H}^4 m_\mathrm{S}^4}{9\left(1+m_\mathrm{H}^2\right)\left(1+m_\mathrm{S}^2\right)^2} - \frac{128\,G^2_{(0,3)}\,m_\mathrm{H}^2\,m_\mathrm{S}^4}{9\left(1+m_\mathrm{S}^2\right)}\right)
\end{aligned}
\tag{B.0.15}
$$

$$- \frac{64\, G_{(0,2)}^2\, m_{\rm H}^2\, m_{\rm S}^4}{9\left(1+m_{\rm S}^2\right)^2}\Bigg).$$

There is again the same universality, *i.e.*, those terms that are independent of the scalar masses are exactly the same as the first two terms in $f_{\lambda_{\rm H/S}}$.

Finally, by defining dimensionless versions of the Higgs and dark mass parameters by the rescalings $m_{\rm H}^2 \to k^2 m_{\rm H}^2$ and $m_{\rm S}^2 \to k^2 m_{\rm S}^2$, their beta functions read

$$\begin{aligned}\beta_{m_{\rm H}^2} = &-2m_{\rm H}^2 - f_{m_{\rm H}^2}\, m_{\rm H}^2 - \frac{9g_2^2 m_{\rm H}^2}{64\pi^2(1+m_{\rm H}^2)} - \frac{9g_2^2 m_{\rm H}^2}{64\pi^2(1+m_{\rm H}^2)^2} - \frac{3g_{\rm Y}^2 m_{\rm H}^2}{64\pi^2(1+m_{\rm H}^2)} \\ &- \frac{3g_{\rm Y}^2 m_{\rm H}^2}{64\pi^2(1+m_{\rm H}^2)^2} + \frac{3m_{\rm H}^2 y_b^2}{8\pi^2} + \frac{3m_{\rm H}^2 y_t^2}{8\pi^2} - \frac{9g_2^2}{64\pi^2} - \frac{3g_{\rm Y}^2}{64\pi^2} - \frac{\lambda_{\rm H}}{16\pi^2(1+m_{\rm H}^2)^2} \\ &- \frac{(1+\zeta)\,\lambda_{\rm p}}{8\pi^2(1+m_{\rm S}^2)^2} + \frac{3y_b^2}{8\pi^2} + \frac{3y_t^2}{8\pi^2}\,,\end{aligned} \tag{B.0.16}$$

and

$$\begin{aligned}\beta_{m_{\rm S}^2} = &-2m_{\rm S}^2 - f_{m_{\rm S}^2}\, m_{\rm S}^2 - \frac{(1+\zeta/2)\,\lambda_{\rm S}}{24\pi^2(1+m_{\rm S}^2)^2} - \frac{3\,(1-\zeta/4)\,g_{\rm D}^2 m_{\rm S}^2}{16\pi^2(1+m_{\rm S}^2)^2} - \frac{3\,(1-\zeta/4)\,g_{\rm D}^2 m_{\rm S}^2}{16\pi^2(1+m_{\rm S}^2)} \\ &- \frac{3\,(1-\zeta/4)\,g_{\rm D}^2}{16\pi^2} - \frac{\lambda_{\rm p}}{4\pi^2(1+m_{\rm H}^2)^2}\,,\end{aligned} \tag{B.0.17}$$

with gravitational contribution

$$f_{m^2} = -\frac{5\,G_{(2,0)}}{2\pi} - \frac{G_{(0,2)}}{3\pi} + \frac{4\,G_{(0,2)}\,m^4}{3\pi\,(1+m^2)^2} + \frac{4\,G_{(0,1)}\,m^2}{3\pi\,(1+m^2)^2} - \frac{G_{(0,1)}}{18\pi\,(1+m^2)^2} - \frac{G_{(0,2)}}{18\pi\,(1+m^2)} \tag{B.0.18}$$

for $m^2 = m_{\rm H}^2$ and $m^2 = m_{\rm S}^2$.

Besides the gravitational contributions, the results presented here differ from standard one-loop beta functions in two ways: i) they automatically contain threshold effects due to a mass-like regulator function; ii) the beta functions for the mass parameters contain terms proportional to $\lambda_{\rm H}$, $\lambda_{\rm S}$ and $\lambda_{\rm p}$ that are non-vanishing in the limit $m_{\rm H}^2, m_{\rm S}^2 \to 0$.

Appendix C

Heat-Kernel Trace of the Squared Dirac Operator in Spaces with Torsion and Vanishing Curvature

In this Appendix, the heat-kernel trace of the squared Dirac operator is computed. This is given by

$$K_\tau = \mathrm{Tr}\left[\exp\left(-\tau\,(-\not{\mathcal{D}}^2)\right)\right]. \tag{C.0.1}$$

We focus on the particular case of homogeneous axial-torsion and vanishing curvature. In this way, the differential operator operator $-\not{\mathcal{D}}^2$ is defined in Eq. (4.2.63).

This approximation allows us to perform a Fourier space representation for the heat-kernel trace, namely

$$K_\tau = v_4\, e^{-\tau A^2/64} \int_q e^{-\tau\, q^2}\, \mathrm{tr}\left[\exp\left(-\frac{\tau}{4}\gamma_5\,\sigma^{\mu\nu}A_\mu\, q_\nu\right)\right], \tag{C.0.2}$$

where tr stands for the trace over Dirac indices. In order to actually compute the momentum space integrals, it is useful to perform an expansion of the exponential inside the remaining trace:

$$\mathrm{tr}\left[\exp\left(-\frac{\tau}{4}\gamma_5\,\sigma^{\mu\nu}A_\mu\, q_\nu\right)\right] = 4 + \sum_{n=1}^{\infty}\frac{(-1)^n\tau^n}{2^{2n}\,n!}\,\mathrm{tr}\left[\gamma_5\,\sigma^{\mu_1\nu_1}\cdots\gamma_5\,\sigma^{\mu_n\nu_n}\right]A_{\mu_1}\cdots A_{\mu_n}\,q_{\nu_1}\cdots q_{\nu_n}\,, \tag{C.0.3}$$

where $\mathrm{tr}\mathbf{1} = 4$ is the zeroth order term. Remarkably, the only nonzero contributions in the sum are with even values of n. These terms will have a trace which will contain even powers of γ_5, which ultimately can be combined into an identity matrix. Relabeling $n \mapsto 2n$, we find

$$\mathrm{tr}\left[\exp\left(-\frac{\tau}{4}\gamma_5\,\sigma^{\mu\nu}A_\mu\, q_\nu\right)\right] = 4 + \sum_{n=1}^{\infty}\frac{\tau^{2n}}{2^{4n}\,(2n)!}\,\mathrm{tr}\left[\sigma^{\mu_1\nu_1}\cdots\sigma^{\mu_{2n}\nu_{2n}}\right]A_{\mu_1}\cdots A_{\mu_{2n}}\,q_{\nu_1}\cdots q_{\nu_{2n}}\,. \tag{C.0.4}$$

Plugging ((C.0.4)) back into (C.0.2), we find

$$\int_q e^{-\tau q^2}\,\mathrm{tr}\left[\exp\left(-\frac{\tau}{4}\gamma_5\,\sigma^{\mu\nu}A_\mu\,q_\nu\right)\right] = 4\int_q e^{-\tau q^2} + \sum_{n=1}^{\infty}\frac{\tau^{2n}}{2^{4n}\,(2n)!}\,\mathrm{tr}\left[\sigma^{\mu_1\nu_1}\cdots\sigma^{\mu_{2n}\nu_{2n}}\right]A_{\mu_1}\cdots A_{\mu_{2n}}\int_q q_{\nu_1}\cdots q_{\nu_{2n}}\,e^{-\tau q^2}\,. \tag{C.0.5}$$

The result for $\mathrm{tr}\left[\sigma^{\mu_1\nu_1}\cdots\sigma^{\mu_{2n}\nu_{2n}}\right]$ can be expressed as a linear combination of products of the flat metric $\delta_{\mu\nu}$. Consequently, for each value of n, the combined expression

$$\mathcal{I} = \mathrm{tr}\left[\sigma^{\mu_1\nu_1}\cdots\sigma^{\mu_{2n}\nu_{2n}}\right]A_{\mu_1}\cdots A_{\mu_{2n}}\int_q q_{\nu_1}\cdots q_{\nu_{2n}}\,e^{-\tau q^2}, \tag{C.0.6}$$

can be recast into the form

$$\mathcal{I} = \sum_{m_1=0}^{n}\sum_{m_2=0}^{2n} c_{m_1,m_2}\,\delta_{n,m_1+m_2}\,(A^2)^{n-m_1}\int_q (q\cdot A)^{2m_1}\,(q^2)^{m_2}\,e^{-\tau q^2}\,, \tag{C.0.7}$$

for a given set of coefficients c_{m_1,m_2}. The integrals over the squared momentum can be further reduced by the replacement

$$(q\cdot A)^{2m_1} \mapsto \frac{\Gamma(m_1+\frac{1}{2})}{\sqrt{\pi}\Gamma(m_1+2)}(A^2)^{m_1}(q^2)^{m_1}, \tag{C.0.8}$$

where the symnbol $\mapsto$ indicates the replacement can only be implemented under the momentum-integral. With this, the remaining integrals can be written as

$$\int_q (q\cdot A)^{2m_1}\,(q^2)^{m_2}\,e^{-\tau q^2} = \frac{\Gamma\left(m_1+\frac{1}{2}\right)}{\sqrt{\pi}\,\Gamma(m_1+2)}(A^2)^{m_1}\int_q (q^2)^{m_1+m_2}\,e^{-\tau q^2}\,. \tag{C.0.9}$$

It then follows that

$$\mathcal{I} = \mathcal{C}_n\,(A^2)^n\int_q (q^2)^n\,e^{-\tau q^2}\,, \tag{C.0.10}$$

where

$$\mathcal{C}_n = \sum_{m_1=0}^{n}\sum_{m_2=0}^{2n} c_{m_1,m_2}\,\delta_{n,m_1+m_2}\,\frac{\Gamma\left(m_1+\frac{1}{2}\right)}{\sqrt{\pi}\,\Gamma(m_1+2)}\,,\quad (n>0). \tag{C.0.11}$$

Remarkably, the last expression can be computed order by order with the built-in function *FindSequenceFunction* from *Mathematica*. Using this function, the following expression for $\mathcal{C}_n$ is obtained:

$$\mathcal{C}_n = \frac{8}{\sqrt{\pi}}\,\frac{\Gamma\left(n+\frac{3}{2}\right)}{\Gamma(n+2)}\,. \tag{C.0.12}$$

Returning to the original integral, we get

$$\int_q e^{-\tau q^2}\,\mathrm{tr}\left[\exp\left(-\frac{\tau}{4}\gamma_5\,\sigma^{\mu\nu}A_\mu\,q_\nu\right)\right] = \sum_{n=0}^{\infty}\frac{\mathcal{C}_n}{2^{4n}\,(2n)!}\,\tau^{2n}\,(A^2)^n\int_q (q^2)^n\,e^{-\tau q^2}\,, \tag{C.0.13}$$

where $\mathcal{C}_0 = 4$ has been defined (which is compatible with (C.0.11) in the limit $n \to 0$) to collect all terms into one single sum. Finally, the remaining integral over q can be computed. Explicitly, it reads

$$\int_q (q^2)^n \, e^{-\tau q^2} = \frac{1}{16\pi^2} \int_0^\infty dq^2 \, (q^2)^{n+1} \, e^{-\tau q^2} = \frac{\Gamma(n+2)}{16\pi^2 \, \tau^{n+2}} \, . \tag{C.0.14}$$

Therefore, we are led to

$$\int_q e^{-\tau q^2} \, \mathrm{tr}\left[\exp\left(-\frac{\tau}{4}\gamma_5 \, \sigma^{\mu\nu} A_\mu \, q_\nu\right)\right] = \frac{1}{16\pi^2 \, \tau^2} \sum_{n=0}^{\infty} \frac{\mathcal{C}_n \, \Gamma(n+2)}{2^{4n} \, (2n)!} \, (\tau \, A^2)^n \, . \tag{C.0.15}$$

Based on (C.0.11), we can make use of *Mathematica* once again to show that the sum in the last expression converges to

$$\sum_{n=0}^{\infty} \frac{\mathcal{C}_n \, \Gamma(n+2)}{2^{4n} \, (2n)!} \, (\tau \, A^2)^n = \frac{1}{8} e^{\tau \, A^2/64} (32 + \tau \, A^2). \tag{C.0.16}$$

Returning to the heat-kernel trace, we finally led to

$$K_\tau = \frac{v_4}{16\pi^2 \, \tau^2} \left(4 + \frac{1}{8} \, \tau \, A^2\right) . \tag{C.0.17}$$

Appendix D

Supplementary Material on (Quantum) Unimodular Gravity

D.1 Alternative formulations of classical UG

The equations of motion of UG can also be obtained by the variation of an action $S_{\rm UG}[g;\Phi]$ defined as

$$S_{\rm UG}[g;\Phi] = S_{\rm G}[g;\Phi] + \int \mathrm{d}^d x\, B\left(\sqrt{|g|} - \omega\right), \tag{D.1.1}$$

with $S_{\rm G}[g;\Phi]$ being a full Diff-invariant gravitational action (e.g., the Einstein-Hilbert action), possibly containing matter fields, and B is a Lagrange multiplier. Note that, when imposing the unimodularity conditon by means of a Lagrange multiplier, the action has to be written as if there are no constraints, *i.e.*, the metric is treated as an unconstrained variable. The equation of motion for B imposes (5.3.1). Apart from being equivalent to imposing the unimodularity condition directly on the determinant of the metric, the formulation of UG with a Lagrange multiplier would bring computational difficulties at the quantum level (for instance, in defining the vertices and consequent Feynman diagrams of the underlying theory).

Another commonly used formulation of UG, based on an enlarged symmetry group, is achieved by writing the full Diff-invariant action $S_{\rm G}[g;\Phi]$ in terms of an unrestricted dynamical metric $\gamma_{\mu\nu}$, which is conformally related to the constrained metric $g_{\mu\nu}$ via [133, 387, 408, 475]

$$g_{\mu\nu} = \gamma_{\mu\nu}\left(\omega^{-2}\det\gamma_{\mu\nu}\right)^{-1/d}. \tag{D.1.2}$$

It is straightforward to check that relation (D.1.2) enforces the unimodularity condition $\det g_{\mu\nu} = \omega^2$ irrespective of any restriction on the new dynamical metric $\gamma_{\mu\nu}$. In terms of this fundamental unconstrained metric, the action is defined by $S_{\rm UG}[\gamma;\Phi] = S_{\rm G}[g(\gamma),\Phi]$, and all geometrical quantities such as covariant derivatives and curvature invariants are constructed in terms of $\gamma_{\mu\nu}$.

In addition to being symmetric under SDiff transformations, the action $S_{\rm UG}[\gamma;\Phi]$ is symmetric

under Weyl rescalings

$$\gamma_{\mu\nu} \mapsto \gamma'_{\mu\nu} = \Omega^2(x)\gamma_{\mu\nu}, \tag{D.1.3}$$

with $\omega' = \omega$, where $\Omega(x)$ is a local dilation. Correspondingly, the action is invariant under the enlarged symmetry group *WTDiff*', characterized by the combined SDiff $\ltimes$ Weyl transformations. The transformation from constrained metric $g_{\mu\nu}$ to dynamical unrestricted metric $\gamma_{\mu\nu}$ is clearly non-invertible (one degree of freedom corresponding to $\det\gamma_{\mu\nu}$ is lost as, by construction, the action is independent of it). This non-invertibility may spoil the equivalence of UG written in terms of $g_{\mu\nu}$ and $\gamma_{\mu\nu}$ [403–407]. So far, this equivalence is only guaranteed at the classical and at 1-loop levels [387].

We close this short discussion on alternative formulations of UG by noting that the classical equivalence of UG and GR extends to Riemann-Cartan formulations of gravity, which are characterized by a non-vanishing torsion field. In [476], the authors considered a first-order formulation of the unimodular version of the Einstein-Cartan action, where the spin density of matter fields (notably, Dirac spinors) act as a source of spacetime torsion. The unimodularity condition is implemented through an unrestricted dynamical vierbein $\tilde{e}^a{}_\mu$ conformally related to the constrained one by

$$e^a{}_\mu = \left(\omega^{-1}\det e^a{}_\mu\right)^{-1/d}\tilde{e}^a{}_\mu, \tag{D.1.4}$$

with $\det e^a{}_\mu = \sqrt{-g}$. In the first-order formulation of UG, the field equation of the vierbein is traceless, in conformity with the torsion-free UG scenario.

D.2 The decomposed Hessian

In this Appendix we report the Hessians employed in the computation of the beta functions of the gravitational couplings. Expanding the gravitational part of the flowing action (5.4.10) up to second order in the fluctuation field h leads to the expressions

$$\Gamma^{(2)}_{\mathrm{TT}} = \mathcal{Z}_{k,\mathrm{TT}}\left[f_k^{(0,1)}\left(\Delta_2 + (\gamma_2 - 1)\bar{R}\right) - f_k^{(1,0)}\right]\left(\Delta_2 + \frac{2\gamma_2 - 1}{2}\bar{R}\right) \tag{D.2.1a}$$

$$\Gamma^{(2)}_{\xi\xi} = \frac{2\mathcal{Z}_{k,\xi}}{\alpha}\left(\Delta_1 + \frac{2\gamma_1 - 1}{2}\bar{R}\right)^2 \tag{D.2.1b}$$

$$\Gamma^{(2)}_{\sigma\sigma} = \frac{9\mathcal{Z}_{k,\sigma}}{8}\left[\mathbf{P}_k\left(\Delta_0 + \frac{3\gamma_0 - 1}{3}\bar{R}\right) + \mathbf{Q}_k\right]\left(\Delta_0 + \frac{3\gamma_0 - 1}{3}\bar{R}\right)(\Delta_0 + \gamma_0\bar{R})^2 \tag{D.2.1c}$$

$$\Gamma^{(2)}_{C\bar{C}} = \sqrt{2}\mathcal{Z}_{k,C}\left(\Delta_1 + \frac{2\gamma_1 - 1}{2}\bar{R}\right), \tag{D.2.1d}$$

where we have defined

$$\mathbf{P}_k = f_k^{(2,0)} + \frac{1}{4}\bar{R}^2 f_k^{(0,2)} + 4\,\bar{R}\, f_k^{(1,1)} + \frac{2}{3}f_k^{(0,1)}, \tag{D.2.2a}$$

$$\mathbf{Q}_k = \frac{1}{3}f_k^{(1,0)} + \frac{2}{9}\bar{R}\, f_k^{(0,1)}. \tag{D.2.2b}$$

Furthermore, as defined in the main text, we define the coarse-graining operator for each spin-s sector as $\Delta_s = \Delta_{\mathrm{L}s} - \gamma_s \bar{R}$, where the endomorphism parameters are introduced such that the choice $\gamma_0 = \gamma_{\frac{1}{2}} = \gamma_1 = \gamma_2 = 0$ implements the Lichnerowicz-Laplacians and $\gamma_0 = 0$, $\gamma_{\frac{1}{2}} = 1/4$, $\gamma_1 = 1/4$ and $\gamma_2 = 2/3$ provide the Bochner-Laplacian. As the matter action is already second order in the fields, its Hessian elements are given by

$$\Gamma^{(2)}_{\phi\phi} = \Delta_{\mathrm{L}0} \tag{D.2.3a}$$

$$\Gamma^{(2)}_{A^{\mathrm{T}}A^{\mathrm{T}}} = \Delta_{\mathrm{L}1} \tag{D.2.3b}$$

$$\Gamma^{(2)}_{A^{\mathrm{L}}A^{\mathrm{L}}} = \frac{1}{\zeta}\Delta_{\mathrm{L}0} \tag{D.2.3c}$$

$$\Gamma^{(2)}_{\psi\bar{\psi}} = i\not{\nabla} \tag{D.2.3d}$$

$$\Gamma^{(2)}_{c\bar{c}} = \Delta_{\mathrm{L}0}. \tag{D.2.3e}$$

D.3 Heat kernel evaluation and trace technology

We follow the standard heat kernel techniques to compute the functional traces needed in Chapter 5. We restrict the calculations below to $d = 4$. On general grounds, as we briefly discussed in Chapter 4, a functional trace can be expanded in terms of heat kernel coefficients [13, 477, 478], namely

$$\mathrm{Tr}_{(s)}\big[W(\Delta_s)\big] = \frac{1}{16\pi^2}\sum_{n=0}^{\infty}\int_x \sqrt{g}\, Q_{2-n}[W]\ \mathrm{tr}\big[\mathbf{b}_{2n}(\Delta_s)\big], \tag{D.3.1}$$

with Q_n-functional defined (for arbitrary real n) according to

$$Q_n[W] = \frac{(-1)^k}{\Gamma(n+k)}\int_0^{\infty} dz\, z^{n+k-1}\,\frac{d^k W(z)}{dz^k}, \tag{D.3.2}$$

where k denotes some (arbitrary) positive integer satisfying the following restriction $n+k > 0$. Moreover, $\mathrm{tr}\big[\mathbf{b}_{2n}(\Delta_s)\big]$ denotes the trace of the (non-integrated) heat kernel coefficient $\mathbf{b}_{2n}(\Delta_s)$ associated with the coarse-graining operator Δ_s. When the background is evaluated over a sphere S^4, we can express

$$\mathrm{tr}\big[\mathbf{b}_{2n}(\Delta_s)\big] = c_s\,\bar{R}^n\,, \tag{D.3.3}$$

where c_s denotes a numerical coefficient depending on the choice of the coarse-graining operator. In Tables D.1 and D.2, we report the relevant c_s-coefficients for the analysis presented in Chapter 5.

For the Litim's cutoff (5.5.3), the Q_n-functionals can be computed analytically even for a general function of the form $f_k(\bar{R}, \bar{R}^2_{\mu\nu})$. Due to specific properties of this choice of profile function, only a finite number of Q_n-functionals (with negative n) lead to non-vanishing results. As a consequence, the heat kernel expansion in (D.3.1) involve only a finite number of terms.

Since the fRG equation written in the York basis features traces over differential constrained fields, spurious eigenvalues of the coarse-graining operator must be properly removed. In the main text this

s	$n=0$	$n=2$	$n=4$	$n=6$	$n=8$	$n=10$	$n=12$
0	1	$\frac{5}{6}$	$\frac{749}{2160}$	$\frac{26141}{272160}$	$\frac{130117}{6531840}$	$\frac{203161}{61585920}$	$\frac{925711}{2037934080}$
1	3	$\frac{3}{2}$	$\frac{259}{720}$	$\frac{4931}{90720}$	$\frac{1373}{241920}$	$\frac{8527}{20528640}$	$\frac{261865}{13450364928}$
2	5	$-\frac{5}{6}$	$-\frac{1}{432}$	$\frac{311}{54432}$	$\frac{109}{1306368}$	$-\frac{317}{12317184}$	$-\frac{6631}{4483454976}$

Table D.1: c_s-coefficients associated with the Bochner-Laplacian as the coarse-graining operator. All the coefficients were computed within the 4-sphere background.

s	$n=0$	$n=2$	$n=4$	$n=6$	$n=8$	$n=10$	$n=12$
0	1	$\frac{1}{6}$	$\frac{29}{2160}$	$\frac{37}{54432}$	$\frac{149}{6531840}$	$\frac{179}{431101440}$	$-\frac{1387}{201755473920}$
1/2	4	$-\frac{1}{3}$	$-\frac{11}{2160}$	$\frac{31}{544320}$	$\frac{41}{26127360}$	$\frac{31}{492687360}$	$\frac{10331}{3228087582720}$
1	3	$-\frac{1}{2}$	$\frac{19}{720}$	$-\frac{5}{18144}$	$-\frac{11}{2177280}$	$-\frac{19}{143700480}$	$-\frac{347}{67251824640}$
2	5	$-\frac{25}{6}$	$\frac{719}{432}$	$-\frac{23125}{54432}$	$\frac{101981}{1306368}$	$-\frac{952135}{86220288}$	$\frac{50728409}{40351094784}$

Table D.2: c_s-coefficients associated with the Lichnerowicz-Laplacian as the coarse-graining operator. All the coefficients were computed within the 4-sphere background.

was indicated with the inclusion of an appropriate number of primes in some functional traces. These "primed" traces can be computed according to [172, 179, 180]

$$\mathrm{Tr}^{\prime\cdots\prime}_{(s)}\big[W(\Delta_s)\big] = \mathrm{Tr}_{(s)}\big[W(\Delta_s)\big] - \sum_{l\in M_s} D_l(s)W(\lambda_l(s)), \tag{D.3.4}$$

where $M_s = \{s, s+1, \cdots, m-1+s\}$ with m denoting the number of spurious modes ("primes"). Moreover, $\lambda_l(s)$ denotes the l-th eigenvalue of the "interpolating" background Laplacian Δ_s defined on the 4-sphere and $D_l(s)$ represents the degree of degeneracy associated with $\lambda_l(s)$. For the calculation performed in Chapter 5, the relevant expressions when $s = 0$ or 1 are given by

$$\lambda_l(s) = \frac{(l+3)\,l-s}{12}\,\bar{R} - \gamma_0\,\delta_{0,s}\,\bar{R} + \left(\frac{1}{4}-\gamma_1\right)\delta_{1,s}\,\bar{R}\,, \tag{D.3.5a}$$

$$D_l(s) = \frac{(2l+3)\,(l+2)!}{6\,l!}\delta_{0,s} + \frac{l\,(l+3)\,(2l+3)}{2}\delta_{1,s}\,. \tag{D.3.5b}$$

D.4 Anomalous dimensions

Here we report the (non-vanishing) contributions to the anomalous dimensions of the graviton modes and ghost fields. The expressions are presented within the semi-perturbative approximation where all anomalous dimensions contributions on the RHS of the equations are set to zero. We omit the k-dependence for simplicity. For the graviton modes, the gravitational contribution to the anomalous dimension of $\eta_{\rm TT}$ and η_σ yield the following results

$$\begin{aligned}\eta_{\rm TT}\big|_{\rm grav} = \frac{G}{432\pi}\Bigg[&54+\frac{90}{(1+\rho)^4}-\frac{4(53\beta_\rho-69)}{(1+\rho)^3}-\frac{1656-155\beta_\rho+\alpha(290\beta_\rho-3252)}{(1-2\alpha)(1+\rho)^2}\\&+\frac{20(50+2\alpha(87\alpha-95)-\beta_\alpha)}{(1-2\alpha)^2(1+\rho)}+\frac{18}{(1-6\alpha-2\rho)^4}+\frac{8(12\beta_\alpha+4\beta_\rho-3)}{(1-6\alpha-2\rho)^3}\\&+\frac{76(3\beta_\alpha+\beta_\rho)-8\alpha(15+87\beta_\alpha+29\beta_\rho)}{(1-2\alpha)(1-6\alpha-2\rho)^2}-\frac{8(11+2\alpha(87\alpha-47)+5\beta_\alpha)}{(1-2\alpha)^2(1-6\alpha-2\rho)}\Bigg],\end{aligned} \tag{D.4.1a}$$

$$\begin{aligned}\eta_\sigma\big|_{\rm grav} = \frac{G}{432\pi}\Bigg[&-504-\frac{720}{(1+\rho)^4}+\frac{8(291+23\beta_\rho)}{(1+\rho)^3}-\frac{22\alpha(5\beta_\rho-138)-47\beta_\rho+1494}{(1-2\alpha)(1+\rho)^2}\\&+\frac{2\left(660\alpha^2-532\alpha+8\beta_\alpha+113\right)}{(1-2\alpha)^2(1+\rho)}-\frac{144}{(1-6\alpha-2\rho)^4}-\frac{8(42\beta_\alpha+14\beta_\rho-51)}{(1-6\alpha-2\rho)^3}\\&-\frac{4(\alpha(66\beta_\alpha+22\beta_\rho-42)-57\beta_\alpha-19\beta_\rho+9)}{(1-2\alpha)(1-6\alpha-2\rho)^2}-\frac{4(4\alpha(33\alpha-65)-8\beta_\alpha+85)}{(1-2\alpha)^2(1-6\alpha-2\rho)}\Bigg].\end{aligned} \tag{D.4.1b}$$

The ghost anomalous dimension is given by

$$\eta_c = \frac{G}{270\pi}\left[\frac{5(3\beta_\rho-4)}{(1+\rho)^2}+\frac{20}{1+\rho}-\frac{4(7+9\beta_\alpha+3\beta_\rho)}{(1-6\alpha-2\rho)^2}+\frac{148}{1-6\alpha-2\rho}\right]. \tag{D.4.2}$$

D.5 UG and background-field approximation

In the background-field approximation, the unimodular background effective action splits in a transverse diffeomorphism-invariant part and a gauge-fixing part in the form

$$\Gamma_k[\bar g,\varphi,\Psi] = \bar\Gamma_k[g,\Psi]+\hat\Gamma_k[\bar g,\varphi], \tag{D.5.1}$$

with $\hat\Gamma_k[\bar g,\varphi]\approx S_{k,\rm gf}[\bar g,h]+S_{k,\rm gh}[\bar g,\text{ghosts}]$, where $\varphi=(h,\bar C,C,\bar c,c)$ is the fluctuating multiplet comprising the metric fluctuation and the ghosts associated with *TDiff* and U(1) gauge symmetries. The multiplet $\Psi=(\phi,A,\psi)$ collects the matter part. The covariant approach provides a local invariance associated with the use of the background-field method, namely a split transformation of the background metric and the fluctuation field which renders the full metric invariant, i.e.,

$$g_{\mu\nu}(\bar g,h)\ \mapsto\ g_{\mu\nu}(\bar g+\delta_{\rm split}\bar g,h+\delta_{\rm split}h)=g_{\mu\nu}(\bar g,h). \tag{D.5.2}$$

As briefly discussed in Section 2.3, this split transformation is tantamount to guaranteeing background independence (see [95, 101, 124] for a discussion in the context of the FRG approach). For the linear split of the metric, $g_{\mu\nu} = \bar{g}_{\mu\nu} + h_{\mu\nu}$, the split transformation is given by $\delta_{\text{split}}\bar{g}_{\mu\nu} = -\chi_{\mu\nu}$ and $\delta_{\text{split}}h_{\mu\nu} = \chi_{\mu\nu}$, with $\chi_{\mu\nu} = \chi_{\mu\nu}(x)$ being a local transformation parameter. For the non-linear exponential parameterization, more convenient for unimodular gravity, the explicit form of $\delta_{\text{split}}h_{\mu\nu}$ is not straightforward. In this case, we denote $\delta_{\text{split}}h_{\mu\nu} = \mathcal{N}^{\alpha\beta}_{\mu\nu}[\bar{g}, h]\chi_{\alpha\beta}$, and its explicit form can be determined by an iterative procedure (see [141, 142]). In the following, we discuss on the corresponding functional identity associated with the split symmetry.

The invariance of $\bar{\Gamma}_k$ under local split transformations[1], i.e., $\delta_{\text{split}}\bar{\Gamma}_k[g, \Psi] = 0$, leads to the following functional identity written in schematic form:

$$\frac{\delta\bar{\Gamma}_k}{\delta\bar{g}} - \mathcal{N}[\bar{g}, h] \circ \frac{\delta\bar{\Gamma}_k}{\delta h} = 0, \tag{D.5.3}$$

where the $\circ$ notation indicates a space-time integration and a contraction of all indices and it is understood that $h(\bar{g}, g)$. By acting with $(\delta/\delta\bar{g} + \delta/\delta h)$ on (D.5.3) and noting that, at $h = 0$, we have $\mathcal{N}[\bar{g}, 0] = \mathbb{1}$ and $\delta_{\bar{g}}\mathcal{N}[\bar{g}, h]|_{h=0} = 0$, the functional identity (D.5.3) turns into

$$\left.\frac{\delta^2\bar{\Gamma}_k}{\delta\bar{g}^2}\right|_{h=0} - \left.\frac{\delta^2\bar{\Gamma}_k}{\delta h^2}\right|_{h=0} = \left[\frac{\delta\mathcal{N}}{\delta h} \circ \frac{\delta\bar{\Gamma}_k}{\delta\bar{g}}\right]_{h=0}. \tag{D.5.4}$$

By requiring that the background is on-shell, *i.e.*, $\bar{g} = \bar{g}_{\text{EoM}}$, the right-hand side of (D.5.4) vanishes, and the background and the fluctuation two-point correlation functions agree in the exponential parameterization:

$$\left.\frac{\delta^2\bar{\Gamma}_k}{\delta\bar{g}^2}\right|_{h=0} = \left.\frac{\delta^2\bar{\Gamma}_k}{\delta h^2}\right|_{h=0}. \tag{D.5.5}$$

The projection adopted for the anomalous dimensions consists of taking two derivatives w.r.t to quantum fields of the flow equation. Therefore, applying a scale derivative on both sides of (D.5.5) provides an identification of the anomalous dimensions of the graviton modes to be proportional to the background anomalous dimensions. Although the background-field approximation is still useful, Eq. (D.5.3) is not preserved along the flow as it does not correspond to the modified Nielsen identity, mNI = 0, namely, [95, 101, 124, 213, 479],

$$\text{mNI} = \frac{\delta\Gamma_k}{\delta\bar{g}} - \mathcal{N}[\bar{g}, h] \circ \frac{\delta\Gamma_k}{\delta h} - \left\langle\left[\frac{\delta}{\delta\bar{g}} - \mathcal{N}[\bar{g}, h] \circ \frac{\delta}{\delta h}\right]\hat{\Gamma}_k\right\rangle + \Xi_k[\bar{g}, \varphi], \tag{D.5.6}$$

where $\Xi_k[\bar{g}, \varphi]$ is a regulator-dependent contribution. Therefore, for our purposes and for technical reasons, we have chosen to go one step further and also consider a hybrid closure of the system of beta

[1] Actually, the full effective action explicitly breaks the split symmetry since the gauge-fixing and regulator terms are not shift-symmetric. Hence, the Ward identity associated with shift symmetry is actually deformed by those explicit-breaking sources. Nevertheless, ultimately, one is interested in integrating down to $k = 0$ which eliminates the spurious breaking coming from the regulator. As for the gauge-fixing, it arises as a BRST-exact term and, therefore, can be handled in conjunction with the Slavnov-Taylor identity. Since we are working in the background approximation where fluctuations are turned off at the level of the flow equation after the computation of the Hessian, we simply ignore those symmetry-breaking contributions.

functions by improving the background-field approximation with anomalous dimensions computed in an independent way via the vertex expansion employing a flat background metric.

Bibliography

[1] Georges Aad et al. A detailed map of Higgs boson interactions by the ATLAS experiment ten years after the discovery. *Nature*, 607(7917):52–59, 2022. [Erratum: Nature 612, E24 (2022)].

[2] Giulio Maria Pelaggi, Francesco Sannino, Alessandro Strumia, and Elena Vigiani. Naturalness of asymptotically safe Higgs. *Front. in Phys.*, 5:49, 2017.

[3] Georges Aad et al. Observation of a new particle in the search for the Standard Model Higgs boson with the ATLAS detector at the LHC. *Phys. Lett. B*, 716:1–29, 2012.

[4] Serguei Chatrchyan et al. Observation of a New Boson at a Mass of 125 GeV with the CMS Experiment at the LHC. *Phys. Lett. B*, 716:30–61, 2012.

[5] N. Cabibbo, L. Maiani, G. Parisi, and R. Petronzio. Bounds on the Fermions and Higgs Boson Masses in Grand Unified Theories. *Nucl. Phys. B*, 158:295–305, 1979.

[6] Dario Buttazzo, Giuseppe Degrassi, Pier Paolo Giardino, Gian F. Giudice, Filippo Sala, Alberto Salvio, and Alessandro Strumia. Investigating the near-criticality of the Higgs boson. *JHEP*, 12:089, 2013.

[7] J. Silk et al. *Particle Dark Matter: Observations, Models and Searches*. Cambridge Univ. Press, Cambridge, 2010.

[8] Emanuele Berti et al. Testing General Relativity with Present and Future Astrophysical Observations. *Class. Quant. Grav.*, 32:243001, 2015.

[9] Peter J. Mohr, David B. Newell, and Barry N. Taylor. CODATA Recommended Values of the Fundamental Physical Constants: 2014. *Rev. Mod. Phys.*, 88(3):035009, 2016.

[10] James W. York, Jr. Role of conformal three geometry in the dynamics of gravitation. *Phys. Rev. Lett.*, 28:1082–1085, 1972.

[11] G. W. Gibbons and S. W. Hawking. Action Integrals and Partition Functions in Quantum Gravity. *Phys. Rev. D*, 15:2752–2756, 1977.

[12] Reinhold A Bertlmann. *Anomalies in quantum field theory*, volume 91. Oxford university press, 2000.

[13] Robert Percacci. *An Introduction to Covariant Quantum Gravity and Asymptotic Safety*, volume 3 of *100 Years of General Relativity*. World Scientific, 2017.

[14] T. W. B. Kibble. Lorentz invariance and the gravitational field. *J. Math. Phys.*, 2:212–221, 1961.

[15] Dennis W. Sciama. The Physical structure of general relativity. *Rev. Mod. Phys.*, 36:463–469, 1964. [Erratum: Rev.Mod.Phys. 36, 1103–1103 (1964)].

[16] F. W. Hehl, P. Von Der Heyde, G. D. Kerlick, and J. M. Nester. General Relativity with Spin and Torsion: Foundations and Prospects. *Rev. Mod. Phys.*, 48:393–416, 1976.

[17] I. L. Shapiro. Physical aspects of the space-time torsion. *Phys. Rept.*, 357:113, 2002.

[18] Andrzej Trautman. Einstein-Cartan theory. 6 2006.

[19] Milutin Blagojević and Friedrich W. Hehl, editors. *Gauge Theories of Gravitation: A Reader with Commentaries*. World Scientific, Singapore, 2013.

[20] Oleg Melichev and Roberto Percacci. On the renormalization of Poincaré gauge theories. 7 2023.

[21] J.L. Anderson and D. Finkelstein. Cosmological constant and fundamental length. *Am. J. Phys.*, 39:901–904, 1971.

[22] J.J. van der Bij, H. van Dam, and Yee Jack Ng. The Exchange of Massless Spin Two Particles. *Physica A*, 116:307–320, 1982.

[23] W. Buchmuller and N. Dragon. Gauge Fixing and the Cosmological Constant. *Phys. Lett. B*, 223:313–317, 1989.

[24] W. Buchmuller and N. Dragon. Einstein Gravity From Restricted Coordinate Invariance. *Phys. Lett. B*, 207:292–294, 1988.

[25] W.G. Unruh. A Unimodular Theory of Canonical Quantum Gravity. *Phys. Rev. D*, 40:1048, 1989.

[26] M. Henneaux and C. Teitelboim. The Cosmological Constant and General Covariance. *Phys. Lett. B*, 222:195–199, 1989.

[27] William G. Unruh and Robert M. Wald. Time and the Interpretation of Canonical Quantum Gravity. *Phys. Rev. D*, 40:2598, 1989.

[28] George FR Ellis, Henk Van Elst, Jeff Murugan, and Jean-Philippe Uzan. On the trace-free einstein equations as a viable alternative to general relativity. *Classical and Quantum Gravity*, 28(22):225007, 2011.

[29] Steven Weinberg. The Cosmological Constant Problem. *Rev. Mod. Phys.*, 61:1–23, 1989.

[30] R. Percacci. Unimodular quantum gravity and the cosmological constant. *Found. Phys.*, 48(10):1364–1379, 2018.

[31] B. P. Abbott et al. Observation of Gravitational Waves from a Binary Black Hole Merger. *Phys. Rev. Lett.*, 116(6):061102, 2016.

[32] B. P. Abbott et al. GW170817: Observation of Gravitational Waves from a Binary Neutron Star Inspiral. *Phys. Rev. Lett.*, 119(16):161101, 2017.

[33] Kazunori Akiyama et al. First M87 Event Horizon Telescope Results. I. The Shadow of the Supermassive Black Hole. *Astrophys. J. Lett.*, 875:L1, 2019.

[34] Kazunori Akiyama et al. First M87 Event Horizon Telescope Results. II. Array and Instrumentation. *Astrophys. J. Lett.*, 875(1):L2, 2019.

[35] Kazunori Akiyama et al. First M87 Event Horizon Telescope Results. III. Data Processing and Calibration. *Astrophys. J. Lett.*, 875(1):L3, 2019.

[36] Kazunori Akiyama et al. First M87 Event Horizon Telescope Results. IV. Imaging the Central Supermassive Black Hole. *Astrophys. J. Lett.*, 875(1):L4, 2019.

[37] Kazunori Akiyama et al. First M87 Event Horizon Telescope Results. V. Physical Origin of the Asymmetric Ring. *Astrophys. J. Lett.*, 875(1):L5, 2019.

[38] Kazunori Akiyama et al. First M87 Event Horizon Telescope Results. VI. The Shadow and Mass of the Central Black Hole. *Astrophys. J. Lett.*, 875(1):L6, 2019.

[39] Kazunori Akiyama et al. First M87 Event Horizon Telescope Results. VII. Polarization of the Ring. *Astrophys. J. Lett.*, 910(1):L12, 2021.

[40] Kazunori Akiyama et al. First M87 Event Horizon Telescope Results. VIII. Magnetic Field Structure near The Event Horizon. *Astrophys. J. Lett.*, 910(1):L13, 2021.

[41] Kazunori Akiyama et al. First Sagittarius A* Event Horizon Telescope Results. I. The Shadow of the Supermassive Black Hole in the Center of the Milky Way. *Astrophys. J. Lett.*, 930(2):L12, 2022.

[42] Kazunori Akiyama et al. First Sagittarius A* Event Horizon Telescope Results. IV. Variability, Morphology, and Black Hole Mass. *Astrophys. J. Lett.*, 930(2):L15, 2022.

[43] Kazunori Akiyama et al. First Sagittarius A* Event Horizon Telescope Results. V. Testing Astrophysical Models of the Galactic Center Black Hole. *Astrophys. J. Lett.*, 930(2):L16, 2022.

[44] Kazunori Akiyama et al. First Sagittarius A* Event Horizon Telescope Results. VI. Testing the Black Hole Metric. *Astrophys. J. Lett.*, 930(2):L17, 2022.

[45] Tessa Baker et al. Novel Probes Project: Tests of gravity on astrophysical scales. *Rev. Mod. Phys.*, 93(1):015003, 2021.

[46] Stephen Hawking and Roger Penrose. *The nature of space and time*, volume 3. Princeton University Press, 2010.

[47] N. D. Birrell and P. C. W. Davies. *Quantum Fields in Curved Space*. Cambridge Monographs on Mathematical Physics. Cambridge Univ. Press, Cambridge, UK, 2 1984.

[48] Gerard t Hooft and MJG1974AnIHP Veltman. One-loop divergencies in the theory of gravitation. In *Annales de l'IHP Physique théorique*, volume 20, pages 69–94, 1974.

[49] Steven M Christensen and Michael J Duff. Quantizing gravity with a cosmological constant. *Nuclear Physics B*, 170(3):480–506, 1980.

[50] Julian S. Schwinger. On gauge invariance and vacuum polarization. *Phys. Rev.*, 82:664–679, 1951.

[51] Bryce S. DeWitt. Quantum Field Theory in Curved Space-Time. *Phys. Rept.*, 19:295–357, 1975.

[52] Bryce Seligman DeWitt. *The global approach to quantum field theory*, volume 114. Oxford University Press, USA, 2003.

[53] Stanley Deser and P. van Nieuwenhuizen. Nonrenormalizability of the Quantized Dirac-Einstein System. *Phys. Rev. D*, 10:411, 1974.

[54] Stanley Deser, Hung-Sheng Tsao, and P. van Nieuwenhuizen. Nonrenormalizability of Einstein Yang-Mills Interactions at the One Loop Level. *Phys. Lett. B*, 50:491–493, 1974.

[55] S. Deser and P. van Nieuwenhuizen. Nonrenormalizability of the Quantized Einstein-Maxwell System. *Phys. Rev. Lett.*, 32:245–247, 1974.

[56] GW Gibbons and MJ Perry. Quantizing gravitational instantons. *Nuclear Physics B*, 146(1):90–108, 1978.

[57] AO Barvinsky and GA Vilkovisky. The generalized schwinger-dewitt technique in gauge theories and quantum gravity. *Physics Reports*, 119(1):1–74, 1985.

[58] A. O. Barvinsky, A. Yu. Kamenshchik, and I. P. Karmazin. The Renormalization group for nonrenormalizable theories: Einstein gravity with a scalar field. *Phys. Rev. D*, 48:3677–3694, 1993.

[59] Ilya L. Shapiro and Hiroyuki Takata. One loop renormalization of the four-dimensional theory for quantum dilaton gravity. *Phys. Rev. D*, 52:2162–2175, 1995.

[60] Christian F. Steinwachs and Alexander Yu. Kamenshchik. One-loop divergences for gravity non-minimally coupled to a multiplet of scalar fields: calculation in the Jordan frame. I. The main results. *Phys. Rev. D*, 84:024026, 2011.

[61] Marc H. Goroff and Augusto Sagnotti. QUANTUM GRAVITY AT TWO LOOPS. *Phys. Lett. B*, 160:81–86, 1985.

[62] Marc H Goroff and Augusto Sagnotti. The ultraviolet behavior of einstein gravity. *Nuclear Physics B*, 266(3-4):709–736, 1986.

[63] AO Barvinsky and GA Vilkovisky. The effective action in quantum field theory: two-loop approximation. In *Quantum field theory and quantum statistics: essays in honour of the sixtieth birthday of ES Fradkin. V. 1.* 1987.

[64] Anton EM van de Ven. Two-loop quantum gravity. *Nuclear Physics B*, 378(1-2):309–366, 1992.

[65] Zvi Bern, Clifford Cheung, Huan-Hang Chi, Scott Davies, Lance Dixon, and Josh Nohle. Evanescent Effects Can Alter Ultraviolet Divergences in Quantum Gravity without Physical Consequences. *Phys. Rev. Lett.*, 115(21):211301, 2015.

[66] Steven Weinberg. *The Quantum theory of fields. Vol. 1: Foundations.* Cambridge University Press, 6 2005.

[67] N. E. J Bjerrum-Bohr, John F. Donoghue, and Barry R. Holstein. Quantum gravitational corrections to the nonrelativistic scattering potential of two masses. *Phys. Rev. D*, 67:084033, 2003. [Erratum: Phys.Rev.D 71, 069903 (2005)].

[68] Claus Kiefer. *Quantum gravity*, volume 124. Clarendon, Oxford, 2004.

[69] K. S. Stelle. Renormalization of Higher Derivative Quantum Gravity. *Phys. Rev. D*, 16:953–969, 1977.

[70] J. Julve and M. Tonin. Quantum Gravity with Higher Derivative Terms. *Nuovo Cim. B*, 46:137–152, 1978.

[71] ES Fradkin and Arkady A Tseytlin. Renormalizable asymtotically free quantum theory of gravity. *Physics Letters B*, 104(5):377–381, 1981.

[72] IG Avramidy and AO Barvinsky. Asymptotic freedom in higher-derivative quantum gravity. *Physics Letters B*, 159(4-6):269–274, 1985.

[73] M. Ostrogradsky. Mémoires sur les équations différentielles, relatives au problème des isopérimètres. *Mem. Acad. St. Petersbourg*, 6(4):385–517, 1850.

[74] Richard P. Woodard. Ostrogradsky's theorem on Hamiltonian instability. *Scholarpedia*, 10(8):32243, 2015.

[75] Aaron Held and Hyun Lim. Nonlinear evolution of quadratic gravity in 3+1 dimensions. *Phys. Rev. D*, 108(10):104025, 2023.

[76] K. S. Stelle. Classical Gravity with Higher Derivatives. *Gen. Rel. Grav.*, 9:353–371, 1978.

[77] Ignatios Antoniadis and ET Tomboulis. Gauge invariance and unitarity in higher-derivative quantum gravity. *Physical Review D*, 33(10):2756, 1986.

[78] John F. Donoghue and Gabriel Menezes. Gauge Assisted Quadratic Gravity: A Framework for UV Complete Quantum Gravity. *Phys. Rev. D*, 97(12):126005, 2018.

[79] John F. Donoghue and Gabriel Menezes. Massive poles in Lee-Wick quantum field theory. *Phys. Rev. D*, 99(6):065017, 2019.

[80] John F. Donoghue and Gabriel Menezes. Arrow of Causality and Quantum Gravity. *Phys. Rev. Lett.*, 123(17):171601, 2019.

[81] John F. Donoghue and Gabriel Menezes. Unitarity, stability and loops of unstable ghosts. *Phys. Rev. D*, 100(10):105006, 2019.

[82] Damiano Anselmi. Fakeons, Microcausality And The Classical Limit Of Quantum Gravity. *Class. Quant. Grav.*, 36:065010, 2019.

[83] Damiano Anselmi. Fakeons And Lee-Wick Models. *JHEP*, 02:141, 2018.

[84] Damiano Anselmi and Marco Piva. Quantum Gravity, Fakeons And Microcausality. *JHEP*, 11:021, 2018.

[85] Damiano Anselmi. Fakeons and the classicization of quantum gravity: the FLRW metric. *JHEP*, 04:061, 2019.

[86] Alberto Salvio. Quadratic Gravity. *Front. in Phys.*, 6:77, 2018.

[87] Leonardo Modesto and Ilya L. Shapiro. Superrenormalizable quantum gravity with complex ghosts. *Phys. Lett. B*, 755:279–284, 2016.

[88] Bob Holdom and Jing Ren. QCD analogy for quantum gravity. *Phys. Rev. D*, 93(12):124030, 2016.

[89] Bob Holdom and Jing Ren. Quadratic gravity: from weak to strong. *Int. J. Mod. Phys. D*, 25(12):1643004, 2016.

[90] Bob Holdom. A ghost and a naked singularity; facing our demons. In *Scale invariance in particle physics and cosmology*, 5 2019.

[91] John F. Donoghue. Is the spin connection confined or condensed? *Phys. Rev. D*, 96(4):044003, 2017.

[92] Gustavo P. de Brito. Quadratic gravity in analogy to quantum chromodynamics: Light fermions in its landscape. 9 2023.

[93] Damiano Anselmi. Absence of higher derivatives in the renormalization of propagators in quantum field theories with infinitely many couplings. *Class. Quant. Grav.*, 20:2355–2378, 2003.

[94] C. Wetterich. Quantum scale symmetry. 1 2019.

[95] Alfio Bonanno, Astrid Eichhorn, Holger Gies, Jan M. Pawlowski, Roberto Percacci, Martin Reuter, Frank Saueressig, and Gian Paolo Vacca. Critical reflections on asymptotically safe gravity. *Front. in Phys.*, 8:269, 2020.

[96] Steven Weinberg. Ultraviolet divergences in quantum theories of gravitation. In *General relativity.* 1979.

[97] J. Beringer et al. Review of Particle Physics (RPP). *Phys. Rev. D*, 86:010001, 2012.

[98] Gustavo P. de Brito and Astrid Eichhorn. Nonvanishing gravitational contribution to matter beta functions for vanishing dimensionful regulators. *Eur. Phys. J. C*, 83(2):161, 2023.

[99] Daniel F. Litim and Francesco Sannino. Asymptotic safety guaranteed. *JHEP*, 12:178, 2014.

[100] Daniel F. Litim, Matin Mojaza, and Francesco Sannino. Vacuum stability of asymptotically safe gauge-Yukawa theories. *JHEP*, 01:081, 2016.

[101] Astrid Eichhorn. An asymptotically safe guide to quantum gravity and matter. *Front. Astron. Space Sci.*, 5:47, 2019.

[102] Michael E Peskin. Critical point behavior of the wilson loop. *Physics Letters B*, 94(2):161–165, 1980.

[103] R Gastmans, R Kallosh, and C Truffin. Quantum gravity near two dimensions.[one-loop approximation, background functional method]. *Nucl. Phys., B;(Netherlands)*, 133(3), 1978.

[104] SM Christensen and Michael J Duff. Quantum gravity in 2+ ε dimensions. *Physics Letters B*, 79(3):213–216, 1978.

[105] M. Reuter. Nonperturbative evolution equation for quantum gravity. *Phys. Rev. D*, 57:971–985, 1998.

[106] J. Ambjorn, A. Goerlich, J. Jurkiewicz, and R. Loll. Nonperturbative Quantum Gravity. *Phys. Rept.*, 519:127–210, 2012.

[107] R. Loll. Quantum Gravity from Causal Dynamical Triangulations: A Review. *Class. Quant. Grav.*, 37(1):013002, 2020.

[108] J. Ambjorn, L. Glaser, A. Goerlich, and J. Jurkiewicz. Euclidian 4d quantum gravity with a non-trivial measure term. *JHEP*, 10:100, 2013.

[109] Daniel Coumbe and John Laiho. Exploring Euclidean Dynamical Triangulations with a Non-trivial Measure Term. *JHEP*, 04:028, 2015.

[110] Tobias Rindlisbacher and Philippe de Forcrand. Euclidean Dynamical Triangulation revisited: is the phase transition really 1st order? (extended version). *JHEP*, 05:138, 2015.

[111] Scott Bassler, Jack Laiho, Marc Schiffer, and Judah Unmuth-Yockey. The de Sitter Instanton from Euclidean Dynamical Triangulations. *Phys. Rev. D*, 103:114504, 2021.

[112] Muhammad Asaduzzaman and Simon Catterall. Euclidean dynamical triangulations revisited. *Phys. Rev. D*, 107(7):074505, 2023.

[113] Herbert W. Hamber. Scaling Exponents for Lattice Quantum Gravity in Four Dimensions. *Phys. Rev. D*, 92(6):064017, 2015.

[114] Simon Catterall, Jack Laiho, and Judah Unmuth-Yockey. Kähler-Dirac fermions on Euclidean dynamical triangulations. *Phys. Rev. D*, 98(11):114503, 2018.

[115] Mingwei Dai, Jack Laiho, Marc Schiffer, and Judah Unmuth-Yockey. Newtonian binding from lattice quantum gravity. *Phys. Rev. D*, 103(11):114511, 2021.

[116] Herbert W. Hamber and Lu Heng Sunny Yu. Dyson's Equations for Quantum Gravity in the Hartree-Fock Approximation. 10 2020.

[117] Jan Horak, Jan M. Pawlowski, and Nicolas Wink. Spectral functions in the ϕ^4-theory from the spectral DSE. *Phys. Rev. D*, 102:125016, 2020.

[118] Jannik Fehre, Daniel F. Litim, Jan M. Pawlowski, and Manuel Reichert. Lorentzian Quantum Gravity and the Graviton Spectral Function. *Phys. Rev. Lett.*, 130(8):081501, 2023.

[119] Jens Braun et al. Renormalised spectral flows. *SciPost Phys. Core*, 6:061, 2023.

[120] Rudrajit Banerjee and Max Niedermaier. The spatial Functional Renormalization Group and Hadamard states on cosmological spacetimes. *Nucl. Phys. B*, 980:115814, 2022.

[121] Edoardo D'Angelo, Nicolò Drago, Nicola Pinamonti, and Kasia Rejzner. Wetterich equation on Lorentzian manifolds. 2 2022.

[122] Edoardo D'Angelo and Kasia Rejzner. Lorentzian Wetterich equation for gauge theories. 3 2023.

[123] Edoardo D'Angelo. Asymptotic Safety in Lorentzian quantum gravity. 10 2023.

[124] Jan M. Pawlowski and Manuel Reichert. Quantum Gravity: A Fluctuating Point of View. *Front. in Phys.*, 8:551848, 2021.

[125] Olivier Piguet and Silvio P Sorella. *Algebraic renormalization: Perturbative renormalization, symmetries and anomalies*, volume 28. Springer Science & Business Media, 1995.

[126] Carlo Becchi, Alain Rouet, and Raymond Stora. The abelian higgs kibble model, unitarity of the s-operator. *Physics Letters B*, 52(3):344–346, 1974.

[127] I. V. Tyutin. Gauge Invariance in Field Theory and Statistical Physics in Operator Formalism. 1975.

[128] L. F. Abbott. Introduction to the Background Field Method. *Acta Phys. Polon. B*, 13:33, 1982.

[129] Benjamin Knorr, Alessia Platania, and Marc Schiffer. Configuration space for quantum gravity in a locally regularized path integral. *Phys. Rev. D*, 106(12):126002, 2022.

[130] Kevin Falls. Background independent exact renormalisation. *Eur. Phys. J. C*, 81(2):121, 2021.

[131] M. Yu Kalmykov. Gauge and parametrization dependencies of the one loop counterterms in the Einstein gravity. *Class. Quant. Grav.*, 12:1401–1412, 1995.

[132] M. Yu. Kalmykov, K. A. Kazakov, P. I. Pronin, and K. V. Stepanyantz. Detailed analysis of the dependence of the one loop counterterms on the gauge and parametrization in the Einstein gravity with the cosmological constant. *Class. Quant. Grav.*, 15:3777–3794, 1998.

[133] N. Ohta, R. Percacci, and A. D. Pereira. Gauges and functional measures in quantum gravity I: Einstein theory. *JHEP*, 06:115, 2016.

[134] N. Ohta, R. Percacci, and A. D. Pereira. Gauges and functional measures in quantum gravity II: Higher derivative gravity. *Eur. Phys. J. C*, 77(9):611, 2017.

[135] Jeferson D. Gonçalves, Tibério de Paula Netto, and Ilya L. Shapiro. Gauge and parametrization ambiguity in quantum gravity. *Phys. Rev. D*, 97(2):026015, 2018.

[136] N. Ohta, R. Percacci, and A. D. Pereira. $f(R, R^2_{\mu\nu})$ at one loop. *Phys. Rev. D*, 97(10):104039, 2018.

[137] Andreas Nink. Field Parametrization Dependence in Asymptotically Safe Quantum Gravity. *Phys. Rev. D*, 91(4):044030, 2015.

[138] Holger Gies, Benjamin Knorr, and Stefan Lippoldt. Generalized Parametrization Dependence in Quantum Gravity. *Phys. Rev. D*, 92(8):084020, 2015.

[139] Kevin Falls. Renormalization of Newton's constant. *Phys. Rev. D*, 92(12):124057, 2015.

[140] Gustavo P. De Brito, Nobuyoshi Ohta, Antonio D. Pereira, Anderson A. Tomaz, and Masatoshi Yamada. Asymptotic safety and field parametrization dependence in the $f(R)$ truncation. *Phys. Rev. D*, 98(2):026027, 2018.

[141] Astrid Eichhorn, Stefan Lippoldt, and Vedran Skrinjar. Nonminimal hints for asymptotic safety. *Phys. Rev. D*, 97(2):026002, 2018.

[142] Gustavo P. de Brito and Antonio D. Pereira. Unimodular quantum gravity: Steps beyond perturbation theory. *JHEP*, 09:196, 2020.

[143] Frank Saueressig. *The Functional Renormalization Group in Quantum Gravity*. Springer, 2023.

[144] Christof Wetterich. Exact evolution equation for the effective potential. *Phys. Lett. B*, 301:90–94, 1993.

[145] Ulrich Ellwanger. Flow equations for N point functions and bound states. *Z. Phys. C*, 62:503–510, 1994.

[146] Tim R. Morris. The Exact renormalization group and approximate solutions. *Int. J. Mod. Phys. A*, 9:2411–2450, 1994.

[147] Elisa Manrique and Martin Reuter. Bare versus Effective Fixed Point Action in Asymptotic Safety: The Reconstruction Problem. *PoS*, CLAQG08:001, 2011.

[148] Tim R. Morris and Zoë H. Slade. Solutions to the reconstruction problem in asymptotic safety. *JHEP*, 11:094, 2015.

[149] Mathijs Fraaije, Alessia Platania, and Frank Saueressig. On the reconstruction problem in quantum gravity. *Phys. Lett. B*, 834:137399, 2022.

[150] N. Dupuis, L. Canet, A. Eichhorn, W. Metzner, J. M. Pawlowski, M. Tissier, and N. Wschebor. The nonperturbative functional renormalization group and its applications. *Phys. Rept.*, 910:1–114, 2021.

[151] Benjamin Knorr, Chris Ripken, and Frank Saueressig. Form Factors in Asymptotic Safety: conceptual ideas and computational toolbox. *Class. Quant. Grav.*, 36(23):234001, 2019.

[152] Benjamin Knorr. The derivative expansion in asymptotically safe quantum gravity: general setup and quartic order. *SciPost Phys. Core*, 4:020, 2021.

[153] Diego Buccio, John F. Donoghue, and Roberto Percacci. Amplitudes and Renormalization Group Techniques: A Case Study. 6 2023.

[154] John F. Donoghue. A Critique of the Asymptotic Safety Program. *Front. in Phys.*, 8:56, 2020.

[155] John F. Donoghue and Gabriel Menezes. Higher Derivative Sigma Models. 8 2023.

[156] T. Papenbrock and C. Wetterich. Two loop results from one loop computations and nonperturbative solutions of exact evolution equations. *Z. Phys. C*, 65:519–535, 1995.

[157] M. Reuter and C. Wetterich. Gluon condensation in nonperturbative flow equations. *Phys. Rev. D*, 56:7893–7916, 1997.

[158] M. Pernici and M. Raciti. Wilsonian flow and mass independent renormalization. *Nucl. Phys. B*, 531:560–592, 1998.

[159] Peter Kopietz. Two loop beta function from the exact renormalization group. *Nucl. Phys. B*, 595:493–518, 2001.

[160] Jan M. Pawlowski. On Wilsonian flows in gauge theories. *Int. J. Mod. Phys. A*, 16:2105–2110, 2001.

[161] Holger Gies. Running coupling in Yang-Mills theory: A flow equation study. *Phys. Rev. D*, 66:025006, 2002.

[162] Tim R. Morris and Oliver J. Rosten. A Manifestly gauge invariant, continuum calculation of the SU(N) Yang-Mills two-loop beta function. *Phys. Rev. D*, 73:065003, 2006.

[163] S. P. Klevansky. The Nambu-Jona-Lasinio model of quantum chromodynamics. *Rev. Mod. Phys.*, 64:649–708, 1992.

[164] Joerg Jaeckel. Effective actions for strongly interacting fermionic systems. Other thesis, 9 2003.

[165] Joerg Jaeckel and Christof Wetterich. Flow equations without mean field ambiguity. *Phys. Rev. D*, 68:025020, 2003.

[166] Wei-jie Fu. QCD at finite temperature and density within the fRG approach: an overview. *Commun. Theor. Phys.*, 74(9):097304, 2022.

[167] Jens Braun. Fermion Interactions and Universal Behavior in Strongly Interacting Theories. *J. Phys. G*, 39:033001, 2012.

[168] Tomohiro Inagaki, Taizo Muta, and Sergei D. Odintsov. Dynamical symmetry breaking in curved space-time: Four fermion interactions. *Prog. Theor. Phys. Suppl.*, 127:93, 1997.

[169] Holger Gies and Christof Wetterich. Renormalization flow of bound states. *Phys. Rev. D*, 65:065001, 2002.

[170] Wataru Souma. Nontrivial ultraviolet fixed point in quantum gravity. *Prog. Theor. Phys.*, 102:181–195, 1999.

[171] M. Reuter and Frank Saueressig. Renormalization group flow of quantum gravity in the Einstein-Hilbert truncation. *Phys. Rev. D*, 65:065016, 2002.

[172] O. Lauscher and M. Reuter. Ultraviolet fixed point and generalized flow equation of quantum gravity. *Phys. Rev. D*, 65:025013, 2002.

[173] Dario Benedetti, Pedro F. Machado, and Frank Saueressig. Four-derivative interactions in asymptotically safe gravity. *AIP Conf. Proc.*, 1196(1):44, 2009.

[174] Kevin Falls, Nobuyoshi Ohta, and Roberto Percacci. Towards the determination of the dimension of the critical surface in asymptotically safe gravity. *Phys. Lett. B*, 810:135773, 2020.

[175] Guilherme de Berredo-Peixoto and Ilya L. Shapiro. Conformal quantum gravity with the Gauss-Bonnet term. *Phys. Rev. D*, 70:044024, 2004.

[176] Guilherme de Berredo-Peixoto and Ilya L. Shapiro. Higher derivative quantum gravity with Gauss-Bonnet term. *Phys. Rev. D*, 71:064005, 2005.

[177] Giulia Gubitosi, Robin Ooijer, Chris Ripken, and Frank Saueressig. Consistent early and late time cosmology from the RG flow of gravity. *JCAP*, 12:004, 2018.

[178] Alessandro Codello, Roberto Percacci, and Christoph Rahmede. Ultraviolet properties of f(R)-gravity. *Int. J. Mod. Phys. A*, 23:143–150, 2008.

[179] Pedro F. Machado and Frank Saueressig. On the renormalization group flow of f(R)-gravity. *Phys. Rev. D*, 77:124045, 2008.

[180] Alessandro Codello, Roberto Percacci, and Christoph Rahmede. Investigating the Ultraviolet Properties of Gravity with a Wilsonian Renormalization Group Equation. *Annals Phys.*, 324:414–469, 2009.

[181] K. Falls, D. F. Litim, K. Nikolakopoulos, and C. Rahmede. A bootstrap towards asymptotic safety, 1 2013.

[182] Kevin Falls, Daniel F. Litim, Konstantinos Nikolakopoulos, and Christoph Rahmede. Further evidence for asymptotic safety of quantum gravity. *Phys. Rev. D*, 93(10):104022, 2016.

[183] Kevin G. Falls, Daniel F. Litim, and Jan Schröder. Aspects of asymptotic safety for quantum gravity. *Phys. Rev. D*, 99(12):126015, 2019.

[184] Yannick Kluth and Daniel F. Litim. Fixed points of quantum gravity and the dimensionality of the UV critical surface. *Phys. Rev. D*, 108(2):026005, 2023.

[185] Yannick Kluth and Daniel F. Litim. Functional renormalization for f(R$\mu\nu\rho\sigma$) quantum gravity. *Phys. Rev. D*, 106(10):106022, 2022.

[186] Holger Gies, Benjamin Knorr, Stefan Lippoldt, and Frank Saueressig. Gravitational Two-Loop Counterterm Is Asymptotically Safe. *Phys. Rev. Lett.*, 116(21):211302, 2016.

[187] Astrid Eichhorn. Status update: Asymptotically safe gravity-matter systems. *Nuovo Cim. C*, 45(2):29, 2022.

[188] Astrid Eichhorn and Marc Schiffer. Asymptotic safety of gravity with matter, 12 2022.

[189] Astrid Eichhorn. The microscopic structure of quantum space-time and matter from a renormalization group perspective. *Nature Phys.*, 19(11):1527–1529, 2023.

[190] Pietro Donà, Astrid Eichhorn, and Roberto Percacci. Matter matters in asymptotically safe quantum gravity. *Phys. Rev. D*, 89(8):084035, 2014.

[191] Jan Meibohm, Jan M. Pawlowski, and Manuel Reichert. Asymptotic safety of gravity-matter systems. *Phys. Rev. D*, 93(8):084035, 2016.

[192] Jorn Biemans, Alessia Platania, and Frank Saueressig. Renormalization group fixed points of foliated gravity-matter systems. *JHEP*, 05:093, 2017.

[193] Nicolai Christiansen, Daniel F. Litim, Jan M. Pawlowski, and Manuel Reichert. Asymptotic safety of gravity with matter. *Phys. Rev. D*, 97(10):106012, 2018.

[194] Natália Alkofer and Frank Saueressig. Asymptotically safe $f(R)$-gravity coupled to matter I: the polynomial case. *Annals Phys.*, 396:173–201, 2018.

[195] Astrid Eichhorn, Stefan Lippoldt, Jan M. Pawlowski, Manuel Reichert, and Marc Schiffer. How perturbative is quantum gravity? *Phys. Lett. B*, 792:310–314, 2019.

[196] Christof Wetterich and Masatoshi Yamada. Variable Planck mass from the gauge invariant flow equation. *Phys. Rev. D*, 100(6):066017, 2019.

[197] Gustavo P. de Brito, Antonio D. Pereira, and Arthur F. Vieira. Exploring new corners of asymptotically safe unimodular quantum gravity. *Phys. Rev. D*, 103(10):104023, 2021.

[198] Mikhail Shaposhnikov and Christof Wetterich. Asymptotic safety of gravity and the Higgs boson mass. *Phys. Lett. B*, 683:196–200, 2010.

[199] U. Harst and M. Reuter. QED coupled to QEG. *JHEP*, 05:119, 2011.

[200] Astrid Eichhorn and Aaron Held. Viability of quantum-gravity induced ultraviolet completions for matter. *Phys. Rev. D*, 96(8):086025, 2017.

[201] Nicolai Christiansen and Astrid Eichhorn. An asymptotically safe solution to the U(1) triviality problem. *Phys. Lett. B*, 770:154–160, 2017.

[202] Astrid Eichhorn and Aaron Held. Top mass from asymptotic safety. *Phys. Lett. B*, 777:217–221, 2018.

[203] Astrid Eichhorn and Fleur Versteegen. Upper bound on the Abelian gauge coupling from asymptotic safety. *JHEP*, 01:030, 2018.

[204] Astrid Eichhorn and Aaron Held. Mass difference for charged quarks from asymptotically safe quantum gravity. *Phys. Rev. Lett.*, 121(15):151302, 2018.

[205] Gustavo P. De Brito, Astrid Eichhorn, and Antonio D. Pereira. A link that matters: Towards phenomenological tests of unimodular asymptotic safety. *JHEP*, 09:100, 2019.

[206] Reinhard Alkofer, Astrid Eichhorn, Aaron Held, Carlos M. Nieto, Roberto Percacci, and Markus Schröfl. Quark masses and mixings in minimally parameterized UV completions of the Standard Model. *Annals Phys.*, 421:168282, 2020.

[207] Álvaro Pastor-Gutiérrez, Jan M. Pawlowski, and Manuel Reichert. The Asymptotically Safe Standard Model: From quantum gravity to dynamical chiral symmetry breaking. *SciPost Phys.*, 15(3):105, 2023.

[208] Gaurav Narain and Roberto Percacci. Renormalization Group Flow in Scalar-Tensor Theories. I. *Class. Quant. Grav.*, 27:075001, 2010.

[209] Kin-ya Oda and Masatoshi Yamada. Non-minimal coupling in Higgs–Yukawa model with asymptotically safe gravity. *Class. Quant. Grav.*, 33(12):125011, 2016.

[210] Roberto Percacci and Gian Paolo Vacca. Search of scaling solutions in scalar-tensor gravity. *Eur. Phys. J. C*, 75(5):188, 2015.

[211] Peter Labus, Roberto Percacci, and Gian Paolo Vacca. Asymptotic safety in $O(N)$ scalar models coupled to gravity. *Phys. Lett. B*, 753:274–281, 2016.

[212] Pietro Donà, Astrid Eichhorn, Peter Labus, and Roberto Percacci. Asymptotic safety in an interacting system of gravity and scalar matter. *Phys. Rev. D*, 93(4):044049, 2016. [Erratum: Phys.Rev.D 93, 129904 (2016)].

[213] Astrid Eichhorn, Peter Labus, Jan M. Pawlowski, and Manuel Reichert. Effective universality in quantum gravity. *SciPost Phys.*, 5(4):031, 2018.

[214] Passant Ali, Astrid Eichhorn, Martin Pauly, and Michael M. Scherer. Constraints on discrete global symmetries in quantum gravity. *JHEP*, 05:036, 2021.

[215] Gustavo P. de Brito, Astrid Eichhorn, and Rafael Robson Lino dos Santos. The weak-gravity bound and the need for spin in asymptotically safe matter-gravity models. *JHEP*, 11:110, 2021.

[216] Cristobal Laporte, Antonio D. Pereira, Frank Saueressig, and Jian Wang. Scalar-tensor theories within Asymptotic Safety. *JHEP*, 12:001, 2021.

[217] Astrid Eichhorn, Rafael R. Lino dos Santos, and Fabian Wagner. Shift-symmetric Horndeski gravity in the asymptotic-safety paradigm. *JCAP*, 02:052, 2023.

[218] Gustavo P. de Brito, Benjamin Knorr, and Marc Schiffer. On the weak-gravity bound for a shift-symmetric scalar field. *Phys. Rev. D*, 108(2):026004, 2023.

[219] Astrid Eichhorn and Holger Gies. Light fermions in quantum gravity. *New J. Phys.*, 13:125012, 2011.

[220] Pietro Dona and Roberto Percacci. Functional renormalization with fermions and tetrads. *Phys. Rev. D*, 87(4):045002, 2013.

[221] Jan Meibohm and Jan M. Pawlowski. Chiral fermions in asymptotically safe quantum gravity. *Eur. Phys. J. C*, 76(5):285, 2016.

[222] Astrid Eichhorn and Stefan Lippoldt. Quantum gravity and Standard-Model-like fermions. *Phys. Lett. B*, 767:142–146, 2017.

[223] Astrid Eichhorn, Stefan Lippoldt, and Marc Schiffer. Zooming in on fermions and quantum gravity. *Phys. Rev. D*, 99(8):086002, 2019.

[224] Gustavo P. De Brito, Yuta Hamada, Antonio D. Pereira, and Masatoshi Yamada. On the impact of Majorana masses in gravity-matter systems. *JHEP*, 08:142, 2019.

[225] Jesse Daas, Wouter Oosters, Frank Saueressig, and Jian Wang. Asymptotically safe gravity with fermions. *Phys. Lett. B*, 809:135775, 2020.

[226] Jesse Daas, Wouter Oosters, Frank Saueressig, and Jian Wang. Asymptotically Safe Gravity-Fermion Systems on Curved Backgrounds. *Universe*, 7(8):306, 2021.

[227] Sarah Folkerts, Daniel F. Litim, and Jan M. Pawlowski. Asymptotic freedom of Yang-Mills theory with gravity. *Phys. Lett. B*, 709:234–241, 2012.

[228] Astrid Eichhorn and Marc Schiffer. $d = 4$ as the critical dimensionality of asymptotically safe interactions. *Phys. Lett. B*, 793:383–389, 2019.

[229] Astrid Eichhorn, Jan Henryk Kwapisz, and Marc Schiffer. Weak-gravity bound in asymptotically safe gravity-gauge systems. *Phys. Rev. D*, 105(10):106022, 2022.

[230] Astrid Eichhorn, Yuta Hamada, Johannes Lumma, and Masatoshi Yamada. Quantum gravity fluctuations flatten the Planck-scale Higgs potential. *Phys. Rev. D*, 97(8):086004, 2018.

[231] Astrid Eichhorn, Alessia Platania, and Marc Schiffer. Lorentz invariance violations in the interplay of quantum gravity with matter. *Phys. Rev. D*, 102(2):026007, 2020.

[232] Manuel Reichert and Juri Smirnov. Dark Matter meets Quantum Gravity. *Phys. Rev. D*, 101(6):063015, 2020.

[233] Astrid Eichhorn and Martin Pauly. Constraining power of asymptotic safety for scalar fields. *Phys. Rev. D*, 103(2):026006, 2021.

[234] Yu Hamada, Koji Tsumura, and Masatoshi Yamada. Scalegenesis and fermionic dark matters in the flatland scenario. *Eur. Phys. J. C*, 80(5):368, 2020.

[235] Astrid Eichhorn and Martin Pauly. Safety in darkness: Higgs portal to simple Yukawa systems. *Phys. Lett. B*, 819:136455, 2021.

[236] Kamila Kowalska, Enrico Maria Sessolo, and Yasuhiro Yamamoto. Flavor anomalies from asymptotically safe gravity. *Eur. Phys. J. C*, 81(4):272, 2021.

[237] Kamila Kowalska and Enrico Maria Sessolo. Minimal models for g-2 and dark matter confront asymptotic safety. *Phys. Rev. D*, 103(11):115032, 2021.

[238] Astrid Eichhorn, Martin Pauly, and Shouryya Ray. Towards a Higgs mass determination in asymptotically safe gravity with a dark portal. *JHEP*, 10:100, 2021.

[239] Gustavo P. de Brito, Astrid Eichhorn, and Rafael R. Lino dos Santos. Are there ALPs in the asymptotically safe landscape? *JHEP*, 06:013, 2022.

[240] Kamila Kowalska, Soumita Pramanick, and Enrico Maria Sessolo. Naturally small Yukawa couplings from trans-Planckian asymptotic safety. *JHEP*, 08:262, 2022.

[241] Astrid Eichhorn and Aaron Held. Dynamically vanishing Dirac neutrino mass from quantum scale symmetry. *Phys. Lett. B*, 846:138196, 2023.

[242] Jens Boos, Christopher D. Carone, Noah L. Donald, and Mikkie R. Musser. Asymptotic safety and gauged baryon number. *Phys. Rev. D*, 106(3):035015, 2022.

[243] Jens Boos, Christopher D. Carone, Noah L. Donald, and Mikkie R. Musser. Asymptotically safe dark matter with gauged baryon number. *Phys. Rev. D*, 107(3):035018, 2023.

[244] Abhishek Chikkaballi, Wojciech Kotlarski, Kamila Kowalska, Daniele Rizzo, and Enrico Maria Sessolo. Constraints on Z' solutions to the flavor anomalies with trans-Planckian asymptotic safety. *JHEP*, 01:164, 2023.

[245] Abhishek Chikkaballi, Kamila Kowalska, and Enrico Maria Sessolo. Naturally small neutrino mass with asymptotic safety and gravitational-wave signatures, 8 2023.

[246] Wojciech Kotlarski, Kamila Kowalska, Daniele Rizzo, and Enrico Maria Sessolo. How robust are particle physics predictions in asymptotic safety? *Eur. Phys. J. C*, 83(7):644, 2023.

[247] Astrid Eichhorn, Rafael R. Lino dos Santos, and João Lucas Miqueleto. From quantum gravity to gravitational waves through cosmic strings, 6 2023.

[248] Donald Marolf, Ian A. Morrison, and Mark Srednicki. Perturbative S-matrix for massive scalar fields in global de Sitter space. *Class. Quant. Grav.*, 30:155023, 2013.

[249] Adrian David, Nico Fischer, and Yasha Neiman. Spinor-helicity variables for cosmological horizons in de Sitter space. *Phys. Rev. D*, 100(4):045005, 2019.

[250] Alessia Platania and Christof Wetterich. Non-perturbative unitarity and fictitious ghosts in quantum gravity. *Phys. Lett. B*, 811:135911, 2020.

[251] Alessia Platania. Causality, unitarity and stability in quantum gravity: a non-perturbative perspective. *JHEP*, 09:167, 2022.

[252] Astrid Eichhorn. Steps towards Lorentzian quantum gravity with causal sets. *J. Phys. Conf. Ser.*, 1275(1):012010, 2019.

[253] Elisa Manrique, Stefan Rechenberger, and Frank Saueressig. Asymptotically Safe Lorentzian Gravity. *Phys. Rev. Lett.*, 106:251302, 2011.

[254] Stefan Rechenberger and Frank Saueressig. A functional renormalization group equation for foliated spacetimes. *JHEP*, 03:010, 2013.

[255] Jorn Biemans, Alessia Platania, and Frank Saueressig. Quantum gravity on foliated spacetimes: Asymptotically safe and sound. *Phys. Rev. D*, 95(8):086013, 2017.

[256] Frank Saueressig and Jian Wang. Foliated asymptotically safe gravity in the fluctuation approach. *JHEP*, 09:064, 2023.

[257] Adriano Contillo, Stefan Rechenberger, and Frank Saueressig. Renormalization group flow of Hořava-Lifshitz gravity at low energies. *JHEP*, 12:017, 2013.

[258] W. B. Houthoff, A. Kurov, and F. Saueressig. Impact of topology in foliated Quantum Einstein Gravity. *Eur. Phys. J. C*, 77:491, 2017.

[259] Benjamin Knorr. Lorentz symmetry is relevant. *Phys. Lett. B*, 792:142–148, 2019.

[260] S. Nagy, K. Sailer, and I. Steib. Renormalization of Lorentzian conformally reduced gravity. *Class. Quant. Grav.*, 36(15):155004, 2019.

[261] Jodi Cooley et al. Report of the Topical Group on Particle Dark Matter for Snowmass 2021, 9 2022.

[262] A. Arbey and F. Mahmoudi. Dark matter and the early Universe: a review. *Prog. Part. Nucl. Phys.*, 119:103865, 2021.

[263] Antonio Boveia et al. Snowmass 2021 Cross Frontier Report: Dark Matter Complementarity (Extended Version), 10 2022.

[264] D. S. Akerib et al. Snowmass2021 Cosmic Frontier Dark Matter Direct Detection to the Neutrino Fog. In *Snowmass 2021*, 3 2022.

[265] Rouven Essig et al. Snowmass2021 Cosmic Frontier: The landscape of low-threshold dark matter direct detection in the next decade. In *Snowmass 2021*, 3 2022.

[266] Daniel Carney et al. Snowmass2021 Cosmic Frontier White Paper: Ultraheavy particle dark matter, 3 2022.

[267] Daniel Baxter et al. Snowmass2021 Cosmic Frontier White Paper: Calibrations and backgrounds for dark matter direct detection, 3 2022.

[268] Tsuguo Aramaki et al. Snowmass2021 Cosmic Frontier: The landscape of cosmic-ray and high-energy photon probes of particle dark matter, 3 2022.

[269] Shin'ichiro Ando et al. Snowmass2021 Cosmic Frontier: Synergies between dark matter searches and multiwavelength/multimessenger astrophysics. In *Snowmass 2021*, 3 2022.

[270] Yonatan Kahn et al. Snowmass2021 Cosmic Frontier: Modeling, statistics, simulations, and computing needs for direct dark matter detection. In *Snowmass 2021*, 3 2022.

[271] Rebecca K. Leane et al. Snowmass2021 Cosmic Frontier White Paper: Puzzling Excesses in Dark Matter Searches and How to Resolve Them, 3 2022.

[272] Andrea Mitridate, Tanner Trickle, Zhengkang Zhang, and Kathryn M. Zurek. Snowmass white paper: Light dark matter direct detection at the interface with condensed matter physics. *Phys. Dark Univ.*, 40:101221, 2023.

[273] Gary Steigman and Michael S. Turner. Cosmological constraints on the properties of weakly interacting massive particles. *Nuclear Physics B*, 253:375–386, 1985.

[274] N. Aghanim et al. Planck 2018 results. VI. Cosmological parameters. *Astron. Astrophys.*, 641:A6, 2020. [Erratum: Astron.Astrophys. 652, C4 (2021)].

[275] Fritz Zwicky. The redshift of extragalactic nebulae. *Helvetica Physica Acta*, 6:110–127, 1933.

[276] Vera C. Rubin. The rotation of spiral galaxies. *Science*, 220(4604):1339–1344, 1983.

[277] M. Kawasaki, Kazunori Kohri, and Naoshi Sugiyama. MeV scale reheating temperature and thermalization of neutrino background. *Phys. Rev. D*, 62:023506, 2000.

[278] Steen Hannestad. What is the lowest possible reheating temperature? *Phys. Rev. D*, 70:043506, 2004.

[279] Kazuhide Ichikawa, Masahiro Kawasaki, and Fuminobu Takahashi. The Oscillation effects on thermalization of the neutrinos in the Universe with low reheating temperature. *Phys. Rev. D*, 72:043522, 2005.

[280] Julien Billard et al. Direct detection of dark matter—APPEC committee report*. *Rept. Prog. Phys.*, 85(5):056201, 2022.

[281] Snowmass White Paper Contribution: Physics with the Phase-2 ATLAS and CMS Detectors. 2022.

[282] Jan Kalinowski, Tania Robens, and Aleksander Filip Zarnecki. New Physics with missing energy at future lepton colliders - Snowmass White Paper. In *Snowmass 2021*, 3 2022.

[283] Search for dark matter in final states with a Higgs boson decaying to a pair of b-jets and missing transverse momentum at the HL-LHC. 2022.

[284] Projection of the Mono-Z search for dark matter to the HL-LHC. 2018.

[285] David J. E. Marsh. Axion Cosmology. *Phys. Rept.*, 643:1–79, 2016.

[286] Roberto D Peccei and Helen R Quinn. Cp conservation in the presence of pseudoparticles. *Physical Review Letters*, 38(25):1440, 1977.

[287] Elisa G. M. Ferreira. Ultra-light dark matter. *Astron. Astrophys. Rev.*, 29(1):7, 2021.

[288] Mads T. Frandsen, Matti Heikinheimo, Mattias E. Thing, Kimmo Tuominen, and Martin Rosenlyst. Vector dark matter in supercooled Higgs portal models. *Phys. Rev. D*, 108(1):015033, 2023.

[289] Seyed Yaser Ayazi and Ahmad Mohamadnejad. Conformal vector dark matter and strongly first-order electroweak phase transition. *JHEP*, 03:181, 2019.

[290] Thomas Hambye and Alessandro Strumia. Dynamical generation of the weak and Dark Matter scale. *Phys. Rev. D*, 88:055022, 2013.

[291] E. Aprile et al. First Dark Matter Search Results from the XENON1T Experiment. *Phys. Rev. Lett.*, 119(18):181301, 2017.

[292] E. Aprile et al. Projected WIMP sensitivity of the XENONnT dark matter experiment. *JCAP*, 11:031, 2020.

[293] J. Aalbers et al. First Dark Matter Search Results from the LUX-ZEPLIN (LZ) Experiment. *Phys. Rev. Lett.*, 131(4):041002, 2023.

[294] Yue Meng et al. Dark Matter Search Results from the PandaX-4T Commissioning Run. *Phys. Rev. Lett.*, 127(26):261802, 2021.

[295] Georges Aad et al. Search for invisible Higgs-boson decays in events with vector-boson fusion signatures using 139 fb^{-1} of proton-proton data recorded by the ATLAS experiment. *JHEP*, 08:104, 2022.

[296] Armen Tumasyan et al. Search for invisible decays of the Higgs boson produced via vector boson fusion in proton-proton collisions at s=13 TeV. *Phys. Rev. D*, 105(9):092007, 2022.

[297] Ciaran A. J. O'Hare. New Definition of the Neutrino Floor for Direct Dark Matter Searches. *Phys. Rev. Lett.*, 127(25):251802, 2021.

[298] XENON Collaboration. First dark matter search results from the xenon1t experiment. *Physical Review Letters*, 119(18), Oct 2017.

[299] et al. J. Aalbers. First dark matter search results from the LUX-ZEPLIN (LZ) experiment. *Physical Review Letters*, 131(4), jul 2023.

[300] Astrid Eichhorn, Aaron Held, and Christof Wetterich. Predictive power of grand unification from quantum gravity. *JHEP*, 08:111, 2020.

[301] Albert M Sirunyan et al. Observation of $t\bar{t}H$ production. *Phys. Rev. Lett.*, 120(23):231801, 2018.

[302] M. Aaboud et al. Observation of Higgs boson production in association with a top quark pair at the LHC with the ATLAS detector. *Phys. Lett. B*, 784:173–191, 2018.

[303] F. Englert and R. Brout. Broken Symmetry and the Mass of Gauge Vector Mesons. *Phys. Rev. Lett.*, 13:321–323, 1964.

[304] Peter W. Higgs. Broken symmetries, massless particles and gauge fields. *Phys. Lett.*, 12:132–133, 1964.

[305] Peter W. Higgs. Broken Symmetries and the Masses of Gauge Bosons. *Phys. Rev. Lett.*, 13:508–509, 1964.

[306] Gerald S Guralnik, Carl R Hagen, and Thomas WB Kibble. Global conservation laws and massless particles. *Physical Review Letters*, 13(20):585, 1964.

[307] Gustavo P. de Brito, Astrid Eichhorn, and Marc Schiffer. Light charged fermions in quantum gravity. *Phys. Lett. B*, 815:136128, 2021.

[308] Yu Hamada, Jan M. Pawlowski, and Masatoshi Yamada. Gravitational instantons and anomalous chiral symmetry breaking. *Phys. Rev. D*, 103(10):106016, 2021.

[309] I. L. Buchbinder and E. N. Kirillova. Phase transitions induced by curvature in the Gross-Neveu model. *Sov. Phys. J.*, 32:446–450, 1989.

[310] I. L. Buchbinder and E. N. Kirillova. Gross-Neveu Model in Curved Space-time: The Effective Potential and Curvature Induced Phase Transition. *Int. J. Mod. Phys. A*, 04:143–149, 1989.

[311] T. Inagaki, T. Muta, and S. D. Odintsov. Nambu-Jona-Lasinio model in curved space-time. *Mod. Phys. Lett. A*, 08:2117–2124, 1993.

[312] E. Elizalde, S. Leseduarte, and S. D. Odintsov. Chiral symmetry breaking in the Nambu-Jona-Lasinio model in curved space-time with nontrivial topology. *Phys. Rev. D*, 49:5551–5558, 1994.

[313] L. N. Granda and J. Roldan. Curvature induced phase transition in the Gross-Neveu model on $M^4 \times S^d$. *Class. Quant. Grav.*, 12:1127–1133, 1995.

[314] I. Sachs and A. Wipf. Temperature and curvature dependence of the chiral symmetry breaking in 2-D gauge theories. *Phys. Lett. B*, 326:105–110, 1994.

[315] E. Elizalde, S. Leseduarte, S. D. Odintsov, and Yu. I. Shilnov. Phase structure of renormalizable four fermion models in space-times of constant curvature. *Phys. Rev. D*, 53:1917–1926, 1996.

[316] Shinya Kanemura and Haru-Tada Sato. Approach to D-dimensional Gross-Neveu model at finite temperature and curvature. *Mod. Phys. Lett. A*, 11:785–794, 1996.

[317] Tomohiro Inagaki. Curvature induced phase transition in a four fermion theory using the weak curvature expansion. *Int. J. Mod. Phys. A*, 11:4561–4576, 1996.

[318] Tomohiro Inagaki and Ken-ichi Ishikawa. Thermal and curvature effects to dynamical symmetry breaking. *Phys. Rev. D*, 56:5097–5107, Oct 1997.

[319] B. Geyer and S. D. Odintsov. Gauged NJL model at strong curvature. *Phys. Lett. B*, 376:260–265, 1996.

[320] B. Geyer and S. D. Odintsov. Chiral symmetry breaking in gauged NJL model in curved space-time. *Phys. Rev. D*, 53:7321–7326, 1996.

[321] Gennaro Miele and Patrizia Vitale. Three-dimensional Gross-Neveu model on curved spaces. *Nucl. Phys. B*, 494:365–387, 1997.

[322] Patrizia Vitale. Temperature-induced phase transitions in four fermion models in curved space-time. *Nucl. Phys. B*, 551:490–510, 1999.

[323] J. Hashida, S. Mukaigawa, T. Muta, K. Ohkura, and K. Yamamoto. Curvature induced phase transitions in the inflationary universe: Supersymmetric Nambu-Jona-Lasinio model in de Sitter space-time. *Phys. Rev. D*, 61:044015, 2000.

[324] E. V. Gorbar and V. P. Gusynin. Gap generation for Dirac fermions on Lobachevsky plane in a magnetic field. *Annals Phys.*, 323:2132–2146, 2008.

[325] Tomohiro Inagaki and Masako Hayashi. Topological and Curvature Effects in a Multi-fermion Interaction Model. In *International Workshop on Strong Coupling Gauge Theories in LHC Era: SCGT 09*, pages 184–190, 2011.

[326] Shuji Sasagawa and Hidekazu Tanaka. The separation of the chiral and deconfinement phase transitions in the curved space-time. *Prog. Theor. Phys.*, 128:925–939, 2012.

[327] E. V. Gorbar. Dynamical symmetry breaking in spaces with constant negative curvature. *Phys. Rev. D*, 61:024013, 2000.

[328] D. Ebert, A. V. Tyukov, and V. Ch. Zhukovsky. Gravitational catalysis of chiral and color symmetry breaking of quark matter in hyperbolic space. *Phys. Rev. D*, 80:085019, 2009.

[329] Masako Hayashi, Tomohiro Inagaki, and Hiroyuki Takata. Multi-fermion interaction models in curved spacetime. 12 2008.

[330] E. V. Gorbar. On Effective Dimensional Reduction in Hyperbolic Spaces. *Ukr. J. Phys.*, 54:541–546, 2009.

[331] Hidenori Fukaya, Masayasu Harada, Masaharu Tanabashi, and Koichi Yamawaki, editors. *Strong coupling gauge theories in LHC era. Proceedings, International Workshop, SCGT 09, Nagoya, Japan, December 8-11, 2009*, volume 25, 2010.

[332] Antonino Flachi and Kenji Fukushima. Chiral Mass-Gap in Curved Space. *Phys. Rev. Lett.*, 113(9):091102, 2014.

[333] Andrea Addazi, Pisin Chen, and Antonino Marciano. Emergent inflation from a Nambu–Jona-Lasinio mechanism in gravity with non-dynamical torsion. *Eur. Phys. J. C*, 79(4):297, 2019.

[334] Holger Gies and Riccardo Martini. Curvature bound from gravitational catalysis. *Phys. Rev. D*, 97(8):085017, 2018.

[335] Holger Gies and Abdol Sabor Salek. Curvature bound from gravitational catalysis in thermal backgrounds. *Phys. Rev. D*, 103(12):125027, 2021.

[336] Holger Gies and Stefan Lippoldt. Renormalization flow towards gravitational catalysis in the 3d Gross-Neveu model. *Phys. Rev. D*, 87:104026, 2013.

[337] V. P. Gusynin, V. A. Miransky, and I. A. Shovkovy. Catalysis of dynamical flavor symmetry breaking by a magnetic field in (2+1)-dimensions. *Phys. Rev. Lett.*, 73:3499–3502, 1994. [Erratum: Phys.Rev.Lett. 76, 1005 (1996)].

[338] V. P. Gusynin, V. A. Miransky, and I. A. Shovkovy. Dynamical flavor symmetry breaking by a magnetic field in (2+1)-dimensions. *Phys. Rev. D*, 52:4718–4735, 1995.

[339] Daniel D. Scherer and Holger Gies. Renormalization Group Study of Magnetic Catalysis in the 3d Gross-Neveu Model. *Phys. Rev. B*, 85:195417, 2012.

[340] K. G. Klimenko and R. N. Zhokhov. Magnetic catalysis effect in the (2+1)-dimensional Gross-Neveu model with Zeeman interaction. *Phys. Rev. D*, 88(10):105015, 2013.

[341] Friedrich W. Hehl, J. Dermott McCrea, Eckehard W. Mielke, and Yuval Ne'eman. Metric affine gauge theory of gravity: Field equations, Noether identities, world spinors, and breaking of dilation invariance. *Phys. Rept.*, 258:1–171, 1995.

[342] A. Baldazzi, O. Melichev, and R. Percacci. Metric-Affine Gravity as an effective field theory. *Annals Phys.*, 438:168757, 2022.

[343] Attilio Palatini. Deduzione invariantiva delle equazioni gravitazionali dal principio di hamilton. *Rendiconti del Circolo Matematico di Palermo (1884-1940)*, 43(1):203–212, 1919.

[344] Albert Einstein. Einheitliche feldtheorie von gravitation und elektrizität. *Albert Einstein: Akademie-Vorträge: Sitzungsberichte der Preußischen Akademie der Wissenschaften 1914–1932*, pages 267–273, 2005.

[345] Marco Ferraris, Mauro Francaviglia, and Cesare Reina. Variational formulation of general relativity from 1915 to 1925 "palatini's method" discovered by einstein in 1925. *General relativity and gravitation*, 14:243–254, 1982.

[346] K. Hayashi and T. Nakano. Extended translation invariance and associated gauge fields. *Prog. Theor. Phys.*, 38:491–507, 1967.

[347] Claudio Pellegrini and Jerzy Plebanski. Tetrad fields and gravitational fields. *Kgl. Danske Videnskab. Selskab, Mat. Fys. Skrifter*, 2(4), 1963.

[348] YM Cho. Einstein lagrangian as the translational yang-mills lagrangian. *Physical Review D*, 14(10):2521, 1976.

[349] Alejandro Perez. The Spin Foam Approach to Quantum Gravity. *Living Rev. Rel.*, 16:3, 2013.

[350] Carlo Rovelli and Francesca Vidotto. *Covariant Loop Quantum Gravity: An Elementary Introduction to Quantum Gravity and Spinfoam Theory*. Cambridge Monographs on Mathematical Physics. Cambridge University Press, 11 2014.

[351] J. E. Daum and M. Reuter. Renormalization Group Flow of the Holst Action. *Phys. Lett. B*, 710:215–218, 2012.

[352] Georgios K. Karananas, Mikhail Shaposhnikov, Andrey Shkerin, and Sebastian Zell. Matter matters in Einstein-Cartan gravity. *Phys. Rev. D*, 104(6):064036, 2021.

[353] Mikhail Shaposhnikov, Andrey Shkerin, Inar Timiryasov, and Sebastian Zell. Einstein-Cartan Portal to Dark Matter. *Phys. Rev. Lett.*, 126(16):161301, 2021. [Erratum: Phys.Rev.Lett. 127, 169901 (2021)].

[354] Tom WB Kibble. Lorentz invariance and the gravitational field. *Journal of mathematical physics*, 2(2):212–221, 1961.

[355] Alejandro Perez and Carlo Rovelli. Physical effects of the Immirzi parameter. *Phys. Rev. D*, 73:044013, 2006.

[356] Laurent Freidel, Djordje Minic, and Tatsu Takeuchi. Quantum gravity, torsion, parity violation and all that. *Phys. Rev. D*, 72:104002, 2005.

[357] Mikhail Shaposhnikov, Andrey Shkerin, Inar Timiryasov, and Sebastian Zell. Einstein-Cartan gravity, matter, and scale-invariant generalization . *JHEP*, 10:177, 2020.

[358] Jorge Zanelli. Lecture notes on Chern-Simons (super-)gravities. Second edition (February 2008). In *7th Mexican Workshop on Particles and Fields*, 2 2005.

[359] Alfio Bonanno, Tobias Denz, Jan M. Pawlowski, and Manuel Reichert. Reconstructing the graviton. *SciPost Phys.*, 12(1):001, 2022.

[360] Venzo De Sabbata and Maurizio Gasperini. *Introduction to gravitation*. World Scientific Publishing Company, 1986.

[361] Oleg Igorevich Melichev. *Quantum Aspects of Metric-Affine Gravity*. PhD thesis, SISSA, 2023.

[362] R. Percacci and E. Sezgin. New class of ghost- and tachyon-free metric affine gravities. *Phys. Rev. D*, 101(8):084040, 2020.

[363] Yoichiro Nambu and G. Jona-Lasinio. Dynamical Model of Elementary Particles Based on an Analogy with Superconductivity. 1. *Phys. Rev.*, 122:345–358, 1961.

[364] Ulrich Harst and Martin Reuter. A new functional flow equation for Einstein–Cartan quantum gravity. *Annals Phys.*, 354:637–704, 2015.

[365] Ilya L. Shapiro and Poliane M. Teixeira. Quantum Einstein-Cartan theory with the Holst term. *Class. Quant. Grav.*, 31:185002, 2014.

[366] Riccardo Martini, Gregorio Paci, and Dario Sauro. Covariant spin-parity decomposition of the torsion and path integrals. *Class. Quant. Grav.*, 40(19):195005, 2023.

[367] Ioseph L Buchbinder, S Odintsov, and L Shapiro. *Effective action in quantum gravity*. CRC Press, 1992.

[368] Yuri N. Obukhov, Alexander J. Silenko, and Oleg V. Teryaev. Spin-torsion coupling and gravitational moments of Dirac fermions: theory and experimental bounds. *Phys. Rev. D*, 90(12):124068, 2014.

[369] T. Mariz, J. R. Nascimento, A. Yu. Petrov, L. Y. Santos, and A. J. da Silva. Lorentz violation and the proper-time method. *Phys. Lett. B*, 661:312–318, 2008.

[370] M. Gomes, T. Mariz, J. R. Nascimento, E. Passos, A. Yu. Petrov, and A. J. da Silva. On the ambiguities in the effective action in Lorentz-violating gravity. *Phys. Rev. D*, 78:025029, 2008.

[371] J. F. Assunção, T. Mariz, J. R. Nascimento, and A. Yu Petrov. Induced Chern-Simons modified gravity at finite temperature. *JHEP*, 08:072, 2018.

[372] Martin Reuter and Frank Saueressig. *Quantum Gravity and the Functional Renormalization Group: The Road towards Asymptotic Safety*. Cambridge University Press, 1 2019.

[373] Carlo Pagani and Roberto Percacci. Quantum gravity with torsion and non-metricity. *Class. Quant. Grav.*, 32(19):195019, 2015.

[374] Daniel F. Litim. Optimization of the exact renormalization group. *Phys. Lett. B*, 486:92–99, 2000.

[375] Ivan G Avramidi. *Heat kernel and quantum gravity*, volume 64. Springer Science & Business Media, 2000.

[376] Yu. n. Obukhov. Spectral geometry of the Riemann-Cartan space-time. *Nucl. Phys. B*, 212:237–254, 1983.

[377] V. P. Gusynin, E. V. Gorbar, and V. V. Romankov. Heat kernel expansion for nonminimal differential operators and manifolds with torsion. *Nucl. Phys. B*, 362:449–471, 1991.

[378] Norman H. Barth. Heat kernel expansion coefficient. I. An extension. *J. Phys. A*, 20:857, 1987.

[379] H. I. Arcos and J. G. Pereira. Torsion gravity: A Reappraisal. *Int. J. Mod. Phys. D*, 13:2193–2240, 2004.

[380] Ruben Aldrovandi and José Geraldo Pereira. *Teleparallel Gravity: An Introduction*. Springer, 2013.

[381] Sebastian Bahamonde, Konstantinos F. Dialektopoulos, Celia Escamilla-Rivera, Gabriel Farrugia, Viktor Gakis, Martin Hendry, Manuel Hohmann, Jackson Levi Said, Jurgen Mifsud, and Eleonora Di Valentino. Teleparallel gravity: from theory to cosmology. *Rept. Prog. Phys.*, 86(2):026901, 2023.

[382] M. Krssak, R. J. van den Hoogen, J. G. Pereira, C. G. Böhmer, and A. A. Coley. Teleparallel theories of gravity: illuminating a fully invariant approach. *Class. Quant. Grav.*, 36(18):183001, 2019.

[383] Roberto Casadio, Iberê Kuntz, and Gregorio Paci. Quantum fields in teleparallel gravity: renormalization at one-loop. *Eur. Phys. J. C*, 82(3):186, 2022.

[384] R. L. Workman and Others. Review of Particle Physics. *PTEP*, 2022:083C01, 2022.

[385] Sean M. Carroll. The Cosmological constant. *Living Rev. Rel.*, 4:1, 2001.

[386] Wolfram Weise. The QCD vacuum and its hadronic excitations. In *58th Scottish Universities Summer School in Physics (SUSSP58): A NATO Advanced Study Institute and EU Hadron Physics 13 Summer Institute*, pages 201–232, 4 2005.

[387] R. de León Ardón, N. Ohta, and R. Percacci. Path integral of unimodular gravity. *Phys. Rev. D*, 97(2):026007, 2018.

[388] Enrique Alvarez, Sergio Gonzalez-Martin, and Carmelo P. Martin. Unimodular Trees versus Einstein Trees. *Eur. Phys. J. C*, 76(10):554, 2016.

[389] Daniel J Burger, George F. R. Ellis, Jeff Murugan, and Amanda Weltman. The KLT relations in unimodular gravity. 11 2015.

[390] Antonio Padilla and Ippocratis D. Saltas. A note on classical and quantum unimodular gravity. *Eur. Phys. J. C*, 75(11):561, 2015.

[391] Bartomeu Fiol and Jaume Garriga. Semiclassical Unimodular Gravity. *JCAP*, 08:015, 2010.

[392] R. Bufalo, M. Oksanen, and A. Tureanu. How unimodular gravity theories differ from general relativity at quantum level. *Eur. Phys. J. C*, 75(10):477, 2015.

[393] Raúl Carballo-Rubio, Luis J. Garay, and Gerardo García-Moreno. Unimodular gravity vs general relativity: a status report. *Class. Quant. Grav.*, 39(24):243001, 2022.

[394] Gustavo P. de Brito, Oleg Melichev, Roberto Percacci, and Antonio D. Pereira. Can quantum fluctuations differentiate between standard and unimodular gravity? *JHEP*, 12:090, 2021.

[395] Astrid Eichhorn. On unimodular quantum gravity. *Class. Quant. Grav.*, 30:115016, 2013.

[396] Ippocratis D. Saltas. UV structure of quantum unimodular gravity. *Phys. Rev. D*, 90(12):124052, 2014.

[397] Astrid Eichhorn. The Renormalization Group flow of unimodular f(R) gravity. *JHEP*, 04:096, 2015.

[398] Dario Benedetti. Essential nature of Newton's constant in unimodular gravity. *Gen. Rel. Grav.*, 48(5):68, 2016.

[399] Kevin Falls, Callum R. King, Daniel F. Litim, Kostas Nikolakopoulos, and Christoph Rahmede. Asymptotic safety of quantum gravity beyond Ricci scalars. *Phys. Rev. D*, 97(8):086006, 2018.

[400] Hendrik Antoon Lorentz, Albert Einstein, Hermann Minkowski, Hermann Weyl, and Arnold Sommerfeld. *The principle of relativity: a collection of original memoirs on the special and general theory of relativity.* Courier Corporation, 1952.

[401] J. J. Lopez-Villarejo. TransverseDiff gravity is to scalar-tensor as unimodular gravity is to General Relativity. *JCAP*, 11:002, 2011.

[402] J. J. Lopez-Villarejo. A theorem of equivalence between TransverseDiff theories and scalar-tensor gravity. *J. Phys. Conf. Ser.*, 314:012046, 2011.

[403] Thibaut Josset, Alejandro Perez, and Daniel Sudarsky. Dark energy from violation of energy conservation. *Phys. Rev. Lett.*, 118:021102, Jan 2017.

[404] J. A. Astorga-Moreno, Javier Chagoya, J. C. Flores-Urbina, and Miguel A. Garcia-Aspeitia. Compact objects in unimodular gravity. *JCAP*, 09:005, 2019.

[405] Cristóbal Corral, Norman Cruz, and Esteban González. Diffusion in unimodular gravity: Analytical solutions, late-time acceleration, and cosmological constraints. *Phys. Rev. D*, 102(2):023508, 2020.

[406] Alejandro Perez, Daniel Sudarsky, and Edward Wilson-Ewing. Resolving the H_0 tension with diffusion. *Gen. Rel. Grav.*, 53(1):7, 2021.

[407] Gabriel Leon. Inflation and the cosmological (not-so) constant in unimodular gravity. *Class. Quant. Grav.*, 39(7):075008, 2022.

[408] Enrique Álvarez, Sergio González-Martín, Mario Herrero-Valea, and Carmelo P. Martín. Quantum Corrections to Unimodular Gravity. *JHEP*, 08:078, 2015.

[409] Mario Herrero-Valea and Raquel Santos-Garcia. Non-minimal Tinges of Unimodular Gravity. *JHEP*, 09:041, 2020.

[410] Astrid Eichhorn, Holger Gies, and Michael M. Scherer. Asymptotically free scalar curvature-ghost coupling in Quantum Einstein Gravity. *Phys. Rev. D*, 80:104003, 2009.

[411] Astrid Eichhorn and Holger Gies. Ghost anomalous dimension in asymptotically safe quantum gravity. *Phys. Rev. D*, 81:104010, 2010.

[412] Nicolai Christiansen, Daniel F. Litim, Jan M. Pawlowski, and Andreas Rodigast. Fixed points and infrared completion of quantum gravity. *Phys. Lett. B*, 728:114–117, 2014.

[413] Alessandro Codello, Giulio D'Odorico, and Carlo Pagani. Consistent closure of renormalization group flow equations in quantum gravity. *Phys. Rev. D*, 89(8):081701, 2014.

[414] P. Donà, Astrid Eichhorn, and Roberto Percacci. Consistency of matter models with asymptotically safe quantum gravity. *Can. J. Phys.*, 93(9):988–994, 2015.

[415] Holger Gies and Stefan Lippoldt. Fermions in gravity with local spin-base invariance. *Phys. Rev. D*, 89(6):064040, 2014.

[416] Holger Gies and Stefan Lippoldt. Global surpluses of spin-base invariant fermions. *Phys. Lett. B*, 743:415–419, 2015.

[417] Stefan Lippoldt. Spin-base invariance of Fermions in arbitrary dimensions. *Phys. Rev. D*, 91(10):104006, 2015.

[418] S. Upadhyay, M. Oksanen, and R. Bufalo. BRST Quantization of Unimodular Gravity. *Braz. J. Phys.*, 47(3):350–365, 2017.

[419] Laurent Baulieu. Unimodular Gauge in Perturbative Gravity and Supergravity. *Phys. Lett. B*, 808:135591, 2020.

[420] Laurent Baulieu. Unimodular Gauge and ADM Gravity Path Integral. 12 2020.

[421] Jr. York, James W. Conformatlly invariant orthogonal decomposition of symmetric tensors on Riemannian manifolds and the initial value problem of general relativity. *J. Math. Phys.*, 14:456–464, 1973.

[422] Nobuyoshi Ohta, Roberto Percacci, and Gian Paolo Vacca. Renormalization Group Equation and scaling solutions for f(R) gravity in exponential parametrization. *Eur. Phys. J. C*, 76(2):46, 2016.

[423] Maximilian Demmel, Frank Saueressig, and Omar Zanusso. A proper fixed functional for four-dimensional Quantum Einstein Gravity. *JHEP*, 08:113, 2015.

[424] Maximilian Demmel, Frank Saueressig, and Omar Zanusso. Fixed-Functionals of three-dimensional Quantum Einstein Gravity. *JHEP*, 11:131, 2012.

[425] Juergen A. Dietz and Tim R. Morris. Asymptotic safety in the f(R) approximation. *JHEP*, 01:108, 2013.

[426] Juergen A. Dietz and Tim R. Morris. Redundant operators in the exact renormalisation group and in the f(R) approximation to asymptotic safety. *JHEP*, 07:064, 2013.

[427] Maximilian Demmel, Frank Saueressig, and Omar Zanusso. Fixed Functionals in Asymptotically Safe Gravity. In *13th Marcel Grossmann Meeting on Recent Developments in Theoretical and Experimental General Relativity, Astrophysics, and Relativistic Field Theories*, pages 2227–2229, 2015.

[428] Maximilian Demmel, Frank Saueressig, and Omar Zanusso. RG flows of Quantum Einstein Gravity on maximally symmetric spaces. *JHEP*, 06:026, 2014.

[429] Maximilian Demmel, Frank Saueressig, and Omar Zanusso. RG flows of Quantum Einstein Gravity in the linear-geometric approximation. *Annals Phys.*, 359:141–165, 2015.

[430] Nobuyoshi Ohta, Roberto Percacci, and Gian Paolo Vacca. Flow equation for $f(R)$ gravity and some of its exact solutions. *Phys. Rev. D*, 92(6):061501, 2015.

[431] Sergio Gonzalez-Martin, Tim R. Morris, and Zoë H. Slade. Asymptotic solutions in asymptotic safety. *Phys. Rev. D*, 95(10):106010, 2017.

[432] Nicolai Christiansen, Kevin Falls, Jan M. Pawlowski, and Manuel Reichert. Curvature dependence of quantum gravity. *Phys. Rev. D*, 97(4):046007, 2018.

[433] Natália Alkofer. Asymptotically safe $f(R)$-gravity coupled to matter II: Global solutions. *Phys. Lett. B*, 789:480–487, 2019.

[434] Gustavo P. De Brito, Nobuyoshi Ohta, Antonio D. Pereira, Anderson A. Tomaz, and Masatoshi Yamada. Asymptotic safety and field parametrization dependence in the $f(R)$ truncation. *Phys. Rev. D*, 98(2):026027, 2018.

[435] Benjamin Bürger, Jan M. Pawlowski, Manuel Reichert, and Bernd-Jochen Schaefer. Curvature dependence of quantum gravity with scalars. 12 2019.

[436] O. Lauscher and M. Reuter. Flow equation of quantum Einstein gravity in a higher derivative truncation. *Phys. Rev. D*, 66:025026, 2002.

[437] Daniel F. Litim. Fixed points of quantum gravity. *Phys. Rev. Lett.*, 92:201301, 2004.

[438] Alessandro Codello and Roberto Percacci. Fixed points of higher derivative gravity. *Phys. Rev. Lett.*, 97:221301, 2006.

[439] Dario Benedetti, Pedro F. Machado, and Frank Saueressig. Asymptotic safety in higher-derivative gravity. *Mod. Phys. Lett. A*, 24:2233–2241, 2009.

[440] D. Benedetti, P.F. Machado, and F. Saueressig. Taming perturbative divergences in asymptotically safe gravity. *Nucl. Phys.*, B824:168–191, 2010.

[441] E. Manrique, M. Reuter, and F. Saueressig. Bimetric Renormalization Group Flows in Quantum Einstein Gravity. *Annals Phys.*, 326:463–485, 2011.

[442] Dario Benedetti and Francesco Caravelli. The Local potential approximation in quantum gravity. *JHEP*, 06:017, 2012. [Erratum: JHEP 10, 157 (2012)].

[443] D. Benedetti. On the number of relevant operators in asymptotically safe gravity. *EPL*, 102(2):20007, 2013.

[444] N. Ohta and R. Percacci. Higher Derivative Gravity and Asymptotic Safety in Diverse Dimensions. *Class. Quant. Grav.*, 31:015024, 2014.

[445] Nicolai Christiansen, Benjamin Knorr, Jan M. Pawlowski, and Andreas Rodigast. Global Flows in Quantum Gravity. *Phys. Rev. D*, 93(4):044036, 2016.

[446] K. Falls. Asymptotic safety and the cosmological constant. *JHEP*, 01:069, 2016.

[447] Nicolai Christiansen, Benjamin Knorr, Jan Meibohm, Jan M. Pawlowski, and Manuel Reichert. Local Quantum Gravity. *Phys. Rev. D*, 92(12):121501, 2015.

[448] Benjamin Knorr. Infinite order quantum-gravitational correlations. *Class. Quant. Grav.*, 35(11):115005, 2018.

[449] Tobias Denz, Jan M. Pawlowski, and Manuel Reichert. Towards apparent convergence in asymptotically safe quantum gravity. *Eur. Phys. J. C*, 78(4):336, 2018.

[450] K. Falls and N. Ohta. Renormalization Group Equation for $f(R)$ gravity on hyperbolic spaces. *Phys. Rev. D*, 94(8):084005, 2016.

[451] Djamel Dou and Roberto Percacci. The running gravitational couplings. *Class. Quant. Grav.*, 15:3449–3468, 1998.

[452] Roberto Percacci and Daniele Perini. Constraints on matter from asymptotic safety. *Phys. Rev. D*, 67:081503, 2003.

[453] Roberto Percacci and Daniele Perini. Asymptotic safety of gravity coupled to matter. *Phys. Rev. D*, 68:044018, 2003.

[454] O. Zanusso, L. Zambelli, G.P. Vacca, and R. Percacci. Gravitational corrections to Yukawa systems. *Phys. Lett. B*, 689:90–94, 2010.

[455] Astrid Eichhorn. Quantum-gravity-induced matter self-interactions in the asymptotic-safety scenario. *Phys. Rev. D*, 86:105021, 2012.

[456] Astrid Eichhorn, Aaron Held, and Jan M. Pawlowski. Quantum-gravity effects on a Higgs-Yukawa model. *Phys. Rev. D*, 94(10):104027, 2016.

[457] Yuta Hamada and Masatoshi Yamada. Asymptotic safety of higher derivative quantum gravity non-minimally coupled with a matter system. *JHEP*, 08:070, 2017.

[458] Nicolai Christiansen, Astrid Eichhorn, and Aaron Held. Is scale-invariance in gauge-Yukawa systems compatible with the graviton? *Phys. Rev. D*, 96(8):084021, 2017.

[459] Astrid Eichhorn. Status of the asymptotic safety paradigm for quantum gravity and matter. *Found. Phys.*, 48(10):1407–1429, 2018.

[460] Jan M. Pawlowski, Manuel Reichert, Christof Wetterich, and Masatoshi Yamada. Higgs scalar potential in asymptotically safe quantum gravity. *Phys. Rev. D*, 99(8):086010, 2019.

[461] Gustavo P. De Brito, Yuta Hamada, Antonio D. Pereira, and Masatoshi Yamada. On the impact of Majorana masses in gravity-matter systems. *JHEP*, 08:142, 2019.

[462] C. Wetterich. Effective scalar potential in asymptotically safe quantum gravity. *Universe*, 7(2):45, 2021.

[463] Guillem Domènech, Mark Goodsell, and Christof Wetterich. Neutrino masses, vacuum stability and quantum gravity prediction for the mass of the top quark. *JHEP*, 01:180, 2021.

[464] Mads T. Frandsen, Matti Heikinheimo, Martin Rosenlyst, Mattias E. Thing, and Kimmo Tuominen. Gravitational waves from SU(N)/SP(N) composite Higgs models. *JHEP*, 09:022, 2023.

[465] Gustavo P. de Brito, Astrid Eichhorn, and Shouryya Ray. Light fermions in color: why the quark mass is not the planck mass, 2023.

[466] Públio Rwany Batista Ribeiro do Vale. Possibility of Spontaneous Symmetry Breaking in the Nambu-Jona-Lasinio model with torsion. 6 2023.

[467] Guilherme H. S. Camargo and Ilya L. Shapiro. Anomaly-induced vacuum effective action with torsion: Covariant solution and ambiguities. *Phys. Rev. D*, 106(4):045004, 2022.

[468] Kazuo Kondo. On the geometrical and physical foundations of the theory of yielding. In *Proc. 2nd Japan Nat. Congr. Applied Mechanics*, volume 2, pages 41–47, 1952.

[469] Bruce Alexander Bilby, R Bullough, and Edwin Smith. Continuous distributions of dislocations: a new application of the methods of non-riemannian geometry. *Proceedings of the Royal Society of London. Series A. Mathematical and Physical Sciences*, 231(1185):263–273, 1955.

[470] M. A. Zubkov. Emergent gravity and chiral anomaly in Dirac semimetals in the presence of dislocations. *Annals Phys.*, 360:655–678, 2015.

[471] I. Hamzaan Bridle, Juergen A. Dietz, and Tim R. Morris. The local potential approximation in the background field formalism. *JHEP*, 03:093, 2014.

[472] Alessio Baldazzi and Kevin Falls. Essential Quantum Einstein Gravity. *Universe*, 7(8):294, 2021.

[473] Jan-Eric Daum, Ulrich Harst, and Martin Reuter. Running Gauge Coupling in Asymptotically Safe Quantum Gravity. *JHEP*, 01:084, 2010.

[474] J. E. Daum, U. Harst, and M. Reuter. Non-perturbative QEG Corrections to the Yang-Mills Beta Function. *Gen. Rel. Grav.*, 43:2393, 2011.

[475] Steffen Gielen, Rodrigo de León Ardón, and Roberto Percacci. Gravity with more or less gauging. *Class. Quant. Grav.*, 35(19):195009, 2018.

[476] Yuri Bonder and Cristóbal Corral. Unimodular Einstein–Cartan gravity: Dynamics and conservation laws. *Phys. Rev. D*, 97(8):084001, 2018.

[477] I.L. Buchbinder, S.D. Odintsov, and I.L. Shapiro. *Effective action in quantum gravity*. 1992.

[478] I.G. Avramidi. *Heat kernel and quantum gravity*, volume 64. Springer, New York, 2000.

[479] Mahmoud Safari. Splitting Ward identity. *Eur. Phys. J. C*, 76(4):201, 2016.